



**SAPIENZA**  
UNIVERSITÀ DI ROMA

**Dottorato di ricerca:**  
**Scienze Applicate per la Protezione**  
**dell'Ambiente e dei Beni Culturali**  
**Dipartimento di Scienze della Terra**

**Coordinatore: Adriana MARAS**

**Tutore/i: Silvano MIGNARDI**

**Filippo TERRASI**

**Fabio MARZAIOLI**

**Revisori:**

**Gilberto ARTIOLI**

**Elisabetta BOARETTO**

**Docenti Esaminatori:**

**Marco GIAMELLO**

**Gianluigi DE GENNARO**

**Paolo BALLIRANO**

## **An innovative method to select a suitable fraction for mortar $^{14}\text{C}$ dating: the Cryo2SoniC protocol.**

**Un metodo innovativo per la selezione di una frazione ideale per la datazione delle malte tramite  $^{14}\text{C}$ : il protocollo Cryo2SoniC.**

**Sara NONNI**

**XXVI Ciclo**

# Contents

**Glossary**

**Summary**

**Acknowledgements**

<b>I. Introduction</b>	<b>1</b>
I.1 Mortar dating	1
I.2 Mortar production	2
I.3 Datable fraction isolation	5
<b>II. Implementation and validation of the methodology</b>	<b>8</b>
II.1 Testing CryoSoniC Protocol.	8
<i>II.1.1 Mortar radiocarbon dating: preliminary evaluation of a novel methodology.</i>	9
II.2 The evolution: Methodological aspects and field study applications at CIRCE using CryoSoniC and Cryo2SoniC methods.	17
<i>II.2.1 Application on Medieval Spanish Sites: Aistra, Zornotzegi, Trevino.</i>	21
<i>II.2.2 Publication on NIMB.</i>	30
II.3 Lime Lumps a successful resource	36
II.4 Dating Pozzolana Mortars: a new challenge.	44
<i>II.4.1 Study case: Fiscale Tower and Ostia Marina Excavation.</i>	46
II.5 Drawbacks.	50
<i>II.5.1 Calcareous Aggregate</i>	51
<i>II.5.2 Secondary Calcite Deposition.</i>	53
<i>II.5.3 Fossil Atmospheres.</i>	56
<i>II.5.4 Study case: Ponte di Augusto at Narni.</i>	56
II.6 Control Checks on Collected Fractions.	61
<i>II.6.1 Particles dimension control check using SEM.</i>	62
<i>II.6.2 Recognition of Dead Carbon contaminants with Cathodoluminescence.</i>	72
<i>II.6.3 Differentiation between geological and anthropological calcite by FTIR.</i>	75
II.7 Methods comparison	81
II.8 Resume	88
<b>III. Applicative Section</b>	<b>90</b>
III.1 Castle of Shayzar: a Radiocarbon Publication.	90
III.2 Palazzo Vecchio between antiquity and middle age.	103
III.3 <sup>14</sup> C Investigation on Circo Massimo remains.	112
III.4 Discovering the Domus Romanae inside Palazzo Valentini.	119
III.5 Chronological reconstruction of Roman Basilica in Canosa di Puglia	131
<b>IV. General Resume</b>	<b>139</b>
<b>V. References</b>	<b>143</b>

## Glossary

**AMS Radiocarbon dating** – Determination of the age of a finding belonging in the past to a living organism by measurement of its radiocarbon content, using an Accelerator Mass Spectrometer (AMS). The amount of  $^{14}\text{C}$  atoms is representative of the time elapsed since the death of the organism if a precise atmospheric signature is ascribable to a precise moment in the past.

**Binder** – Generically a *binder* is considered any material or substance that holds or draws other materials together to form a cohesive whole. In this thesis the binder is intended as a building material (a cement) used to connect stones or bricks to form a wall or a covering surface. Usually it is produced by firing limestone (or calcareous basic rocks or gypsum) which produced quicklime that goes to an hydration becoming slaked-lime. From the time of aging depends the quality and durability of the slaked lime.

**Calibration** – The necessary step to pass from a RC age to a Calendar age. If you base on the assumption that the atmospheric radiocarbon concentration has always been the same as it was in 1950 AD (or better as it would have been in a “clean” atmosphere) and that the half-life of radiocarbon is 5568 years, you could get the calendar age directly from the RC age. Indeed this assumption is wrong because  $^{14}\text{C}$  concentration in atmosphere was not constant during the centuries: it has varied and it has done it irregularly. The use of calibration curve allows to switch from a RC age form to a calendar one by a specific software of calculation.

**Calibration Curves** – It represents the evolution and changing of  $\text{CO}_2$  concentration in the atmosphere. According to what we need to date a different calibration curve should be used, changing in relation to the geographic position of material dated. With terrestrial material, the IntCal13 calibration curve should be used, but in the Southern Hemisphere, the ShCal13 curve should be used. For marine (oceanic) samples the Marine13 curve should be used but you need to know about any regional offsets and to use Marine Reservoir Correction Database.

**Cryo2SoniC** – A pretreatment protocol used to select a fraction of mortar suitable to be dated. Its name is an acronym of its three main steps: cryo-breaking, double sonication and centrifugation.

**Lime lump** – Its definition could be understood as several different materials (section II.3), but here it is intended as a nodule of pure binder. Often it is a residue of a bad mixing during the last phases of production of a mortar.

**Limestone** - A sedimentary rock composed largely of the minerals calcite and aragonite, which are different crystal forms of calcium carbonate ( $\text{CaCO}_3$ ). Many limestones are composed from skeletal fragments of marine organisms such as coral or foraminifera.

**Mortar** – A composite materials including a binding material (such as a cement or lime) or a mixture of them, of natural or artificial aggregates (different nature) or a mix of them and water. It has been used as isolating lining materials in cisterns, wells, aqueducts, shafts and duct drains, as supporting materials for pavements and mosaics, as plasters on external and internal walls and as supporting materials for frescoes, as well as joint mortars on masonry structures.

**Secondary calcite** – A newly-formed calcite, grown up from any water activity which determines deposition of calcium carbonate when evaporation of the water leaves a solution supersaturated with the chemical constituents of calcite.

**Years BP** – The standard unit to express a radiocarbon age, where BP is for ‘before present’, and ‘present’ refers to 1950. It is derived from the assumption that the half-life of radiocarbon is 5568 years and the amount of radiocarbon in the atmosphere has been constant as it was at 1950 AD.

## Summary

To date, mortar radiocarbon ( $^{14}\text{C}$ ) dating represents one of the main “open issues” involving the whole radiocarbon community because, after about 50 years of experimentation, the possibility to evaluate absolute chronologies for these artifact by radiocarbon remains still uncertain. This thesis is a report of three years of research on dating of mortars using radiocarbon techniques by AMS. It illustrates the development and applications of an innovative and efficient pretreatment protocol aiming to the selection of a fraction of mortars recording the time of setting.

This adventure started in 2010, with first experimentations of the methodology on a series of laboratory samples. The protocol, named CryoSoniC (a simplified version of the final protocol) was based on a physical (ultrasonication) selection procedure and was performed to test its efficiency on synthetic laboratory samples produced without the addition of aggregates. The experience and its good feedbacks were the object of a publication on Analytical Chemistry in 2011 (Chapter II, Section 1) and allowed us to begin a broad spectrum of activities which, to date, have involved a lot of different Institutions and Universities, in Italy and abroad. The close collaboration between University of Rome Sapienza, Second University of Naples and CIRCE (Centre for Isotopic Research on Cultural and Environmental Heritage) produced first a hotshot protocol applicable on synthetic mortars. Once proved that this selection method worked on a simplified system, the second step was testing the same procedure on more complex matrices: real mortars. To do that, a series of RC analyses were performed on mortars from different archaeological sites. From data analysis, it was shown that the proposed protocol needed some modification in order to obtain a higher purification efficiency.

The implementation of the CryoSoniC method, then, developed into Cryo2SoniC protocol, a procedure easily adaptable to a widespread type of archaeological mortars. This is illustrated in the second section of chapter II, whose object was published in a paper on Nuclear Instrument and Methods in Physics Research B (2013). Analysed samples come from different archaeological sites, from different geographical regions and characterized by different mortar production technologies. All measured radiocarbon ages were compared with their chronological reference allowing accuracy evaluation. Radiocarbon dating was performed on the selected fractions using high-precision (i.e. 0.3% precision) Accelerator Mass Spectrometry (AMS). Results obtained from real historical mortars are discussed and compared with independently estimated chronologies (i.e. radiocarbon dating performed on organic materials such as charcoals, found in the same study site, archaeological references and sometimes also with previous measures performed by other laboratories with other techniques) in order to have a basis for comparison and to give an interpretation of results with a multidisciplinary approach.

Of course during the testing of the procedure over a big number of samples, even of pozzolanic type (subject of a specific section), this protocol did not give back reliable dating in the totality of cases. Differences between analyzed samples were fundamental to cover the most common typologies of mortars potentially present in any archaeological context. Cryo2SoniC drawbacks occurring during the experimentation are discussed in a dedicated section, in order to explain what should be avoided to obtain a correct dating and why some inconveniences happened. It has been found that drawbacks are mainly represented by mortars with fine calcareous aggregates and mortar sampled from a buried environment, which hence experienced groundwater activity, but there are also some particular cases like the mortars hardened in a fossil atmosphere; all these occurrences have been endorsed by applications to real cases.

A specific section has been devoted to a deeper investigation developed on the collected fractions useful for dating and to an additional and precious resource represented by lime lumps. In this work their indispensability when it is not possible to date the bulk mortars, that is to say when Cryo2SoniC does not reach the required selectivity avoiding errors, has been proved. Adding a further tool to obtain a right dating by lime lumps, usually dated as the same.

To better understand radiocarbon results and to guide the choice of the most appropriate treatment for each case, characterizations of mortars were supported by mineralogical-petrographic investigations, such as the observation of thin sections with Optical Microscope (TSOM), scanning electron microscopy (SEM) and X-ray diffraction (XRD) on powders. Petrographic analysis under polarizing light microscopy has been used to identify different mineralogical phases of mortar samples, aggregate nature, and the limestone fragment remains. It also provided the identification of possible features of mortar degradation (organic and inorganic) and, therefore, allowed the selection of a suitable sample for radiocarbon dating. Further detailed microscopic analyses have been carried out by SEM, which allowed to identify contaminant error sources of mortar at small scale.

A further section in the first methodological chapter is focused on the checks performed on selected fractions collected using the separation protocol which wants to prove the Cryo2SoniC capability to isolate only the fraction representative of the binder produced at the setting moment. The check used were: SEM analysis to verify particles minimum size and morphology, CL to recognize eventual traces of geological calcite and FTIR to prove that the main calcite component has an anthropological origin. The section aim is, through the use of different analytical techniques, to define the efficiency of Cryo2SoniC as separation method and to explain why it worked or not, and at the same time to develop a diagnostic tool able to: i) gather information about observed pitfalls of the methodology; ii) preliminarily predict the quality of CryoSoniC isolated fractions.

As last section of the methodological chapter, a comparison of efficiency between the Cryo2SoniC and other methods performed by the Poznan Laboratory based on stepped digestion is reported. The efficiency evaluation consists on comparison of final RC ages performed on same sample series, using the two different pretreatment protocols, with the expected chronological reference.

Once defined all potentialities and limitations of Cryo2SoniC, this work wants to highlight how a simple selection protocol can be useful in the archaeometric field and can be used as a precious tool to solve some unraveled archaeological questions. The importance of studying buildings and in particular mortar structures, that represents a class of founding material almost ubiquitous in archaeological sites, is acknowledged. Finding a method capable to give back the right information about the age of a construction means to hold a precious tool to investigate even inside to most spoiled places reconstructing part of their history.

In the third chapter some cases of real study are reported, where Cryo2SoniC pretreatment has been utilized as a tool to solve some archaeological questions about construction sequences or more generally about the need to confirm chronological attributions. Mortars from different geographical and chronological realities were dated using radiocarbon technology. Applications have been done on different kinds of mortar, from different geographical and chronological sites, made of several materials, from calcareous to pozzolanic aggregates. Among them, in the first section of this applicative chapter the case of Castle of Shayzar in Jordan, object of a publication on Radiocarbon Journal, is illustrated. Several other italian important historical and archeological sites, such as the ancient Circus Maximum and Palazzo Valentini in Rome, the famous Palazzo Vecchio in Florence or the hidden archaeological complex of Canosa di Puglia in the South of Italy, are then included in this section.

This excursus on Cryo2SoniC research wants to prove the reliability of this simple procedure despite diffusion of other more complicated separation methods and then propose it like one of the most useful tools in the field of archaeological research. The use of an absolute dating method – like the radiocarbon one – as an investigative resource could place side by side unknown realities with unclear ones. Final balance of this research is the reliability and efficiency of the Cryo2SoniC method on a widespread spectra of mortar typologies, highlighting its weak points and suggesting alternative solutions such as the purification of lime lumps incased in mortars.

## **Acknowledgments**

Before starting I want to say thank you to all who made possible completing this research.

To prof. Filippo Terrasi and dott. Fabio Marzaioli (Second University of Naples ) who helped me and guide me for years to obtain best results into radiocarbon measures, taught me how to live inside a radiocarbon laboratory and gave me possibility to use all their facilities at CIRCE lab.

To dott. Silvano Mignardi (University of Rome Sapienza) who followed me during this PhD experience with patience and kindness, helping me to make possible important experiences.

To prof. Gilberto Artioli (University of Padoa) who allowed me to use his laboratories at Geosciences Department and gave his contribute to redact this work.

To prof. Elisabetta Boaretto (Weizmann Institute of Science, Israel) who help me with her precious suggestions.

To dott. Michele Secco e dott. Anna Addis (University of Padoa) who supported me and gave me their practical help, collaborating and performing some petrographical and catholodumilicent analysis. And further, they provided me with many interesting mortar samples to analyze (Castles of Forni and Pra di Got).

To dott. Giacomo Eramo (University of Bari Aldo Moro) who supported me, helping with his collaboration and providing to me some samples coming from archaeological areas of Siponto and Canosa di Puglia, from Manfredonia Square Tower and San Leonardo Abbey and performed on the same samples some accurate petrographic analyses.

To prof. Juan Carlos Quiros Castillo (University of the Basque Country, Spain) who collaborated to my research and led to it same of his samples coming from archaeological sites of Zornotzegi, Aistra and Trevino sited at the north of Spain.

To prof. Stefano Lugli (University of Modena and Reggio Emilia) to gave me opportunity to use the experimental equipments above his department and showed to believe in this project. To his student, dott. Marta Caroselli, to gave me all her practical and psychological support during these last months, for having lightened with her positivity and joy of living some difficult moments and for having discovered in her a precious friend.

To prof. Stefano Gialanella and dott. Angela Berloffia (University of Trento) to have made possible the implementation of an idea laying the groundwork for a challenge, developed by shots of FTIR.

To prof. Danuta Michalska (University of Poznan Adam Mickiewicz, Poland) and dott. Justina Czernik (Poznan Radiocarbon Laboratory, Poland) to have given their help to the setting of the



method through the lending of many samples coming from Jericho, Qumran and Krakow already dated and analysed. The comparing of our methods puts the basis to continue our collaboration.

To dott. Paola Baldassarri and dott. Roberto Del Signore (Province of Rome, Archaeological Sector) for allowing me to sampling inside the Archaeological Site of Domus Romanae at Palazzo Valentini, performing research on them and diffusing the relative information. To dott. Mariapia Sammartino (University of Rome Sapienza) to have made possible this important collaboration.

To prof. Gino Crisci, dott. Alessandra Pecci and dott. Domenica Miriello (University of Calabria) who provided samples from Palazzo Vecchio and some petrographic analyses on them. Thanks also to the Superintendence of Archaeological Heritage of Tuscany Region, which allowed to perform analyses on cited material.

To dott. Franco Fratini (ICVBC-CNR, Sesto Fiorentino) who kindly gave me the opportunity to work on particular samples coming from the ancient Ponte di Augusto at Narni, previously studied by him and his colleagues and who supported me and my work with precious suggestions and encouragements, believing in this project.

To dott. Cristina Tonghini (University of Venice Ca'Foscari) and all people involved into Shayzar Project who allowed to apply this new experience on samples of mortar coming from the medieval ruins of Shayzar Citadel (Syria).

To the Archaeological Superintendence of Pompei which allow us to sampling some mortar samples inside the Caste Lovers and Painters at Work Houses in order to perform on them our experiments.

To the Archaeological Superintendence of Rome, together with dott. Maria Erzilia Loreti and dott. Marialuisa Buonfiglio who allowed to sampled mortars from archaeological sites of Torre del Fiscale and Circo Massimo in Rome, necessary for testing the protocol on pozzolanic materials.

To dott. Salvo Barrano who allowed the sampling of mortar to date, inside the Minerva Medica Temple. To prof. Laura Sadori who made possible this collaboration.

To dott. Marcello Turci (University of Bologna Mater Studiorum) and his team of archaeologists, to dott. Andrea Macchia and to the student Andrea Morricone (University of Rome Sapienza) to allow the sampling of some mortars from the archaeological excavation of Porta Marina, useful to improve the protocol setting.

To prof. Adriana Maras who has manage our PhD course with activeness and dedication.

To SEM and XRD technicians of Sapienza (Marco Albano and Stefano Stellino) for their help.

To CIRCE team, all boys and girls, who have gone along with me through this long experience and with who I spent many sweet moments (Egidio, Isabella, Simona, Annalisa, Luisa, Carmina,

Carmine, Manuela, Giuseppe, Lucio, Paola, Antonino, Mario, Nicola and all the other guys met during these last years).

To guys of 'auletta' for having shared with me birthdays, Christmast, degrees, lunch parties and the hard work to be a student of Sapienza.

To all my roommates changed during these years, especially to Eluisa who made my stays in Caserta full of laughs and affection.

To my friend Laura because with her every tragedy turned out into a comedy, and because without her and her company maybe I should never arrived where I am now.

To all my dear friends because made me smile and there were always when I needed of them (Sara, Claudia and go on - sorry but you're too much for this page).

To my family, dad, mum and sisters who believe in me and support all my new adventures.

To mine Gnammy and Attila who gave me their love without any needs of words, expecially when I was down.

To my love, because he has believed in me more than I have could never do, patiently has stood to these final crazy days making me learn that a positive think is the first step to have a happy life.

# I – Introduction

## I.1. Mortar Dating

Lime and Pozzolana mortars are characterized by a long and complex development independently begun in many parts of the globe, a history involving domestic architecture, religious and funerary rituals, early painting and sculpture, stimulating further experiments in pyro-technology that led to pottery, metal and glass. Lime plaster technology developed in many parts of the world, in the time frame between the Aegean Bronze Age (Zouridiakis et al. 1987; Maravelaki et al. 2003) and the 2<sup>nd</sup> century BC in Indonesia (Deloye 1996), but first records indicate that mortars were born in Anatolia and neighboring areas of the Near East. Though long neglected, the study of lime mortars is at last taking its rightful place as an essential component of scientific investigation into the past (Hale 2011). Mortar is commonly understood to be a cementitious material used to link different bricks or building stones. Mortar matrix can be schematically divided in two portions: the binder and the aggregates. The binder represents the most important component of mortars which, if worked with water, forms a easily workable mass capable of hardening in air to form a unique hard structure, comprising the aggregates, capable to resist to mechanical stresses and atmospheric agents (Gottardi, 1978).

Dating ancient buildings and establishing construction phases represent important issues for archaeologists; unfortunately, we are not always facing structures built with materials capable to be analyzed by means of typological or stylistic methodologies aimed to gather information concerning the period of their implementation (Castillo et al. 2011). Moreover, in many cases buildings have been erected in several construction phases along many centuries and/or have been subjected in the past to restorations and reshaping. Reconstructing the chronology of these events may often shed new light on the history of the region they insist on.

To determine the age of buildings, building archaeology has adopted, in recent years, a large volume of analytical tools (Mannoni 1984), but in absence of instrumental methods to determine absolute age, the only option is to rely on historical dates and archaeological markers, which often require the presence of artifacts to be used as “guide fossils” (Hale et al 2003). Currently, absolute chronology of archaeological sites is mostly based on the radiocarbon dating of organic materials uncovered during the excavations, but with many uncertainties related to the history of the analyzed sample and its precise relationship with the building construction time. Absolute dating of a building, without the necessity to appeal to organic materials found at the study site, represents a great advantage to the study of an archaeological site and a sensitive improvement for the historical reconstructions in general.

Mortars naturally record the act of building and the opportunity to apply the  $^{14}\text{C}$  dating tool to this class of materials constitutes a possible breakthrough point in the actual knowledge because:

- they represent a class of materials virtually ubiquitous at archaeological sites, from the Neolithic period on (Rech 2004).
- organic materials and any other object found in the context of the examined structures (e.g. coins and/or ceramics), could be affected by age biases with respect to the building due to their history (i.e. reusage).
- mortars, by absorbing atmospheric  $\text{CO}_2$  during setting, record exactly the time of development of the building.

It is well-known that all building materials based on lime – mortar, concrete, plaster, whitewash – adsorb atmospheric carbon dioxide as they harden. In this way, if the hardening time is negligible with respect to the structure development,  $^{14}\text{C}$  is fixed in all these lime-derived materials at the exact time of construction. From the setting moment  $^{14}\text{C}$  begins decaying, similarly to the organic remains of any plant or animal immediately after its death. Thus if  $^{14}\text{C}$  analysis could be applied to mortar, the radiocarbon tool could be applied in order to estimate the time when the building came into existence (Hale et al. 2003). The principle is simple enough, but its application proved surprisingly difficult as shown by its unclear results over more than 50 years of experimentations.

## I.2. Mortar production

To better understand this issue it is important to briefly describe mortar production technology. Mortar production process begins with the burning of a limestone at temperatures ranging around 800-900 °C by means of traditional lime kilns (Moropoulou et al. 2001) according to the reaction:



This reaction, better known as *calcination*, removes C of fossil origin from the initial (primary) carbonate, producing quicklime (calcium oxide). Quicklime is then watered, undergoing hydration, hence producing slaked lime (calcium hydroxide) according to the reaction:



Slaked lime production is an exothermic reaction and the produced  $\text{Ca(OH)}_2$  crystals (portlandite) are aged under water excess in the form of lime putty. Vitruvius (De Architectura, Book VII) and Plinius (Naturalis Historia, Book V) documented how, according to Roman habits, lime putty was aged for almost 3 years before its usage. During this period, portlandite crystals are rearranged becoming smaller and foil-like (Rodriguez-Navarro et al. 1998), enhancing their future  $\text{CO}_2$  absorption capability. Aged lime putty is mixed, in a variable ratio, with aggregates (e.g., reworked bricks, silica minerals, marble powder, volcanic pyroclastic materials) to increase workability,

hydration and to avoid cracks due to drying during setting (Cazalla et al. 2000, Lawrence et al. 2003). Calcium hydroxide absorbs atmospheric  $\text{CO}_2$  producing calcium carbonate ( $\text{CaCO}_3$ ) according to the reaction:



Slaked lime absorbs  $\text{CO}_2$  from the air over time periods of a few years forming a secondary anthropogenic carbonate. If the burning of the primary carbonate is efficient and no carbonate aggregates are utilized, C composing mortars is ascribable only to the atmospheric  $\text{CO}_2$  (Marzaioli 2011). Problems may arise when other carbonate phases such as aggregates or exogenous carbonates interfere, affecting the signature of the system, with the accurate dating so that it becomes hard isolating and dating the binder C from such a complex matrix.

Summarizing, the main sources of C potentially contributing to a biasing in the final measurement are:

- i) primary carbonates residues (calcinations relics) originating from the incomplete burning of the limestone during the quicklime production process. They lead to an ageing effect producing sensitive age overestimation in the radiocarbon age;
- ii) carbonaceous aggregates used as inert materials during the mortar production phases, again, ageing the mortar dating;
- iii) neo-genesis carbonates precipitated after the interaction of current water or rain, containing variable aliquots of dissolved inorganic carbon (DIC), with the structure for centuries, inducing an overall rejuvenation effect, or ageing if circulating water is from groundwater.



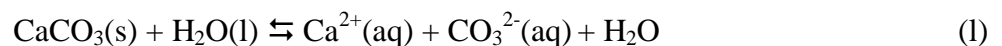
Figure 1. The  $\text{CaCO}_3$  cycle from limestone to binder calcite presented schematically (Hale et al.2003).

The limitations of radiocarbon dating of lime based materials are attributed to contamination of samples from all these carbonaceous substances. Carbonate rocks are in fact mainly made of calcium carbonate that, at the beginning of the sedimentary process, mirrored the carbon isotopes contained in the Earth atmosphere at the time of the precipitation. However, in contrast to the

carbon contained in the lime mixtures of archaeological interest, which have an age comparable with the radiocarbon radioactivity half-life, calcium carbonate of geological origins may be considered completely free of  $^{14}\text{C}$ . This means that each C atom contained in carbonate rocks is " $^{14}\text{C}$ -dead". More in detail, this implies that any molecule of carbonate rock that may contaminate a hardened lime such as grains of carbonate sand added or pieces of under-burned limestone, can sensitively affect the result of radiocarbon dating with a heavy ageing.

The presence of aggregates or pieces of stones would not be a problem if a methodology to remove such phases from the binder in lime mixtures would exist. Actually, even if under the microscope it is possible to distinguish binder (lime) and aggregate (sand), from a practical point of view, it is almost impossible to physically separate all the aggregate from the binder when both are made of carbonates. One has to take into account that even a very small amount of contaminant C can severely affect the measured  $^{14}\text{C}/^{12}\text{C}$  isotopic ratio if its age is very different with respect to that of the bulk.

Lime contained in building materials can be also affected by a dissolution and re-precipitation process of calcium carbonate that can lead to an exchange of carbon atoms hence affecting accurate dating. Typical water sources potentially affecting archaeological and building sites such as rain (mainly for renders), backwater, rising damp (for plasters, renders, and mortars) and going back groundwater, can lead to the dissolution of calcium carbonate. Calcium carbonate has a specific solubility in water and, consequently, binder contained in the mixtures can dissolve in very wet environments such as foundations and underground floors. Binder dissolution in old lime based mixtures can be described as follows:



Once in solution, calcium ions can react with carbonate ions to produce new calcium carbonate crystals. However, in this case the carbonate ion population dissolved in solution is made of both ions from the carbonate dissolution and ions from the atmospheric carbon dioxide, with this latter representing the majority. But carbon concentration in the atmosphere at the dissolution time of the lime may differ from the radiocarbon concentration at the hardening time of the original lime. For this reason, the radiocarbon dating of a lime sample containing even a small amount of re-precipitated calcium carbonate can be affected by errors due to the radiocarbon contents of the newly added calcium carbonate phases (Pesce & Ball 2012).

Hence, accurate dating of aerial mortars can be prosecuted by developing chemical or physical methodologies capable to prevent, by isolation, the dating of other carbonate sources different from the anthropogenic.

### I.3. Datable fraction isolation

Since the 1960s, mortars have been exploited as a potential material for  $^{14}\text{C}$  dating (Delibrias and Labeyrie 1964), and despite the fact that this methodology appears very simple in its principles, some measured  $^{14}\text{C}$  ages showed evident biases with respect to the expected historic ages (e.g., Stuiver and Smith 1965; Baxter and Walton 1970; Van Strydonck et al. 1986, 1992; Ambers 1987; Heinemeier et al. 1997, 2010; Mathews 2001; Hale et al. 2003; Nawrocka et al. 2005, 2009; Lindroos et al. 2007).

Therefore, in order to eliminate observed biasing sources, sample preparation procedures have been implemented since the beginning of the mortar radiometric dating method (Delibrias and Libeyrie 1964). Most of the preparation procedures applied during the last decades consist of a combination of mechanical and chemical treatments (Folk and Valastro 1976; Cherf 1984; Van Strydonck et al. 1986, 1992; Heinemeier et al. 1997; Sonninen and Jungner 2001; Lindroos et al. 2007; Nawrocka et al. 2007, 2009; Goslar et al. 2009; Al-Bashaireh 2013). The most common approaches involve the isolation of the binder atmospheric  $^{14}\text{C}$  signal by means of stepped acid digestion based on the evidence that binder carbonates react faster (i.e. higher solubility in acids) than limestone residuals. To our knowledge, the unique alternative to this methodology is based on the attempt to physically separate the binder carbonates by a combined mechanical/physical procedure (Folk and Valastro 1976; Heinemeier et al. 1997; Nawrocka et al. 2005; Ortega et al. 2012) based on the laboratory isolation of binder calcite. This thesis main objective is the development, testing and application of a procedure based on a series of physical separations capable to produce mortar accurate  $^{14}\text{C}$  dating. The development of the methodology is mostly based on AMS  $^{14}\text{C}$  measurements but is also supported by a series of diagnostic analyses allowing to preliminary characterize analyzed mortar samples. Moreover, 1) aiming to infer independent clues of  $^{14}\text{C}$  dating failure and 2) to develop a bouquet of preliminary analyses indicating the efficiency of isolation of the applied procedure, FTIR, CL and particle morphology inferred by SEM images were performed.

AMS results will represent the main part of the research and for this reason it is useful to explain how raw data are shown and why. Dates may be expressed as either uncalibrated or calibrated years (the latter abbreviated as cal). An uncalibrated radiocarbon date is abbreviated as  $^{14}\text{C}$  yr BP or simply BP (before present, where present is 1950 AD), although the last is also sometimes ambiguously used with dating methods other than radiocarbon, such as stratigraphy. A raw RC date cannot be used directly as a calendar date, because the level of atmospheric  $^{14}\text{C}$  has not been strictly constant during the span of time that can be radiocarbon dated, producing radiocarbon plateaus and wiggles. The level is affected by variations in the cosmic ray intensity, which is, in turn, affected by

variations in the Earth's magnetosphere (Kudela and Bobik 2004). In addition, there are substantial reservoirs of carbon in organic matter, the ocean, ocean sediments (see methane hydrate), and sedimentary rocks. Changes in the Earth's climate can affect the carbon flows between these reservoirs and the atmosphere, leading to changes in the atmosphere's  $^{14}\text{C}$  fraction. The uncalibrated, raw RC date underestimates the actual age by 3000 years at 15000 BP. The underestimation generally runs about 10% to 20%, with 3% of that underestimation attributable to the use of 5568 years as the half-life of  $^{14}\text{C}$  instead of the more accurate 5730 years. To maintain consistency with a large body of published research, the out-of-date half-life figure is still used in all radiocarbon measurements (Radiocarbon Calibration University of Oxford, Radiocarbon Web Info, Version 143 Issued 31/10/2013). The standard radiocarbon calibration curve is continuously being refined on the basis of new data gathered from tree rings, coral, and other studies.

In addition to the natural variation of the curve throughout time, the carbon-14 level has also been affected by human activities in recent centuries. From the beginning of the industrial revolution in the 18<sup>th</sup> century to the 1950s, the fractional level of  $^{14}\text{C}$  decreased because of the admixture of  $\text{CO}_2$  into the atmosphere from the combustion of fossil fuels. This decline, which is known as the Suess effect, also affects the  $^{13}\text{C}$  isotope. Moreover, atmospheric  $^{14}\text{C}$  was almost doubled during the 1950s and 1960s, due to atmospheric atomic bomb tests (Reimer et al. 2004). The raw radiocarbon dates, in BP years, are calibrated to give calendar dates. Standard calibration curves are available, based on comparison of radiocarbon dates of samples that can be dated independently by other methods such as examination of tree growth rings (dendrochronology), deep ocean sediment cores, lake sediment varves, coral samples, and speleothems (cave deposits). In late 2009, the journal *Radiocarbon* announced agreement on the INTCAL09 standard, which extends a more accurate calibration curve to 50,000 years (Reimer et al. 2009). Marine reservoir variations can be partly handled by a special marine calibration curve (Stuiver and Branzionas 1993).

There are two main methods used for calculating age ranges from the calibration curve. The first method to be employed was called the 'intercept method' because it can be done by drawing intercepts on a graph. This method will tell you the years in which the radiocarbon concentration of tree rings is within two standard deviations of your measurement (e.g. between 2940 BP and 3060 BP for the measurement  $3000 \pm 30$  BP). A slightly different method is now more often used which is called the 'probability method'. This requires a computer since the calculations are more complicated. It gives the time range, in which you can be 95% confident that the true value lies. An RC age, calibrated with a margin of error of  $1\sigma$  means to have a 68,3% probability that a measurement repetition gives a mean values plus or minus once the error. A margin of error of  $2\sigma$  means to have a probability of 95,4% if a measurement repetition gives back a mean values plus or



minus twice the error. The calibration will show not a whole interval but a series of time intervals equipped with relative probability intervals. A margin of error of  $2\sigma$  gives a higher reliability degree but wider chronological uncertainty. Once calibrated a radiocarbon date should be expressed in terms of cal BC, cal AD or cal BP. The cal prefix indicates that the dates are the result of radiocarbon calibration using tree ring data. These values should correspond exactly to normal historical years BC and AD. In academic practice calibrated dates are generally presented along with their source uncalibrated dates, as the accuracy of the presently established calibration curve varies by time period.

In the next chapters we will present the datable-fraction-isolation procedure based on the development of a previously applied mechanical/physical procedure (Nawrocka et al. 2005) allowing  $^{14}\text{C}$  dating of mortars. It developed in a collaboration between the Centre for Isotopic Research on Cultural and Environmental Heritage (CIRCE) and Department of Earth Sciences of Sapienza University of Rome. The procedure, described by Marzaioli et al. (2011), was successfully applied to lime lumps under the name of CryoSoniC, and after implementation to Cryo2SoniC. It was applied to real mortars too, leading both to accurate results (Marzaioli et al. 2013; Nonni et al. 2013). The main advantages of the Cryo2SoniC methodology are 1) the complete digestion of the laboratory isolated mortar fraction, avoiding difficulties in handling time-evolved fractions, and 2) the limited number of analyses per mortar to be performed: one for each sample after methodology accuracy evaluation. Further analysis has been performed on Cryo2SoniC produced fractions of calcite in order to independently evaluate their appropriateness for dating. In other words they were analyzed to check some evidences which could explain eventual biases observed on radiocarbon age. This check has been done on selected powder fractions with InfraRed Fourier Transformed Spectroscopy (FTIR), ChatodoLuminescence (CL) analysis and imaging capture with Scanning Electron Microscopy (SEM).

## **II- Implementation and validation of a novel methodology**

### **II.1. Testing CryoSonic Protocol**

Tests on simplified mortars are based on the initial assumption that while secondary carbonate contaminations can be suppressed by choosing the correct location of the sample (i.e. not directly exposed to the atmospheric layer but not completely isolated from the atmospheric CO<sub>2</sub>). It's known that the presence of primary carbonates contaminations represents the main cause of the observed accuracy instability (Van Strydonck et al. 1986). In the first phase of the present work, synthetic mortar samples were produced following the details described by the ancient process of production of mortar. Knowing the isotope signature of laboratory CO<sub>2</sub> air and the absence of any other contaminants source (ie. lack of added aggregates), with the exception of unburned limestone residues, made it possible the check of the suppression efficiency in DC residues comparing RC ages of CryoSonic isolated fractions from synthetic mortars with laboratory air CO<sub>2</sub> signature.

All experimental activity is explained in detail inside the published paper "Mortar Radiocarbon Dating: Preliminary Accuracy Evaluation of a Novel Methodology", of Analytical Chemistry (2011) journal attached as annex to this section.

## II.1.1. Mortar Radiocarbon Dating: Preliminary Accuracy Evaluation of a Novel Methodology.

### Mortar Radiocarbon Dating: Preliminary Accuracy Evaluation of a Novel Methodology

Fabio Marzaioli,<sup>\*,†</sup> Carmine Lubritto,<sup>†</sup> Sara Nonni,<sup>‡</sup> Isabella Passariello,<sup>†</sup> Manuela Capano,<sup>§</sup> and Filippo Terrasi<sup>†</sup>

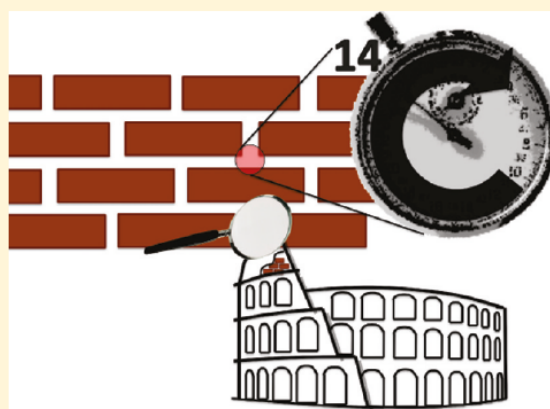
<sup>†</sup>INNOVA, Centre for Isotopic Research on Cultural and Environmental Heritage and Dipartimento di Scienze Ambientali, Seconda Università degli Studi di Napoli, Caserta, Italy

<sup>‡</sup>Centro di Ricerca per le Scienze Applicate all'Ambiente e ai Beni Culturali, Università la "Sapienza" Roma, Roma, Italy

<sup>§</sup>INNOVA, Centre for Isotopic Research on Cultural and Environmental Heritage and Dipartimento di Studio delle Componenti Culturali del Territorio, Seconda Università degli Studi di Napoli, Santa Maria Capua Vetere, Caserta, Italy

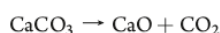
#### Supporting Information

**ABSTRACT:** Mortars represent a class of building and art materials that are widespread at archeological sites from the Neolithic period on. After about 50 years of experimentation, the possibility to evaluate their absolute chronology by means of radiocarbon ( $^{14}\text{C}$ ) remains still uncertain. With the use of a simplified mortar production process in the laboratory environment, this study shows the overall feasibility of a novel physical pretreatment for the isolation of the atmospheric  $^{14}\text{CO}_2$  (i.e., binder) signal absorbed by the mortars during their setting. This methodology is based on the assumption that an ultrasonic attack in liquid phase isolates a suspension of binder carbonates from bulk mortars. Isotopic ( $^{13}\text{C}$  and  $^{14}\text{C}$ ), % C, X-ray diffractometry (XRD), and scanning electron microscopy (SEM) analyses were performed to characterize the proposed methodology. The applied protocol allows suppression of the fossil carbon (C) contamination originating from the incomplete burning of the limestone during the quick lime production, providing unbiased dating for "laboratory" mortars produced operating at historically adopted burning temperatures.

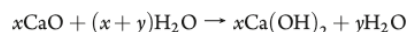


To date, radiocarbon chronology of archeological sites is mostly based on the dating of organic materials found at the study site. Hence, significant gaps may be introduced between  $^{14}\text{C}$  dates and the real age of the site or the studied event.<sup>1</sup> Using mortars (MOs) to evaluate the age of artifacts represents a sensitive improvement in radiocarbon dating methodology of archeological events. Mortars and plasters were extensively used to construct floors, walls, roads, aqueducts, and even to create art. As a result, these materials are virtually ubiquitous at archeological excavations since 7000 B.C.<sup>2</sup> They also represent a valid tool to assess the chronology of artifacts when they were found on bedrocks or lie on different strata or can be used as a survey tool to preliminarily evaluate the opportunity to proceed with excavations if the site matches its supposed age.<sup>3</sup>

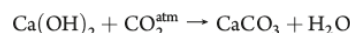
Aerial mortars were, historically, produced by a sequential production phase: (i) limestone (LS) was burnt in high temperature (800–1000 °C) furnaces to produce calcium oxide (quick lime) in the calcination process:



(ii) quick lime (QL) was slaked in water to produce calcium hydroxide (slaked lime) and preserved under water excess ( $y$ ) forming a lime putty:<sup>4</sup>



(iii) slaked lime (SL), mixed with inert materials, was used undergoing hardening because of the absorption of atmospheric  $\text{CO}_2$ <sup>5</sup> and loss of water:



In principle the unique source of carbon present in the mortar is the  $\text{CO}_2$  absorbed during the manufacture of the building. Hence, dating of MOs can be performed because  $\text{CO}_2$  absorption records the time of mortar setting and this latter is negligible

Received: October 28, 2010

Accepted: January 21, 2011

Published: February 21, 2011

with respect to  $^{14}\text{C}$  half-life ( $5730 \pm 40$  years<sup>6</sup>). Unfortunately the presence of different contamination sources can lead to contradictory results.<sup>5,7–10</sup> Several studies identify the inefficient suppression of the contamination originating from the original carbonate residues surviving the burning of the LS one of the main reasons for the systematic errors in mortar dating methodology.<sup>5,7,9–11</sup>

A large effort has been devoted by the scientific community to find a reliable  $^{14}\text{C}$  dating of mortars, and time has been spent in attempting an efficient isolation of the atmospheric  $\text{CO}_2$  signal, preserved in the binder phase of the mortar carbonate, from other carbonaceous sources, whose coexistence in the mortar matrix leads to a significant aging effect on the measured ages. The current state of the art approaches point to the binder signal isolation mainly by means of a partial acid attack. This methodology, proposed first by Delibrias and Labeyrie,<sup>7</sup> is based on the evidence of a different reaction rate for the carbonates as a function of their diagenesis (i.e., binder carbonates react faster than limestone lumps<sup>7,9,12</sup>) and widely applied leading to a series of contradictory results.<sup>1,3,5,7–9</sup> Partial acid attack was recently reviewed suggesting the isolation of a series of  $\text{CO}_2$  partly digested fractions reflecting the isotopic signal absorbed during their diagenesis.<sup>13</sup> To our knowledge, the unique alternative to this methodology is based on the attempt to separate the binder carbonates by a combined mechanical/physical procedure<sup>5,11,14</sup> based on the laboratory isolation of calcite crystals produced as the consequence of atmospheric  $\text{CO}_2$  absorption.

An important aspect regarding the protocol validation for mortar dating is the characterization of their stable isotopes ratios.<sup>10,15</sup> Van Strydonck et al.<sup>10</sup> and Nawrocka et al.,<sup>11</sup> in both procedures (i.e., chemical and physical/mechanical), suggest a stable isotope  $^{13}\text{C}$ -back correction (see section 1 of the Supporting Information for details) for the measured ages attempting to suppress the effects of dead C contamination. This procedure is based on the main assumption of the absence of C isotopic discrimination (fractionation) along mortar processing. To our knowledge, most of the studies analyzing this process use the isotopic fractionation experienced by atmospheric  $\text{CO}_2$  during the absorption to characterize the mortar setting. Pachiardi et al.<sup>15</sup> as well as Kosednar-Legenstein et al.<sup>16</sup> found a measurable fractionation effect during this phenomenon. This effect was interpreted as an overall Rayleigh type distillation process.<sup>17</sup>

In order to (i) maintain the concept of the isolation of a fraction from the mortar preserving the isotopic signature of the atmospheric  $\text{CO}_2$  and (ii) allow a reliable dating without performing partial acid digestions and several radiocarbon measurements of complex interpretation, we decided to investigate a modified mechanical/physical procedure for mortar radiocarbon dating.

To avoid combined effects, we performed an accuracy evaluation of the proposed methodology on a simplified version of mortars, influenced by only one (i.e., unburnt LS C, ref 10) of the supposed sources of uncertainty affecting accurate chronology reconstructions by means of mortars. In order to preliminarily evaluate the accuracy of the procedure in dead C suppression and to characterize the entire process, in this paper we simulated a simplified mortar production protocol (i.e., no aggregates were added to the mortar) in the laboratory environment. This test allowed

us to primarily verify the agreement of the isolated binder signal ( $^{13}\text{C}$  and  $^{14}\text{C}$ ) with the measured atmospheric one and, secondarily, to better characterize the mortar production process with a specific emphasis on verified isotopic fractionations.

## EXPERIMENTAL SECTION

**Synthetic Mortar Production.** Laboratory synthetic mortar production simulates the original mortar sequential production phases with the exception of the addition of inert materials. During our simulation, we also tested the influence of different temperatures on the quick lime manufacturing. In detail, a carbonaceous rock of about 30 kg mass was chosen to synthesize the laboratory mortar. Scraps ( $n = 3$ , randomly sampled from LS) were powdered by means of a rotary tool and used for the characterization of the initial matrix in terms of % C, mineralogy (i.e., XRD),  $^{13}\text{C}$  and  $^{14}\text{C}$ .

With the aim to simulate the quick lime production phase, six different (not pulverized) LS fragments of approximately 15 g underwent burning in a muffle furnace capable of reaching up to 1100 °C. In detail, each of the original 6 samples was burnt for 1 h at 700, 800, 900, 1000, and 1100 °C and for 1.5 h at 700 °C. The muffle thermal cycle was controlled by means of a temperature controller allowing the oven to reach the set temperature in approximately 1 h, maintaining it for the programmed time (e.g., 1 h), and switching off the oven when the set time elapsed. Produced QLs (QL 700, QL 800, QL 900, QL 1000, QL 1100, QL 700\_1.5) were subsequently pulverized and underwent % C,  $^{13}\text{C}$ , and  $^{14}\text{C}$  analyses.

A stoichiometric excess of deionized water was added to the pulverized quicklimes (about 4 g) in beakers to simulate the slaked lime product phase. With the aim to increase the yield of the reaction over the experimental periods and simulate an aging of the  $\text{Ca}(\text{OH})_2$  crystals, the beakers were ultrasonically treated for 60 min. It is well documented how excess water as well as low temperatures increase the dissolution of  $\text{CO}_2$  in the aqueous strong alkaline environment leading to a general speeding up of the  $\text{CO}_2$  absorption process (carbonatation) by the slaked lime.<sup>16,18</sup> For 3 weeks, samples were kept at 4–6 °C to increase the  $\text{CO}_2$  dissolution process and for 2 successive weeks at 25 °C to facilitate mortar carbonate hardening in a temperature controlled environment. The produced MOs (MO 700, MO 700\_1.5, MO 800, MO 900, MO 1000, MO 1100), after pulverization, underwent % C,  $^{13}\text{C}$ , and  $^{14}\text{C}$  analyses, and MO 700 and MO 900 were analyzed by SEM.

**Laboratory  $\text{CO}_2$  Air Sampling.** During the whole carbonatation phase (5 weeks), two spot samples of laboratory air  $\text{CO}_2$  (1st and 4th week) were sampled to have an isotopic reference to be compared to our mortar binder signal.  $\text{CO}_2$  was purified by other atmospheric gases, according to Bertolini et al.,<sup>19</sup> by means of a dynamic cryogenic system, capable of isolating  $\text{CO}_2$  from other air gases with no observed fractionation.

**Isolation of the Atmospheric  $\text{CO}_2$  Signal from the Mortar Carbonate.** Our protocol is based on a modification of the procedure described by Nawrocka et al.<sup>11</sup> It is based on the assumption that binder carbonates are characterized by an easily breakable aggregation structure (i.e., by means of ultrasonication attacks). Our working hypothesis is that this step operates the binder signal isolation from the unburnt LS

residuals by breaking the binder minerals and originating a suspension of carbonates characterized by a slower sedimentation velocity ( $v_{\text{sed}}$ ) because of their smaller average diameter ( $d_p$ ).<sup>20</sup>

In details, (i) bulk mortar breaking: bulk mortars (5–10 g) were submerged in liquid nitrogen for about 5 min and rapidly moved into an oven at 80 °C. After at least three cycles, raw materials were crushed by means of gentle hammering. (ii) Suspension production: thermally broken materials, still containing the binder and the LS residues, underwent ultrasonication in an excess of deionized/decarbonated water for 30 min in a beaker generating a suspension (SU) of binder. (iii) Suspension isolation: the liquid phase of the produced suspension was gently siphoned in 50 mL Falcon centrifuge tubes and centrifuged for 5 min at 8.5 krpm to separate the suspension from the water medium. The water filling the tubes was gently removed, and the SU fraction was dried overnight at 70 °C. The protocol isolated suspensions (SU 700, SU 700\_1.5, SU 800, SU 900, SU 1000, and SU 1100) underwent <sup>13</sup>C and <sup>14</sup>C analyses, and SU 700 and SU 900 were analyzed with SEM.

**% C Measurements.** % C determinations were performed by means of a Thermo 1112 Flash elemental analyzer. Samples were weighed ( $n = 3$ ) in tin cups. Empty tin cups and calibration and check standards were run together with unknown samples.

**Isotope Analyses.** <sup>13</sup>C and <sup>14</sup>C analyses were performed by means of a complete orthophosphoric acid (H<sub>3</sub>PO<sub>4</sub>) attack. Ampoules for isotope analyses<sup>23</sup> containing the carbonate materials and a frozen excess of H<sub>3</sub>PO<sub>4</sub> [85%] were evacuated (<10<sup>-3</sup> mbar) and detached from the line after isolation. H<sub>3</sub>PO<sub>4</sub> digestion was developed in an oven (85 °C) for a period of 2 h. Produced gases underwent cryogenic purification by means of a vacuum line<sup>18</sup> to separate evolved CO<sub>2</sub>. Carbon dioxide was split in two subaliquots: (i) for the stable isotope ratio determination and (ii) for the radiocarbon sample pretreatment/measurements.

Stable isotope analyses were performed by means of a Thermo Delta Plus isotope ratio mass spectrometer directly on the CO<sub>2</sub> via dual inlet using a lab tank as reference. In order to correct for eventual procedure induced fractionations, three internationally recognized carbonate reference materials (IAEA C1, C2,<sup>23</sup> and NBS 19) were used for the normalization procedure. <sup>13</sup>C abundances are expressed according to the  $\delta$  notation<sup>24</sup> as permil of excess with respect to the Peedee belemnite (PDB) primary reference material:

$$\delta^{13}\text{C} = \frac{(^{13}\text{C}/^{12}\text{C})_{\text{sample}} - (^{13}\text{C}/^{12}\text{C})_{\text{PDB}}}{(^{13}\text{C}/^{12}\text{C})_{\text{PDB}}} \times 1000$$

Radiocarbon analyses were performed on the graphite developed from the CO<sub>2</sub> following the zinc reduction process.<sup>21</sup> With the aim to check for the entire procedure accuracy, reproducibility, and induced background, IAEA C1 (background), IAEA C2 (normalization), and several check standards were prepared following the same procedure. Graphite samples were measured by means of the CIRCE-AMS system for the measurement of radiocarbon isotopic ratios.<sup>25</sup> For the purposes of this study, we present <sup>14</sup>C data, according to Stuiver and Pollach,<sup>26</sup> in both pMC (percent of modern carbon), mostly used for geochemical

scopes and to express the post 1950s ages, and radiocarbon (R.C.) age.

$$\text{pMC} = \frac{(^{14}\text{C}/^{13}\text{C})_{\text{sample}} \Big|_{-25\text{‰}}}{(^{14}\text{C}/^{13}\text{C})_{\text{OXI}} \Big|_{-19\text{‰}}} \times 100$$

$$^{14}\text{F} = \frac{(^{14}\text{C}/^{13}\text{C})_{\text{sample}} \Big|_{-25\text{‰}}}{(^{14}\text{C}/^{13}\text{C})_{\text{OXI}} \Big|_{-19\text{‰}}}; \quad \text{R.C. age} = -8033 \ln ^{14}\text{F}$$

In both measured isotopic ratios of the sample and the primary standard (OXI) are corrected for isotopic fractionation to a  $\delta^{13}\text{C}$  value of -25 and -19‰, respectively. Moreover, when pMC notation is used, the OXI isotopic ratio is scaled for decay to 1950. In this study, some <sup>14</sup>C measurements are converted in R.C.ages, via calibration, in calendar ages and expressed in A.D. years, reporting B.C. dates as negative A.D. values. Calibration of R.C.ages was performed by means of Calib 6.0<sup>27</sup> software; other radiocarbon data (i.e., <sup>14</sup>F > 1) were directly converted in A.D. ages by means of CALIBomb.<sup>28</sup> All these dates are reported by means of the probability-weighted averages of the medians of the calibrated ranges, while error bars represent 1 and 2 $\sigma$  maximum and minimum ranges.

**Partial Acid Attack.** With the aim to improve the suppression efficiency on the unique dead C contaminated SU samples, we applied a partial acid digestion (SU 700\_PA and SU 700\_1.5\_PA). In our case, by knowing that for the 700 suspensions there was an amount of dead carbon varying between 16 and 25% left (see later and Figure 3), we decided to process 100 g of suspension with the stoichiometric amount of acid necessary to digest only 10% of the C. At the end of the CO<sub>2</sub> purification, the residual liquid phase was checked for the neutral pH.

**XRD/SEM analyses.** About 10 g of material was sampled and grinded to a minimum particle diameter of 270 mesh. The powder was loaded in the tray of a Phillips PW 1800 X-ray diffraction instrument, and the spectra were acquired by means of Co K-alpha radiation.

SEM images were taken at the Surfaces Thin Films and Nano Structures (STN) Laboratory in the Physics Department at the University of L'Aquila with a LEO 1503 apparatus equipped with a field effect gun. The beam was typically operated at 1 kV.

**Data Analysis.** Replicated measurements are reported as weighted averages using the error of the weighted average (internal error) as dispersion index. If the  $\chi^2$  test of the H<sub>0</sub> hypothesis: "the internal error is not statistically different from the standard error (external error) of the sampled population" is not verified at a level of significance of 95%, the standard error is used for dispersion estimation purposes. The usage of different position/dispersion indicators will be specified in parentheses.

Comparison of the data will be performed by means of a  $t$  test for the means. The results of the comparison indicate no difference between the means if the level of agreement of the test ( $1 - \alpha$ ) lies within 0.05 and 0.95.

Table 1. % C,  $\delta^{13}\text{C}$  and pMC Measured on the Laboratory Produced Quick Limes and Laboratory Mortars

	sample ID	% C	$\delta^{13}\text{C}$ (mil)	pMC (%)
quick limes	QL700	$8.6 \pm 0.3^a$	$2.36 \pm 0.02$	$2.30 \pm 0.06$
	QL700 1.5	$8.9 \pm 0.2^a$	$2.64 \pm 0.01$	$0.83 \pm 0.03$
	QL800	$0.38 \pm 0.03^a$	$-9.3 \pm 0.7^a$	N.M. <sup>b</sup>
	QL900	$0.34 \pm 0.02^a$	$-22.92 \pm 0.04$	N.M. <sup>b</sup>
	QL 1000	$0.143 \pm 0.003^a$	$-16.52 \pm 0.05$	N.M. <sup>b</sup>
	QL1100	$0.20 \pm 0.03^a$	$-18.70 \pm 0.04$	N.M. <sup>b</sup>
laboratory mortars	MO 700	$10.3 \pm 0.1^a$	$-1.88 \pm 0.02$	$20.3 \pm 0.1$
	MO 700 1.5	$9.6 \pm 0.2^a$	$-2.01 \pm 0.02$	$21.9 \pm 0.2$
	MO 800	$3.7 \pm 0.3^a$	$-14.9 \pm 0.01$	$94.3 \pm 0.4$
	MO 900	$5.4 \pm 0.4^a$	$-15.15 \pm 0.01$	$97.9 \pm 0.4$
	MO 1000	$5.2 \pm 0.9^a$	$-21.98 \pm 0.02$	$97.4 \pm 0.4$
	MO 1100	$4.4 \pm 0.7^a$	$-19.2 \pm 0.02$	$100.2 \pm 0.4$

<sup>a</sup> Values represent weighed mean  $\pm$  standard error on  $n = 3$  samples. <sup>b</sup> N.M. stands for not measured.

## RESULTS AND DISCUSSION

**LS Characterization.** The initial limestone carbonate showed an average % C content of  $10.2 \pm 0.2\%$  (mean  $\pm$  standard error), a  $\delta^{13}\text{C}$  of  $2.9 \pm 0.2\text{‰}$ , and a pMC of  $0.12 \pm 0.05\%$ . All measurements were in agreement with the values expected for a sedimentary carbonate: (i) % C around 12% (the theoretical % C value for the pure calcite ( $\text{CaCO}_3$ )), (ii)  $\delta^{13}\text{C}$  comparable to the isotope signature of cretaceous carbonates ( $+1$  to  $+3\text{‰}$ <sup>29,30</sup>), and (iii) depleted radiocarbon abundances, related to the ancient age of the carbonaceous material. XRD analysis evidenced how the initial material was composed of low magnesium calcite crystals. Low Mg contents of the original material avoid the possibility of formation of magnesian mortars characterized by slower carbonation velocities<sup>31</sup> not compatible with our experimental times.

**QL Production Process.** The calcination process appeared very sensitive (i.e., % C,  $\delta^{13}\text{C}$ ) to the temperatures of the applied treatment (Table 1). QL produced at 700 °C, independent of the applied time of combustion (QL 700 and QL 700\_1.5), is depleted with respect to the original carbonate. For these samples, the observed degree of C depletion indicates inefficient calcinations (about 80% of LS C is still present in the samples). QL produced at temperatures ranging between 800 and 900 °C are sensitively depleted with respect to MO 700 series but slightly enriched with respect to the ones produced in the 1000–1100 °C range. It can be noted how efficient calcination happens (i.e., less than 1% of the LS C remains in the QLs) only for temperatures  $\geq 800$  °C.

$\text{MgCO}_3$  dissolves in the 450–520 °C range while  $\text{CaCO}_3$  dissolves in the 700–900 °C range.<sup>32</sup> Thermal dissolution of calcite happens at 898 °C at 1 bar of pressure of pure  $\text{CO}_2$ , and the calcination temperature decreases with the lowering of the  $\text{CO}_2$  concentration.<sup>33</sup> This evidence fits the observed threshold behavior of calcination well, with the small C loss up to 800 °C probably attributable to the selective  $\text{MgCO}_3$  thermal dissolution.

Measured QL  $\delta^{13}\text{C}$  values (Table 1) were in statistical agreement with the measured LS only for calcination temperatures of 700 °C. For calcination temperatures higher than 700 °C, a strong depletion in the  $^{13}\text{C}$  signature is observable. Calcination temperatures higher than 700 °C induce a sensitive isotopic fractionation in the residual/lost carbon. We observed a

preferential loss of the heavier stable isotope of carbon leaving the residual  $\text{CaCO}_3$  depleted in  $^{13}\text{C}$ . This process is better known as the inverse isotope effect,<sup>34</sup> in opposition to the normal fractionation predicting enrichment in the heaviest isotope composition of the residue of calcination.

Our measurements raise some questions about the literature-suggested  $^{13}\text{C}$  back correction.<sup>10,11</sup> Indeed, this correction is based also on the assumption of preservation of the isotopic signature of the LS in the MO even after calcination, implying the absence of isotopic fractionation during the production of QL. Measured fractionations constitute a good explanation for previous bibliographic evidence of depleted  $\delta^{13}\text{C}$  mortar carbonates values until levels lower than the atmospheric  $\text{CO}_2$  level.<sup>11,16</sup> These observations were justified by supposing the usage of aggregates for MO production with a C isotopic signature different from the one occurring in the cretaceous<sup>11</sup> or by hypothesizing a carbonation with depleted biogenic  $\text{CO}_2$ .<sup>16</sup> To our knowledge, no studies have been published underlying a possible isotopic fractionation during the calcination as a possible explanation for the observed degrees of depletion in the mortar matrixes.

The measured radiocarbon signals on QL 700 and QL 700\_1.5 (Table 1) were strongly depleted in  $^{14}\text{C}$ . These values were in agreement with the one measured on the three replicates of the original LS ( $0.12 \pm 0.05\%$ ). A  $t$  test comparison of  $1.1 \pm 0.8\%$  (weighted average on the pMCs of the QL 700 and QL 700\_1.5) with this latter confirms the agreement between these measurements. Then, hereafter, we use this value as a representative of the QL  $^{14}\text{C}$  signature independent of the calcination temperature applied.

**Carbonatation Process.** Laboratory  $\text{CO}_2$  absorption over the experimental period leads to a mass increase (data not shown) ranging between 34 and 37% for the QLs produced at temperatures  $\geq 800$  °C. For the 700 °C QL series, the mass increases only from 8 to 20%. The theoretical mass increase for the complete reaction of carbonation (i.e., 79%) implies a yield of carbonation close to 50% for the QL produced at  $T$  higher than 700 °C and much slower for not completely calcinated samples.

The % C (Table 1) measurements on MO replicates confirm the overall success of the carbonation procedure: all measured MO % C values were significantly enriched with respect to the respective QLs. The % C reached by the MO 700 and MO 700\_1.5 was not statistically different from the % C of the LS

**Table 2.** Fraction of Limestone Residual C Constituting the Mortar Carbonate ( $\chi_1$ ),  $\delta^{13}\text{C}$ , and pMC of the Binder Phase of the Mortar Evaluated by Means of the Isotopic Mass Balance

sample ID	$\chi_1$	$\delta^{13}\text{C}$ binder	pMC binder
MO 700	$0.83 \pm 0.03$	$-22 \pm 4$	$113 \pm 32$
MO700_1.5	$0.92 \pm 0.02$	$-54 \pm 14$	$255 \pm 97$
MO 800	$0.10 \pm 0.01$	$-15.6 \pm 0.1$	$105 \pm 2$
MO 900	$0.06 \pm 0.01$	$-14.62 \pm 0.05$	$105 \pm 1$
MO 1000	$0.03 \pm 0.01$	$-22.13 \pm 0.04$	$100 \pm 1$
MO 1100	$0.05 \pm 0.01$	$-19.22 \pm 0.02$	$105 \pm 2$

carbonate. The % C of other MO carbonates were significantly depleted with respect to the 700 °C series but constant independent of the temperature of the QL production

The % C data reported in Table 1 can be used to estimate some important details about the carbonation process. It is possible to evaluate (Table 2) the fraction of limestone residual C ( $\chi_1$ ) composing the mortar carbonate by performing the ratio between the % C measured on the QL and the relative produced MO. It must be noted how, because of the incomplete carbon removal of the LS C during calcination, the  $\chi_1$  characterization of MO 700 and MO 700\_1.5 is sensitively higher than other MOs. These characteristics make these samples (i) a material not easily usable for constructive uses given the low hardening ratio related to the low CO<sub>2</sub> absorption; (ii) an extremely high dead C contaminated material; (iii) a less sensitive tool for the binder  $\delta^{13}\text{C}$ /pMC estimations (higher uncertainties affecting the mass balance approach (see the next paragraph for details)). SEM analyses on the laboratory produced mortars (Figure 1A and B) clearly confirm their different nature, with the MO 700 characterized by a coarser and more angular structure than MOs produced from the LS calcinated at 900 °C.

It appears that carbonation differentiates the two subsets of mortars: the first produced by the carbonation of the QL 700 series characterized by low atmospheric CO<sub>2</sub> absorption rates (i.e., most of the C constituting these samples is ascribable to LS), higher % C, and preservation of the crystalline aspect of the initial carbonate. The second by QLS produced at temperatures higher than 700 °C is characterized by higher rates of CO<sub>2</sub> absorption, lower % C and the development of regular surfaces.

$\delta^{13}\text{C}$  and pMC values (Table 1) also confirm the absorption of CO<sub>2</sub> from the laboratory atmosphere, being both different by their respective  $\delta^{13}\text{C}$  and mean pMC ( $1.1 \pm 0.8\%$ ) of the QLS. MO 1000 and MO 1100 were found comparable to the previously observed  $\delta^{13}\text{C}$  of laboratory synthesized mortars.<sup>15</sup>

**Evaluating the Binder Isotopic Signature and Carbonation Fractionation.** Assuming that C composing our synthetic mortar carbonate (m) is ascribable to two sources, (i) the LS carbonate (l) survived the burning for the quick lime production, (ii) the carbonate forming the binder (b) produced by the carbonation of the slaked limes is characterized by a characteristic carbon isotopic fingerprint <sup>13</sup>C (i.e.,  $\delta^{13}\text{C}$  or pMC). With the hypothesis of a homogeneous dispersion of the two source signals, it is possible to evaluate the isotopic content of the binder present in the mortar (see section 2 of the Supporting Information for details) by applying the isotopic mass balance (IMB) using as input data the  $\chi_1$  (Table 2), the  $\delta^{13}\text{C}$ , and pMC of the QL and of the MO (Table 1, see section 3 of the Supporting Information for details). Assuming all the values (Table 2) are representative of an independent replicate set for the evaluation

of the  $\delta^{13}\text{C}$  and pMC of the binder, we estimate them to be, respectively,  $-19 \pm 6\%$  and  $102 \pm 25\%$ .

The evaluation of both the <sup>13</sup>C and <sup>14</sup>C signatures of the binder is affected by an uncertainty of about 1 order of magnitude higher than the atmospheric variability (see later) over the reference period addressable to MO 700 and MO 700\_1.5 (see the previous paragraph). Rejection of these values gives an evaluated  $\delta^{13}\text{C}$  and pMC signature of the binder phase of  $-19 \pm 2\%$  and  $102 \pm 1\%$ , respectively, not altering the average values but significantly affecting their index of dispersion.

Over the whole carbonation period, CO<sub>2</sub> constituting the laboratory atmosphere was sampled and the estimated  $\delta^{13}\text{C}$  and pMC were, respectively,  $-11 \pm 1\%$  and  $100 \pm 2\%$ . It can be noted how the measured values are evidence of a sensitive fossil C source that can significantly affect the depleted measured isotopic values of CO<sub>2</sub> with respect to the clear air values.

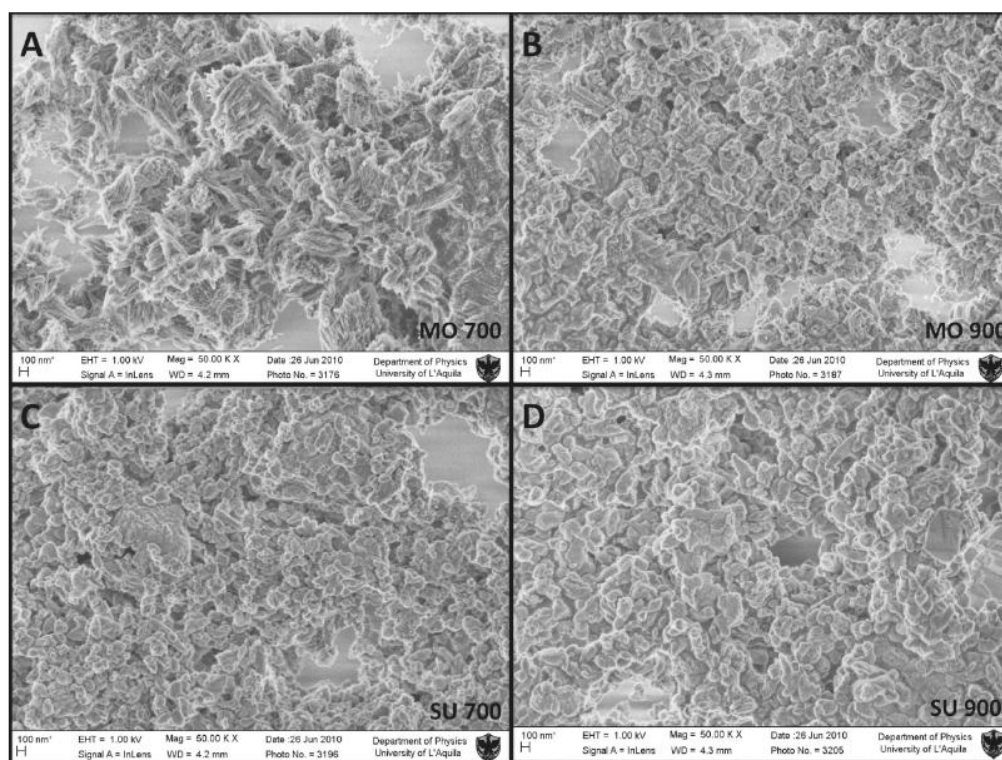
The binder estimated IMB  $\delta^{13}\text{C}$  should exactly preserve the signature of the atmospheric CO<sub>2</sub> if no isotopic fractionation is observed during carbonation, while binder radiocarbon estimations should appear in agreement with the atmosphere independent of the presence/absence of this fractionation. In our case, the *t* test between the measured <sup>13</sup>C values (i.e., atmosphere  $-11 \pm 1\%$  and binder  $-19 \pm 2\%$ ) indicates a small fractionation. This finding was in agreement with a previous study<sup>16</sup> simulating the absorption of CO<sub>2</sub> from a pure Ca(OH)<sub>2</sub>/water solution at different CO<sub>2</sub> pressures. In this study, the observed <sup>13</sup>C CaCO<sub>3</sub>/CO<sub>2</sub> fractionation was found to decrease as soon as the partial pressure of CO<sub>2</sub> approaches the atmospheric values. The observation of a measurable fractionation process during MO carbonation agrees also with Pachiaudi et al.<sup>15</sup> but points out the possibility of shallower atmosphere/mortar C fractionation with respect to this study.

IMB evaluated binder pMC values are in agreement with the measured atmosphere <sup>14</sup>CO<sub>2</sub>. In this case, the significance of the absence of a difference between the atmosphere and the binder is valid. This last result is a clue to the good practice of the <sup>14</sup>C measurement and correction procedure applied at the CIRCE laboratory.

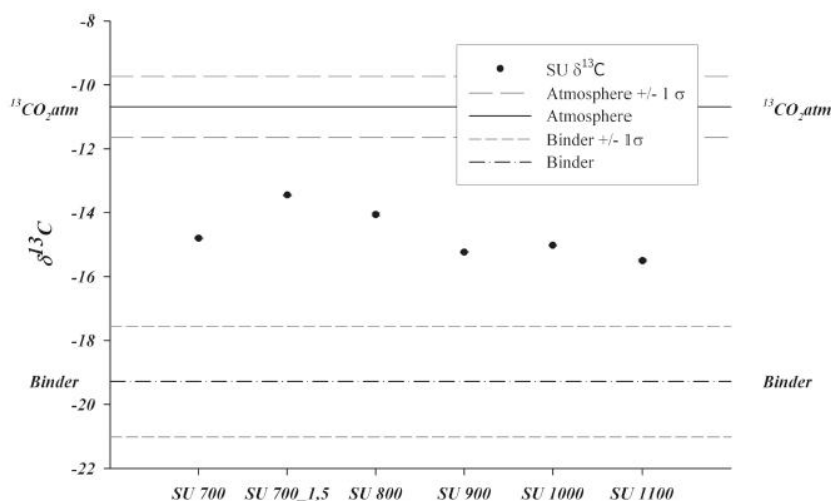
**Binder Signal Isolation Procedure.** Considering the suspension phase <sup>13</sup>C values (Figure 2) as independent replicates of the same phase (i.e., the binder), we evaluate the suspension signal in  $-14.7 \pm 0.3\%$ . The data variability affecting the suspension <sup>13</sup>C measurements is very narrow, compatibly with the directly measured atmospheric <sup>13</sup>CO<sub>2</sub> and underlies a good reproducibility of the applied procedure for the binder signal <sup>13</sup>C isolation. SU values lie between the atmospheric value ( $-11 \pm 1\%$ ) and the IMB evaluated binder signal ( $-19 \pm 2\%$ , see previous paragraph for details). Comparison of SU with IMB  $\delta^{13}\text{C}$  values, with the two deviations of the order of 2–3 $\sigma$ , indicates the fair effectiveness of dead C suppression provided by the applied isolation procedure for all the types of MO analyzed in this study.

SEM analyses on the isolated suspensions (Figure 1C,D) do not show any particular difference between the samples independent of their history, confirming the apparent effective suppression of the LS fossil signal in agreement with the results found by application of the <sup>13</sup>C tool.

Suspension <sup>14</sup>C signals converted in calendar ages show a different behavior from what is evidenced by looking at <sup>13</sup>C (Figure 3). Radiocarbon, in fact, evidences a different behavior in the efficiency of the dead C contamination suppression. Our procedure gave reliable results (comparable to the atmosphere CO<sub>2</sub> and IMB <sup>14</sup>C values) only when calcination temperatures



**Figure 1.** Scanning electron microscopy images of the laboratory produced mortars (i.e., MO 700 (A) and MO 900 (B)) and the suspensions isolated by the same samples (i.e., SU 700 (C) and SU 900 (D)).

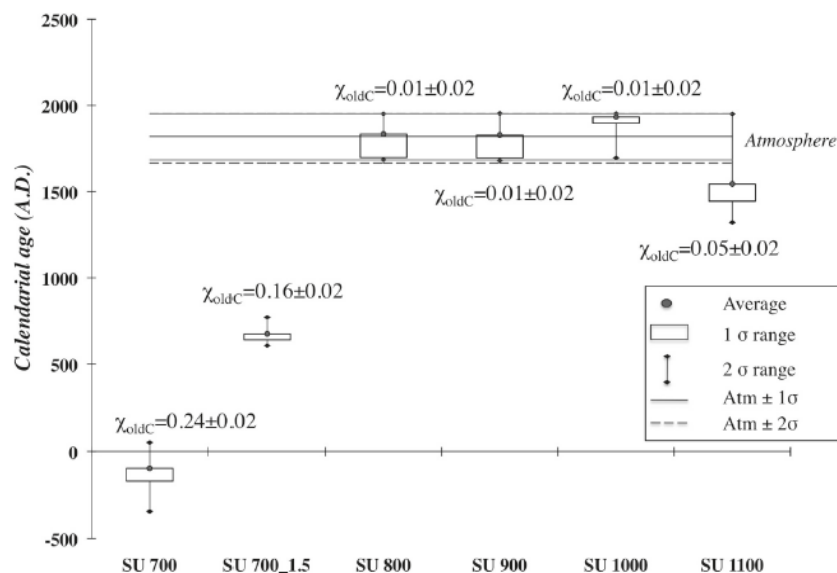


**Figure 2.** Measured  $\delta^{13}\text{C}$  values of the suspension isolated from the mortars following this study proposed isolation procedure compared with the isotopic signature of the laboratory air  $\text{CO}_2$  (directly measured) and the binder signal evaluated by means of the mass balance approach with the rejection of MO700 and MO700\_1.5 outliers (see the text for details).

were  $\geq 800$  °C. For temperatures of quick lime production lower than 800 °C, most of the C constituting the mortars (i.e., 83 and 92%, Table 2) was of limestone origin so that our procedure fails in the efficient suppression (i.e., 100%) of the original limestone residues leading to an aging effect of about 2000 years for SU 700 and 1200 years for SU 700\_1.5. Radiocarbon measurements performed on these suspensions together with the pMC values measured on the atmosphere and quick limes (i.e.,  $1.1 \pm 0.8\%$ )

can be used to evaluate the relative contribution of the residual limestone carbonate ( $\chi_{\text{old}}$ ) by an ulterior application of an IMB (Figure 3, see the Supporting Info for details). Residual C fractions in statistical agreement with zero show no significant difference from the atmospheric  $\text{CO}_2$  value. These measurements allow us to estimate the suppression efficiency of the proposed procedure by comparing the  $\chi_{\text{oldC}}$  of the SU with the  $\chi_1$  present in the laboratory mortar carbonate. Suppression





**Figure 3.** Calibrated radiocarbon ages (expressed in A.D., assigning B.C. dates as negative A.D. values) measured on the suspension phases extracted by the laboratory produced MO carbonates and laboratory atmospheric CO<sub>2</sub>. Weighted averages and 1–2σ ranges are reported for each of the measured values together with the fraction of C of limestone origin ( $\chi_{\text{oldC}}$ ) still present in the sample.

efficiencies measured were not compatible with 100% only for suspensions originating from MO 700 and 700\_1.5 (i.e.,  $72 \pm 2\%$  and  $83 \pm 2\%$ ). These materials represent a sort of outlier in the commonly applied production process of mortars because it is commonly accepted that because calcination efficiently happens at temperatures in the 800–1000 °C range,<sup>3,34,35</sup> they were not used for constructive uses.

The sensitivity of the applied methodology based on <sup>14</sup>C measurements is about 3-fold better than that based on <sup>13</sup>C. These results suggest using the <sup>13</sup>C tool just as an exploratory (not constraining) analysis preceding the more sensitive and expansive <sup>14</sup>C analysis of the isolated suspensions.

The partial acid digestion applied to the SU 700 and 700\_1.5 samples (i.e., SU 700\_PA and SU 700\_1.5\_PA) yielded  $78.6 \pm 0.3$  and  $81.2 \pm 0.7$  pMC, respectively, showing no improvement in the dead carbon suppression. In our case, as also observed by van Strydonk et al.<sup>10</sup> in the case of very powdery mortars, partial acid digestion was not effective for the isolation of the atmospheric CO<sub>2</sub> preserved in the binder.

## CONCLUSIONS

This study explores the possible application of the radiocarbon dating methodology to evaluate mortar ages by means of a novel physical procedure aiming to isolate the binder from other carbonate sources commonly leading to sensitive aging effects on the absolute chronology evaluation of studied sites. This goal was achieved by reproducing a simplified mortar production process in the laboratory that performed even at different calcination temperatures and characterizing its intermediate phases aiming to estimate reference values useful for procedure accuracy evaluations. The laboratory mortar production process allowed us (i) to show sensitive <sup>13</sup>C isotopic fractionation during the limestone calcination according to the treatment temperatures, (ii) to underline shallow <sup>13</sup>C isotopic discrimination during the QL carbonation. Both findings raise some questions about the literature suggested <sup>13</sup>C-backcorrection hypothesizing a lack of isotopic discrimination over the mortar production procedure. In this

framework it is important to notice how, aiming to dating purposes, this correction would result in higher values of the conventional age, implying inaccuracy of the correction model.

Produced mortars, after their characterization, were processed for the isolation of the binder signal and analyzed. All measured <sup>13</sup>C values on the suspension phases were in slight agreement with the atmospheric <sup>13</sup>CO<sub>2</sub> of the laboratory air. Radiocarbon ages were in agreement with the atmospheric reference for applied temperatures of calcination higher than 700 °C. Only when the QL is produced at temperatures lower than 800 °C, a sensitive dead C effect is observable. The applied partial acid digestion did not improve the aging effect introduced in these sample processings. Such disagreement, anyhow, should not influence the protocol applicability to archeological samples because calcination and subsequent carbonation is not efficient at these temperatures. Given the overall successful character of the proposed methodology in the dead C suppression of unburnt limestone origin, a second phase of testing will be performed on real field mortars. Comparison of the observed results with other independent chronology estimations will be used to further refine the methodology.

## ASSOCIATED CONTENT

**S** Supporting Information. Additional information as noted in text. This material is available free of charge via the Internet at <http://pubs.acs.org>.

## AUTHOR INFORMATION

### Corresponding Author

\*Address: Via Vivaldi, 43 81100, Caserta, Italy. Phone and fax: +390823274814. E-mail: [fabio.marzaioli@unina2.it](mailto:fabio.marzaioli@unina2.it).

## ACKNOWLEDGMENT

We thank Dr. Luca Ottaviano of the Department of Physics, University of L'Aquila (Italy) for the SEM analyses, Dr. Leonardo

Nucetelli of Servizio Di Polizia Scientifica for the XRD analyses, and Dr. Joseph Sepe for reviewing this manuscript.

## REFERENCES

- (1) Ringbom, A.; Hale, J.; Heinemeier, J.; Lancaster, L.; Lindroos, A. *Am. Sci.* **2003**, *91* (2), 130–137.
- (2) Bensted, J. In *Cement: Past, Present and Future*; Dartford Greenwich University Press: Dartford, U.K., 1997.
- (3) Rech, J. A.; Near, E. *Archaeol.* **2004**, *67* (4), 212–219.
- (4) Rodriguez-Navarro, C.; Hansen, E.; Ginell, W. S. *J. Am. Ceram. Soc.* **1998**, *81* (11), 3032–3034.
- (5) Folk, R. L.; Valastro, S. *J. Field Archaeol.* **1976**, *3* (2), 203–208.
- (6) Godwin, H. *Nature* **1962**, *195* (4845), 984–984.
- (7) Delibrias, G.; Labeyrie, J. *6th International Conference on Radiocarbon and Tritium Dating*, Pullman, WA, 1965; p 344.
- (8) Stuiver, M.; Smith, C. S. *6th International Conference on Radiocarbon and Tritium Dating*, Pullman, WA, 1965; p 338.
- (9) Baxter, M. S.; Walton, A. *Nature* **1970**, *225*, 937–938.
- (10) Van Strydonck, M.; Dupas, M.; Dauchot-Dehon, M.; Pachiardi, Ch.; Marechal, J. *Radiocarbon* **1986**, *28* (2A), 702–710.
- (11) Nawrocka, D.; Michniewicz, J.; Pawlyta, J.; Padzur, A. *Geochronometria* **2005**, *24*, 109–115.
- (12) Sonninen, E.; Jungner, H. *Radiocarbon* **2001**, *43* (2A), 271–273.
- (13) Lindroos, A.; Heienmeier, J.; Ringbom, A.; Brasken, M.; Sveinbojornstodtir, A. *Radiocarbon* **2007**, *49* (1), 47–67.
- (14) Heinemeier, J.; Jungner, H.; Lindroos, A.; Ringbom, A.; von Konow, T.; Rud, N. *Nucl. Instrum. Methods Phys. Res., Sect. B* **1997**, *123*, 487–495.
- (15) Pachiardi, J. M.; Van Strydonck, M.; Dupas, M.; Dauchot-Dehon, M. *Radiocarbon* **1986**, *28* (2A), 691–697.
- (16) Kosednar-Legenstein, B.; Dietzel, M.; Leis, A.; Stingl, K. *Appl. Geochem.* **2008**, *23*, 2425–2437.
- (17) Van Strydonck, M.; Dupas, M.; Keppens, E. *Radiocarbon* **1989**, *31* (3), 610–618.
- (18) Cazalla, O.; Rodriguez-Navarro, C.; Sebastian, E.; Cultrone, G. *J. Am. Ceram. Soc.* **2000**, *83* (5), 1070–1076.
- (19) Bertolini, T.; Rubino, M.; Lubritto, C.; D'Onofrio, A.; Marzaioli, F.; Passariello, I.; Terrasi, F. *J. Mass Spectrom.* **2005**, *40* (8), 1104–1108.
- (20) Zamba, I. C.; Stamatakis, M. G.; Cooper, F. A.; Themelis, P. G.; Zambas, C. G. *Mater. Charact.* **2007**, *58*, 1229–1239.
- (21) Marzaioli, F.; Borriello, G.; Passariello, I.; Lubritto, C.; De Cesare, N.; D'Onofrio, A.; Terrasi, F. *Radiocarbon* **2008**, *50* (1), 139–149.
- (22) McCrea, J. M. *J. Chem. Phys.* **1950**, *18*, 849–857.
- (23) Rozanski, K.; Stichler, W.; Gonfiantini, R.; Scott, E. M.; Beukens, R. P.; Kromer, B.; van der Plicht, J. *Radiocarbon* **1992**, *34* (3), 506–519.
- (24) McKinney, C. R.; McCrea, J. M.; Epstein, S.; Allen, H. A.; Urey, H. C. *Rev. Sci. Instrum.* **1950**, *21* (8), 724–730.
- (25) Terrasi, F.; De Cesare, N.; D'Onofrio, A.; Lubritto, C.; Marzaioli, F.; Passariello, I.; Rogalla, D.; Sabbarese, C.; Borriello, G.; Casa, G.; Palmieri, A. *Nucl. Instrum. Methods Phys. Res., Sect. B* **2008**, *266*, 2221–2224.
- (26) Stuiver, M.; Polach, H. A. *Radiocarbon* **1977**, *19* (3), 355–363.
- (27) Stuiver, M.; Reimer, P. J.; Reimer, R. *CALIB Radiocarbon Calibration*, version 6.0; 2010, <http://www.calib.org>.
- (28) Reimer, P. J.; Reimer, R. *CALIBomb Radiocarbon Calibration*, html program; 2010, <http://www.calib.org>.
- (29) Jenkyns, H. C.; Gale, A. S.; Corfield, R. M. *Geol. Mag.* **1994**, *131*, 1–34.
- (30) Wissler, L.; Funk, H.; Weissert, H. *Palaeogeogr., Palaeoclimatol., Palaeoecol.* **2003**, *200*, 187–205.
- (31) Zheng, L.; Xuehua, C.; Mingshu, T. *Cem. Concr. Res.* **1992**, *22* (1), 1–5.
- (32) Paama, L.; Pitkanen, I.; Ronkkomaki, H.; Peramaki, P. *Thermochim. Acta* **1998**, *320* (1–2), 127–133.
- (33) Elert, K.; Rodriguez-Navarro, C.; Pardo, E. S.; Hansen, E.; Cazalla, O. *Stud. Conserv.* **2002**, *47* (1), 62–75.
- (34) McNaught, A. D.; Wilkinson, A. In *Compendium of Chemical Terminology*, 2nd ed.; Blackwell Science: Oxford, U.K., 1997.
- (35) Moropoulou, A.; Bakolas, A.; Aggelakopoulou, E. *Cem. Concr. Res.* **2001**, *31*, 633–639.

## **II.2. The evolution: methodological aspects and field study applications at CIRCE using CryoSoniC and Cryo2SoniC methods.**

Observed results obtained from synthetic mortars, encouraged to test CryoSoniC accuracy evaluation on genuine mortars sampled from archeological sites of known or independently constrained age (i.e., other  $^{14}\text{C}$  dates on different materials). Giving the test efficiency of the proposed methodology in suppressing the DC signal coming from unburned limestone residues (Marzaioli et al. 2011) now, the main aim is to check the effectiveness of the methodology on the suppression of eventual aggregates related effects. This has been the subject of a paper published on *Nuclear Instruments and Methods in Physic Research B* on 2013, as Proceeding of the AMS12 Conference held in Wellington (New Zealand) on March 2011. It highlights the necessity to change the original protocol CryoSoniC into a new one, able to obtain good results with the changing of investigated prime materials (section II.2.1).

The first trial on real mortar was performed on some archaeological samples coming from three medieval Spanish sites. In such cases, difficulties to obtain good results grow up proportionally to the presence of different calcareous sources constituting the old mortar. Testing the first CryoSoniC version showed that sometimes discrepancies can be observed with respect to archaeological evidences. This usually happens when calcite components inside mortar are represented not only by the binder but also by aggregates and neo-genic compounds. Here below will be shown how CryoSoniC worked on samples coming from three different Spanish sites: Aistra, Zornotzegi and Trevino. Results, if compared, showed some discrepancies because while the selection protocol worked for some samples, it didn't do for others. Hence, these patchy answers enhanced the need of uploading the old version to the new one. After having recorded a first positive match between RC dating and archaeological conditions performed on samples from first site - Aistra - two negative matches between RC dating and archaeological references performed on samples from other sites - Zornotzegi and Trevino (section II.2.1) were recorded. These failures requested a change on the selection protocol features in order to improve it and obtain a more efficient new one. These experimental evidences drove the development of a 2<sup>nd</sup> generation CryoSoniC successively renamed Cryo2SoniC.

The uploading rose from observations made on measurements performed by a differential ultrasonication time setting on the same archaeological sample. Starting from the principle assumed for CryoSoniC, that used the ultrasonication as the key step to select the right fraction to date, a test based on differentiated ultrasonication times intervals was applied. A time trend of 10, 30, 45 and 60 minutes of ultrasonication performed on the same sample (ZOR07 UE1112 from Zornotzegi) was set. Along the ultrasonication temporal gradient applied, suspended fractions with different  $^{14}\text{C}$

ages were isolated and dated. Information collected through this simple experiment have been useful to define the basis of changes applicable to the original CryoSoniC (Table1). The main info is the difference recorded between first ultrasonication step of 10 min and the following others: the first step produce a fraction older by almost 1000 years than the following (Figure 2) while the steps performed at 30,45,60 min of ultrasonication, show similar results. Last three steps are statistically accepted as the same, considering them inside  $3\sigma$ .

Stressing here the point that all measurements are performed on the total suspension, time trend  $^{14}\text{C}$  ages of suspension can be interpreted as a first very old fraction suddenly entering the suspension being mixed over time with younger fractions. Hypothesizing that the first produced fraction is somehow related to fine aggregates, one can conclude that pretreatment protocol could be divided in two steps: the first probably contaminated with fine carbonatic aggregates and the second free of such contamination. Here by on we hypothesize that the same conclusions can be applied also to the calcite due to secondary deposition. Differences between radiocarbon isotopic signatures of two collected fractions will be heavier if stronger is the presence of calcareous sources (dead carbon or newborn calcite).

The enhanced differences allowed us to propose a new protocol based on the splitting of the original ultrasonication step, that became a double step: from here the CryoSoniC turned into Cryo2SoniC. In detail, the original ultrasonication procedure (Marzaioli et al. 2011; section II.1) was split into two sub-phases obtaining a fraction called sand from the first step of 10 minutes and fraction called susp from the second step of 30 minutes, which will go to substitute the homonymous fraction found using the oldest method. Different selected fractions are carrier of two different RC dating depending on number and importance of DC sources present inside the analyzed samples. In our opinion first fraction accounting for fine and/or diagenetic calcite, should be more easily affected by contaminations than the second, that, on the contrary, should results as a carrier of a chronological information closer to the real value. Watching values of final RC ages reported into Table 1, it could be noticed that every measure is very old and probably affected by a strong DC contamination. Although results were sensitively different from archaeological references, their contribute was very useful to catch new evidences to put a starting point to elaborate a new protocol. Applying it to archaeological samples from Spanish sites of Zornotzegi and Trevino which didn't find good comparison with first separation method (CryoSoniC ) it has been shown a successful dating adopting the ultimate version (Cryo2SoniC). Their cases of studies are going to be discussed below.

Table 1. Results of time trend test applied on an archaeological mortar sample from Zornotzegi site. Calibrated Age are written taking into account the oldest and youngest age of the calibration intervals.

Time Interval (minutes)	RC Age (years BP)	Err RCage	Calibrated Age 1 $\sigma$	Calibrated Age 2 $\sigma$
Susp 10'	4122	50	2865-2579 BC	2880-2497 BC
Susp 30'	3448	51	1876-1689 BC	1893-1626 BC
Susp 45'	3507	50	1897-1749 BC	1954-1691 BC
Susp 60'	3268	29	1605-1500 BC	1619-1458 BC

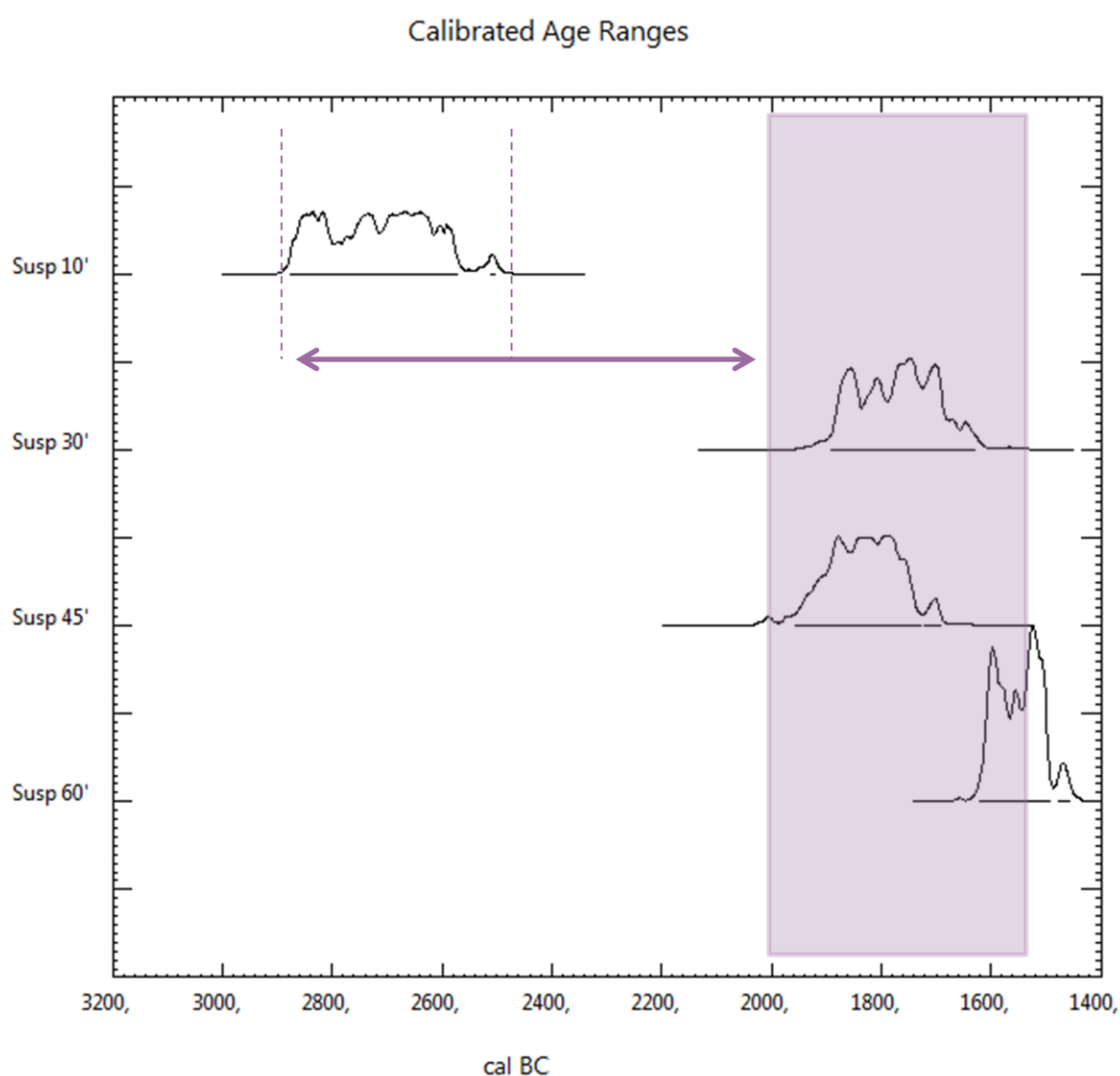


Figure 2. Graphic showing the gap between first step of time interval of ultrasonication (10 min) and others steps using longer time intervals. Has been enhanced chronological similarity between fractions obtained after 30 min of treatment.

Due to these experimental observations (which showed a progressive leveling of the RC age along the applied time of ultrasonication) the CryoSoniC procedure has been updated to **Cryo2SoniC**, in order to increase the dead carbon contamination suppression efficiency observed in conventional CryoSoniC purified samples (Figure 3). Cryo2SoniC can be resumed as follow:

1. **Cryogenical breaking.** According to Nawrocka al. (2005) about 5 g of mortar were submerged in liquid nitrogen till the achievement of thermal equilibrium and immediately transferred into an oven at 80°C. This cycle was repeated almost three times and mortars were broken by means of gentle hammering. An alternative to gentle breaking by hammering is a soft manual disaggregation without a stronger crushing especially when treated material is easily breakable. In this way the risk to produce unwanted fine grain-size particles not coming from binder is reduced. To make a manual breaking on mortar pieces it is necessary to wait that material comes back to ambient temperature after it has been submerged into liquid nitrogen.
2. **Size selection.** The produced fragments (spanning a wide range of particle size) were sieved and only particles with size below 500 µm were selected and stored in a 75 ml beaker. Then ~40 mL of deionized/decarbonated water (DDW) was added.
3. **1<sup>st</sup> ultrasonic selection.** After complete sedimentation (~12 hr), the selected powder was rewetted with 40 mL of DDW and ultrasonicated for 10 min. DDW-containing suspended mortar particles was totally removed and transferred to a Falcon 50-mL centrifuge tube. This fraction of binder represents the fraction potentially affected by dead carbon contamination and/or diagenetic calcite (*sand*) due to the probable presence of very fine carbonaceous grains sands entering the suspension easily and before binder particles.
4. **2<sup>nd</sup> ultrasonic selection.** Residual powder, decanted on the bottom of the beaker after the first ultrasonic attack totally unaffected by first selected fraction (*sand*), underwent to another ultrasonication for 30 min in excess (~40 mL) of DDW. About 30 mL of water were collected by siphoning and stored in another Falcon centrifuge tube, taking great care not to induce a new suspension of the sediments. This last fraction, according to our experimental experience, represents the suspension guaranteeing accurate dating (*susp*).
5. **Centrifugation.** The Falcon centrifuge tube containing *susp* carbonates, and the other containing the *sand* fraction, were centrifuged at 8.0 krpm in a rotor of 10 cm mean radius for 5 min and oven-dried overnight (80 °C).

The selected fractions (*susp* and *sand*) were weighed and prepared for AMS measurement. About 40 mg (up to 15 mg) of powders from selected fractions and carbonate standards samples (i.e. IAEA C1 and C2; Rozanski et al. 1992) were digested under vacuum to develop CO<sub>2</sub> by means of a

complete orthophosphoric acid attack (McCrea 1950) for 2 hr at 85 °C. The developed CO<sub>2</sub> was cryogenically purified from other gasses, reduced to graphite on iron powder catalyst according to the CIRCE sealed-tube reaction protocol (the zinc process) following Marzaioli et al. (2008), and analyzed to measure <sup>14</sup>C isotopic ratios using the CIRCE AMS system (Terrasi et al. 2008). Measured <sup>14</sup>C ratios were converted to <sup>14</sup>C ages (Stuiver and Polach 1977) and calibrated to absolute (i.e. calendar) ages by means of the CALIB v 6.0 program (Stuiver and Reimer 1993) using the IntCal09 atmospheric calibration data set (Reimer et al. 2009). All <sup>14</sup>C dates are reported i) as intervals comprised between the highest/lowest calendar age identified by the projection of measurement intervals (1 or 2σ) on the absolute age axes using the IntCal09 calibration curve, ii) as a combination of multiple intervals (%) reflecting the projection of RC value on IntCal09 calibration curve.

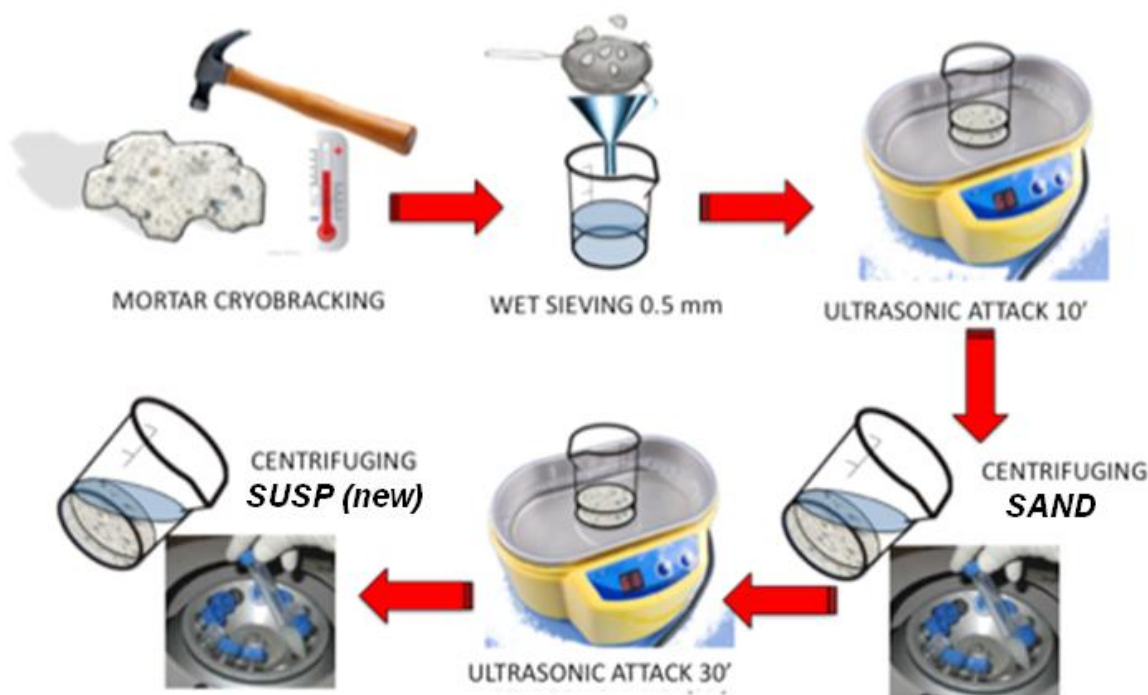


Figure 3. Schematic representation of the Cryo2SoniC procedure. The upgraded version needs two steps of ultrasonication to isolate the fraction usefull to date (susp).

### II.2.1. Application on Medieval Spanish Sites: Aistra, Zornotzegi, Trevino

Some <sup>14</sup>C measurements have been performed on genuine mortars using the CryoSoniC technique to be discussed and compared with independently estimated absolute chronologies (i.e., radiocarbon/archaeometrical dating). CryoSoniC applied to mortars of three Spanish sites was tested on samples from Aistra at first, obtaining good results, and then on samples from Zornotzegi and Trevino sites not getting the expected results. This unexpected failure experience moved us to change the protocol into an improved version of itself: the Cryo2SoniC. Applying it on problematic

samples, final results were obtained which confirm archaeological expectations for all examined cases. In the following the three different successful experiences obtained changing the pretreatment protocol are illustrated case by case.

### Study sites description

#### *San Julian e Santa Basilisa di Aistra*

The church of San Julian e Santa Basilisa in Zalduondo (Figure 4) represents one of the most ancient and best preserved medieval churches of the Álava province in the Basque country (Spain). The chronology of this structure is mostly based on formal and stylistic analyses of windows and walls, and it is still contradictory (Arbeiter et al.1994; Azkarate 1988, 2003). Over the 2006–2009 period, the church underwent deeper analyses allowing the better constraining its chronology in the framework of the Aistra village archaeological project performed in collaboration with the Institute of archaeology UCL (University College London). Thanks to a series of  $^{14}\text{C}$  dates (mostly bones, 20 of them are shown in Figure 8) and other archaeological evidences, church construction was attributed to the fourth phase of the Aistra village (i.e., 10th century A.D.; Castillo 2006; 2007; 2008; 2009). Two samples belonging to the external walls of the church of San Julian were sampled (AISTRA 1 and AISTRA 2). Stratigraphic interpretation of the structure and comparison with available data, drove the choice of the samples for this site: AISTRA 1 was sampled from the north eastern corner of the structure and supposed to belong to the first phase of development of the church; AISTRA 2 was sampled from the south eastern facing wall of the church and hypothesized to be of a later age (Castillo et al. 2011).



Figure 4. *San Julian and Santa Basilisa church di Aistra (Zalduondo, Alava) with two sampling points: AISTRA1 and AISTRA2 (Castillo et al.2011).*





Figure 5 . Santa Maria of Zornoztegi church (Salvatierra, Agurain, Alava) with the sampling area (on the left) and ZOR07 sample (on the right).

### *Santa Maria di Zornoztegi*

The Santa Maria di Zornoztegi village is situated in the eastern Álava province. This archeological site developed continuously over the period from the 5<sup>th</sup> to the 14<sup>th</sup> century with a first settlement during the bronze age (Castillo 2010). Santa Maria di Zornoztegi is characterized by the presence of the so called “fallen chapel”, a religious building, nowadays mostly dismantled because of materials re-usage (Azkarate 1988, 2003; Utrero Agudo 2006). The fallen chapel is founded on a previous structure by means of a basement of filling raw materials. Pottery analysis, architectural styles and several radiocarbon measurements on organic materials (mostly charcoals and bones, some of them shown in Figure 9) found at the study site during archaeological sample processing (i.e. flotation), allowed the precise constraint of the chronology of the structure in the first half of the 12<sup>th</sup> century A.D. To avoid weather exposure contaminations, one sample situated few centimeters from the surface of the north facing wall of this structure (ZOR07) was sampled and analyzed (Figure 5).

### *Treviño Castle (Burgos)*

The town, which is nowadays a small rural center, is located at the bottom of a hill that is still known as «El Castillo». On this hill, large amounts of archaeological remains have been found and the archaeological deposits from the 10<sup>th</sup> - 12<sup>th</sup> centuries confirm that during this period it was a manorial castle articulated into several areas with different functions. Keeping in mind that the formation of the village systems begun in this area much earlier than the 10<sup>th</sup> century, a mortar sample from one of the devastation surfaces of the fortification wall (CTV07 - US 1502) has been taken (Figure 6). Two could be the interpretative settings: the wall was made in an early moment of the castle occupation, implying the *incastellamento* process 10<sup>th</sup> century; or alternatively it was

made later in the framework of the royal town. The studies of the trenches and excavations allowed us to verify the existence of a continuous occupation from the 10<sup>th</sup> century in the hilltop (Castillo et al 2011). Radiocarbon dating could help us to know its chronological setting.



*Figure 6. Wall stretch of the Treviño castle where has been done the sampling.*

### **<sup>14</sup>C Data Analyses**

Cryo2SoniC methodology was applied to suppress the C contamination in the analyzed mortar samples by means of a sequence of physical separations as described in Marzaioli et al. (2013) and at the beginning of the section 2. <sup>14</sup>C calibrated ages at 2 $\sigma$  were compared with archaeological expectations. A *t* test for the means was used to compare these results. The *t* test indicates no difference between the means if the level of agreement observed lies within 0.05 and 0.95 which, from here on, will be conventionally called the 2 $\sigma$  level. When explicitly stated, given a number of <sup>14</sup>C dates referring to coherent samples, the weighted mean of these ages calibrated using IntCal09 is referred to as calibrated weighted age. The calibrated weighted age dispersion is used to estimate the error of the weighted average if a  $\chi^2$  test on the significance of the weighted mean at 0.05 was successful. To distinguish two suspended fractions collected using the first or late version of separation protocol, is going to be used the (\*) to indicate the samples collected through CryoSoniC while no one additional symbols is going to be added to samples collected using Cryo2SoniC.

## Results and discussion

### *San Julian e Santa Basilisa di Aistra*

Figure 8 and Table 2, results arising from the radiocarbon dating performed on organic materials found at the Aistra site using CryoSoniC method. The  $2\sigma$  ranges are plotted as dispersion indexes for the measured distributions of the calendar ages. Measured absolute ages on the mortar *suspensions* (*AISTRA1\_susp\** and *AISTRA\_susp\**) appear in agreement at  $2\sigma$  level. Measured calendar ages on the *susp* fractions showed a slightly different behavior with respect to the expected age of the Church (10<sup>th</sup> century), being *AISTRA1\_susp\** in agreement at  $1\sigma$  level and *AISTRA2\_susp\** lying slightly upon  $2\sigma$  (Marzaioli et al. 2013). This observation indicates later ages for the *AISTRA2* sample probably attributable to a secondary stage of the structure in agreement with archaeological analyses of the San Julian e Santa Basilisa church (Arbeiter 1994). Petrographic analysis showed a mortar composed by a quartz sandy aggregate (Figure 7).

### *Santa Maria di Zornotzegi*

ZOR07 mortar sample was processed at first with the conventional CryoSoniC procedure. Measured radiocarbon age on *ZOR07susp\** ( $4122 \pm 50$  BP, means a calibrated range of  $1\sigma$ : 1017-1151 AD) compared to the expected age of the site (i.e., first half of the 12<sup>th</sup> century A.D.) indicates a failure of the CryoSoniC procedure in DC suppression (i.e., sensitively older ages than expected). ZOR07 was, hence, re-processed according to the updated Cryo2SoniC procedure with the aim of increasing the efficiency in binder carbonates selection producing *ZOR07sand* and *ZOR07susp* (Table 2). A significant effect of rejuvenation induced by the procedure is evident when comparing *ZOR07susp* with *ZOR07sand* (Figure 9; Marzaioli et al. 2013). Measured radiocarbon age on the *ZOR07susp* was in agreement with the estimated average age of the site: 11<sup>th</sup> – 12<sup>th</sup> century and with the major part of measure performed on biological samples collected at the same site (Figure 9).

### *Treviño castle*

Processing mortar sample with traditionally CryoSoniC method and finding a date unmatched with the archaeological attribution, has been repeated the measurement processing the same sample taken from the core of the ancient wall (CTV07) with Cryo2SoniC method and then analyzed. Result of radiocarbon dating on *CTV07\_susp* (773-941 AD at  $1\sigma$  level; Figure10, Table 2) show again a rejuvenation phenomenon if compared with the first measure (*CTV07susp\**). This confirms not only the successful application of Cryo2SoniC despite of the old CyoSoniC but also the chronological reference of the wall fixed at the 10<sup>th</sup> century.

## Conclusions

Over the application of the CryoSoniC to the first study sites (i.e. the Spanish sites) an improvement in the accuracy of the selection method was necessary because of observed pitfalls. The reason of the differential failure of the first CryoSoniC protocol is connected to the mortar composition. Aistra samples were mortars characterized by a quartzous sandy aggregate, which may not affect final dating with an additional DC component. From this information could be deduced that CryoSoniC work on mortars like ones from Aistra (showing a positive feedback) but that probably it doesn't work on other kinds of mortars. Unfortunately there are no petrographical info about Zornotzegi and Trevino samples to interpret but through the observation on RC results could be affirmed that Zornotzegi and Trevino samples were composed differently from Aistra ones. About them could be hypothesized i.e. the presence of an aggregate different from quartz, such as a calcareous one. Presence of unburned limestone residues could be not considered the cause of the aging because has been proved that these kind of contaminants are avoided by the use of the CryoSoniC separation protocol (Marzaioli et al.2011). CryoSoniC as first version, demonstrated to be capable to work both on synthetic and archaeological mortars, with restriction on the lasts to not have other calcareous sources than the eventually unburned limestone residues (i.e. samples from Aistra). The CryoSoniC inapplicability to a generic archaeological sample of unknown composition (like sample from Zornotzegi and Trevino) is connected to its inability to assure a selection of material eligible for a radiocarbon dating, especially when the DC source is not restricted to calcinations relicts. Application of the improved method (Cryo2SoniC) at the opposite, has given results better compatible with archaeological references showing its capability to lock DC contamination on the first *sand* fraction while second selected *susp* fraction was an eligible carrier for an accurate information.

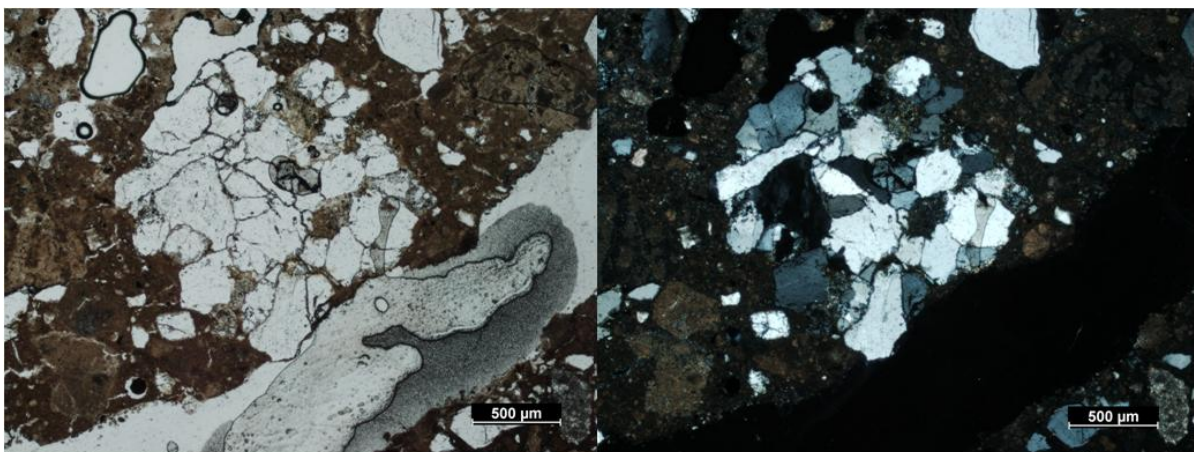


Figure 7. Images at optical microscope in transmitted light (parallel nicols and crossed nicols) where it is shown the quartz nature of the aggregate (Aistra mortars).

Table 2 . Spanish medieval samples from three studied sites, with RC age, calibration and chronological references. SU: stratigraphic unit. Calibrated ages reported as time interval using lowest and highest value of the calibration. (\*) indicates samples collected using the CryoSoniC, all the others are samples collected using Cryo2SoniC.

SAMPLES	SU	RC Ages (years BP)	Err RC	Calibrated Age 1σ	Calibrated Age 2σ	Chronological Reference
AISTRA 1 susp*	-	1160	26	783-943 AD	779-967 AD	10 <sup>th</sup> century
AISTRA 2 susp*	-	1035	28	990-1020 AD	900-1034 AD	
ZOR07 susp*	1106	1357	54	621 - 765 AD	586 - 776 AD	
ZOR07 sand	1106	1284	29	673-771 AD	662-777 AD	11 <sup>th</sup> -12 <sup>th</sup> century
ZOR07susp	1106	978	40	1017-1151 AD	993-1156 AD	
CTV07 susp*	1501	1380	26	646-661 AD	620-671 AD	
CTV07 sand	1501	1359	29	648-673 AD	617-763 AD	10 <sup>th</sup> century
CTV07susp	1501	1184	57	772-944 AD	689-977 AD	

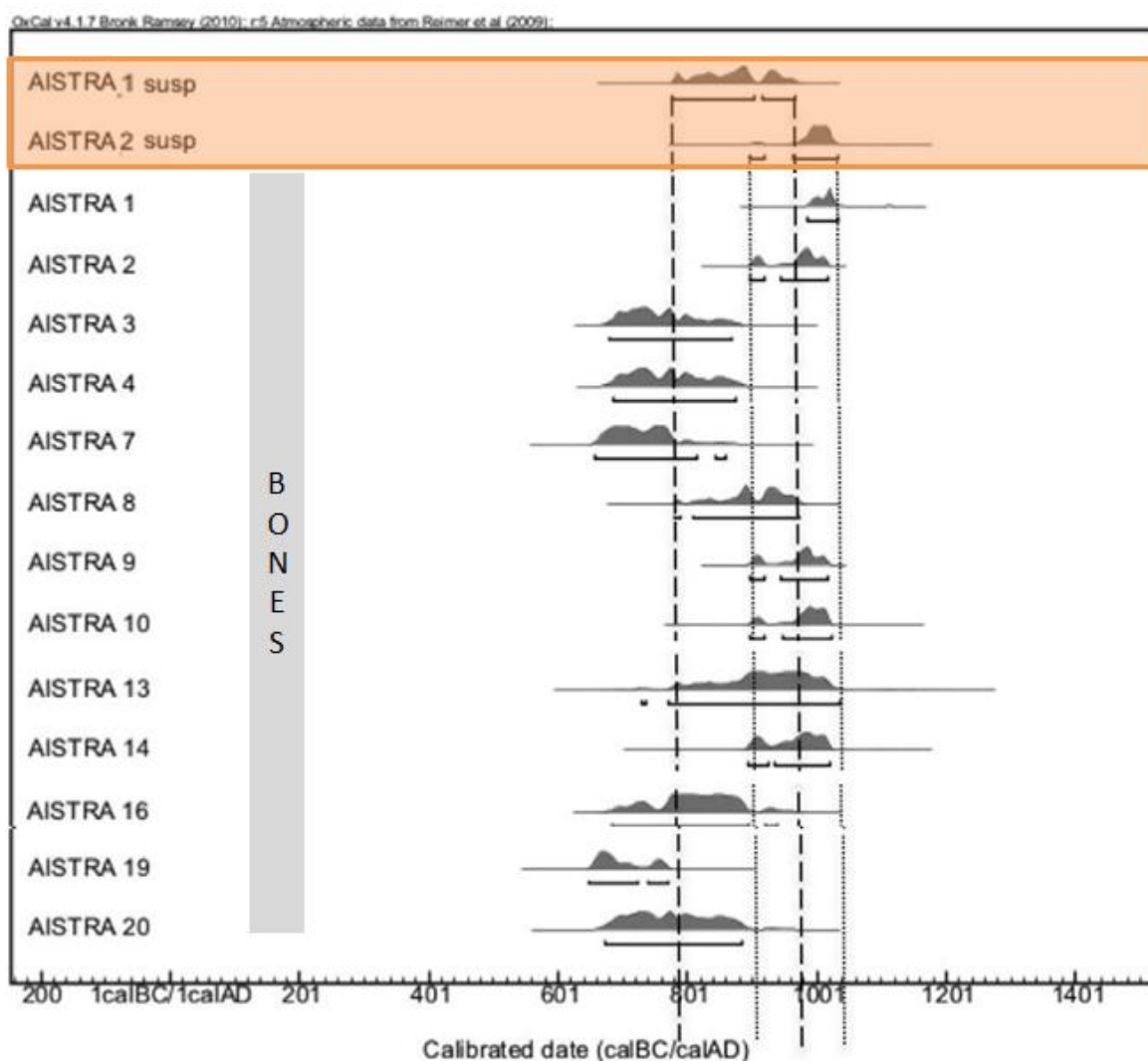


Figure 8. Measured calendar ages (age distributions and 2σ ranges) for the Aistra susp\* fractions (upper section) compared with the measurements of organic samples (bones) from the same site (AISTRA n). Dashed lines represent 2σ intervals for the susp fractions (modified from Marzaioli et al.2013).

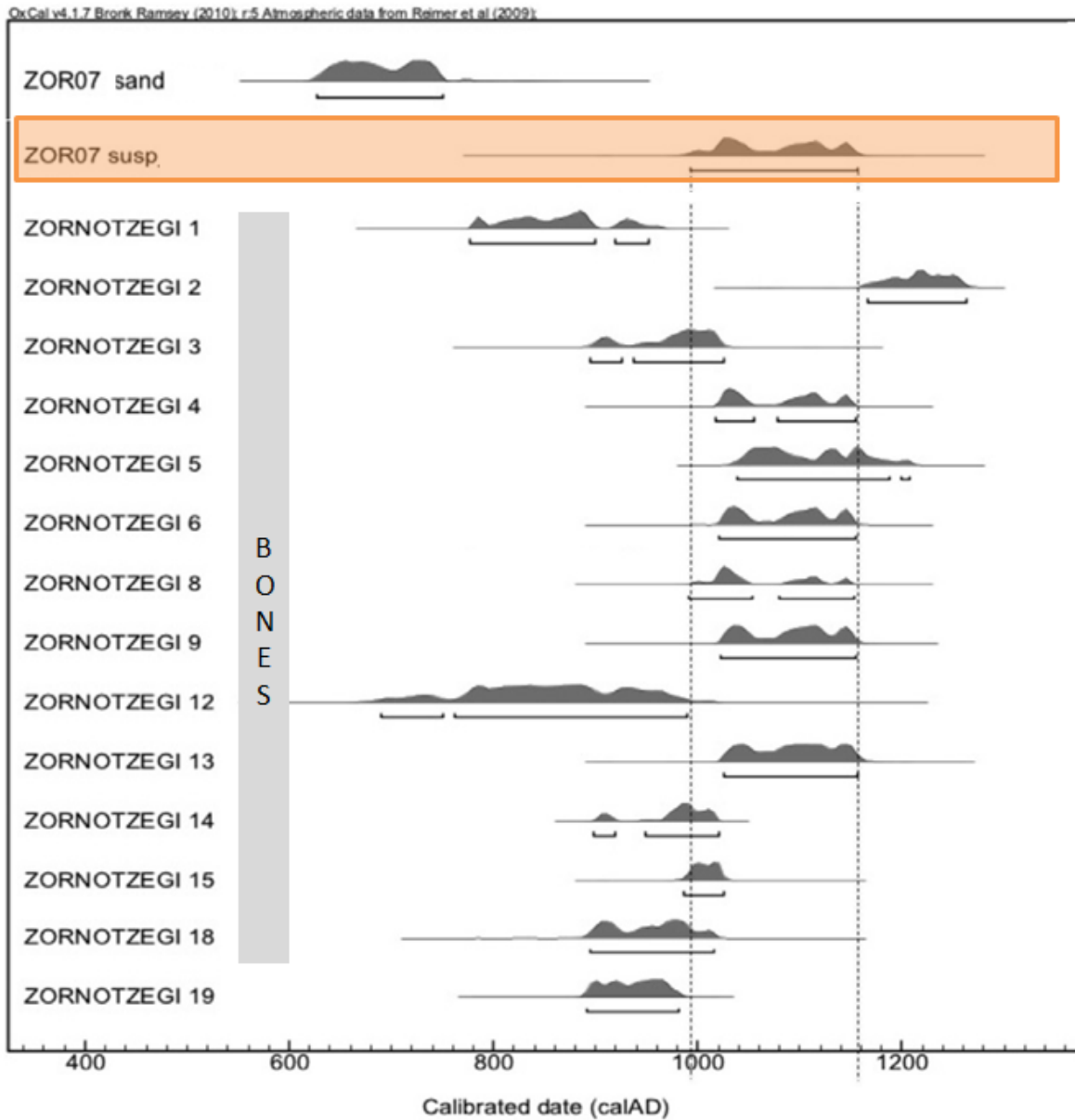


Figure 9. Upper zone: observed difference in the radiocarbon age of Cryo2SoniC fractions (sand and susp) produced by the modified CryoSoniC protocol for the Zornotzegi sample (ZOR07). ZOR07 susp compared with the measurements of organic samples from the same site. Dashed lines represent  $2\sigma$  intervals for the susp fractions (modified from Marzaioli et al. 2013).

### Radiocarbon Age vs. Calibrated Age

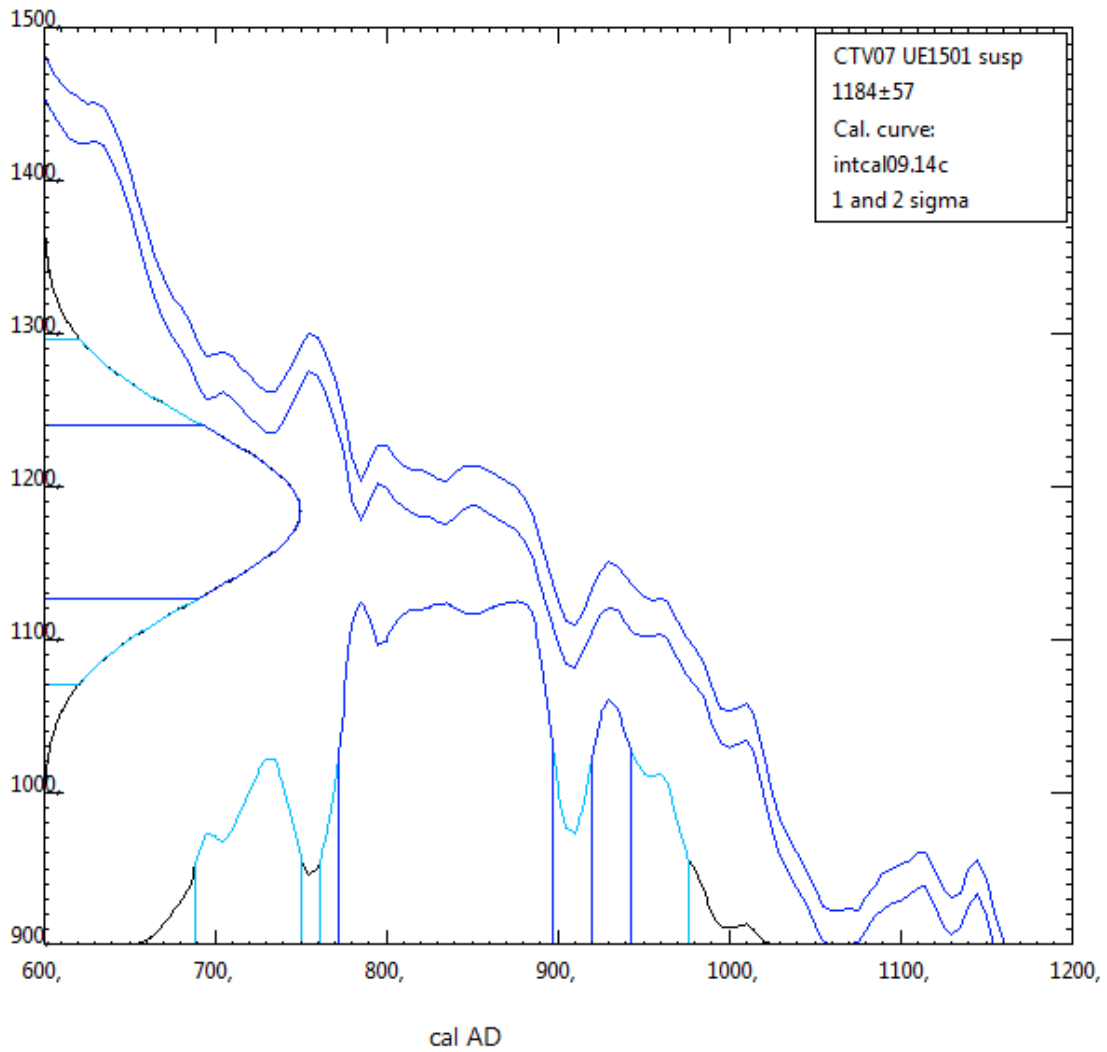


Figure 10. Calibration of CTV susp RC age: attributable to 10<sup>th</sup> century or at the first phases of fortification.

## II.2.2. Publication on NIMB.

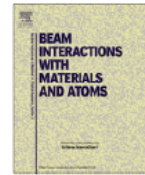
Nuclear Instruments and Methods in Physics Research B 294 (2013) 246–251



Contents lists available at SciVerse ScienceDirect

Nuclear Instruments and Methods in Physics Research B

journal homepage: [www.elsevier.com/locate/nimb](http://www.elsevier.com/locate/nimb)



### Accelerator mass spectrometry $^{14}\text{C}$ dating of lime mortars: Methodological aspects and field study applications at CIRCE (Italy)

Fabio Marzaioli<sup>a,\*</sup>, Sara Nonni<sup>b</sup>, Isabella Passariello<sup>a</sup>, Manuela Capano<sup>c</sup>, Paola Ricci<sup>a</sup>, Carmine Lubritto<sup>a</sup>, Nicola De Cesare<sup>d</sup>, Giacomo Eramo<sup>e</sup>, Juan Antonio Quirós Castillo<sup>f</sup>, Filippo Terrasi<sup>a</sup>

<sup>a</sup> CIRCE, INNOVA and Seconda Università degli Studi di Napoli, Dipartimento di Scienze Ambientali, Caserta, Italy

<sup>b</sup> Dipartimento di Scienze della Terra, "Sapienza" Università di Roma, Italy

<sup>c</sup> CIRCE, INNOVA and Dipartimento di Studio delle Componenti Culturali del Territorio, Seconda Università degli Studi di Napoli, Santa Maria Capua Vetere, Caserta, Italy

<sup>d</sup> CIRCE, INNOVA and Seconda Università degli Studi di Napoli, Dipartimento di Scienze della Vita, Caserta, Italy

<sup>e</sup> Dipartimento di Scienze della Terra e Geoambientali, Università degli Studi di Bari "Aldo Moro", Bari, Italy

<sup>f</sup> Universidad del País Vasco-Euskal Herriko Unibertsitatea, Dipartimento di Geografía, Prehistoria y Arqueología, Vitoria-Gasteiz, Spain

#### ARTICLE INFO

##### Article history:

Received 30 June 2011

Received in revised form 31 August 2012

Available online 14 September 2012

##### Keywords:

Binder carbonates isolation procedure

Lime lumps

Archaeometry

Artifact absolute chronology determination

#### ABSTRACT

Centre for Isotopic Research on Cultural and Environmental heritage (CIRCE) has, recently, obtained some promising results in testing the feasibility of mortar radiocarbon dating by means of an ad hoc developed purification procedure (CryoSonic: Cryobreaking, Sonication, Centrifugation) applied to a series of laboratory mortars. Observed results encouraged CryoSonic accuracy evaluation on genuine mortars sampled from archeological sites of known or independently constrained age (i.e., other  $^{14}\text{C}$  dates on different materials).

In this study, some  $^{14}\text{C}$  measurements performed on genuine mortars will be discussed and compared with independently estimated (i.e., radiocarbon/archaeometrical dating) absolute chronologies of two Spanish sites. Observed results confirm the agreement of the CryoSonic mortar dates with the archaeological expectations for both examined cases.

Several authors reported the possibility of obtaining accurate radiocarbon dates of mortar matrices by analyzing lime lumps: binder-related particles of different sizes exclusively composed of calcium carbonate.

In this paper, preliminary data for the absolute chronology reconstruction of the Basilica of the cemetery complex of Ponte della Lama (Canosa di Puglia, Italy) based on lime lumps will also be discussed. Dating accuracy will be quantified by comparing  $^{14}\text{C}$  data on mortar lime lumps from a funerary inscription of known age found near the Basilica, in the same study site. For this site, a comparison between absolute chronologies performed by bulk and CryoSonic purified lime lumps, and charcoal incased in mortars (when found) will also be discussed.

Observed results for this site provide evidence of how bulk lime lump dating may introduce systematic overestimations of the analyzed sample while CryoSonic purification allows accurate dating.

© 2012 Published by Elsevier B.V.

#### 1. Introduction

Mortars represent a class of construction materials virtually ubiquitous at archeological sites from the Neolithic period on [1]. Mortar matrix can be schematically divided in two portions: the binder and the aggregates.

\* Corresponding author. Tel.: +39 0823274814; fax: +39 0823274605.

E-mail addresses: [fabio.marzaioli@unina2.it](mailto:fabio.marzaioli@unina2.it) (F. Marzaioli), [sara.nonni@uniroma1.it](mailto:sara.nonni@uniroma1.it) (S. Nonni), [isabella.passariello@unina2.it](mailto:isabella.passariello@unina2.it) (I. Passariello), [manuela.capano@unina2.it](mailto:manuela.capano@unina2.it) (M. Capano), [paola.ricci@unina2.it](mailto:paola.ricci@unina2.it) (P. Ricci), [carmine.lubritto@unina2.it](mailto:carmine.lubritto@unina2.it) (C. Lubritto), [nicola.decesare@unina2.it](mailto:nicola.decesare@unina2.it) (N. De Cesare), [giacomo.eramo@uniba.it](mailto:giacomo.eramo@uniba.it) (G. Eramo), [quiros.castillo@ehu.es](mailto:quiros.castillo@ehu.es) (J.A. Quirós Castillo), [filippo.terradi@unina2.it](mailto:filippo.terradi@unina2.it) (F. Terrasi).

Based on the process determining the setting, the binders can be distinguished in aerial or hydraulic form also if intermediate classes are produced by adding different aliquots of inert materials (e.g., pozzolana, crushed bricks) [2].

Aggregates used to produce mortars vary both in size and type of material (e.g., crushed bricks, silicate minerals, marble powder). They are usually mixed with the lime putty (aged slaked lime) with the aim of increasing material workability and avoiding cracks due to drying during setting [3,4]. Usage of materials characterized by sensitive concentrations (>15%) of aluminates and amorphous silicates [5] (i.e., pozzolana, volcanic ashes, crushed bricks) confers light hydraulic properties to lime mortars. This constituted, since Roman times, a breakthrough in mortar production technology



allowing the speeding up of mortar hardening and increasing mortar mechanical resistance [6].

While hydraulic mortars mostly harden because of hydration reactions, aerial binders hardening is due to the process of carbonation: the multistep reaction of atmospheric CO<sub>2</sub> with the slaked lime (Ca(OH)<sub>2</sub>) to produce calcium carbonate (CaCO<sub>3</sub>). This process makes the binder of aerial mortars an interesting proxy preserving, virtually unvaried, the signature of the atmospheric CO<sub>2</sub> absorbed over the period of mortar hardening.

Binder carbonates can be used to date artifacts:

- i) If the hardening period (usually a few years) is negligible with respect to the radiocarbon decay constant (5730 a [7]) and the expected uncertainty on the measured radiocarbon age (few decades for our laboratory [8]);
- ii) if the calcination (Carbonatic rock → quick lime) was performed attaining high efficiencies (i.e., no C residuals (calcinations relics) survived in the quick lime).

Several drawbacks [9] have been observed since the beginning of the experiments on <sup>14</sup>C dating of mortars [10]. These fluctuations are related to the partial failure of the mortar radiocarbon dating working hypotheses. For example, the presence of exogenous carbonate contaminations affecting the sample and low efficiencies in isolating the binder from calcareous aggregates can lead to sensitive biases resulting in a contamination effect altering the measured age of samples. Hence, mortars sampled from the surface of a wall can be affected by exogenous carbonate contaminations (i.e., running water depositing dissolved inorganic carbon over centuries) while mortars sampled too deep can be affected by low carbonation velocities both leading to <sup>14</sup>C rejuvenation. Nevertheless the most recalcitrant source of contamination affecting mortars is represented by the calcination relics of limestone surviving into the mortar and preserving a Dead Carbon (DC) fingerprint. An innovative methodology aiming to suppress calcination relics C by means of a sequence of physical separations (i.e., Cryo-SoniC) has been recently developed and tested at CIRCE [11]. Cryo-SoniC showed its overall effectiveness for laboratory samples produced at *T* ranging from 800 to 1100 °C simulating only the binder phase with no aggregates interactions.

With the aim of checking the effectiveness of the methodology on field samples, including the suppression of eventual “aggregates effects”, in this paper we applied our procedure to genuine mortars from two sites in Spain.

Lime lumps radiocarbon dating has been reported as an accurate methodology for mortar radiocarbon dating [12,13]. Lime lumps *in sensu stricto* are binder-related nodules often rounded and porous, appearing distinctly in the mortar matrix [14]. Their origin is not agreed upon: (i) some argue their genesis comes from a poor mixing of the lime putty with aggregates [13]; (ii) some attribute their development to dry slaking (i.e., the mixing of wet sand with burnt lime fragments (quick limes)) [15]; (iii) some others attribute lime lumps development to the carbonate crust that forms on top of lime putty when maturing [16]. The evident advantage of dating lime lumps is that they represent the binder already purified by aggregates. Eventual contributions of calcination relics in the lime lumps cannot be inferred in advance on the sample to be analyzed since (i) they appear in the same mineral form (calcite) as the lime lump; (ii) the Optical Microscopy (OM) methodology cannot be directly applied to the sample to be dated. In this study some data regarding lime lumps dating will be discussed and compared with dating of charcoal encased in mortar. These kinds of charcoal have been used to study artifact chronologies by Berger [17]. Moreover the application of the Cryo-SoniC procedure to lime lumps will be discussed in terms of its accuracy evaluation for one Italian study site.

## 2. Methods

### 2.1. Study sites description

#### 2.1.1. San Julian e Santa Basilisa di Aistra

The church of San Julian e Santa Basilisa in Zaldondo represents one of the most ancient and best preserved medieval churches of the Álava province in the Basque country (Spain). The chronology of this structure is mostly based on formal and stylistic analyses of windows and walls, and it is still contradictory. Over the 2006–2009 period, the church underwent deeper analyses allowing the better constraining of its chronology in the framework of the Aistra village archaeological project performed in collaboration with the Institute of archaeology UCL (University College London). Thanks to a series of <sup>14</sup>C dates (mostly bones, 20 of them are showed in Fig. 1) and other archaeological evidences, church construction was attributed to the fourth phase of the Aistra village (i.e., 10th century A.D.) [18].

Two samples belonging to the external walls of the church of San Julian were sampled (AISTRA 1 and AISTRA 2). Stratigraphic interpretation of the structure and comparison with available data, guided the choice of two samplings for this site: AISTRA 1 was sampled from the north eastern corner of the structure and supposed to belong to the first phase of development of the church; AISTRA 2 was sampled from the south eastern facing wall of the church and hypothesized to be of a later age [19].

#### 2.1.2. Santa Maria di Zornotzegi

The Santa Maria di Zornotzegi village is also situated in the eastern Álava province. This archeological site developed continuously in the period from the 5th to the 14th century with a first settlement during the bronze age [20]. Santa Maria di Zornotzegi is characterized by the presence of the so called “fallen chapel”, a religious building, nowadays mostly dismantled because of its materials re-use. The fallen chapel is founded on a previous structure by means of a basement of filling raw materials. Pottery analysis, applied architectural styles and several radiocarbon measurements on organic materials (mostly charcoals and bones, 20 of them shown in Fig. 2) found at the study site during archaeological sample processing (i.e., flotation), allowed the precise constraint of the chronology of the structure in the first half of the 12th century A.D.

To avoid weather exposure contaminations, one sample situated few centimeters from the surface of the north facing wall of this structure (ZOR07) was sampled and analyzed.

#### 2.1.3. Cemetery complex of Ponte della Lama

The cemetery complex of Ponte della Lama, discovered in the beginning of the '50s, is found near the city of Canosa di Puglia (Apulia, Southern Italy). It developed in a period ranging from 2nd to 6th century A.D. along the *via Traiana*. The complex is composed of different structures, among them (i) the catacombs representing one of the most important examples for the Apulia region for extension and preservation [21]; (ii) the Basilica founded around the 4th century A.D. This artifact plays an important role in the cemetery complex and some questions regarding this structure are still unsolved. First of all the chronology of the Basilica development/usage is not very well defined and, secondly, an abrupt discontinuity in the usage of raw building materials regarding the north-facing side of the structure requires deeper analyses. Radiocarbon dating of mortars, combined with chemical and petrographic analyses, were applied for the definition of the Basilica development. Basilica lime mortars contain (i) calcination relics of biomicritic limestone origins; (ii) carbonate aggregates (a sensitive fraction of total aggregates) whose dimensions vary from medium to fine sand sizes.

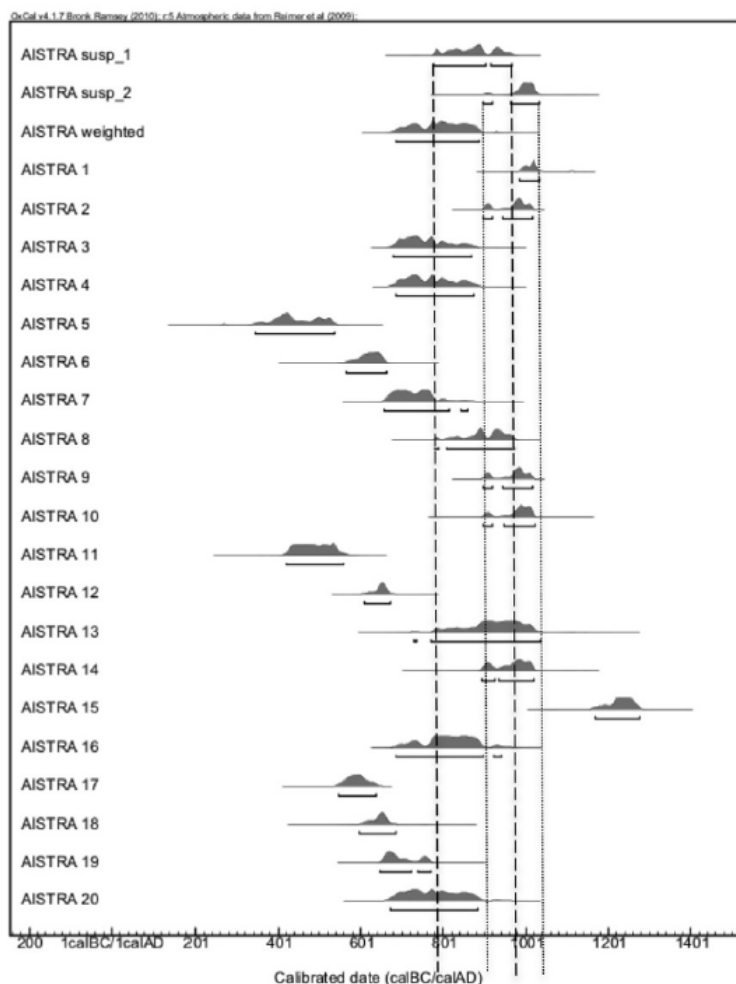


Fig. 1. Measured calendar ages (age distributions and  $2\sigma$  ranges) for the Aistra susp fractions (AISTRA susp\_1 and AISTRA susp\_2, first two age distributions) compared with the Aistra site average age (weighted average of measured  $^{14}\text{C}$  values, AISTRA weighted) and the measurements of organic samples from the same site (AISTRA 1–20). Dashed lines represent  $2\sigma$  intervals for the susp fractions.

Two Wall Stratigraphic Contexts (WSCs) of the Basilica were sampled: CPLM 12L and CPLM 18L and lime lumps extracted. Bulk lumps (CPLM 12L\_lump and CPLM 18L\_lump) underwent CryoSonic procedure (CPLM 12L\_susp\_lump and CPLM 18L\_susp\_lump). Inside CPLM18L mortar encased charcoal was also found which underwent sample processing and measurement according to Berger [17].

An epigraph with an inscription engraved upon fresh mortar applied during the grave sealing was discovered in the catacombs belonging to the same archaeological context. Thanks to the inscription: “*Sine collega Flavius Rufius Placidus*” the epigraph was attributed to 481 A.D. Epigraph mortar manufacture appeared grosser with respect to the Basilica ones. With the aim of procedure accuracy evaluation, one lime lump (CPLM1\_lump), its CryoSonic produced fraction (CPLM1\_susp\_lump) and one encased charcoal sample extracted from the same WSC were extracted and radiocarbon dated.

## 2.2. Samples pretreatment and $^{14}\text{C}$ measurement

The main goal of the CryoSonic procedure for mortar radiocarbon dating is the isolation of the carbonate fraction merely attrib-

utable to the carbonation of slaked lime. Sampled mortars underwent:

1. **Cryogenical braking:** Following Nawrocka et al. [22], mortar pieces (about 5 g) were submerged in liquid nitrogen until they reached thermal equilibrium and transferred immediately into an oven at  $80\text{ }^\circ\text{C}$ . This cycle was repeated almost three times. At the end of these freezing/thawing cycles mortars were broken by gentle hammering.
2. **Size selection:** Fractured material, spanning over a wide range of particle size, was wet filtered, in decarbonated/deionized water (DDW), at  $500\text{ }\mu\text{m}$ .
3. **Ultrasonic selection:** Filtered particles after complete sedimentation and water removal, were re-wet with 40 ml of DDW and ultrasonicated for 30'. Only materials being suspended (*susp*) by the induced ultrasonic shock (i.e., finer and more fragile particles) were selected by siphoning about 30 ml of the water into a centrifuge tube.
4. **Centrifugation:** Centrifuge vials containing *susp* carbonates were centrifuged @  $7874g$  for 5' and oven dried ( $T = 80\text{ }^\circ\text{C}$ ) overnight.

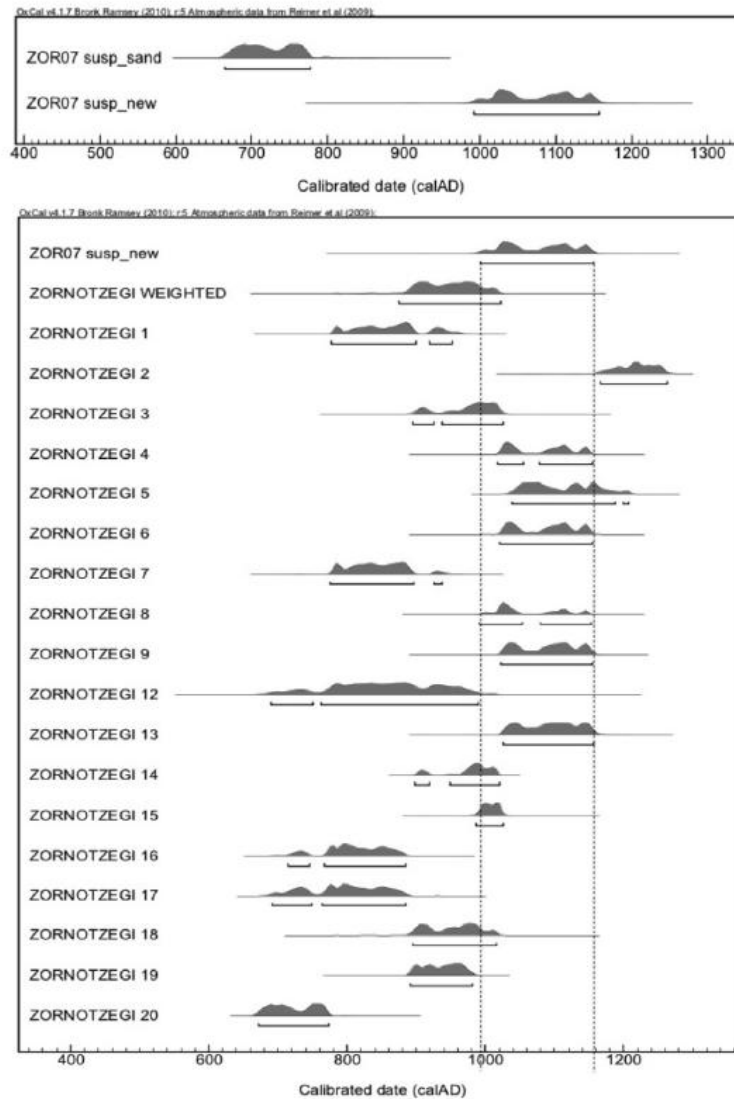


Fig. 2. Upper panel: observed difference in the radiocarbon age of *susp* fractions (*susp\_sand* and *susp\_new*) produced by the modified CryoSonic protocol for the Zornotzegi sample (ZOR07). Lower panel: comparison of the ZOR07 *susp\_new* with the site average age (ZORNOTZEGI weighted) and the measurements of organic samples from the same site (ZORNOTZEGI 1–20). Dashed lines represent  $2\sigma$  intervals for the *susp\_new* fractions.

Due to some experimental observations (data not shown in this paper) the CryoSonic procedure was later updated in order to increase the DC contamination suppression efficiency observed in conventional CryoSonic purified samples. In detail, we split the original ultrasonication procedure (step 3) in two sub-phases: (i) the first ultrasonication was applied for 10' producing the *susp\_sand* fraction; (ii) the second was applied, after a complete removal of the liquid phase and the adding of 40 ml of clean DDW, for 30' producing the *susp\_new* fraction.

Weighted *susp* fractions (up to 15 mg of material) and carbonate standards samples (i.e., IAEA C1 and C2 [23]) were converted into  $\text{CO}_2$  by means of orthophosphoric acid digestion [24] for 2 h @ 85 °C.

Charcoal samples found in the mortars were pretreated according to Berger [17] and combusted together with normalization/check standards and background samples (blank).

Produced  $\text{CO}_2$  was cryogenically purified by other gasses, reduced to graphite on iron powder catalyst according to the CIRCE sealed tube reaction protocol [25] and measured for  $^{14}\text{C}$  isotopic ratios determination [26]. Measured radiocarbon ratios were converted to R.C. ages [27] and calibrated to absolute ages by means of OxCal 4.1 [28].

### 3. Results and discussion

#### 3.1. San Julian e Santa Basilisa di Aistra

Fig. 1 shows results arising from the radiocarbon dating performed on organic materials found at the Aistra site. Church average age was estimated by weight averaging measured  $^{14}\text{F}$  abundances [27] of samples reported in Fig. 1 (AISTRA 1–20), evaluating its R.C. age and calibrating it by means of Oxcal 4.1 (AISTRA

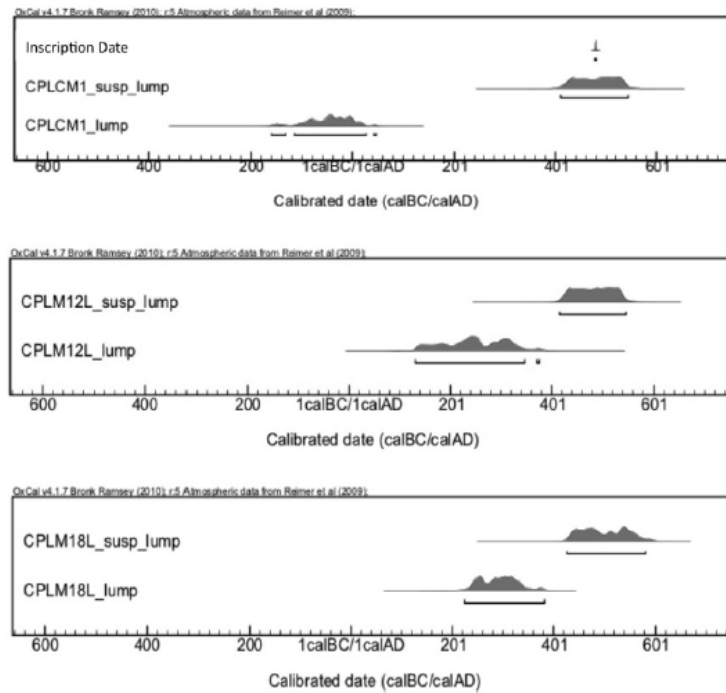


Fig. 3. Measured calendar ages for the Ponte della Lama samples. For each sample both lump (CPLCM1\_lump, CPLM 16L\_lump and CPLM 18L\_lump) and *susp\_lump* (CPLCM1\_susp\_lump, CPLM 16L\_susp\_lump and CPLM 18L\_susp\_lump) calendar ages are shown, for CPLCM1 also the established age of the funerary epigraph is displayed.

weighted).  $2\sigma$  ranges are also plotted as dispersion indexes for the measured distributions of the calendar ages. Measured absolute ages on the mortar *susps* (AISTRA *susp\_1* and AISTRA *susp\_2*) appear in agreement at  $2\sigma$  level. Measured calendar ages on the *susp* fractions showed a slightly different behavior with respect to the expected age of the Church (AISTRA weighted), being AISTRA *susp\_1* in agreement at  $1\sigma$  level and AISTRA *susp\_2* lying slightly upon  $2\sigma$ . This observation indicates later ages for the AISTRA 2 sample probably attributable to a secondary stage of the structure in agreement with archaeological analyses of the San Julian e Santa Basilisa church [19] (see Section 2).

### 3.2. Santa Maria di Zornotzegi

Structure average age was estimated by weight averaging measured  $^{14}\text{F}$  abundances [27] of samples reported in Fig. 2 (ZORNOTZEGI 1–20), evaluating its R.C. age and calibrating it by means of Oxcal 4.1 (ZORNOTZEGI weighted). For this site ZOR07 mortar was processed according to the conventional CryoSonic procedure. Measured radiocarbon age on ZOR07\_susp ( $4122 \pm 50$  B.P.) compared to the expected age of the site (i.e., first half of the 12th century A.D.) indicates a failure of the CryoSonic procedure in DC suppression (i.e., older ages than expected). ZOR07 was, hence, re-processed according to the updated CryoSonic procedure with the aim of increasing the efficiency in binder carbonates selection producing ZOR07\_susp\_sand and ZOR07\_susp\_new.

A significant effect of rejuvenation induced by the procedure is evident when comparing ZOR07\_susp\_new with ZOR07\_susp\_sand (Fig 2 (upper panel)). Measured radiocarbon age on the ZOR07\_susp\_new was in agreement with the estimated average age of the site (ZORNOTZEGI weighted, Fig. 2 (lower panel)).

### 3.3. Cemetery complex of Ponte della Lama

For this archeological site available data includes encased charcoals, bulk lime lumps and CryoSonic purified *susp\_lumps*. Accuracy evaluation in lime lumps dating, for this site, was performed by comparing measured radiocarbon activities on one lime lump extracted from an epigraph of well constrained age (CPLCM1 see methods).

Given the accurate results generally observed using bulk lime lumps [12,13] for radiocarbon dating, lime lumps from this site had been originally acid digested [24] following the protocol applied at CIRCE for carbonates. Observed results on CPLCM1 indicate a measurable DC effect affecting the radiocarbon age estimation of the mortar when bulk lump is used (CPLCM 1\_lump (Fig. 3)). CPLCM 1\_lump, in fact, appeared to be compatible with the 1st century B.C. Because of their formation process, lime lumps do not contain aggregates, hence observed discrepancies can be exclusively attributed to the presence of calcination relics. This experimental observation lead us to apply the CryoSonic classical procedure also to lumps. Residues (up to 10 mg) of the previously dated bulk lumps were pretreated to produce *susp\_lump* fractions and measured. It can be noted how the application of CryoSonic efficiently removed the effect of calcination relics on measured radiocarbon ages leading to unbiased age for the epigraph sample (CPLCM1\_susp\_lump).

A similar effect (i.e., smaller but significant DC) was observed for the other two analyzed lime lumps (CPLM12L\_lump and CPLM 16L\_lump) compared to CPLM12L\_susp\_lump and CPLM 16L\_susp\_lump.

Also in this case the application of the CryoSonic procedure to produce *susp\_lump* fractions brought all the other  $^{14}\text{C}$  ages to values compatible with the archeological expectations for the Basilica

(4th century A.D.) reducing the lime lumps observed DC effect virtually to zero.

Difference in the DC contamination affecting the analyzed lime lumps (i.e., CPLCM1 lump appeared sensitively older than the CPLM12L\_lump and CPLM 16L\_lump) well matches some observations on the technology used during mortar production. CPLCM1, in fact, turned out to be produced by means of a grosser manufacturing process probably leading to higher amounts of calcination relics in the examined mortars.

Dating of charcoal intrusions in the mortar matrix revealed, again, a strong DC contamination evidenced by corresponding calendar ages of 10th century B.C. and 1st century B.C. respectively for the CPLCM1 and CPLM 18 L samples. This observation is attributable to the lack of carbonate suppression during the coal pretreatment also if ad hoc methodologies [17] were applied.

#### 4. Conclusions

Radiocarbon dating of mortars has been attempted since the '60s with still ambiguous results. The method development can lead to sensitive improvement for the applied archaeology allowing dating of artifacts, from the Neolithic period on, with no need for organic materials and no risk of wrong age estimations because of material recycling. In this paper, after the development and testing of a new methodology for mortar radiocarbon dating (CryoSonic) at CIRCE, some applications to genuine field mortars are shown. Observed results on San Julian e Santa Basilisa di Aistra church were in agreement with the archaeometrical expectations. Santa Maria di Zornotzegi results revealed the necessity to update the classical CryoSonic procedure. Observed results, after the application of the updated CryoSonic procedure led to accurate  $^{14}\text{C}$  dating also for this site.

Our data on lime lumps revealed how the dating of this class of materials can be affected by significant offsets strictly connected to the technology applied for the calcination of the primary limestone during mortar production. For the Ponte della Lama site this effect was visible for all the analyzed lumps, and the production of purified *susp\_lump* fractions efficiently removed DC contamination attributable to this interfering source.

Also if more experiments should be produced, this work shows the general applicability of the CryoSonic procedure to extract a carbonate fraction capable of guaranteeing accurate radiocarbon dating from mortars. Data presented in this paper clearly indicate how the procedure validation must be supported by a series of geological analyses (i.e., thin sections + optical microscopy, XRD) sustaining some, otherwise assumed, scenarios for the correct data interpretation.

#### Acknowledgments

The authors are grateful to the anonymous referee and to the managing editor for their review of the paper and for their valuable suggestions.

#### References

- [1] J.A. Rech, *Near Eastern Archaeology* 67 (2004) 212–219.
- [2] A. Moropoulou, K. Polikreti, A. Bakolas, P. Michailidis, *Cem. Concr. Res.* 33 (6) (2003) 891–898.
- [3] O. Cazalla, C. Rodriguez-Navarro, E. Sebastian, G. Cultrone, M.J. De la Torre, *J. Am. Ceram. Soc.* 83 (2000) 1070–1076.
- [4] P. Lawrence, M. Cyr, E. Ringot, *Cem. Concr. Res.* 33 (2003) 1939–1947.
- [5] A. Moropoulou, A.S. Cakmak, G. Biscontin, A. Bakolas, E. Zendri, *Construction and Building Materials* 16 (8) (2002) 543–552.
- [6] Vitruvius, *De Architectura*, Book II, V. Frank Granger's translation (Heinemann, 1931).
- [7] H. Godwin, *Nature* 195 (1962) 984.
- [8] F. Terrasi, N. De Cesare, A. D'Onofrio, C. Lubritto, F. Marzaioli, I. Passariello, D. Rogalla, C. Sabbarese, G. Borriello, G. Casa, A. Palmieri, *Nucl. Instr. Meth. Phys. Res.* 266 (2008) 2221–2224.
- [9] M. VanStrydonck, M. Dupas, M. Dauchot-Dehon, Ch. Pachiaudi, J. Marechal, *Radiocarbon* 28 (2A) (1986) 702–710.
- [10] G. Delibrias, J. Labeyrie, 6th International Conference on Radiocarbon and Tritium Dating, Pullman, WA, 1965.
- [11] F. Marzaioli, C. Lubritto, S. Nonni, I. Passariello, M. Capano, F. Terrasi, *Anal. Chem.* 83 (2011) 2038–2045.
- [12] G. Pesce, G. Quarta, L. Calcagnile, M. D'Elia, P. Cavaciocchi, C. Lastrico, R. Guastella, *Radiocarbon* 51 (2009) 867–872.
- [13] A. Lindroos, J. Henemeier, A. Ringbom, M. Brasken, A. Sveinbojmsdottir, *Radiocarbon* 49 (2007) 47–67.
- [14] J. Elsen, *Cem. Concr. Res.* 36 (2006) 1416–1424.
- [15] K. Callebaut, K. Van Balen, in: *Proceedings of the International workshop on Urban Heritage and Building Maintenance VII "Maintenance and restrengthening of materials and structures: Plaster"*, Zürich, 2000, pp. 65–72.
- [16] S. Bruni, F. Cariati, P. Fermo, P. Cairati, G. Alessandrini, L. Toniolo, *Archeometry* 39 (1) (1997) 1–7.
- [17] R. Berger, *Radiocarbon* 34 (3) (1992) 880–889.
- [18] A. Reynolds, J.A. Quirós Castillo, *Despoblado de Aistra (Zalduondo)*, *Arkeoikuskua* 06, pp. 94–100; 07, pp. 159–167; 08, pp. 209–211 (2007–2010).
- [19] J.A.Q. Castillo, F. Marzaioli, C. Lubritto, *Arqueología De La Arquitectura* 8 (2011) 13–24.
- [20] J.A. Quirós Castillo, *Final report of the Zornotzegi (Salvatierra-Agurain) Archaeological Project*, 2010.
- [21] D. Nuzzo, A. Rocco, G. Disantarsa, *The journal of Fasti online*, Associazione Internazionale di Archeologia Classica, Roma, 2008.
- [22] D. Nawrocka, J. Michniewicz, J. Pawlyta, A. Padzur, *Geochronometria* 24 (2005) 109–115.
- [23] K. Rozanski, W. Stichler, R. Gonfiantini, E.M. Scott, R.P. Beukens, B. Kromer, J. van der Plicht, *Radiocarbon* 34 (3) (1992) 506–519.
- [24] J.M.J. McCrea, *Chem. Phys.* 18 (1950) 849–857.
- [25] F. Marzaioli, G. Borriello, I. Passariello, C. Lubritto, N. De Cesare, A. D'Onofrio, F. Terrasi, *Radiocarbon* 50 (1) (2008) 139–149.
- [26] F. Terrasi, N. De Cesare, A. D'Onofrio, C. Lubritto, F. Marzaioli, I. Passariello, D. Rogalla, C. Sabbarese, G. Borriello, G. Casa, A. Passariello, *Nucl. Instr. Meth. Phys. Res.* 266 (2008) 2221–2224.
- [27] M. Stuiver, H.A. Polach, *Radiocarbon* 19 (3) (1977) 355–363.
- [28] B.C. Ramsey, *Radiocarbon* 51 (1) (2009) 337–360.

### **II.3. Lime Lumps: a successful resource.**

Lime lump dating has been tested in order to evaluate the possibility to date an archaeological mortar independently by its aggregates composition. First testing on lime lumps found that the radiocarbon dating produced many positive feedbacks (Van Strydonck et al 1992; Lindroos 2005; Pesce et al. 2009, 2012). All these trials are associated with the usage of the whole lump material as the best proxy to find the binder age assuming that an appropriate selection of the lump is sufficient to obtain accurate results. In this chapter experimental clues indicating how lime lumps represent a system potentially affected by DC contamination (i.e. calcination relics) will be discussed and the choice of a selection protocol assuring calcination relics suppression with high efficiency will be developed and tested in order to guarantee successful mortar dating.

A lime lump in *sensu stricto* is a binder-related nodule often rounded and porous, appearing distinctly in the mortar matrix. It is a common element whose presence is independent of the site, the construction period, the manufacture typology and the raw materials employed in the preparation of the mortar mixture (Bakolas et al. 1995; Bugini and Toniolo, 1990). The lime lumps origin is not agreed yet upon: (i) some authors argue their genesis comes from a poor mixing of the lime putty with aggregates (Lindroos et al. 2007); (ii) some others attribute their development to dry slaking (i.e., the mixing of wet sand with burnt lime fragments (quick limes)) (Callebaut and Van Balen 2000); (iii) some others attribute lime lumps development to the carbonate crust that forms on top of lime putty when maturing (Bruni et al. 1997).

Lime lumps are similar to binder constituting the surrounding matrix (Franzini et al. 1990; Bruni et al. 1997; Bakolas et al., 1995) with only differences in their micro-morphology (some authors hypothesize that crystals in these lumps developed over a shorter time period compared to the crystals of the matrix; Bruni et al. 1997). These differences are described by Bakolas and colleagues as: “The matrix of the mortar surrounding the lumps appear to be of compact texture with smaller porosity in respect to the lumps” and, moreover, “in many cases the growth of the binder crystals is greater than the lumps” (Bakolas et al., 1995).

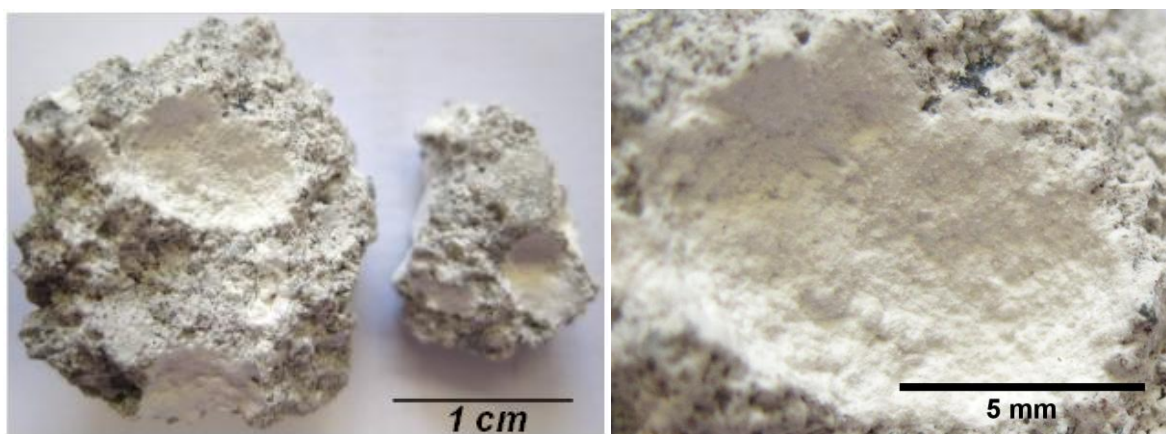
For a successful application of the “pure lime lumps” dating technique to identify suitable lime lumps and distinguish them from several other types of nodules commonly found embedded within old mixtures is fundamental. These ‘troublemakers’ include:

- unburned pieces of limestone (Leslie & Hughes, 2002, Ingham, 2005, Elsen, 2006);
- over burned pieces of limestone (Leslie & Hughes 2002, Ingham, 2005, Elsen, 2006, Elsen et al., 2004);

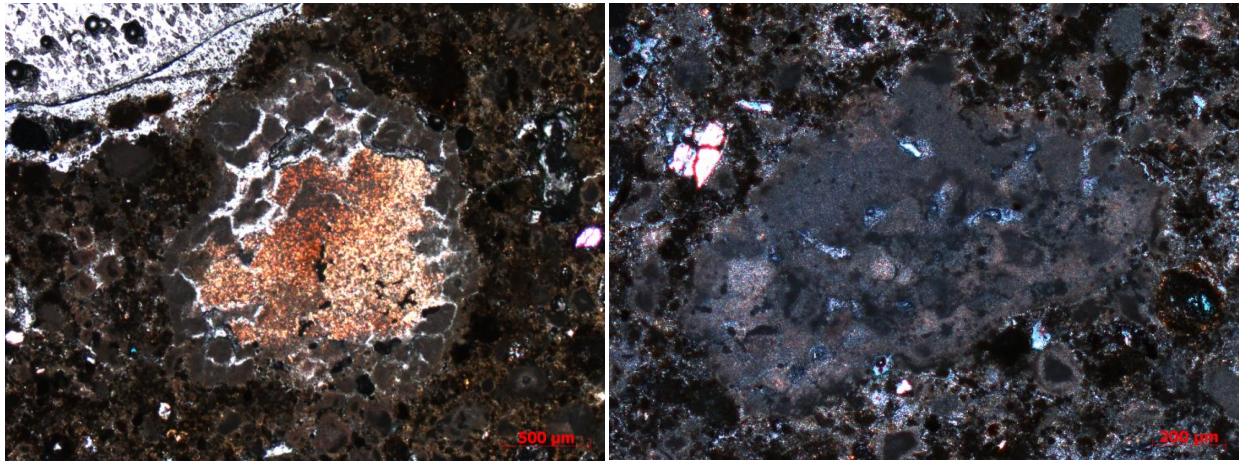
- pieces of burned limestone containing high concentrations of silica (these arise when the stone used for the lime production contains high quantity of impurities (Elsen et al., 2004, Bakolas et al., 1995));
- concretions of recarbonated lime (Pesce & Ball 2012);
- lumps of pure calcium carbonate due to the carbonation of lime putty (Leslie & Hughes 2002; Franzini et al. 1990; Bugini & Toniolo 1990; Ingham 2005; Elsen 2006; Elsen et al. 2004; Bakolas et al. 1995).

Among these, only the lumps belonging to the latter group should be selected for radiocarbon purposes with all fitted expedients. If this is the case, the evident advantage of dating lime lumps is that they are a faithful representation of the binder with no aggregates influences. A binder purified by a hypothetical aggregate implies that dead carbon signal owned by aggregates is avoided and the eventual dead carbon source affecting lime lumps could be limited to the presence of calcinations relicts (from an incomplete burning of the original carbonate). That is why the lime lumps offer a great challenge in the suppression of mortar contamination problems.

First of all, the most important step is the sampling: select a good lime lump is the first step for a successful dating. Lumps of pure lime are easily identifiable in old lime mixtures as they exhibit a white, rounded and floury complexion (Figure 11). Surface hardness of this type of lump is very low making them extremely delicate to handle and easily damaged (Pesce & Ball 2012). The surfaces of lime lumps have a floury appearance while those of under burned lumps and sand grains appear denser resembling stone. Evaluation of the superficial hardness is a useful method for distinguishing between similar lumps (incompletely burn limestone or roundly grains of milky quartz). Even performing a crude test, by hand, using a needle point, allows these different types of



*Figure 11. Pure lime lumps in a specimen of air lime mortar and detail of the lime lump (right hand side); (Pesce & Ball 2012).*



*Figure 12. Photomicrograph of a lime lump with calcination relicts, suitable for dating only applying the CryoSoniC procedure (left). Photomicrograph of a lime lump without evident calcination relicts (right), theoretically useful for dating even if measured as it is.*

lumps to be effectively distinguished. During the sampling it is required to pay a lot of attention: for example, when the inner part of the masonry is accessible, it is always important to consider the possible re-carbonation of lime lumps and the depth from which samples within the wall should be taken. Care is needed to avoid unusual situations such as water pockets and mixtures not belonging to the original structure such as pieces of plaster applied after its construction. In the same manner samples taken deep inside the wall, where incompletely or delayed carbonated lime may be present, should be avoided. In this case it is useful to remember that the carbonation process initiates from the external surfaces of a structure and progresses towards the inner region at decreasing speed. This is a condition to apply not only to the sampling of lime lumps but also to a generic mortar sampling. When a suitable depth of sampling is reached, a lump containing sufficient material for the radiocarbon dating must be identified. In the case that a single lump does not contain sufficient material, multiple lumps from the same region of the masonry can be pooled and utilized (in archaeological terms this means from the same stratigraphic unit) (Pesce & Ball 2012).

Being most of the successful  $^{14}\text{C}$  dating experiences based on the measurement of the bulk lime lump (i.e. without any kind of pretreatment), a key role is covered by the selection of lime lumps free of DC contaminant sources. Therefore, before their analysis, it is necessary to examine the samples under an optical stereo microscope to confirm their and eventually mechanically remove particles of aggregate that may adhere to their surface.

Anyway stereoscope analysis alone cannot assure that analyzed lime lumps are totally made of pure lime. It is possible to gain important information on lime lump calcination degree by checking the sample material by thin section analyses under polarizing microscope (Figure 12). Anyway no certainty in lump selection can be supposed because, even if it is admitted that thin section can



efficiently identify the presence of DC, lumps to submit to  $^{14}\text{C}$  analysis cannot be the same observed with the thin section. In Figure 12 (on the right) for example a lime lump theoretically eligible for a direct dating is shown, however there is not the assurance that lime lumps picked up from the same piece of mortar exhibit the same habits. So, in order to overcome these biases sensitively affecting the dating, the collection of data aimed to statistically infer the nature of lime lumps incased in a mortar sample should be performed. Lime lumps frequencies in a mortar sample, anyway, are sometimes not so high to produce precise statistics assuring that the selected sample will avoid biased dating.

These motivations are sufficient to justify the usage of pretreatment method (i.e. the CrySoniC) looking at increasing the suppression of DC interferences in order to produce accurate dating.

The advantages of this approach are linked to the possibility to obtain a good accuracy on lime lumps, independently from their nature: pure and DC contaminated. This could be possible using the CrySoniC pretreatment on lime lumps, after-written. The advantage of the selection protocol is the drastic reduction in the risk of contamination, selecting the calcite portion representative of the binder and avoiding the dating of calcinations relicts.

Where Accelerator Mass Spectrometry (AMS) is utilized for radiocarbon dating, a mass of lime lumps of about 10 mg to date bulk and at least 30 mg to pure lime lumps is required. As shown in Figure 13, selected powder will be stored in a beaker and covered with about 50 ml of double distilled water (DDW) and then submitted to an ultrasonication attack of about 30 minutes.

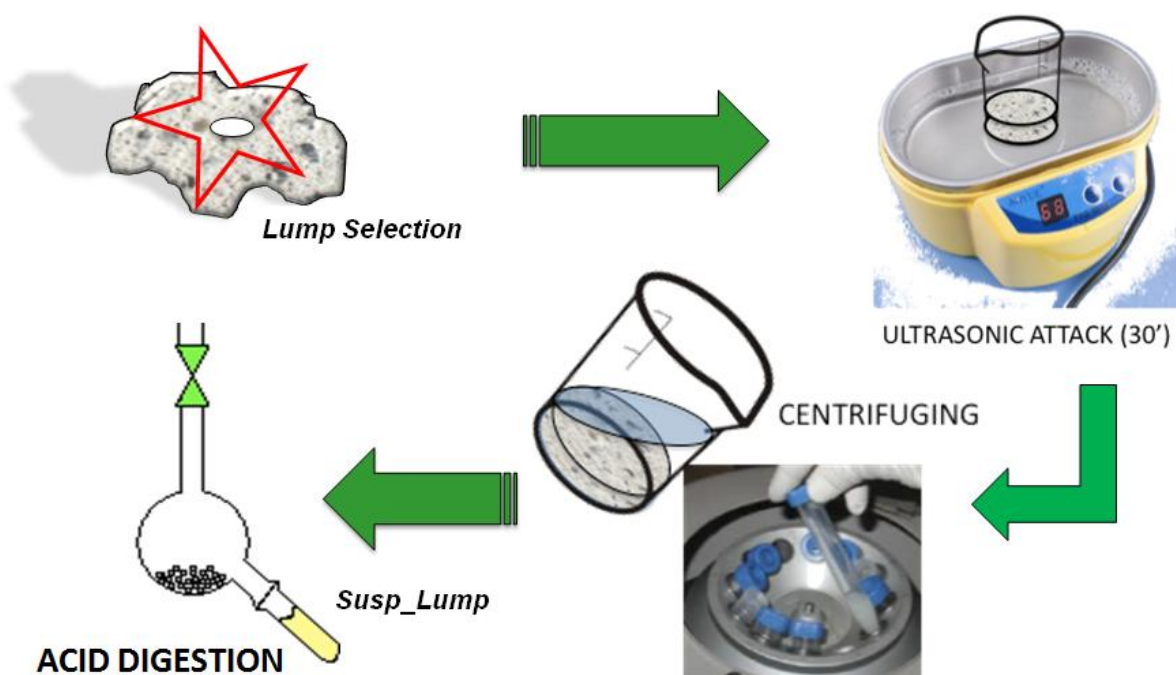


Figure 13. CrySoniC protocol applied to lime lumps to produce the *susp\_lump* fraction to analyze.

The water, containing all smaller lime lumps particles in suspension, will be collected, taking care to not move the original material settled on the bottom of the beaker. Suspended fraction will be centrifuged in order to collect the solid component, which will be dried and weighted. Once the selected portion to analyze has been collected, calcite is converted to CO<sub>2</sub> using a phosphoric acid attack (H<sub>3</sub>PO<sub>4</sub>). The CO<sub>2</sub> extracted from the sample is, then, reduced to graphite and measured in the AMS for the carbon isotopic ratios (according to Marzaioli et al. 2008, 2011, 2013). A first application of such technique has been reported into Marzaioli et al. (2013), attached to section II.2.2 and another new case of study is reported in section III.5.

To put in evidence the potential of the CryoSonic application to lime lumps dating three study cases are going to be shown: the first two show how CryoSonic purification doesn't highlight any outer contamination, showing a coherent dating between lime lump measured as the same and the pretreated one and demonstrating also to be a precious tool on thorny situation as mortar with calcareous aggregates are; the last testifies how the use of CryoSonic on lime lump could give an accurate dating despite the one found when dating bulk lime lump (without pre-treatment), very far from the dates suggested by literature.

The first case is related to the application to a set of samples picked up from the old Square Tower otherwise named 'Torre del Monaco' at the castle of Manfredonia. This tower is the unique testimony of the ancient nucleus built between 1256 and 1258 AD remained after the strong modifications done lately on the entire structure by Aragona Royal family (Torraiuoli 2008). Petrographic analysis of mortar sample (MC1) showed the presence of lime lumps, calcination relicts, earthy aggregates and calcareous sand, with a medium size particle dimension. The Cryo2Sonic protocol performed on bulk mortar gave a *susp* fraction whose dating unmatched with archaeological references (Table 3). The aging of the dating performed on the bulk mortar, was due most probably to calcareous sand present as aggregates, which evidently reached the collected material. Reason of this contamination could be linked to calcareous materials different from the binder, present in the mortar matrix and to the nature of these materials. Their softer nature could determine their crumbling during the ultrasonication process and the production of fraction dimensionally equal or finer than the binder particles. As attested by Goslar et al. (2009) presence of biocalcarene fragments, such it was for this sample, is found to be an obstacle to a successful radiocarbon dating. Analyses performed on lime lump collected from MC1 sample gave both good feedbacks, better than the one performed on bulk mortar (with Cryo2Sonic). Material from lime lump was divided into two sub-fractions: one portion measured as bulk and the other pre-treated with CryoSonic protocol up to obtainment of a fraction called *susp\_lump*. Calibrated results obtained from these two fractions matched with medieval archaeological reference, covering years

Table 3. All measured RC ages with relatives errors and calibrated results, distinguishing between Square Tower sample from Manfredonia Castle (MC) and mortar sample from the Sacuidic Castle (SAC). Bold type has been used to show dates which match with archaeological references.						
Sample	Type	RC age	Err RC age	Calibration 1 $\sigma$	Calibration 2 $\sigma$	Archaeological Reference
MC	Susp	1643	29	349 - 432 AD	269 - 533 AD	1280 – 1282 AD
	Lump	<b>700</b>	<b>35</b>	<b>1270 - 1379 AD</b>	<b>1257 - 1389 AD</b>	
	Susp_lump	<b>617</b>	<b>41</b>	<b>1298 - 1384 AD</b>	<b>1289 - 1406 AD</b>	
GM86	Lump	<b>953</b>	<b>33</b>	<b>1126 – 1152 AD</b>	<b>1021 – 1158 AD</b>	1099 AD as lower limit
	Susp_lump	<b>929</b>	<b>38</b>	<b>1041 – 1155 AD</b>	<b>1023 – 1205 AD</b>	
SAC9	Susp	1688	68	255 - 423 AD	211 - 540 AD	End of 13 <sup>th</sup> century
	Lump	1619	41	396 - 532 AD	343 - 543 AD	
	<b>Susp_lump</b>	<b>814</b>	<b>41</b>	<b>1207 - 1264 AD (92%)</b>	<b>1155 - 1280 AD</b>	

between 1280 – 1282 AD as affirmed by written sources (Table 3; Figure 14). The result of a t-test between *MCI\_lump* and *MCI\_susplump*, showed that these measurements are statistically not different, therefore it could be affirmed that both are in agreement with expected age. Likeness of dating results, on lime lumps and on pre-treated lime lump, could be explained by the absence of calcinations relicts inside the selected lime lump. An analogous situation could be observed on a sample coming from foundation of Modena Cathedral, Italy (GM86). Measurement of lime lump as it is (*GM86\_lump*) and of its CryoSonic product (*GM86\_susplump*) were used as precious tool to verify archaeological supposition without performing any further analysis on bulk mortar, which it known to be composed by a calcareous aggregate. As before, selected lime lump was divided into two subunits where one was measured as bulk and the other measured only after CryoSonic pre-treatment (producing a susp-lump fraction). Their radiocarbon measurements lead to a dating that perfectly match with chronological reference, showing an optimum reliability of this technique and a coherence between each result. Their archaeological reference fixed 1099 AD as lower limit for cathedral foundation, and the results are in very good agreement (Table 3).

Measurements performed on mortars sampled from Sacuidic Castle (end of 13<sup>th</sup> century, Forni, Italy) highlighted that dating of fractions collected from Cryo2Sonically pre-treated bulk mortars (*susp*) gave inconstant results because of a strong dead carbon contamination (see chapter II.5.1). Contamination was due to a silt calcareous fraction in the mortar. This situation, similar to the above mentioned, was solved using lime lump as a precious resource and following the cited preparation methods. There is a difference with Manfredonia and Modena samples here, there were

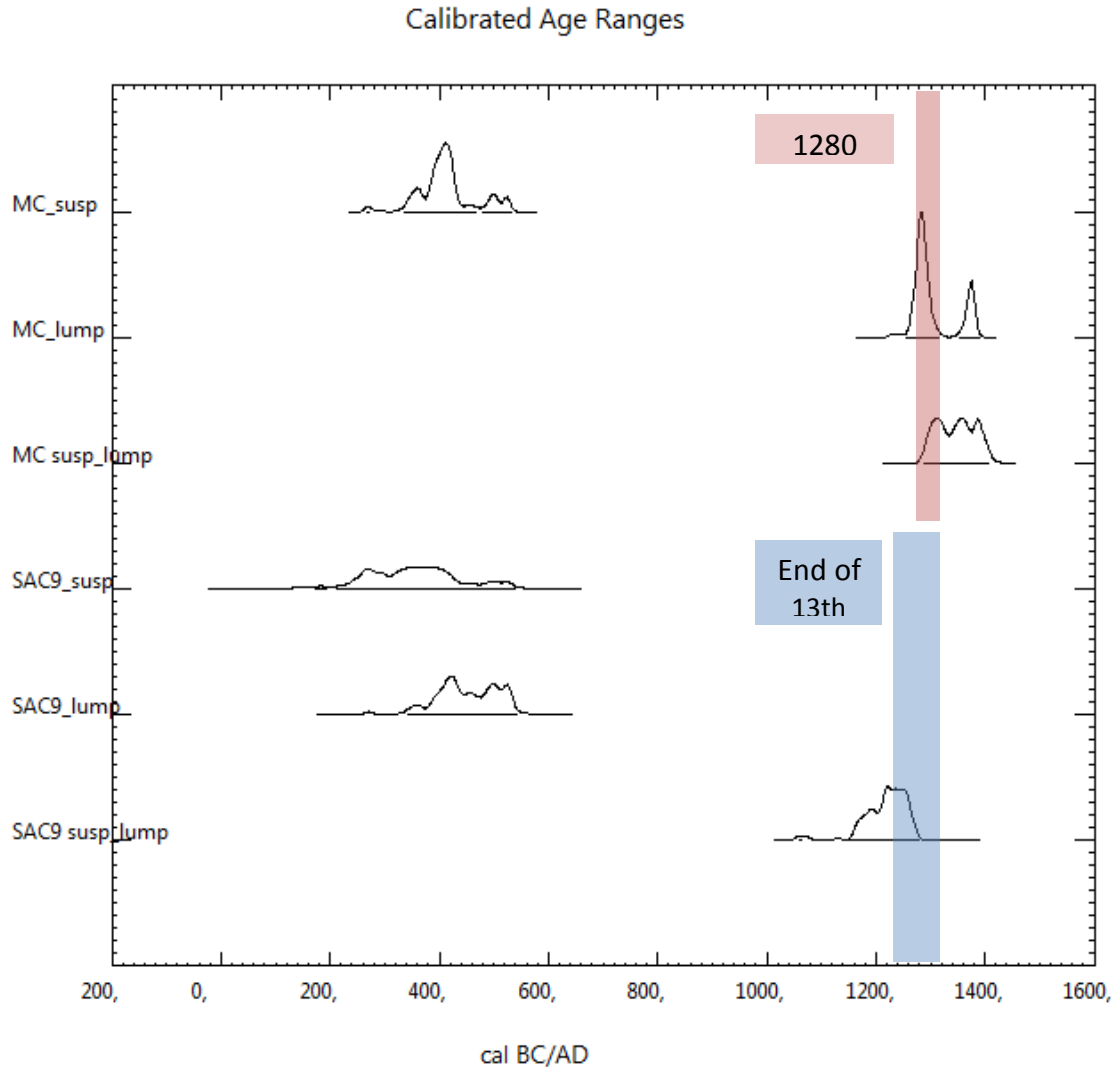


Figure 14. Calibrated ages of samples from Square Tower of Manfredonia Castle (MC) and from Sacuidic Castle (SAC9) with relative references. It is clear how dates from pretreated lime lumps gave better results.

two clearly different measures: one, contaminated by dead carbon (on lime lump as it is: *lump*) and one, did not (on pretreated lime lump: *susp\_lump*). The only dating according with archaeological reference is the one found from the *susp\_lump* fraction while the measurement performed on the bulk of the lime lump gave back an age older than the expected (Table 3; Figure 14). Many other analyses has been performed on lime lumps as they are or on their cryosonicated powders: all of them will be shown below in the Application Section (from III.3 to III.5). Basing on these preliminary tests it could be affirmed that:

- Lime lumps are a precious resource attempting to date a mortar, especially when it is characterized by the usage of calcareous materials (i.e. sand, silt, crumbling fragments of limestone or biocalcarene);

- Lime lumps could be used as the same but the success of the dating is not ensured even if there is a careful choice of materials (i.e. a statistically robust sample lime lumps characterization);
- The safest way to adopt, aiming to a good dating, is to collect enough material (one big lime lump or a pooling of small ones to reach a minimum of above 30 mg) from the same piece of mortar in order to pre-treat it with CryoSonic protocol, obtaining *susp\_lump* fractions. This procedure will avoid eventual dead carbon contamination coming from calcinations relicts.

## II.4. Dating Pozzolana Mortars: a new challenge.

Typologies of aggregate along with the nature of the binder can change depending on the availability of raw materials and the final destination of mortars. Usage of materials characterized by significant concentrations (>15%) of aluminates and amorphous silicates (i.e., pozzolana, volcanic ashes, crushed bricks) as aggregates confer light hydraulic properties to lime mortars (Moropoulou et al. 2002). This constituted, since Roman times, a breakthrough in mortar production technology allowing the speeding up of mortar hardening also under hard climatic conditions and increasing mortar mechanical resistance. In this section a focus on pozzolana mortars coming from roman area will be discussed.

The term *pozzolana* originates from Vitruvius, who described a volcanic soil, *pulvis puteolanum* from a village named Puteoli (nowadays Pozzuoli) placed in the active volcanic Campi Flegrei district on the northern shore of the Bay of Naples. According to Vitruvius, mixing this soil with lime would make the mortar harder and durable. In geological terms the deposit is a loose pyroclastic surge deposit (fine-grained, vitreous material deposited from horizontal blasts during a violent volcanic eruption).

Similar volcanic materials are also common in the Rome area, originating from the Monti Sabatini volcano NW of Rome and the Colli Albani volcano SE of Rome. Rome is founded on the deposits of these volcanoes, which have usually been utilized as pozzolana to furnish building raw material. For radiocarbon dating is important to consider that both volcanoes overlie a Mesozoic limestone basement. This means that ascending magmas interacted (i.e. calcinating and reacting) with the limestone foundation before reaching the surface (Rittmann 1933): therefore those Roman pozzolana deposits can be characterized by the presence of dead carbon sources. The experience and skill of Roman builders later led to what is universally known as pozzolanic mortars (Massazza 1993) where the improved properties in the hardening are based on chemical reactions between the slaked lime and the amorphous aluminosilicates of volcanic origin, mainly zeolites or high alkali glass. In the fundamental work of *De Architectura*, which was considered a handbook for Roman builders, Vitruvius described this material as one capable to harden both in air and underwater, opening the way to the so-called hydraulic mortars (i.e. mortars able to harden under water, *De Architectura* 2.6). When volcanic ash was not available, finely ground pottery and ceramics were used to induce hydraulicity to the material (*cocciopesto*), a technique that originated in Minoan Crete (Moropoulou et al. 2000). It has to be remarked here that the word cement (*opus caementicium*) in ancient Roman times referred to the concrete masonry of monuments composed of centimeter sized brick and tuff fragments (*caementa*), which are bonded by hydraulic mortars

with alkali-rich, calcium-alumino-silicate volcanic ash sands. Only in recent times the meaning has changed to refer to modern clinker-based materials (Artioli 2010).

The Roman pozzolana mortar is completely different from aerial one and its radiocarbon dating, to date, has been characterized by several problems (Hale et al. 2003; Lindroos 2005; Ringbom et al. 2006, 2008, 2011; Hodgins et al. 2011). In the case of non-hydraulic mortars the method has been studied experimentally and the problems are fairly well understood (Folk and Valastro, 1976; Pachiardi et al. 1986; Ambers 1987; Heinemeier et al. 1997; Lindroos et al. 2007; Marzaioli 2011; Al-Bashaireh 2013; Marzaioli et al. 2013; Nonni et al. 2013). The main issue is related to the presence of old, radiocarbon-dead carbonate, characterizing incompletely calcined limestone residues and calcite grains present in commonly used geological mortar fillers (such as sand and gravel). Pozzolana mortars have many problems such as:

- Less binder carbonate available than in lime mortar;
- Chemical activity for very long time;
- Continuous production of carbonates whenever exposed to atmospheric CO<sub>2</sub> (Ringbom et al. 2011);
- Recurring presence of re-crystallizations for several reasons, like weather (air exposed structures) or groundwater (deep buried structures) activities or due to their impermeable nature that retains pockets with un-reacted Ca(OH)<sub>2</sub>. This will continue to react with CO<sub>2</sub> to form carbonates whenever the mortar is distributed by breaking or crushing hence coming in contact with the atmosphere;
- Post depositional, hydrothermal alterations which affected pyroclastic deposit used as source of raw prime material (Jackson and Marra 2006);
- Lower permeability to atmospheric CO<sub>2</sub> than aerial mortars;
- Eventual presence of carbonate nodules, similar to lime lumps, derived from volcanic activity and founded inside pozzolanic ashes (Miriello et al. 2010) or carbonate minerals due to geological origins (i.e. limestone basement near magmas veins);
- Probable presence of natural carbonates from limestone or marble used as additives for surface and finishing wall layers.

All these issues could shift final radiocarbon dating result to younger or even older ages than the real one. Despite their importance Pozzolana mortars have received less attention than non-hydraulic mortars, mostly because they have been found to be more difficult to be dated (Lindroos et al. 2011). Anyway a successful dating of such materials has an enormous potential and can be considered a challenge in the field of archaeology.

#### II.4.1. Study case: Fiscale Tower and Ostia Marina Excavation.

In this section various successful  $^{14}\text{C}$  dating attempts on different samples of mortars coming from two archaeological sites near Rome, will be illustrated to prove that also pozzolanic mortar typology can be dated by means of Cryo2SoniC separation method. The examined samples have been collected from the site of Tor Fiscale located in the Aqueduct Park along the ancient Via Latina and Porta Marina Excavation into the famous Archaeological Area of Ostia Antica. Three samples, two from Porta Marina (OST4 and OST6) and one from Tor Fiscale (ToFi1), will be discussed.  $^{14}\text{C}$  results have been integrated by additive mortar preliminary analysis such as petrographic observations performed in thin sections, with an optical polarizing microscope (ZEISS D-7082 Oberkochen) under parallel and crossed nicols. This analysis can be indicative for the detection of eventual DC sources of contamination such as deposition of secondary calcite or any calcium carbonate materials distinguished from binder. All the samples were constrained to chronological references determined by means of archaeological criteria, in particular findings of stamped bricks, both attributable to the Hadrian Emperor (123-126 AD), into the investigated wall structures. This will be used as comparison term with the radiocarbon dates found after Cryo2SoniC pretreatment of pozzolana mortars utilized to build up the wall. About the sites, Porta Marina is an archaeological excavation in progress (Valeri 2001; David et al. 2009; David and Turci, 2011; David and Gonzales Muro, 2011; Morricone et al. 2013), which brought to light some building structures of a suburban neighborhood of different historical periods, including a public bath building called Maritime Baths. OST4 and OST6 samples came from a monumental pool with three statue-niches (Figure 15.A), probably part of a *frigidarium*, renamed “Bath of Silenum” after the discovery of a festoon with

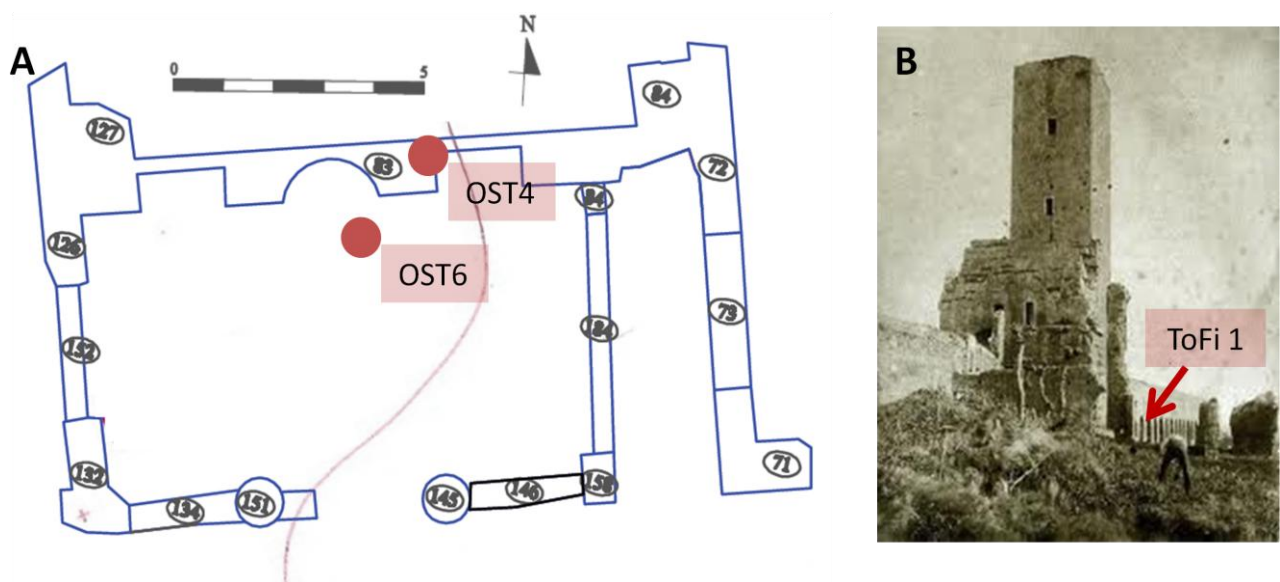


Figure 15. Sampling points at Bath of Silenum at Ostia Antica (A) and at the basement of Tor Fiscale (B).



Table 4. All RC ages and relatives calendar ages for analyzed samples. Repetitions on OST6 susp has been signed with a different apex. Archaeological reference is a *terminus post quem*: 126 AD.

Sample	Location	RC Age (years BP)	Err RC Age	Calibrated 1 $\sigma$	Calibrated 2 $\sigma$
OST4 susp M	USM 83 (N wall)	1857	32	125-215 AD (95%)	80 -234 AD
OST6 susp	US 168 (floor)	1876	73	65 - 230 AD	5 BC - 262 AD (92%)
OST6 susp'		1880	46	73 - 172 AD (87%)	48 - 240 AD (98%)
OST6 susp''		1960	52	3 BC – 84 AD (83%)	95 – 139 AD (98%)
OST6 susp'''		1918	44	48 - 130 AD (89%)	1 BC - 219 AD
ToFi 1 sand	W side of Claudio pillar	1881	60	70 -182 AD (82%)	1 BC - 257 AD (98%)
ToFi 1 susp		1859	71	77 - 235 AD	0 - 340 AD

satyr and sileni. Several brick-stamps found inside structures, dated between 123-126 AD, seem to indicate the structure development during the Hadrian period. The pool, changing its destination use, seems to have been used at least to the end of the 4<sup>th</sup> century (David 2011). Brick-stamps can be considered here a *terminus post quem* (TPQ) otherwise as a lower age limit. The same chronological reference is attributed to ToFi1 sample, a mortar sample coming from the roman basement (Hadrian period) of Tor del Fiscale (Figure 15.B): an ancient medieval tower built along Roman Claudio and Felice aqueducts.

Observation in thin sections confirm the hydraulic nature of both samples, ascribable to an aggregate composed mainly by volcanic glass, pozzolana and leucitite fragments that easily develop in CSH and AFm phases. A binder/aggregate ratio (B/A) higher for Ostia samples (2:1) than Tor Fiscale (1:1) is balanced by a significant presence of lime lumps inside binder matrix of ToFi1 (45% inside of the binder portion) with respect to OST6 (at last 30%). The presence of lime lumps represent an important advantage trying to perform radiocarbon dating, because it increases CaCO<sub>3</sub> available for dating. The presence of a source of contamination can be attributed to the presence of secondary calcite depositions inside pozzolana and binder voids in all observed samples. Moreover ToFi1 samples could be also characterized by the presence of possible calcareous residues (derived from ascended movements of lavas through limestone basement; Rittman 1933) and unburned limestone fragments.

Radiocarbon measurements show results in perfect agreement with the archaeological references. OST4, sampled in the north wall of the Bath of Silenum near an Hadrian brick-stamp (USM 83),

shows a match confirming the age of mortar (Table 4 and Figure 16). OST6, sampled from the floor of the same structure (US 168), was assigned from archeologists to an age presumably going from

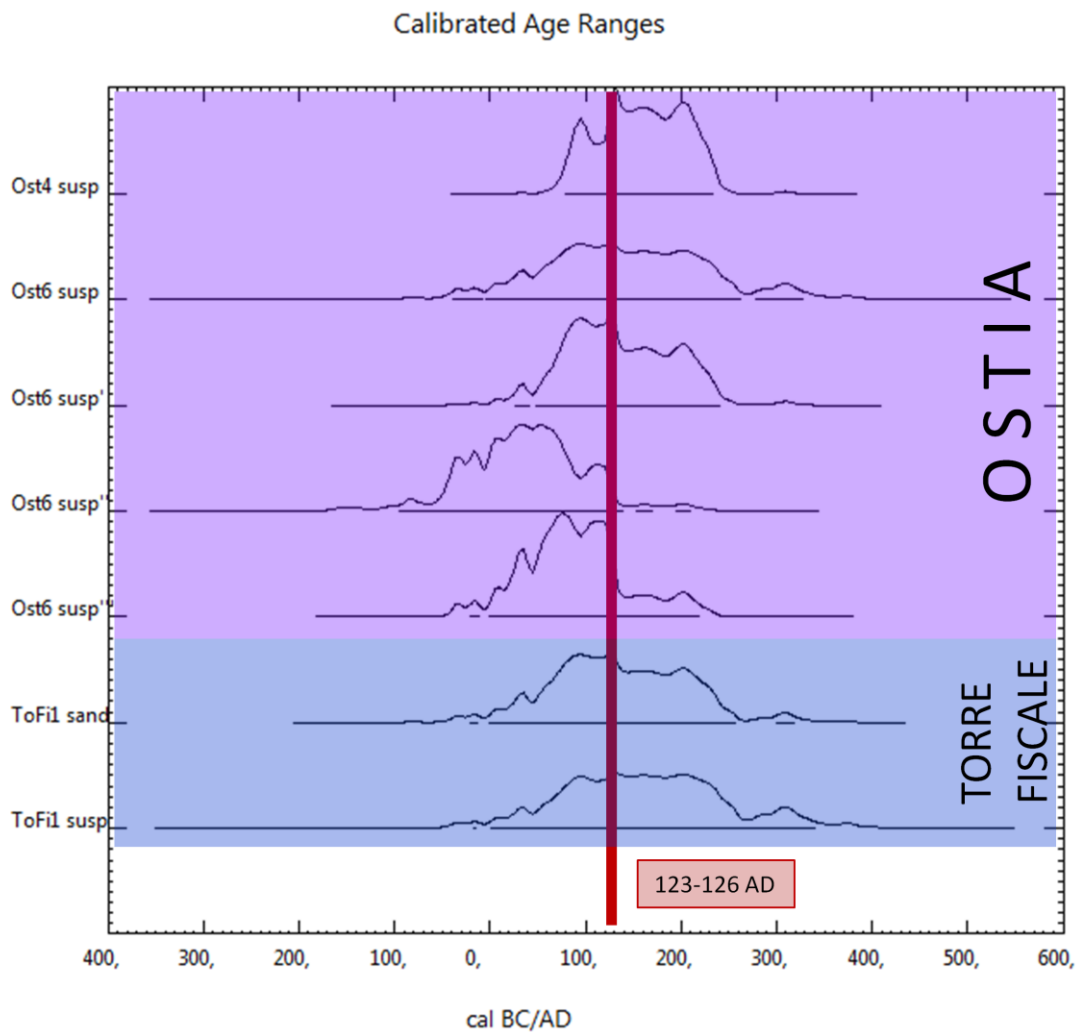


Figure 16. Calibrated ages of pozzolanic samples from Ostia Antica (Ost) and Tor Fiscale (ToFi).

123 AD to the 4<sup>th</sup> century (last use of this site). On this mortar (OST6) also a reproducibility test was performed. The original piece of mortar underwent four times to replicates of the pretreatment procedure before its measurement with the AMS (Cryo2SoniC, graphitization and pressing into Al cathodes as described by Nonni et al. 2013), obtaining four different samples to date (Table 4 and Figure 16). Resulting RC ages, found from repetitions, allow, by means of the Bayesian outlier analysis, the definition of the repetition variability for the Cryo2SoniC procedure. Observed combined variability (i.e. error of the weighted mean) over 4 replicates led to 22 RC years dispersion (i.e. about .3% on the  $F^{14}$ ) comparable with machine repeatability.

Observation of OST6 results allow to quantify Cryo2SoniC pretreatment reproducibility. This is an important finding because often, research on pozzolana mortars found high variability when trying to date such matrices. Of course this is only a preliminary test that need to be confirmed on large scale and with so much more repetitions than four.

More over no statistical difference (at 2 sigma) was found between OST6 and OST 4 radiocarbon dates and archaeological expectations confirming a good accuracy of the applied methodology also when dealing with pozzolana mortars.

Finally, the mortar sample from Tor Fiscale Roman basement ToFi1, sampled near to an Hadrian brick-stamp, gave, after the application of Cyo2SoniC, an RC age compatible with this archaeological time reference. After calibration all samples show a perfect agreement with Hadrian reference (Figure 16), demonstrating that Cryo2SoniC protocol is able to obtain accurate dating of mortars with pozzolanic aggregates and to give the raise to reproducible results. In this case successful results have been obtained despite a lower availability of carbonate binder, pozzolana aggregate with possible calcareous residues, unburned limestone fragments and the attested abundant presence of secondary calcite deposition into the voids.

For the examined samples Cryo2SoniC method resulted as a successful tool to obtain right radiocarbon dating from pozzolana mortars.

## II.5. Drawbacks

According to the several experiments performed during this research a series of drawbacks occurred during the radiocarbon dating of mortars. They can be related to the original composition of the mortar or to depositional events involving the studied samples.

The development of an integrated study on archaeological mortars involving both their radiocarbon dating and petrographic characterization, allowed to define the events when Cryo2SoniC protocol was not sufficient to obtain a fraction representative of binder calcite and able to guarantee an accurate dating of the setting moment. In details it has been seen that Cryo2soniC method results confirm that the procedure allows to:

- suppress dead carbon contamination coming from unburned limestone residues as results of an incomplete calcinations (see section II.1);
- obtain successful radiocarbon dating from mortar with a sandy (see section II.2) or pozzolanic aggregate (see section II.4);
- efficiently avoid dead carbon contamination (using its simplified version CryoSoniC) when dating lime lumps (see section II.3).

Although this pretreatment seems to be a valid tool for absolute chronology estimations in the field of archaeological research, during its testing/validation some failures or variability in results accuracy have been observed. Changeable results involved the analyses of:

- mortars with fine calcareous aggregates;
- mortars which underwent a groundwater submersion over their history, for a time interval sufficient to activate the dissolution re-precipitation process;
- mortars whose setting took place in a particular environment, such as an eruption or a fossil atmosphere;
- mortars composed by fragments of re-used mortars;
- mortars sampled deeply inside a masonry structure.

In this paragraph all these cases of inaccuracy will be experimentally studied on real archaeological mortars with the exception of the last point that will be discussed into the final section of the applicative chapter when discussing the results obtained from the ancient roman bridge in Narni (Italy).

## II.5.1 Calcareous aggregates

The worst category of mortars to date, without any doubt, is the one that have calcareous materials as aggregate. The greater presence of probable sources of contaminants increases the probability of a failure of the dating process. Even if we are using a method taking advantage by a physical process separating two chemically identical matrices, the risks to apply a poor selection criteria is essentially related to the dimensional similarities of interferences with original binder particles. Failure risks are mostly due to the i) possibility to have a calcareous aggregate composed by very fine particles (i.e. calcareous sand, foraminifera elements); ii) possibility to have a coarse calcareous aggregate with a high tendency to produce fine particles under mechanical strain (like ultrasonication).

Some examples to understand Cryo2SoniC variability in the binder selection efficiency when it is applied to archaeological mortars potentially strongly contaminated by dead carbon sources will be used to clarify this procedure accuracy reproducibility. To date, alternative dating methods to Cryo2SoniC did not reach acceptable results when compared to archeological references. In this framework three study cases will be discussed: samples taken from i) the vault of Teutonic Knights Tavern inside San Leonardo abbey in Lama Volara; ii) ruins of an ancient Roman colony, Siponto, along Apulian Adriatic seaboard; iii) ruins of three destroyed Castles placed in Trentino ( northern Italy).

The application of Cryo2SoniC separation method to the samples took from the vault of Teutonic Knights Tavern inside San Leonardo abbey (now definitely collapsed) provided results which proved separation efficiency, although they did not match with archaeological reference (Table 5). The chronological reference for this site reports that the Tavern (MSL) was built in 1327, beside monastery walls, by Teutonic Knights, an ancient monastic-military and hospitality order born in the holy-land during third crusade. Thanks to a petrographic analysis both presence of lime lumps, calcination relicts, earthy aggregates and calcareous sand, with a very coarse dimension, has been detected. *MSL\_sand* and *MSL\_susp* RC ages focus between 15<sup>th</sup> – 17<sup>th</sup> centuries, they are perfectly equal to each other but also much younger than 1327 AD. This inconsistency could be explained with two different answers. First, considering that conservation conditions of this medieval building were so bad to determine the collapsing of the whole structure in 2011 AD, it's probable that the sampled masonry point was interested by weathering. The flowing of meteoric water could have determined the dissolution of the old binder and precipitation of secondary calcite with a different radiocarbon isotopic signature, of course younger than the original binder. <sup>14</sup>C enrichment of the original binder signal with a modern signal of newly formed calcite could have determined a

Table 5. Calibrated and RC ages of *susp* fractions analyzed samples. Mortars come from San Leonardo Abbey (MSL); Siponto ancient city (SIP) and from three castles Cuol di Ciastel (CDC), Sacuidic (SAC) and Prà di Got (PDG). Bold type highlighted compatible results.

Sample	Radicarbon Age (years BP)	Err RC	Calibrated Age 1 $\sigma$	Calibrated Age 2 $\sigma$	Archaeological References
MSL	328	29	1512 - 1635 AD	1479 - 1643 AD	1327 AD
SIP	1693	29	264 - 399 AD	257 - 416 AD	12 <sup>th</sup> – 13 <sup>th</sup> centuries
CDC91	10701	61	10711 - 10621 BC	10794 - 10594 BC	4 <sup>th</sup> century
CDC91'	11233	57	11283 - 11139 BC	11335 - 10988 BC	
CDC91''	10464	54	10593 - 10272 BC	10616 - 10188 BC	
CDC91'''	11076	50	11140 - 10952 BC	11166 - 10802 BC	
CDC29	<b>1608</b>	<b>59</b>	<b>403 - 536 AD</b>	<b>326 - 583 AD (98%)</b>	
CDC42	10974	45	10969-10783 BC	11034 – 10716 BC	
SAC9	1688	68	255 - 423 AD	211 - 540 AD (99%)	End of 13 <sup>th</sup> century
SAC20	1605	32	414 - 532 AD	395 - 540 AD	
SAC24	1390	34	631 - 664 AD (93%)	597 - 680 AD	
SAC18	1418	36	608 - 651 AD	572 - 661 AD	
PDG59	3305	26	1615 - 1532 BC	1663 - 1511 BC	9 <sup>th</sup> -10 <sup>th</sup> centuries
PDG2	2535	34	791 - 570 BC	798 - 541 BC	
PDGs	<b>1117</b>	<b>26</b>	<b>894 - 971 AD</b>	<b>881 - 990 AD</b>	

rejuvenation of the expected age, although secondary calcite signal coming from weather activity is usually successfully suppressed during Cryo2SoniC selection (see section II.4). Higher probability goes to the second answer: masonry structure interested by sampling could has been modified during its usage, so dated sample probably owns to a successive construction or structure-modification phase. It's worth noting that 1327 AD, represent a terminus post quem (TPQ), in other words that it is not improbable to find RC Ages younger than TPQ. In this case, it was verified that Cryo2SoniC was able to eliminate dead carbon contamination coming from calcareous aggregates like calcareous sand, when it is composed by coarse sized particles.

Samples from the ancient Siponto (SIP) instead, are characterized by biocalcarene fragments and fine calcareous sand as aggregate. Biocalcarene is a clastic rock made of calcareous particles with sandy dimensions ( $\sim 63 \mu\text{m}$ ), linked together by a calcareous cement ( $< 63 \mu\text{m}$ ). Additional particles of aggregates are fragments of marine organisms like shells of muscles or foraminifera. In this case collected *susp* fraction drastically unmatched with the archaeological references fixed between 12<sup>th</sup> and 13<sup>th</sup> century (Laganara et al.2011). This aging effect is attributable to calcareous sands present as aggregates inside mortars, which evidently entered suspended fraction. This occurred because of their fine sizes or soft nature of aggregates (ultrasonic stress could determine the eventual release of a calcareous finer fraction): the presence of biocalcarene fragments is

attested as an obstacle to radiocarbon dating success also in literature (Goslar et al. 2009). Similar results have also been obtained on Jericho and Qumran samples as they are characterized by the presence of biomicrite fragments as aggregates (see section II.7).

The analysis of samples from ruins of three Castles near Forni (Cuol di Ciastel (CDC), Pra di Got (PDG) and Sacuidic (SA); Gelichi et al. 2008), belonging to three different timeframes, could be used as an additional testing of mortar containing fine carbonaceous aggregates, similar to what shown on Siponto samples. This set of mortars is characterized by a silt calcareous fraction, with a variable abundance over the different samples. RC ages of samples from the three Castles are reported below (Table 5). Positive feedback concerned only two samples (PDGs and CDC29 highlighted in the Table 5) on fourteen analyzed. With CDC91 repeated 4 times in order to perform a reproducibility test similarly to what have been done on mortars with pozzolanic aggregate, but the outcomes has been definitely wrong and unsuccessful: all repetitions made, gave back an age strongly contaminated by dead carbon influence (Table 5). These results clearly show how Cryo2SoniC method is rarely efficient when applied to mortars characterized by fine calcareous component dimensionally converging to the fraction to isolate ( $d < 62 \mu\text{m}$ ).

### **II.5.2. Secondary calcite depositions**

Cryo2SoniC pretreatment and successive radiocarbon measurements of mortar samples affected by secondary calcite deposition originated by meteoric water provided consistent results (see section II.4 and section III.1). However real problems with dating occurred when this secondary calcite is due to dissolution/re-precipitation phenomena involving groundwater. Indeed the age of several samples, collected in different archaeological sites was significantly affected by the deposition of secondary calcite due to the interaction of the mortar with groundwater. Their common property was their position: all of them have been sampled from buried structures in a geological area interested by rising groundwater. Examples of this situation are mortars coming from two archaeological sites: the area of Domus Romanae in the underground of Palazzo Valentini and the buried structures/foundation of the roman Minerva Medica Temple, both placed in the centre of Rome. They are two sites characterized by a buried environment, recently excavated, a suspicious presence of rising groundwater attested by historical sources and geological inspections (Ventriglia 1971; Baldassarri 2008) as well as sporadic flooding of the ancient structures as reported by archaeologists.

The main aging of samples coming from Palazzo Valentini (PVAL) is linked to mortars from the deepest archaeological layer identified as a *platea caementita*, otherwise an ancient walking surface

Table 6. RC ages and relatives calibrated ages of *susp* fractions performed on samples coming from Palazzo Valentini (PVAL) and Minerva Medica Temple (TMM). All them are so far from archaeological references.

Sample	Radicarbon Age (years BP)	Err RC	Calibrated Age 1 $\sigma$	Calibrated Age 2 $\sigma$	Archaeological References
PVAL1	3005	65	1375 - 1131 BC	1411 - 1053 BC	1 <sup>st</sup> - 2 <sup>nd</sup> centuries
PVAL16	3171	41	1494 - 1415 BC	1523 - 1323 BC	
TMM1	2683	71	905 - 797 BC	1017 - 754 BC	4 <sup>th</sup> century
TMM2	2567	35	802 - 603 BC	808 - 550 BC	
TMM3	2439	43	735 - 411 BC	754 - 405 BC	
TMM4	3568	63	2021 - 1779 BC	2046 - 1743 BC	1 <sup>st</sup> century
TMM5	3790	80	2390 - 2049 BC	2467 - 1984 BC	

dated back to the end of 1<sup>st</sup> and beginning of 2<sup>nd</sup> century AD. It was built to waterproofing the area from groundwater coming from Quirinal slopes which flooded till the Fori Imperiali area forming an aquifer till nowadays. The corresponding RC ages show a inaccurate age of more than a thousand years older than 1<sup>st</sup>-2<sup>nd</sup> centuries (Table 6; Figure 17). Similar results have been obtained for the samples from the freshly excavated structures of Minerva Medica Temple (TMM) and some pre-existent walls under its floor, which are respectively archaeologically attributed to 4<sup>th</sup> and 1<sup>st</sup> centuries, respectively (Barbera 2007; Biasci 2000). In this case mortars gave experimental calibrated ages much older than 3000 years BC (Table 6; Figure 17). Both sites have strongly aged RC dating and a strongly presence of secondary calcite deposition due to a nearby aquifer (Ventriglia 1971). This inconsistent aging cannot be due to some calcareous aggregates as the

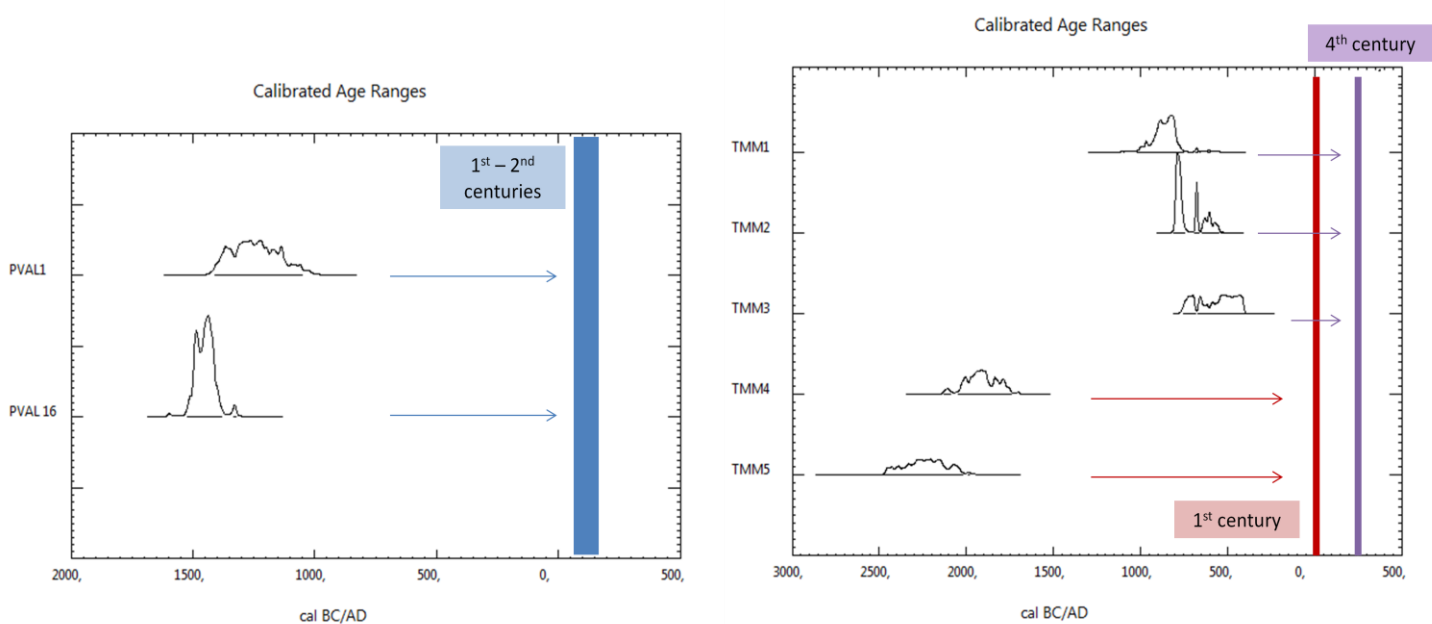
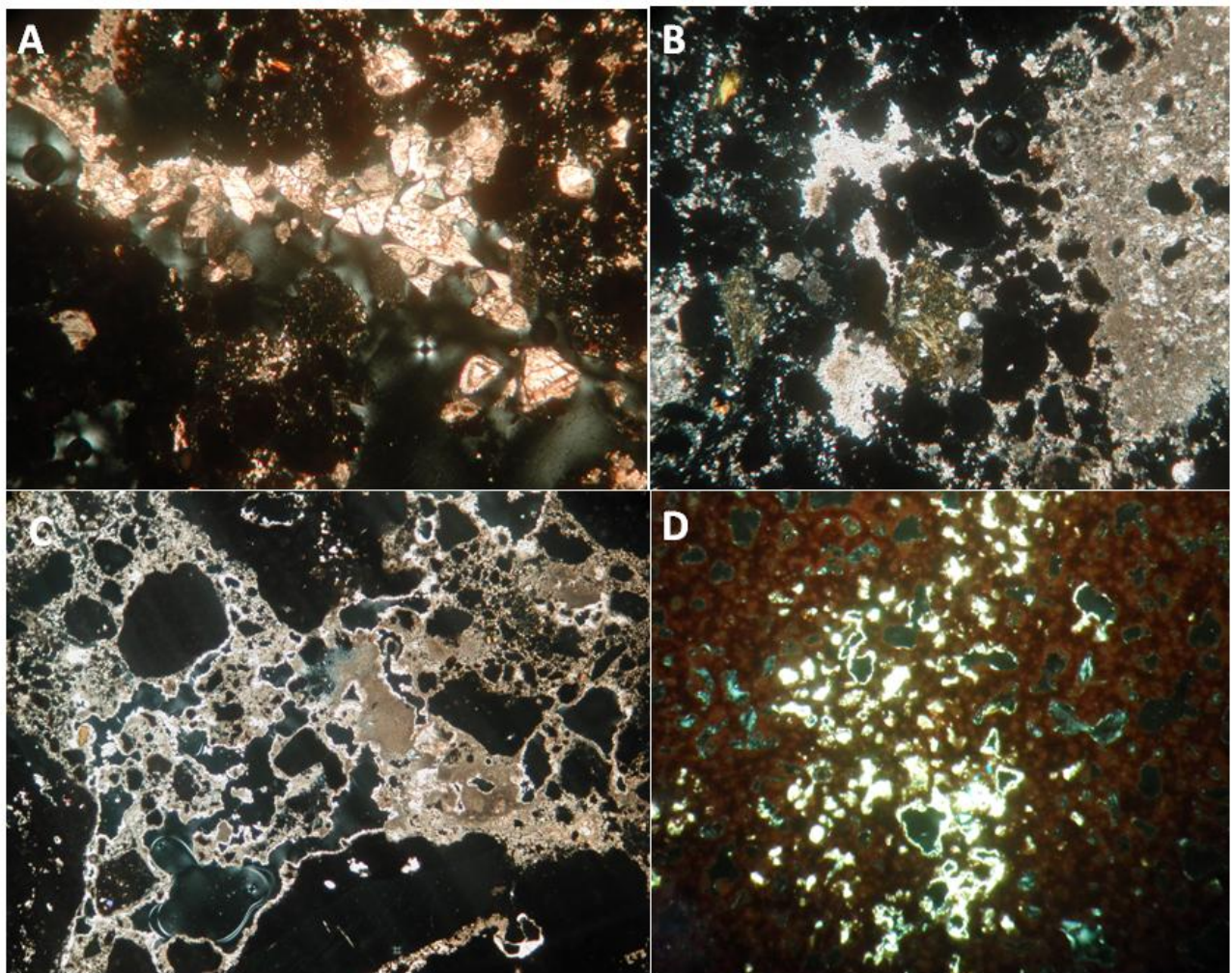


Figure 17. Calibrated ages of samples coming from Palazzo Valentini (left) and Minerva Medica Temple (right). All analyzed mortars show an aging effect due to DC contamination by secondary calcite deposition from groundwater.



petrographic analysis of both sets of samples showed only the occurrence of pozzolanic fragments (brown to reddish brown and yellow scoria, Lancaster 2005) and it has been previously showed how Cryo2SoniC protocol is generally successful for such a kind of materials. The aging cannot be due to unburned limestone fragments, not detected by microscopic observations, and because even in this case Cryo2SoniC was found to be able to suppress this particular kind of signal from fraction to dating. The unique calcitic element characterizing studied mortars and differing from binder matrix was identified as secondary calcite depositions filling all voids and porosity (of the binder and tuffs fragments) as well as replacing of original binder itself (Figure 18). The subsequent depositions have been recognized as the cause of aging and the carrier of dead carbon contamination. A contamination very difficult to suppress even more if original structure has been often submerged and its mortar components undergone an almost complete substitution of the original binder.



*Figure 18. Secondary calcite depositions inside all samples from Minerva Medica Temple observable by TSOM: A - Calcite crystals growing inside voids (TMM4; 20X crossed nicols); B - calcite crystals completely filling porosity (TMM5; 2,5X crossed nicols) and C - partially substituting binder matrix (TMM1; 2,5X crossed nicols); D - calcite crystals grown inside pozzolana voids (TMM1, 20X crossed nicols).*

### II.5.3. Fossil Atmospheres

The last drawback discussed in this chapter deals with the radiocarbon dating of mortars coming from Pompei. Pompei is a famous Italian archaeological site whose story is about unique: it was an ancient Roman city involved in a Vesuvian eruption in 79 AD. It concerns a singular case, surely a rare one, which could help future studies on analogue mortar samples from volcanic areas.

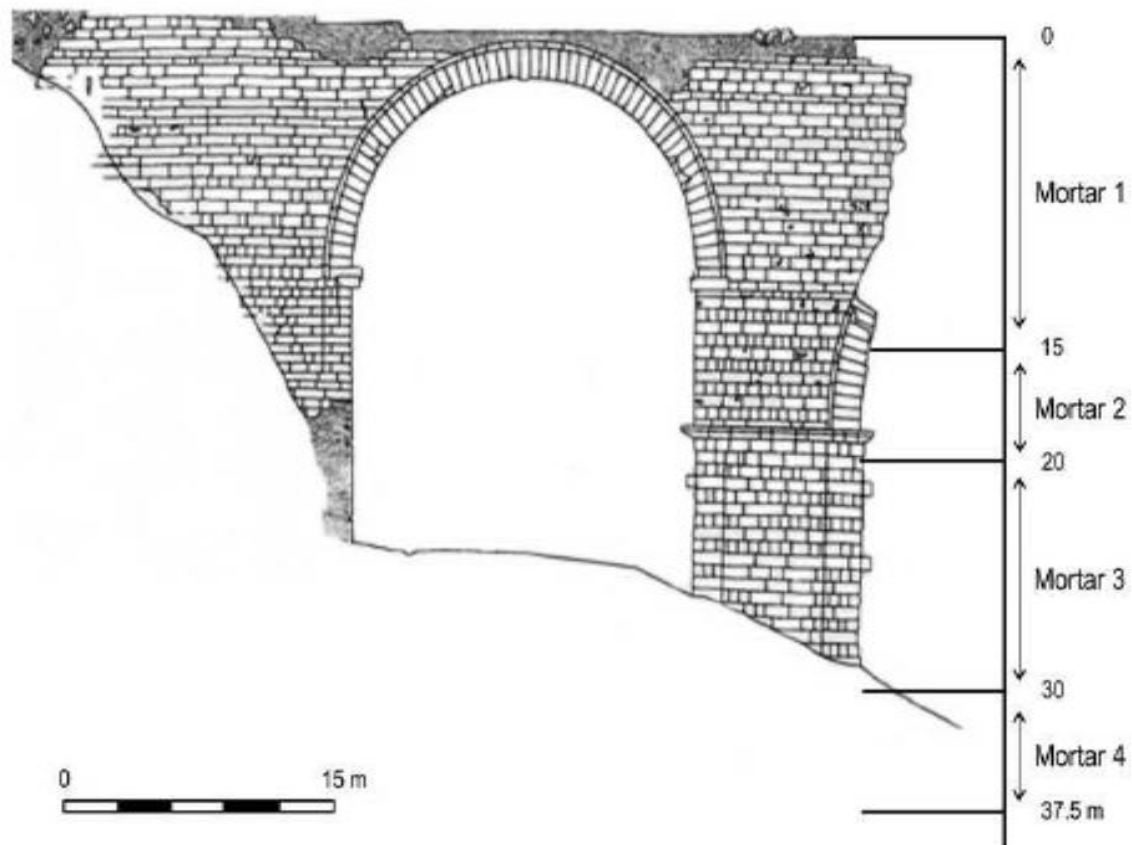
From Region IX Insula 12 in Pompei two beautiful and still well preserved residential structures were discovered: the House of Painters at Work and the House of Chaste Lovers. Two samples were analyzed: one of mortar from to a masonry wall of a *cubiculum* inside the House of Chaste Lovers (PCUB) and one of pure plaster from a wall of the House of Painters at Work (PPIT). The House of Chaste Lovers were involved into a restoration at the time of eruption (79 AD), as the same of many others houses in Pompei which had been strongly damaged by the 62 AD earthquake. According to this, the PCUB sample should be dated between 62 and 79 AD. The House of Painters at Work takes its name from the fact that a crew of painters was working on the decorations of its salon during the eruption. This event produced a layer of fresh plaster which hardened during the eruption and consequently adsorbed fossil CO<sub>2</sub> coming from the volcano. RC dating on PPIT, as expected, resulted in a date that did not match the archeological reference of 79 AD, showing a very strong contamination (Table 7). Interestingly, the dating of sample coming from the close House of Chaste Lovers gave an age much older than the expected (Table 7). This finding could be attributed to the presence of a fossil atmosphere induced by the volcano activity in the nearby or to a strong contamination from calcareous nodules found inside similar Pompeian mortar and easily confusable with lime lumps as reported by Miriello et al. 2010. First hypothesis is the most likely.

Sample	Radicarbon Age (years BP)	Err RC	Calibrated Age 1 $\sigma$	Calibrated Age 2 $\sigma$	Archaeological References
PCUB	2654	69	899 - 786 BC	994 - 553 BC	62 – 79 AD
PPIT	16312	95	17628 - 17445 BC	17901 - 17016 BC	79 AD

### II.5.4 Study case: Ponte di Augusto at Narni, a complicate challenge of success.

The aim is to date a series of mortar sampled from different levels of Ponte di Augusto at Narni and then comparing results with archaeological expectations. Although the samples were not all pozzolanic mortars, this case represents a study case that allows to check applicability of Cryo2SoniC method to hydraulic mortar with an hydraulic binder and with an aggregate which induce an hydraulic behavior.

One of the biggest Roman bridges, with arches spanning over more than 20 meters, was built during Roman period in 27 BC close to Narni, crossing the river Nera. This is the so-called Ponte di Augusto, which formed a part of the extension of the Flaminia consular way. Of this structure only one arch, which was not the largest, is still standing. Its chord is 20 m, and its height at the intrados is 27 m. The abutments, piers and arches were made of three-leaf type masonry with an outer skin of well cut travertine ashlar and an inner core of cast lime concrete. The ruins of the Ponte di Augusto bridge have been investigated over recent years in order to assess its seismic resistance. These studies allowed the sampling of four types of mortar through four vertical core drillings inside bridge structure. A simple visual evaluation revealed that four types of mortar were used to construct the bridge forming a distinguishable stratigraphy (Cantisani et al. 2007; Drdracky et al. in press). The mortars were made of a binder and a coarse aggregate, have a strong cohesion and good mechanical characteristics and for this reason they look similar to modern concrete. In this section are reported the results of the analysis of three of four samples (PN1, PN2 and PN4) belonging respectively to first, second and fourth level of height (Figure 19).



*Figure 19. Vertical distribution of lime mortars/concrete in the pierce core in a draw of Ponte di Augusto ruins.*

### Petrographic Aspects

Observations made by Drdracky et al. (in press) enabled us to recognize four types of mixtures which were set according to a particular sequence. Here below their observations are reported.

*Type 1* mortar (PN1 sample), from the top to a depth of -17 m, with the function of filling the top of the pier, exhibits an earthy appearance and low cohesion. Binder/aggregate ratio: 1:3; binder structure: microsparitic; binder color: light brown. Aggregate composition: carbonatic rocks (biomicrite, biosparite), chert, quartz. *Type 2* mortar (PN2 sample), from -15 m to -20 m, is characterized by a whitish binder, big fragments of travertine and very good cohesion, which is influenced by the high quality of the binder. It has been shown that its high hydraulicity was achieved by calcinations of local cherty limestone, and not by inserting any particular additives (Cantisani et al. 2002). Its use could be due to the need to withstand the rather high stresses present in that particular position of the pier, directly below the arch. Binder/aggregate ratio: 1:2-1:3; binder structure: not homogeneous (micritic and partly strongly recrystallized); binder color: whitish. Aggregate composition: travertine, carbonatic rocks, chert, quartz. The mortar of the foundations (*type 4* - PN4 sample), up to a height of 7 m above the rock basement which at the present time corresponds to the ground level, is characterised by a dark grey binder, good cohesion, big fragments of travertine and abundant presence of tuff fragments. The presence of this material makes the mortar strongly porous. Binder/aggregate ratio: 1:2-1:3; binder structure: microsparitic; binder color: dark gray. Aggregate composition: travertine, tuff, piroxene, leucite (Cantisani et al. 2007).

Many lime lumps were detected after sampling but our samples were lacking of them because they were utilised for previous studies (Cantisani et al. 2002, 2007; Drdracky et al. in press).

### Methods

All samples were processed with Cryo2SoniC method in order to obtain fractions suitable for radiocarbon dating. Collected fractions, corresponding to a *susp* and a *sand* type for each sample, underwent the analytical setup already described into section II.2 and in Nonni et al. (2013). Same fractions have been analyzed twice to increase the statistical reliability during AMS measurement (Terrasi et al. 2008) and than the average of two values of the same sample has been made when statistically possible. Only for PN1 a lime lump was found, and it was measured as bulk and after CryoSoniC pretreatment (Marzaioli et al. 2013).

### Results

Radiocarbon dating of mortar of samples coming from Ponte di Augusto should have been coherent with the age of imperial construction (27 BC) fixed as *terminus post quem*. As reported in Table 8,

Table 8. RC Ages of all samples. Indicate calibration values considering the maximum and minimum age and singular intervals (proportions in %); \* indicates the presence of a mean value between two RC Age results obtained from same suspension.

Sample	Type	RC Age	Err RCAge	Calibrated Age 1 $\sigma$	Calibrated Age 2 $\sigma$	Archaeological Reference
PN1	Sand	5306	137	4262-4032 BC (82%)	4373 -3893 BC (94%)	27 BC
	Susp*	4430	169	3343 -2912 BC	3528 - 2832 BC (90%)	
	Lump*	1347	85	614 - 722 AD	548 - 884 AD	
	Susp lump*	3046	79	1413 - 1210 BC	1455 - 1053 BC	
PN2	Susp	1807	73	126 - 261 AD (79%) 280 - 325 AD (21%)	63 - 394 AD	
PN4	Sand	573	62	1308-1362 AD (63%) 1386- 1417 AD (37%)	1291-1436 AD	
	Susp*	469	161	1306- 1363 AD (18%) 1385-1528 AD (55%) 1551- 1634 AD (26%)	1220-1694 AD (93%) 1727- 1813 AD (5%)	

two of analyzed samples (PN2, PN4) resulted younger than archaeological reference, while one (PN1) was found to be older.

Errors associated to RC Ages are very high but this depends on the low current signals produced by cathodes during AMS measurements. The theoretical relationship between *sand* and *susp* ages has been maintained with the first one resulting always older than the second. The same theoretical proportion was maintained also between suspension ages and analyses performed on bulk *lump* and *susplump* for PN1 sample, that although resulted still older than the archaeological reference (27 BC), are much younger than *sand* and *susp*. The aging is probably attributable to carbonatic rocks, such as biomicrite and biosparite, present inside mortar as aggregates; their fine particles dimension contaminated the selected fraction with a dead carbon component. To explain the failure of the measurement performed on *lump* and *susp lump* theoretically made of pure binder, the lack of an accurate cleaning before the pretreatment processes and the occurrence of contaminating particles from aggregates are very probable. Eventual residues of fine mortar particles probably had shifted to aging final results, less than what happened for mortar bulk but always significant to obtain a wrong age. PN2 showed a RC age close to the archaeological reference and slightly moved toward younger ages than 27 BC. It is a very hydraulic material, and this result is very important to prove applicability of Cryo2SoniC method and generally radiocarbon dating procedure. Observed younger ages could be due to the inner position of sampled mortar with respect to the surface of the pillar. Probably the aging is attributable to the different aeration gradient along the depth into the pillar or, alternatively, to a secondary calcite deposition detected inside sample in the form of recrystallized binder. This enhanced presence of dissolution-precipitation phenomena is probably related to the

presence of river water bringing neogenesis carbonates. Aggregates potentially affecting the correct age estimation were travertine fragments, but for the analyzed samples as was for PN4, their dimensions were not compatible with suspended fraction particles average size (see section II.6.1). Travertine is also a rock with a good hardness which avoids accidental suspension inside suspended fraction due to mechanical solicitations as instead, could be for biomicrite rock. Sample PN4 registers a final age younger than expected and younger than the other samples. Its heavy rejuvenation could be related to the presence of ions exchanging phenomena due to its close proximity to river waters and to the depth of its position far from air and submerged for long time. In the last option, binder capability to exchange CO<sub>2</sub> with the atmosphere is lower than the one of higher part of the pillar.

### Conclusions

The possibility to date hydraulic structures with hydraulic binder and aggregate which induce an hydraulic behavior has been investigated. Results could be comfortable if it is highlighted the possibility to date a mortar similar to a modern concrete. At the same time this archaeological site had some peculiarities which made the measurement of building age a complicate goal, such as the presence of biomicritic aggregates (in PN1), a strong crystallizing activity of new calcite (in PN2), a strong closeness to the river (in PN4) and an inner position inside pillar (in all them). These are all clues to consider if in the future mortars from a similar structure will be going to be measured.

## II.6. Control Checks on Suspended Fractions

Calcite is a common mineral phase in archaeological artifacts, environment and study sites and it may have geogenic, biogenic or anthropogenic origins. Geogenic calcite derives mainly from limestone, chalk and marble, biogenic calcite from eggshells and certain mollusk shells, while anthropogenic calcite is the product of pyrotechnology (plaster and mortar are common anthropogenic materials). Simple chemical analysis is therefore not sufficient to distinguish between calcinated anthropogenic, biogenic and geogenic calcite. Sometimes micromorphological analysis can differentiate among these different typologies of calcite (Courty et al. 1989) but there are also situations where it is not easily possible. The nature of calcite of CryoSonic produced fractions (*susp* and *sand* type) can only be indirectly inferred by comparing their radiocarbon signature with the archeological reference. Of course, the existence of other methods which eventually combined, can be utilized to verify fraction properties represents an independent diagnostic tool to confirm the effectiveness of their selection. In this section we report on the attempt to differentiate anthropogenic from geogenic calcite using the infrared spectroscopy, cathodoluminescence analysis and SEM observations in order to better characterize selected fractions.

SEM will be utilized to check the effectiveness of dimensional micrometric selection and absence of contaminant particles based on their particular morphology.

Cathodoluminescence (CL) microscopy will verify the pureness of a selected fraction highlighting eventual calcite particles of geological origin (i.e. older) by means of its different degree of luminescence.

FTIR investigation inferring the different IR light absorption at given frequencies between geogenic (i.e. more crystalline) calcite and anthropogenic calcite will be used to discriminate between contaminated and uncontaminated fractions.

Once evaluated the effectiveness of these tools for fraction characterization over an exhaustive dataset of already dated fractions, they can be used (specially the CL) as faster and cheaper decisional tests in order to decide about the fate of produced fractions in terms of dating.

## II.6.1 Particles dimension control check using SEM

Some collected fractions to check their minimum particles dimension using SEM imaging section were analyzed, with the aim to evaluate the size dimension of selected particles.

During the Cryo2SoniC selection method, the only mechanical constraint designed to select particle size, is the sieving step. The sieve cuts cryobreaking produced powders diameters below 500  $\mu\text{m}$  hence applying a very raw selection on the powder. To test capability of Cryo2SoniC to separate binder particles through a combined mechanical and physical procedure SEM images analysis was used. It is known that fraction  $< 38 \mu\text{m}$  includes both particles of mechanical (aggregates and/or unburned limestone fraction) and chemical (binder fraction) origin, yielding a contaminated fraction (Lindroos et al. 2007). Literature reports that geological particles of mechanical origin have grain size  $>1 \mu\text{m}$ , whereas chemical reactions produce colloids that flocculate and grow, generating finer particles. This fact has been demonstrated for subaerial media (Wilson and Spengler 1996; Seinfeld and Pandis 2006) and for aqueous media (Davis and Kent 1990; Salama and Wilson 2000). Therefore, particles  $<1 \mu\text{m}$  must be produced by crystal nucleation and growth. Several experimentations simulating mortar production show that binder carbonates are characterized by 200-400 nm fine grain size (Genestar and Pons 2003; Stefanidou and Papayianni 2005; Marzaioli et al. 2011) due to the high hardening rates of lime mortar (Moropoulou et al. 2000; Lanas et al. 2004; El-Turki et al. 2007; Kosendar-Legenstein et al. 2008). The rather high rate of carbonation leads to the isolation of the atmospheric  $^{14}\text{CO}_2$  signal absorbed by the mortars during their setting (Ortega et al. 2012). Therefore, our work aims to verify that Cryo2SoniC is optimized as a procedure able to obtain particles of  $<1 \mu\text{m}$ , which ensures that all the carbonate separated has been generally generated by slaked lime carbonation, and consequently, that the carbon we are measuring corresponds to atmospheric carbon.

Although the best way to know size distribution could be using a particle-analyzer able to discriminate particles between 0,4 to 2  $\mu\text{m}$ , here we were limited to observe the separated and collected fractions for some archeological site through SEM imaging analysis to check the minimum and average size collected, as well as their morphology in order to ensure the absence of binder contaminants. Morphology observation can be useful to particle origin identification: a freshly crushed shape derives from a detrital origin while roundness and similar shape should be a feature of particle derived from a suspension activity.

Analyses were performed on *susp* and *susp\_lump* fractions coming from seven different archeological sites. Analyzed suspensions are not always produced from samples leading to



accurate dating when compared to respective archaeological references. This could be an additional clue to better understand why radiocarbon dating failed.

Analyzed *susp* fractions derive from Minerva Medica Temple (TMM2), Palazzo Vecchio (PVEC 201), Narni Bridge (PN1, PN2), Palazzo Valentini (PVAL 13), Ostia Marina Excavation (OST6D) and Krakow Marquet Square Excavation (KR14, KR38). Only one *susp\_lump* fraction was analyzed belonging to PN1 sample.

### SEM Analyses

SEM-EDS analysis has been carried out on metalized samples. Metallization was performed with an Emitech K550X thinly layering Au on calcite powder. The analysis has been performed using a FEI-Quanta 400 Scanning Electron Microscope, coupled with an Energy Dispersive X-ray Spectroscopy operated at 20 kV.

The magnification of the obtained images is not higher than 50000x as the acquisition of images was difficult because of a bad conductive surface.

### Results and Conclusions

Table 9 summarizes all samples analyzed and relative SEM and  $^{14}\text{C}$  results. According to this dataset it can be affirmed that:

- All samples leading to a correct radiocarbon age should be free of contaminants. A series of collected images testify the absence of contaminant in these cases: there were no angular or splinter fractured particles on captured images at 5,3 and 1  $\mu\text{m}$ . Samples characterized by splinter particles but leading to an accurate radiocarbon age can be explained with presence of a pozzolanic (non calcareous) aggregate.
- Samples with wrong radiocarbon dating should contain some contaminant inside collected fractions. This leads to two different cases: a) there are splinter fractured particles on captured images, when mortar composition registers a calcareous component as aggregates; b) mortar is contaminated by a secondary calcite deposition which is not detectable with image analysis.
- Images proved that mean size collected by suspensions is above 1  $\mu\text{m}$ , while minimum size is below it. This ensures that main component of our collected suspended fractions derive from slaked lime carbonation step.

Of course the presence of very fine particles  $<1 \mu\text{m}$  indicates capability of Cryo2Sonic technique to select the right size fraction to date but it does not ensure lack of contaminants particles.

Table 9. Synthesis of SEM analysis applied on some representative samples. Type column indicates if original mortar had a pozzolanic (P) or sandy-calcareous (C) aggregate. Particles <1  $\mu\text{m}$  in all samples were observed, not the same for angular particles.

Sample	Type	Fraction analyzed	Accurate RC Age	Particles < 1 $\mu\text{m}$	Presence of angular particles	Reference Figure
PN1	P	susp	No	X	X	20
		Susp_lump	No	X	X	
PN2	P	susp	No	X		
OST 6D	P	susp	Yes	X		21
PVAL 1	P	susp	No	X	X	22
PVAL 13	P	susp	Yes	X		23
CMAx 2	P	susp	Yes	X		24
CMAx 3	P	susp	Yes	X	X	25
PVEC 201	C	susp	Yes	X		26
KR 38	C	susp	Yes	X		27
KR 14	C	susp	Yes	X		
TMM 4	P	susp	No	X	X	28

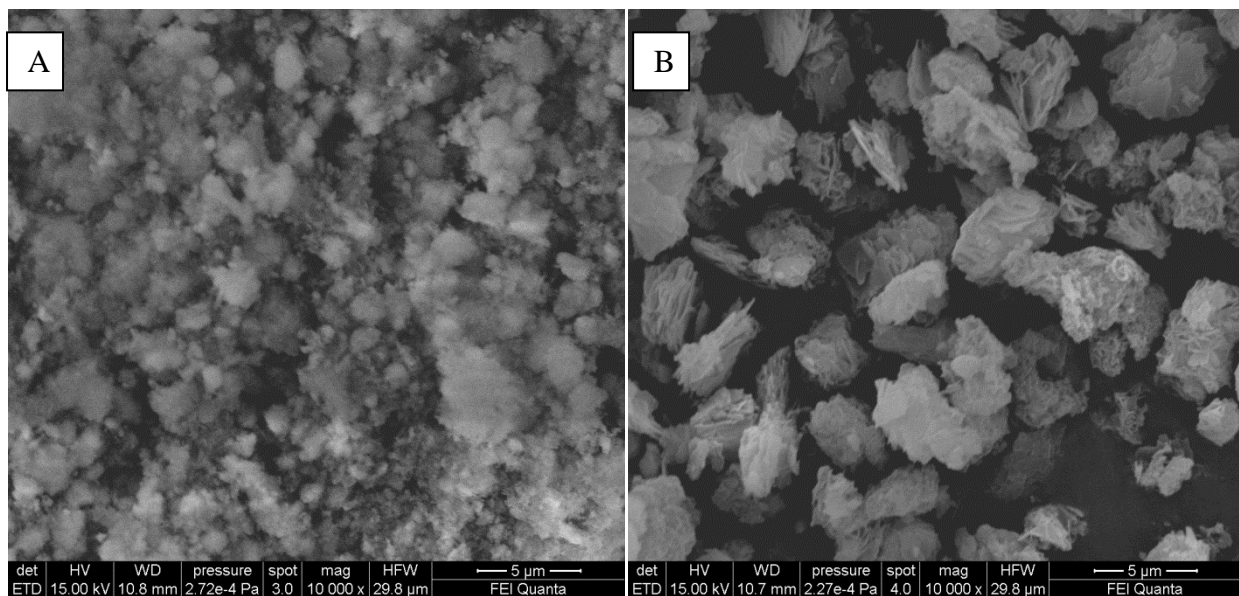


Figure 20. SEM images of PN2\_susp (A) and PN1\_susplump (B). A: visible particle dimension < 1  $\mu\text{m}$  and absence of splintery shaping. According to its final age younger than reference, indication of absence of dead carbon contaminants can be inferred. B: structures made of on-organized and un-homogeneous sheets, found also into the sample PN1\_susp. These angular and sheet-shaping particles could be connected with re-crystallization phenomena due to dissolution/re-precipitation processes which could explain the aging of these samples. Similar micromorphology were observed by Courty *et al.* (1989) and regarded weathering activity.

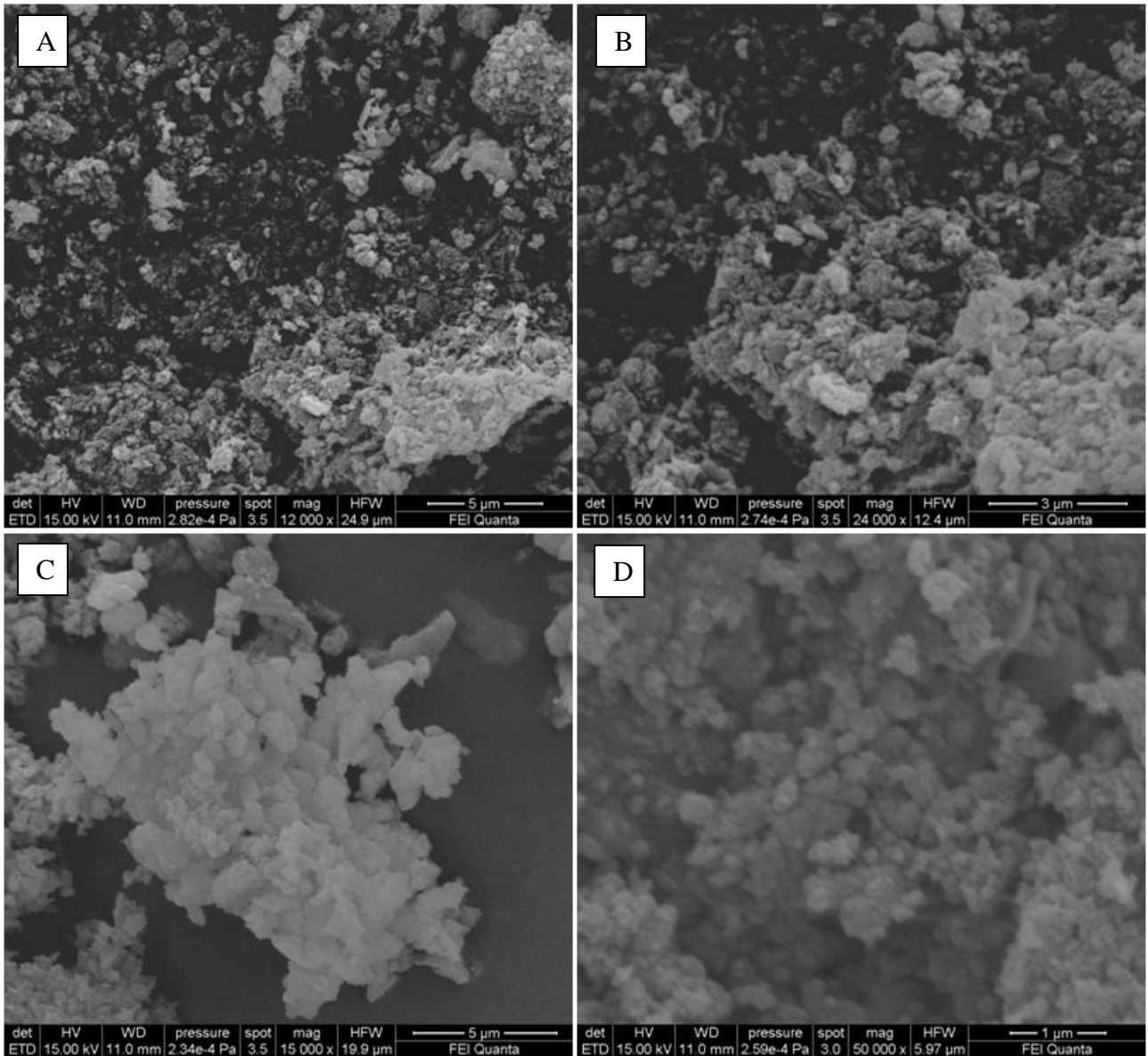


Figure 21. SEM images of OST6D\_susp at different magnifications. In all the images angular splinter particles are absent. Roundness is maintained and particles size is attested  $< 1 \mu\text{m}$ .

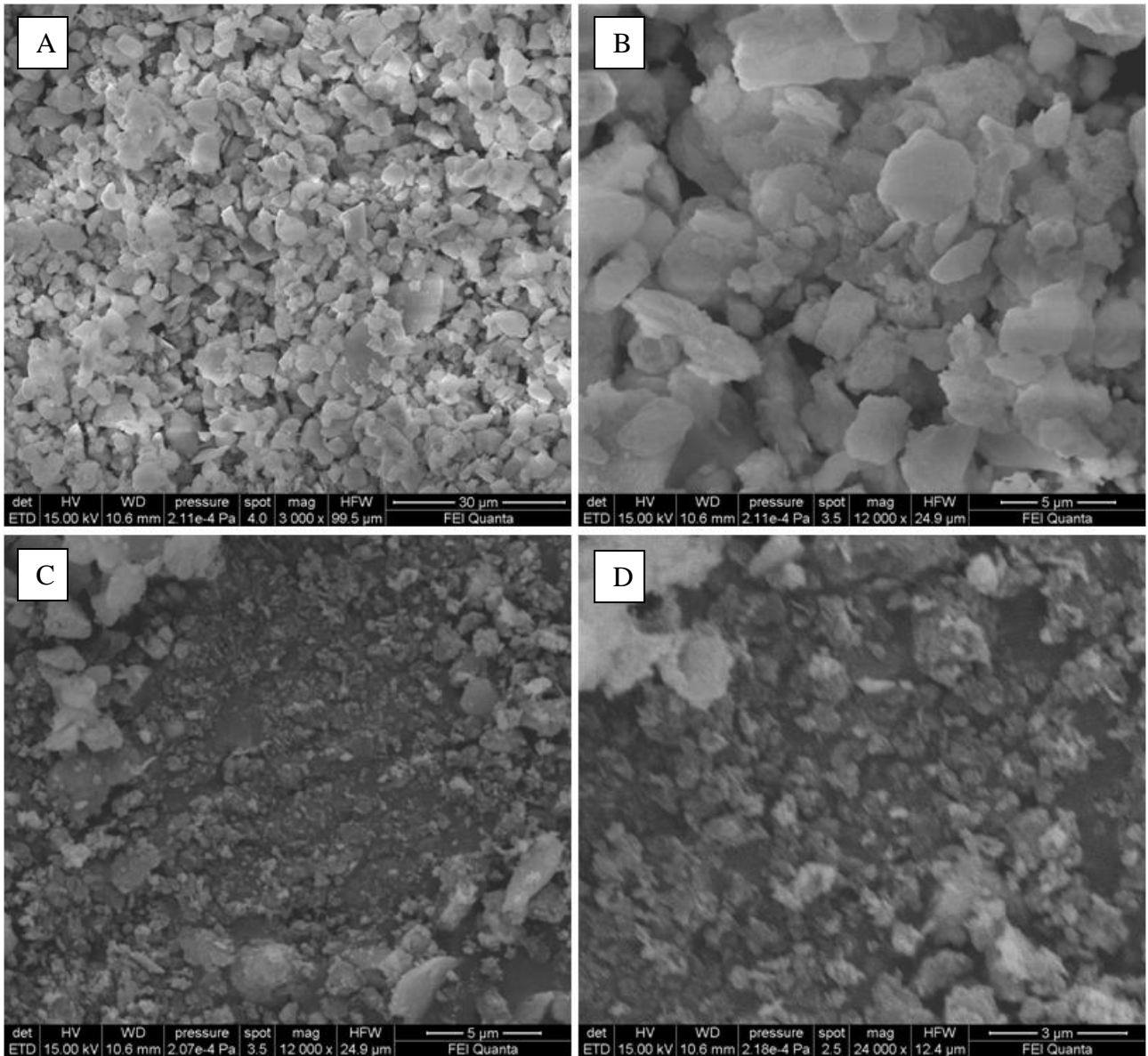


Figure 22. SEM images of PVALI\_susp at different magnifications. The images show the presence of some angular shaped particles ( A, B, C) which decrease at lower dimensions (D). PVALI\_susp gave an RC Age older than the expectations, but it should due to dead carbon coming from secondary calcite deposition generated by groundwater activities. In this case splinter morphology could own to pozzolanic aggregate so it could not be the reason of radiocarbon dating failure. Real contaminants instead should not be visible because their particles formed with a chemical process like binder ones.

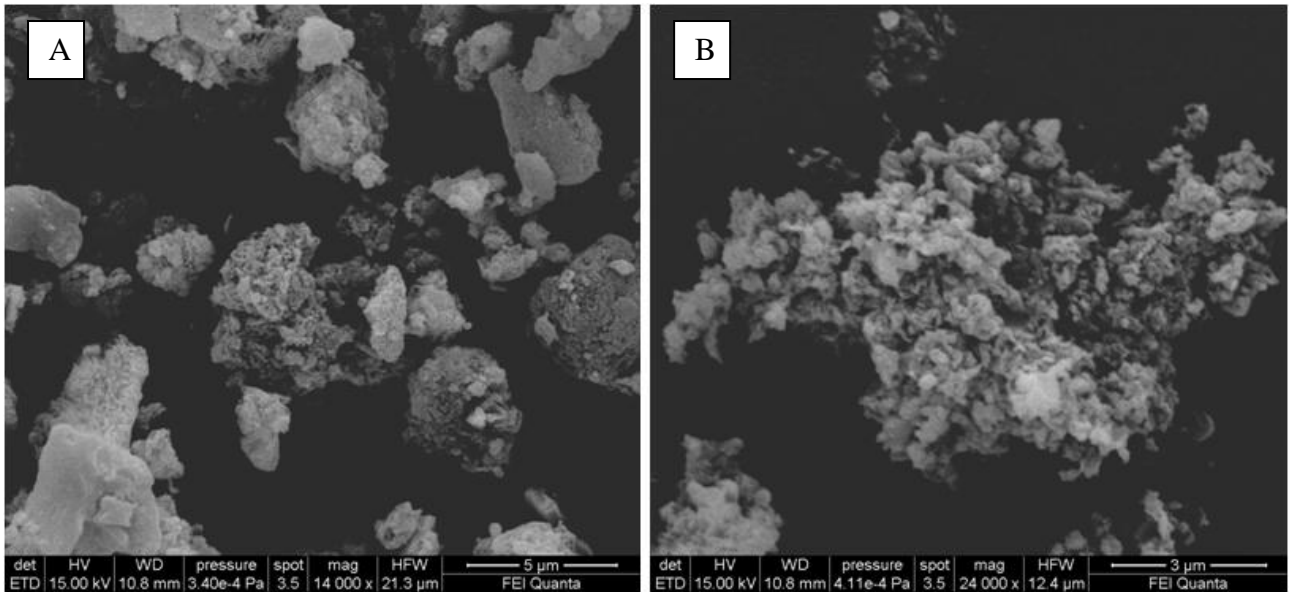


Figure 23. SEM images of PVAL13\_susp at different magnifications, showing particle minimum sizes  $<1 \mu\text{m}$ . Sample is made of particle with a fluffy shape, indicating their flocculating origin, and of some particles with geometrical shapes. These latter, probably deriving from aggregate portion, are usually bigger than  $5 \mu\text{m}$  and did not influenced radiocarbon dating because of their non calcareous origin (pozzolanic).

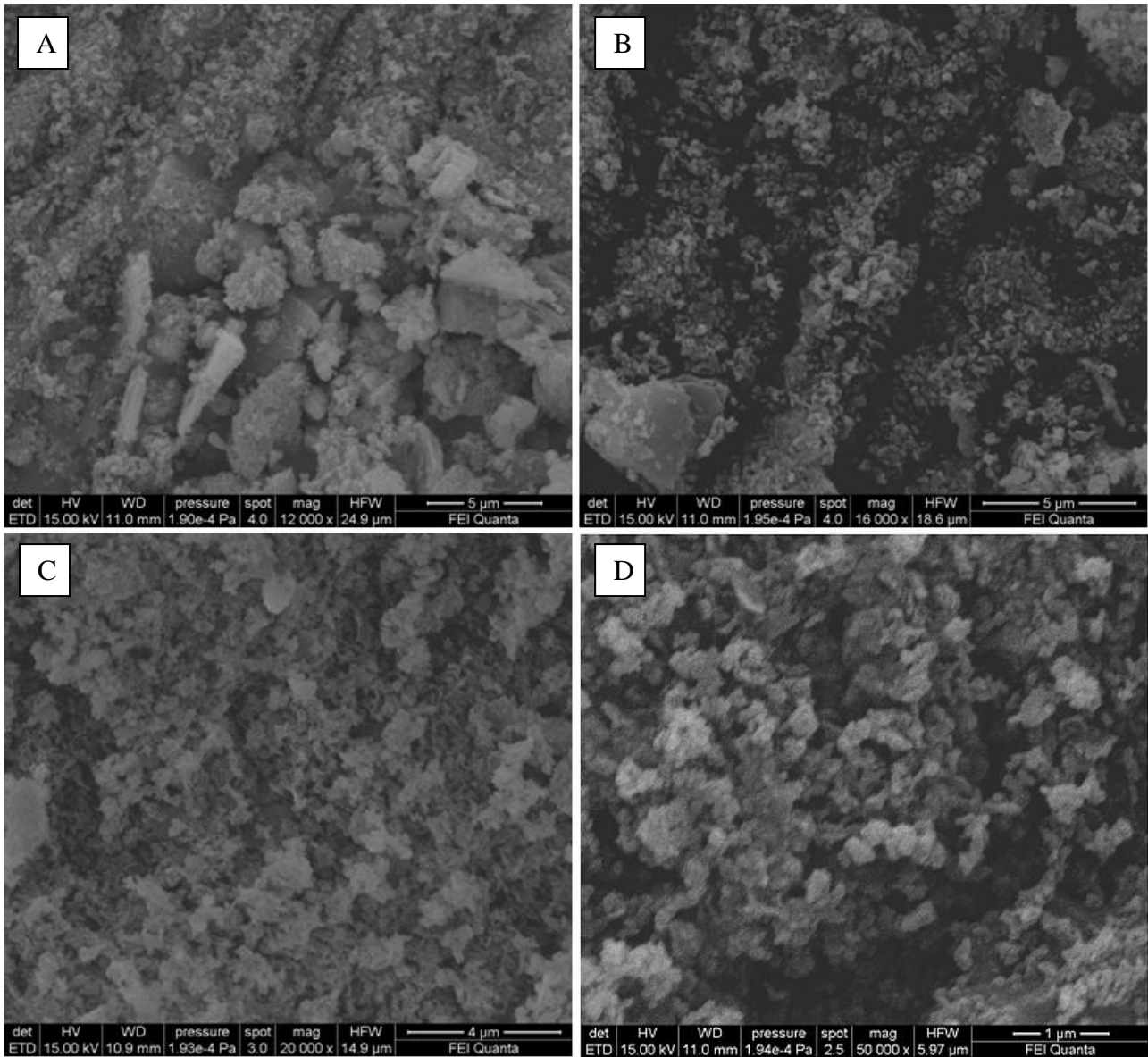


Figure 24. SEM images of CMAX2\_susp at different magnifications. All images show a minimum particle size  $<1 \mu\text{m}$ , in particular in D, the particles show clearly a rounded shape deriving from chemical production process of the binder portion.

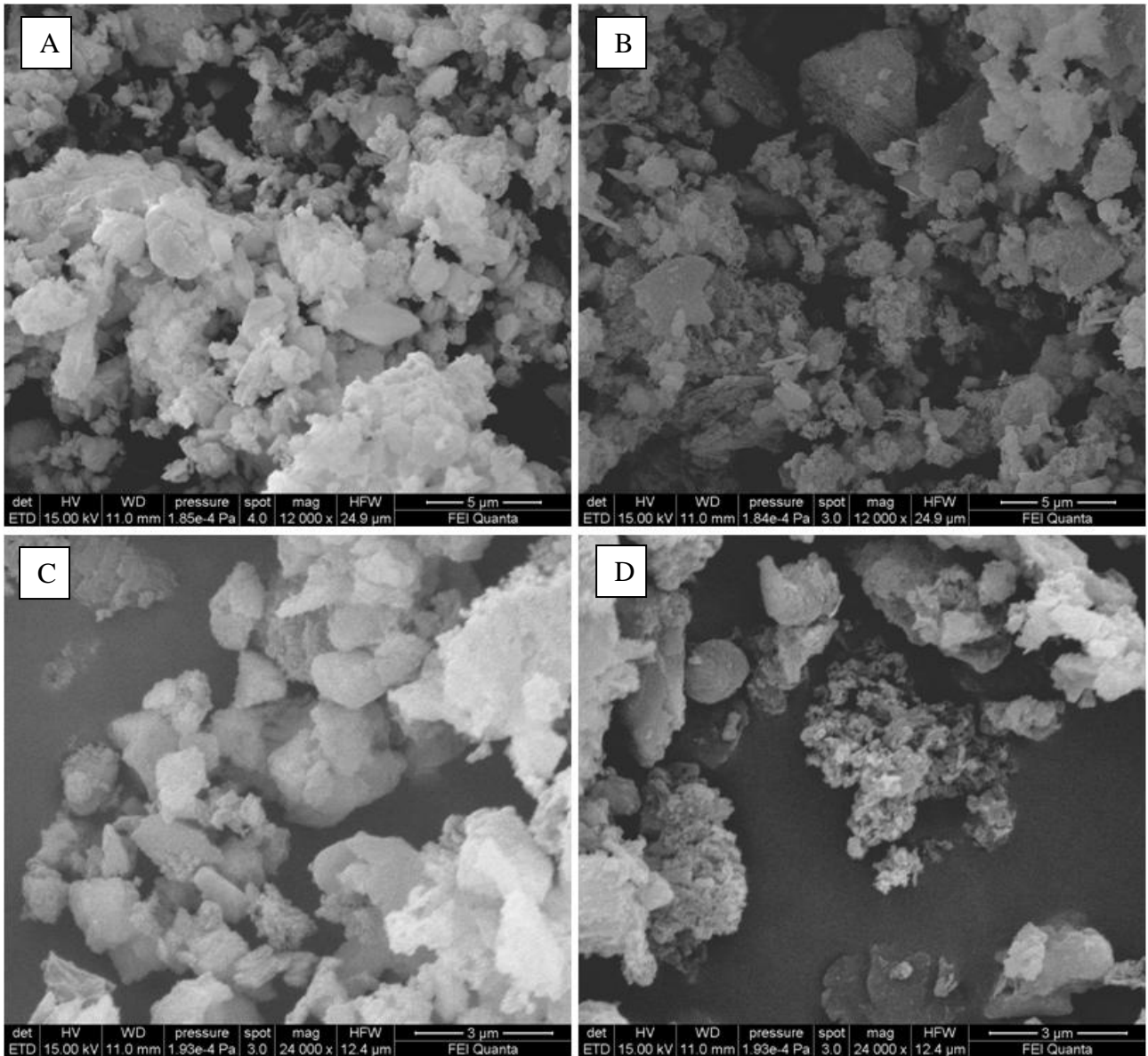


Figure 25. SEM images of CMAX3\_susp at different magnifications. C and D images show the presence of particles with size  $<1 \mu\text{m}$ , even if the average dimension seems to be higher. Smallest particles have a rounded shape while more splinter elements among particles of dimension  $>2,5 \mu\text{m}$  are visible. RC age was in agreement with archaeological reference, also in this case angular particles have a pozzolanic character.

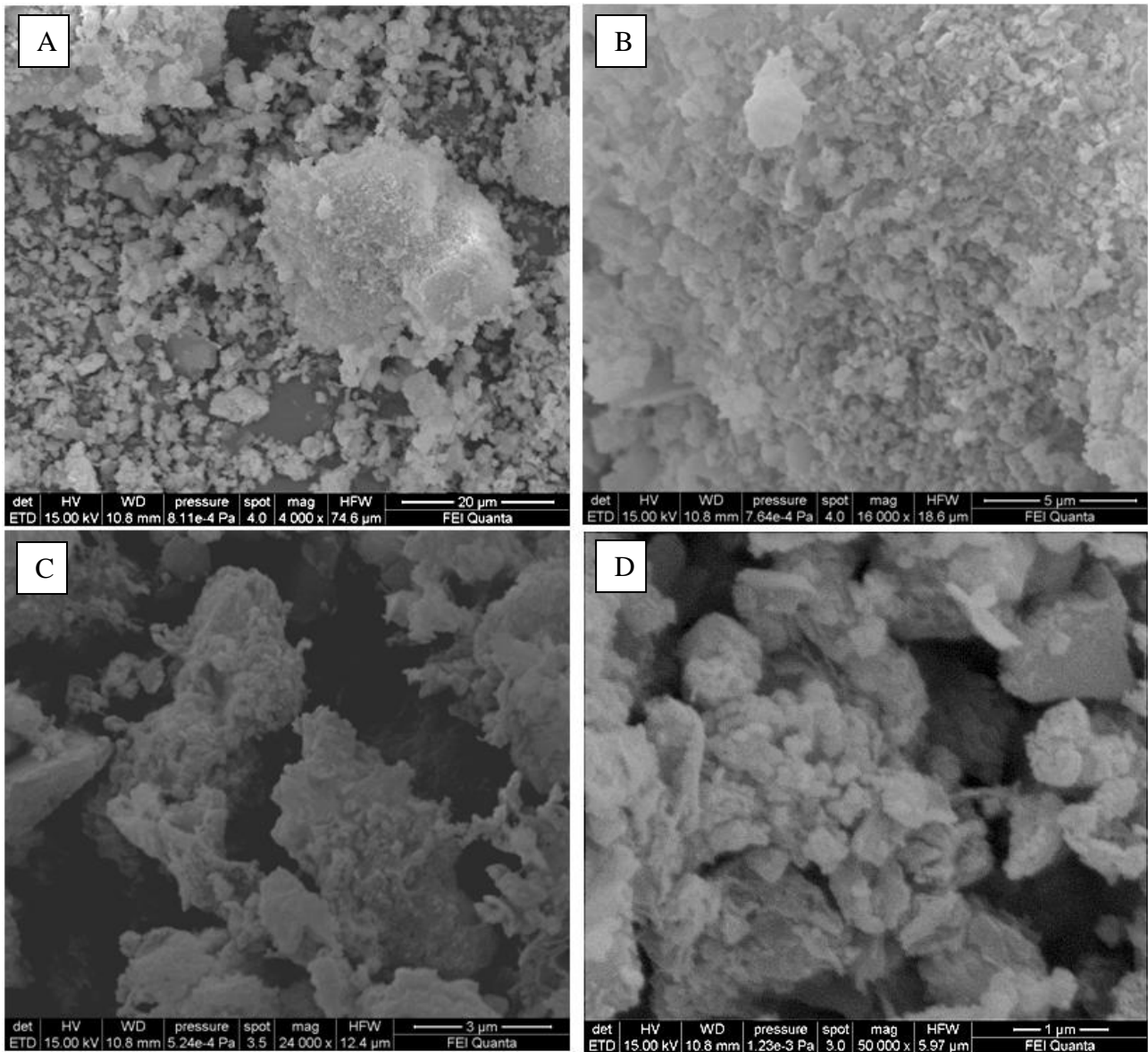


Figure 26. SEM images of PVAL201\_susp at different magnifications. Images confirm the presence of particles with size  $< 1 \mu\text{m}$  (D), linked each others to form aggregate structures dimensionally variable from 1 to several microns. Some sporadic acicular structures with size  $> 3 \mu\text{m}$  are detected. They represent geological material, most probably a part of sandy aggregate (not calcareous), which does not affect the radiocarbon dating. In D (higher magnification) some sheet shapes, probably related to re-crystallization phenomena are visible.



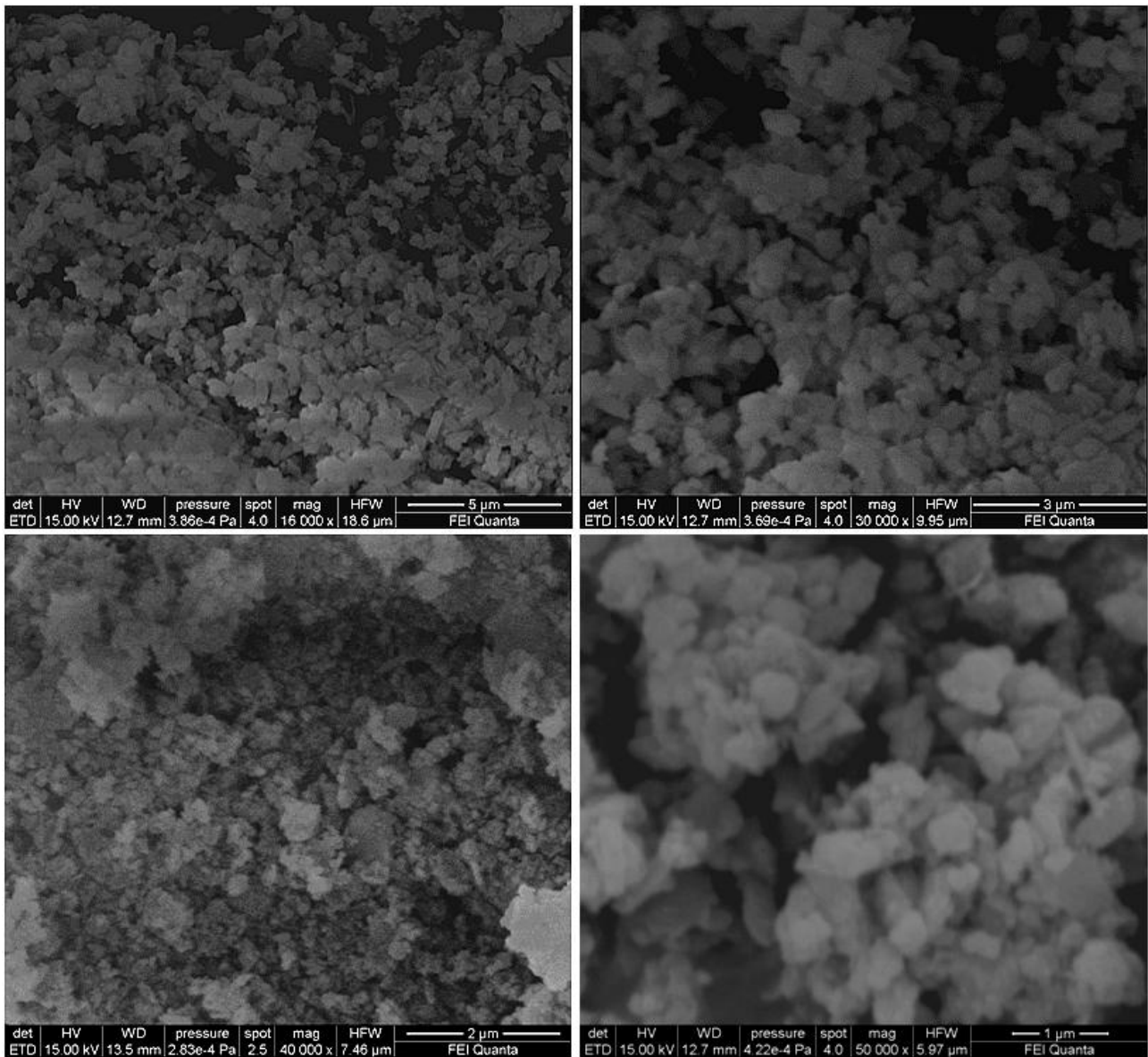


Figure 27. SEM images of KR38\_susp (A,B,D) and KR14\_susp (C) at different magnifications. The minimum size of suspended particles is  $<1 \mu\text{m}$  and there is no evidence of splinter fractured elements. Uniformity of morphology is repeated on both analyzed samples.

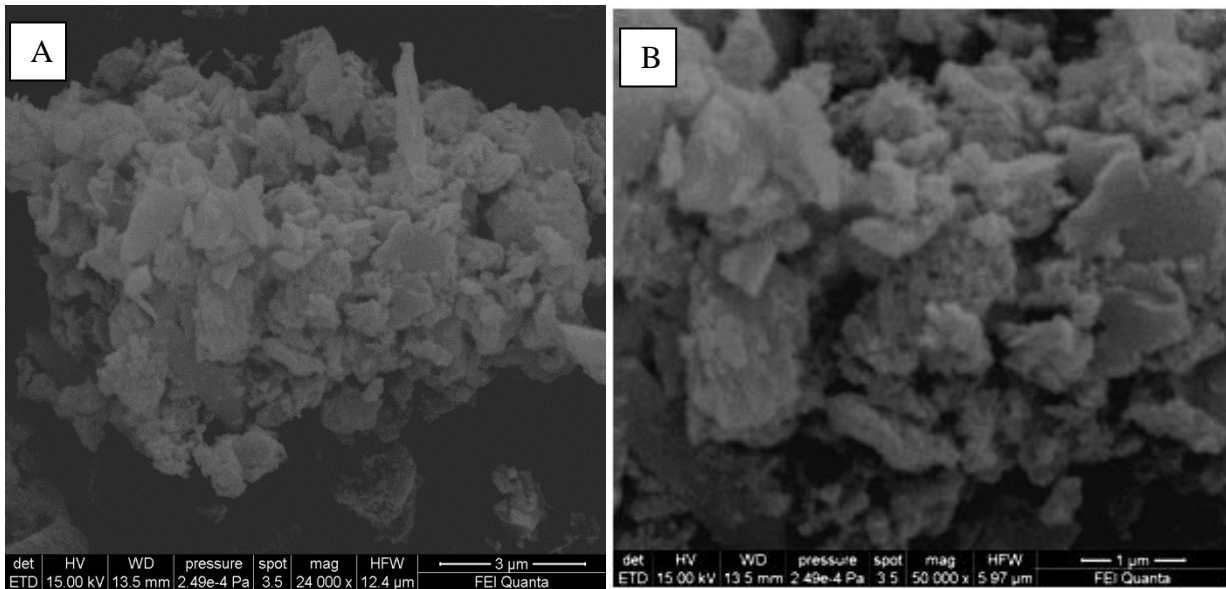


Figure 28. Magnifications at 24000 X and 50000 X performed on TMM4\_susp, showing the presence of particles with size  $<1\mu\text{m}$  and particles with angular shape (especially in A). RC age of TMM4\_susp did not match archeological constraints because buried structures were affected by groundwater activity which contaminated masonry mortar determining an aging in final radiocarbon dating (section II.5.2). Particles with angular shape probably own to pozzolanic component of mortar.

## II.6.2 Searching for dead carbon contaminants with CathodoLuminescence (CL).

CL is a sensitive analytical technique to detect small variations in trace element chemistry in many minerals and especially in zoned minerals and mineral cements (Marshall 1988, Pagel et al. 2000). The mineral group of carbonate has been extensively studied by means of CL. Quoting Machel (2000): “Cathodoluminescence petrography is a popular tool in investigation of carbonate rocks and their diagenesis.” The luminescence properties of calcite have been known since 1950’s (Medlin 1959) and they have been used in geosciences ever since (Pagel et al.2000), often in combination with other techniques such as SEM-EDX, PIXE, SIMS, etc. (Habermann et al.2000).

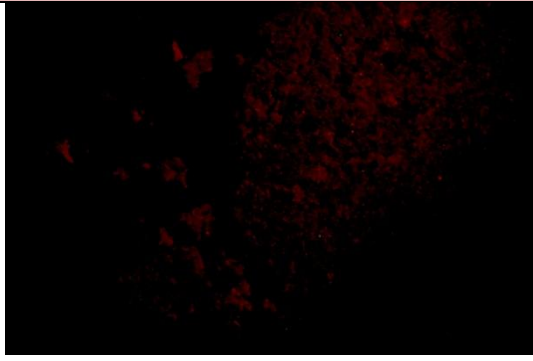
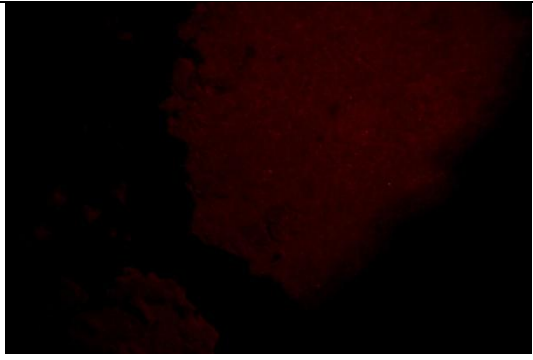


In CL the sample is placed in a vacuum chamber and irradiated with an electron beam. During this cathodic excitation several kinds of interactions between the electrons and solids occur. In CL the emitted, long wavelength electromagnetic radiation in the visible and near visible region is observed either visually or spectrometrically. During irradiation a valence electron is captured by conduction band and when it returns to equilibrium state a long wavelength photon is emitted. The wavelength is determined by the energy gap between the excited state and the equilibrium state. The transition may be split up into several steps (Pagel et al. 2000). Only one type of energy transition is relevant for the type of carbonates studied: CL activation by trace element activators in major element


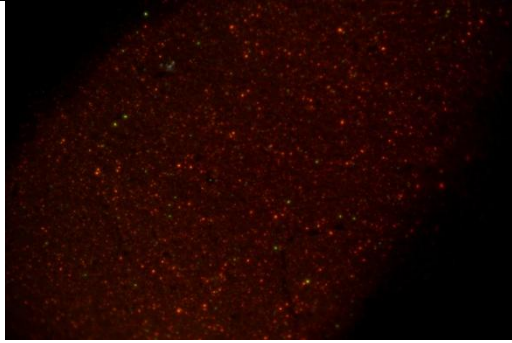
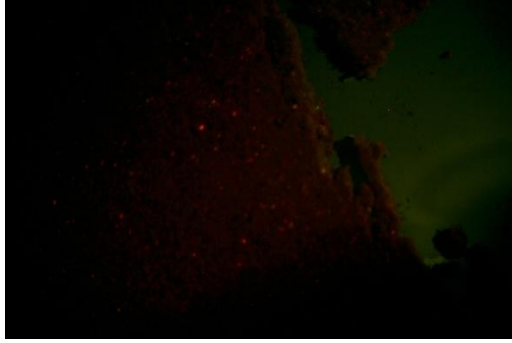
positions in the calcite lattice. Typical activators are the transition elements, rare earth elements (REE) and actinides. Luminescent centers and non-luminescent centers have been observed in correspondence to manganese and iron respectively (Habermann et al. 2000). In practice, the only activator we have utilized so far is manganese in the calcite, dolomite or aragonite lattice. The role played by  $Mn^{2+}$  ion is unquestionable as it causes a radiative transition when substituting  $Ca^{2+}$  in distorted octahedral sites of the calcite structure (Medlin 1959). Substitution determines an orange cathodoluminescence of calcite due to the presence of  $Mn^{2+}$  cations. As suggested by Habermann et al. (2000) and Cazenave et al. (2003) different interpretations reflect the different process and genetic conditions of the formation of calcite (i.e. hydrothermal, sedimentary, etc.). CL has a potential on mineralogical studies also what about quartz, feldspar and plagioclase (Lindroos 2005). Here we just consider a qualitative use of CL survey to verify the presence of geological calcite (limestone) inside selected fraction of binder obtained from archaeological sample treatment. Observation of CL images could discriminate mineralogical composition of grains contained inside *susp* and *sand* fractions knowing that: binder calcite is usually dark brown in color with variations from tile-red to nearly black (depending on poor to slightly luminescent) (Labeyrie and Delibrias 1964); quartz CL color is blue; K-feldspars are green; limestone fragments are red-orange; hydraulic components are deep-blue; secondary “young” calcite has a bright yellow-orange color (much brighter than binder calcite) (Lindroos 2005).

Powders have been homogenized in an agate mortar and then put on a thin section glass. Cathodoluminescence images were obtained using a petrographic microscope (NIKON Labophot2-POL) equipped with a cold cathode stage (Cambridge Image Technology Ltd, CL8200 MK3 model) operated at a voltage of 15 kV and current of 200 A. Collection was performed using a CANON Reflex EOS 600D.

The observations have been performed on suspended fractions already radiocarbon dated. Samples that presented both bad than good accuracies when compared to archaeological references and consequently representing DC contaminated and free composition, underwent CL. Analyzed samples come from five different sites: the Wielka Waga at the Krakow Market Square (KR), Palazzo Valentini in Rome (PVAL), Palazzo Vecchio in Florence (PVEC) and Qumran settlement in Death Sea region (Q3). CL analyses gave back some encouraging results: comparing RC ages found for each *susp*, with their relative CL images it can be affirmed that Cryo2SoniC protocol seems to be a really successful selective method. When contamination particles appeared, the bulk mortar accounted for fine calcareous aggregate, such as it happened for PVEC201 (see section III.2)

or for Qumran site (see section II.7). All the investigated cases shown an overall agreement between radiocarbon results and *susp* cathodoluminescence (Table 10).

Sample	CTL Image
<p><b>KR14 susp</b></p> <p>It shows an overall uniformity of luminescence, which is representative both of a uniform composition and of an absence of geological highly luminescent calcite grains, according with its RC age. Absence of grain referred to its quartz aggregate component.</p>	 <p style="text-align: right;">4x</p>
<p><b>KR14 sand</b></p> <p>As the sample has the same RC age of KR14_susp it shows a comparable behavior with CTL observation. Even in this case, there is no evidence of geological calcite particles or sandy aggregates components.</p>	 <p style="text-align: right;">4x</p>
<p><b>PVAL14 susp</b></p> <p>Radiocarbon dating was in agreement with archaeological expectations and CL images confirm this result: the sample is composed exclusively of binder particles.</p>	 <p style="text-align: right;">10x</p>
<p><b>PVAL13 susp</b></p> <p>Archaeologically and chronologically (RC age) attributed to the same period of PVAL14 and PVAL15, its CL image shows the absence of highly luminescent grains.</p>	 <p style="text-align: right;">10x</p>

<p><b>PVAL15 susp</b></p> <p>Chronologically similar to PVAL14 and PVAL13, its CL image is coherent with ones of others samples and with expectations of absence of dead C contamination. Its CL image shows a mass of binder particles completely free of calcite grains of geological origin as already seen for the previous ones.</p>	 <p>4x</p>
<p><b>PVEC201 susp</b></p> <p>Into this fraction many light spots attributable to grains of geological calcite are visible together with others attributable to quartz and feldspar. This represents a clue for a not accurate selection. In this case final RC age is strongly DC contaminated and far from the archaeological expectation value.</p>	 <p>4x</p>
<p><b>Q3 susp</b></p> <p>It represents a DC contaminated sample, whose contamination is testified by its CL image: high abundance of luminescent grains confirms an inefficient selection due to the presence of a biomicrite sand as aggregates. It reflects a strongly aged dating.</p>	 <p>10x</p>

### II.6.3. FT-IR as an alternative analytical toll to investigate material suitable for RC dating

Infrared spectroscopy is capable to reveal the presence of different calcium carbonate polymorphs, on the basis of different infrared absorption behavior. For this reason, an investigation has been performed on selected fractions of material collected after Cryo2SoniC pre-treatment on archaeological mortars, to check the possibility to discriminate suspensions with calcite of different origin. In particular, our experiment is based on work of Chu et al. (2008), where the possibility to differentiate between anthropogenic and natural calcite using FT infrared spectroscopy is reported. Fourier transform infrared spectroscopy (FTIR) represents a common and useful tool for studying organic and inorganic compounds. It provides information not only on the type of calcium carbonate polymorphs, but also on the extent of atomic order. FTIR measurements are usually fast, require very low amounts of material and can be operated on-site (Weiner and Goldberg, 1990). It is

based on the interaction between radiation in the infrared region and the molecules of the sample. It thus provides information on the nature of the atomic bonds as well as their structural organization. Moreover, it can provide information on the extent of atomic order of the mineral phase (Farmer, 1974). In calcite three of the infrared absorption peaks (called  $\nu_3$ ,  $\nu_2$  and  $\nu_4$ ) correspond to the asymmetric stretch ( $\nu_3$  :  $1420\text{ cm}^{-1}$ ), out-of-plane bending ( $\nu_2$  :  $874\text{ cm}^{-1}$ ) and in-plane bending ( $\nu_4$  :  $713\text{ cm}^{-1}$ ) vibrations of the carbonate ions, respectively (White, 1974). Beniash et al. (1997) observed that the peak intensity ratio  $\nu_2/\nu_4$  reflects the extent of atomic disorder in the calcite crystal, and following these observations Chu et al. (2008) noticed that  $\nu_2/\nu_4$  ratios of some plaster samples from archaeological sites are still high compared to geological calcite. Data show that disorder introduced into the calcite crystal lattice exposed to high temperatures can be preserved over long periods of times and together with diagenesis effects of the environment, determines a variability in  $\nu_2/\nu_4$  ratios. It was determined that the lower limits of  $\nu_2/\nu_4$  ratios by analyzing limestone rock samples and sparry calcite, is around 3 (Beniash et al. 1997; Chu et al. 2008). The upper limit was determined by experimentally heating limestone and determining whether or not it was completely transformed into calcium oxide: a  $\nu_2/\nu_4$  ratio between 5.8 and 7.2. The  $\nu_2/\nu_4$  ratios of plaster samples obtained from archaeological sites of various ages, lie within the range defined by the two endmembers: modern plaster and geological calcite samples. Observed indexes fall between 3 and 6, indicating that in some cases, the plaster may still contain some of the primary anthropogenic calcite component. Chu et al. (1998) affirm that this  $\nu_2/\nu_4$  ratio can be used to identify plaster samples only if they were completely burnt and diagenesis phenomenon is negligible, and therefore might retain their original radiocarbon content. Of course, an archeological mortar unlikely could reflect these conditions, but maybe a *susp* fraction could. A *susp* fraction, selected with the Cryo2SoniC method and which have already Radiocarbon dated with constraint archaeological ages, can be considered a system of ideological “pure binder”. In this prospective a *susp* fraction with a good radiocarbon dating feedback should theoretically show a  $\nu_2/\nu_4$  ratio higher as possible.

### Materials and Methods

Samples were transformed in KBr pellets before analysis. Measurements were performed in pure dry atmosphere to remove humidity and  $\text{CO}_2$  signals with a Fourier Transform Infrared Spectrometer Varian 4100 (Excalibur series), with a resolution of  $4\text{ cm}^{-1}$  over a spectral range of  $4000\text{--}400\text{ cm}^{-1}$ .

FTIR measurements were carried out in transmission mode on KBr pellets containing a suitable amount of specimen. The  $\nu_2/\nu_4$  ratio is estimated by dividing the height of the  $\nu_2$  peak by the height of the  $\nu_4$  peak. The baselines were subtracted between the closest minima on either side of the

measured peak, considering that heights of peaks measured is influenced by the choice of baseline (Chu et al. 1998). The analytical uncertainty in measurement of the  $v_2/v_4$  ratios is  $\pm 0.2$ . Each sample was measured from two to five times and each measurement was from a different part of the sample (as done in Chu et al. 2008).

The amount of material sample to be added to KBr powder has been evaluated carrying out tests on specimens containing from 0.1 up to 1.0 wt % of a standard calcite material (Carlo Erba RPE ACS with 99,5% pureness). Their results are visualized in Table 11. The results of this first phase highlighted that the most suitable concentration of calcite is 0.1 %, as for higher values the relevant absorption lines had intensities too strong to remain in the instrumental range. Once a suitable ratio of calcite vs KBr had been determined, a series of repeated tests was carried out with the main purpose to evaluate the precision of the method (Table 12).

A further test was performed on a calcite sample obtained from a hardening experiment carried out with a pure  $\text{Ca}(\text{OH})_2$  standard material (99% pure portlandite), to test the IR sensitivity upon newly crystallized calcite. Observed  $v_2/v_4$  index over a single sample was in agreement with previous expectations (much more higher than the calcite (Table 12)).

Analyses were successively performed on a series of archaeological samples (Table 12) from Palazzo Valentini, in Rome (PVAL), Palazzo Vecchio in Florence (PVEC), Circo Massimo in Rome (CMAX), Ponte di Augusto in Narni (PN) and Wielka Waga in Krakow (KR). Samples were prepared testing two kind of dilution with KBr: 0,5% and 0,1% in weight. Pads were differentiated in three types: bulk (sample crushed in agate mortar as the same), *susp* (suspension selected by Cryo2SoniC theoretically representative of the binder), *sand* (suspension selected by Cryo2SoniC potentially contaminated).

Table 11. Measures performed by FTIR on reference samples to acquire specific terms of comparison.				
Sample	Absorbance		$v_2/v_4$	Kind of Material
	on $v_2$	on $v_4$		
<b>To check the optimal concentration</b>				
CaCO <sub>3</sub> synth 0,1%	0.095	0.103	0.922	CaCO <sub>3</sub> Carlo Erba RPE ACS 99,5%
CaCO <sub>3</sub> synth 0,5%	0.279	0.355	0.786	
CaCO <sub>3</sub> synth 1%	0.19	0.39	0.487	
<b>To evaluate precision of the method</b>				
CaCO <sub>3</sub> synth 0,1%	0.094	0.101	0.931	CaCO <sub>3</sub> Carlo Erba RPE ACS 99,5%
CaCO <sub>3</sub> synth 0,1%	0.096	0.104	0.923	
CaCO <sub>3</sub> synth 0,1%	0.095	0.104	0.913	
CaCO <sub>3</sub> synth 0,1%	0.095	0.103	0.922	
CaCO <sub>3</sub> synth 0,1%	0.094	0.102	0.921	
Synth Binder 0,1%	0.04	0.005	8	CaCO <sub>3</sub> da $\text{Ca}(\text{OH})_2$ purissimo

## Results

The results of FTIR analyses of synthetic samples, were in agreement with Chu et al. (2008). They showed a  $\nu_2/\nu_4$  ratio lower than 3 for samples composed of pure geological calcite and 8 for sample obtained from an “homemade” plaster produced from a standard calcium hydroxide (Table 11). This last data is a very good one, considering that time of setting used was limited to 48 hours.

There is a good reproducibility on the same sample and a decrease of  $\nu_2/\nu_4$  ratio when concentration grows up (Table 11). Once working optimal conditions were established, FTIR measurements on archaeological samples starting from bulk samples measurements was performed. In detail, two pozzolanic mortars (PVAL13 and CMAX8) were examined by means of KBr pads at 0,5%. The values of  $\nu_2/\nu_4$  were above 3–3.5 due to no selection of binder portion, probably attributable to the carbonate component of aggregates, unburned limestone residues or secondary calcite crystals (due to weather or groundwater resurgence).

The following step consisted of FTIR analyses performed on pads of *susp* and *sand* fractions (collected with Cryo2Sonic). Expectations over  $\nu_2/\nu_4$  ratios are the higher the ratios the less is the DC contaminants. This last condition is strictly connected to the success of RC dating. Collected  $\nu_2/\nu_4$  ratio showed a general non homogeneity in results if matched with respective RC ages (Table 12). Some *susp* fractions measured as KBr pads at 0,5% (not shown) produced often a saturated spectrum, where the high presence of silica determined a covering of  $\nu_2$  peak by Si-O-Si peak ( $1000\text{ cm}^{-1}$ ). This inconvenient was bypassed using pads at 0,1% in concentration that didn't maintain same  $\nu_2/\nu_4$  ratio whit the changing of dilution (see PVAL13 in Table 12).

According with measured RC Ages, samples from Palazzo Valentini (PVAL 13/14/15e) are expected to bring to similar results independently by their typology (*sand* and *susp*). Agreements were observed on FTIR measurements performed on *sand-susp* fractions belonging to PVAL14 but they were not for fractions coming from PVAL13 and PVAL15 that showed couple of  $\nu_2/\nu_4$  ratios from slightly different (PVAL15) to significantly different (PVAL13). Expected ratios should not only be, as close as possible, but also as near as possible to 8 when a successful RC dating confirms the absence of DC contaminations. All experimental results are comprised between the ratio range suggested by Chu et al. (2008) for archaeological samples (3-6) and partially included in the range for completely binder-made samples (5.7-7.2), although they are still far from having a constant value. There is also an anomalous high value (PVAL13 sand 0,1%), maybe indicating that it contains almost only anthropogenic calcite (Table 12). This anomaly should be more deeply investigated by means of further measurements.

Samples from Circo Massimo as the previous, are not coherent with their dating: CMAX from 1 to 5, for example, should have same  $\nu_2/\nu_4$  ratios because belonging to the same US and moreover lead



Sample	Absorbance		$\nu_2/\nu_4$	Calibrated RC age	Chronological Reference
	on $\nu_2$	on $\nu_4$			
PVAL 13 Bulk 0.5%	0.203	0.063	3.22	-	-
PVAL 13 Susp(1) 0.5%	0.198	0.048	4.12	337 – 421 AD ( $2\sigma$ )	Beginning of 4 <sup>th</sup> century
PVAL 13 Sand(1) 0.5%	0.155	0.023	6.74	238 – 335 AD ( $1\sigma$ )	
PVAL 13 Sand(1) 0.1%	0.001	0.021	21.00		
PVAL 14 Sand(1) 0.1%	0.006	0.038	6.33	130 -323AD ( $2\sigma$ )	
PVAL 14 Susp(1) 0.1%	0.006	0.038	6.33	259 – 408 AD ( $1\sigma$ )	
PVAL 15 Sand 0.1%	0.028	0.11	3.93	85 – 321 AD ( $2\sigma$ )	
PVAL 15 Susp 0.1%	0.021	0.107	5.10	140 - 334 AD ( $1\sigma$ )	
CMAX 8 Bulk 0.5%	0.183	0.053	3.45	-	
CMAX 1 Susp 0.1%	0.008	0.064	8.00	111 BC – 75 AD ( $2\sigma$ )	Second half of 1 <sup>st</sup> to first half of 2 <sup>nd</sup> century
CMAX 2 Susp 0.1%	0.005	0.025	5.00	164 BC – 64 AD ( $2\sigma$ )	
CMAX 3 Susp 0.1%	0.016	0.051	3.19	352 BC – 124 AD ( $2\sigma$ )	
CMAX 4 Sand 0.1%	0.014	0.053	3.79	24 – 125 AD ( $1\sigma$ )	
CMAX 5 Susp 0.1%	0.011	0.038	3.45	43 BC – 80 AD ( $1\sigma$ )	
CMAX 6 Susp 0.1%	0.006	0.036	6.00	37 CB – 208 AD ( $1\sigma$ )	
CMAX 7 Susp 0.1%	0.006	0.038	6.33	379 BC – 129 AD ( $2\sigma$ )	
PVEC 201 Sand(b) 0.1%	0.02	0.09	4.50	55 BC – 69AD ( $2\sigma$ )	
PVEC 201 Susp 0.1%	0.035	0.158	4.51	402 – 668 AD ( $2\sigma$ )	
PVEC 208 Susp 0.1%	0.006	0.047	7.83	889-1389 AD ( $2\sigma$ )	
KR 14 Susp 0.1%	0.068	0.278	4.09	1428-1520 AD ( $2\sigma$ )	Second half of 15 <sup>th</sup> century
KR 38 Susp 0.1%	0.077	0.327	4.25	1402 – 1516 AD ( $1\sigma$ )	

to the same RC Ages. This did not happen and a great variability was observed, going from 3 to 8 value of  $\nu_2/\nu_4$  ratio. Taking into account only  $\nu_2/\nu_4$  ratios, you might mistakenly infer a contamination of geological calcite on samples like CMAX 4/5/6 that, according to  $^{14}\text{C}$ , are instead free of DC. All samples have similar RC results, are in agreement with archaeological reference and consequently should show high values of  $\nu_2/\nu_4$  ratios which are typical of the absence of DC contamination. According to Chu et al. (2008) and our preliminary characterization only CMAX1 could be defined as a totally anthropogenic calcite fraction.

Data collected from PVEC samples (code for mortars coming from Palazzo Vecchio) are not totally in agreement with RC Ages. PVEC208 is characterized by a successful dating so should bring to high  $\nu_2/\nu_4$  ratio close to upper limit fixed for totally pure anthropogenic calcite material, but it did not. On the contrary, PVEC 201, is in agreement with archaeological dating only with the sand fraction while *susp* one presents a rejuvenation tendency which should be translated in higher  $\nu_2/\nu_4$  ratios. From Table 12 an intermediate situation can be seen, with both  $\nu_2/\nu_4$  ratios around 4.5 value, which is a ratio lower than expected. It should be noted the absence of  $\nu_2/\nu_4$  ratio differences

between the sample without contamination and the sample with a rejuvenating contamination at FTIR level should also be observed.

Finally, samples from Krakow Market Square excavation having a positive match between RC age and archaeological expectations should be free of DC contaminants. This should be translated into high  $\nu_2/\nu_4$  ratios, but on the contrary, measured FTIR data on KR samples showed a disagreement with this condition:  $\nu_2/\nu_4$  ratios fixed around 4, with values lower than expected.

### Conclusions

Measurements of  $\nu_2/\nu_4$  ratio on selected fraction using FTIR technology can be defined as a developing method. According to Chu et al 2008, low values of  $\nu_2/\nu_4$  ratio are due to the presence of geological calcite; however, our experimental results showed that low values, can be obtained also in samples which are not affected by dead carbon contamination. Hypothesizing that accurate RC dating should bring to the absence of DC contaminations, the observed incongruence between these values and  $\nu_2/\nu_4$  ratios could be due to several causes, different from the incomplete removal of geological calcite. These causes could be: i) presence of a high silicate signal (e.g. in samples with hydraulic components or fine sandy aggregate) which gave a problematic interpretation of FTIR calcite peaks, ii) FTIR data could be affected by procedure of sample preparation.

Although FTIR results are sometimes in agreement with measured RC ages and provisions of pureness from contaminants,  $\nu_2/\nu_4$  ratios calculation couldn't be considered a useful and trusty method to check relative abundances of anthropogenic calcite respect geological one. The results of the application of this method in the present case are not both constant and reproducible; therefore, it seems that  $\nu_2/\nu_4$  ratios calculation couldn't be a trustworthy method without further deeper and wider applications to different cases.

## II.7. Methods Comparison

In this section a series of comparisons between mortar pre-treatment methods adopted by the Poznan Radiocarbon Laboratory in Poland and the CIRCE will be shown aiming to compare observed results. Comparison will be performed on the measured calendar age of several mortar samples coming from different archaeological sites with constrained age. Each sample underwent two different preparation protocols and results compared with each other and with archaeological references, in order to define the most accurate pre-treatment. The common aim of the applied procedures is to collect the right mortar binder fraction. To achieve this CIRCE applied the Cryo2SoniC while the Poznan laboratory utilised a mechanical separation coupled with stepped acid digestion based on already published works: Goslar et al. (2009), Nawarocka and Michniewicz (2011) and Michalska et al. (2013). The analyzed samples come from three different archaeological sites:

- A wall of the Hesmonean Palace in Jericho (AA code);
- A perimetral wall of the Great Scales (Wielka Waga) under the Krakow Market Square (KR code);
- A ruin of the Roman settlements of Qumran at the west coast of the Dead Sea (Q code).

Before dating procedure, the petrographic analysis of the selected mortar samples has been carried out in order to characterize the type of binder and aggregate.

### Sample Description

Jericho sample is an aerial mortar, whose aggregate shows the distinct presence of less dense and brittle foraminiferous limestone (Figure 29 B, C, D) as well as scattered small pieces of foraminifera shells dispersed throughout the entire binder (Goslar et al. 2009).

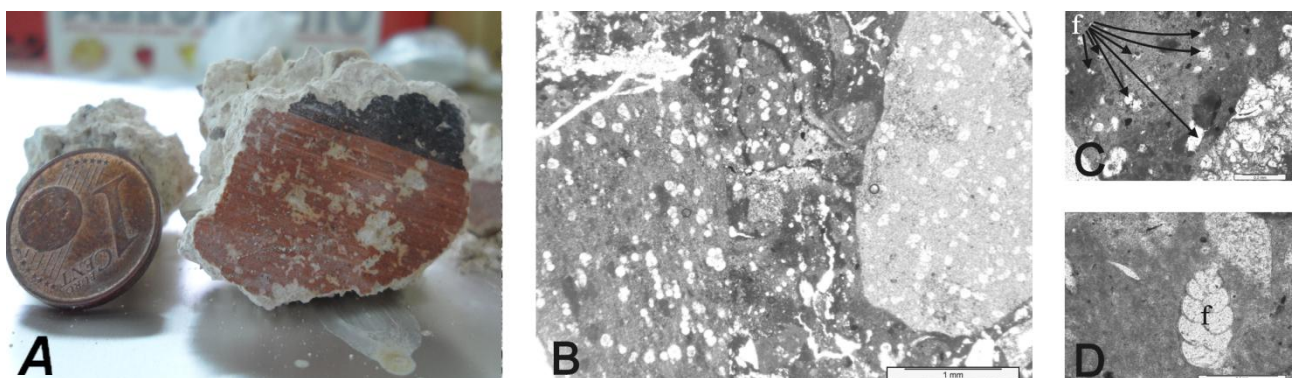


Figure 29. Photograph: A – AA25 sample before treatment (1 cent diameter is 15 mm); Photomicrographs of AA25 sample (polarizing light microscopy, XN): B panoramic view, C and D magnified views of AA25 image; C- Small, crumbled foraminifera pieces (f); D – a whole foraminifera shell (f); (Goslar et al. 2009).

Qumran samples show similar petrographic features as they are a mixture of flints, limestones and dolomites and mortars showed the distinct presence of scattered shells and crumbled limestone with less dense foraminiferous litho types (Michalska et al. 2013). Identification and characterization (i.e. dimension) of carbonaceous aggregate is very important taking into account the necessity of “dead carbon” suppression, because as already discusses (section II.5), the probability to find a DC contamination increases directly with the presence of very fine particles.

Krakow samples, instead, have a completely different composition based on the use of quartz sand as aggregate. They contain mainly grains of quartz and less numerous grits of cherts, fragments of feldspars, granitoid rocks, sandstone and mudstone. Most samples contained macroscopically observable white false lime lumps formed as a result of mortar recrystallization, which could have a significant influence on the final dating.

From material observations of these samples two different risks have been highlighted: the aging on Middle East samples (from Qumran and Jericho) and the a combination of rejuvenating/aging effects on Polish samples (from Krakow).

### Methods

Poznan Radiocarbon Laboratory applied slightly different methodologies to samples according to the examined site. Poznan methodology could be summarized in a multiple step of soft crushing, crumbling and sieving with the aim to select a fine fraction (changeable between 63 - 80  $\mu\text{m}$  and 45 - 63  $\mu\text{m}$ ). Each fraction underwent to a stepped acid digestion reaction following the method described by Lindroos et al. (2007). Ensuring the collection of the required amount of gas for AMS measurements, the mortar fraction to date was selected discriminating each fraction collected at different time intervals. Obtained age functions were mathematically separated in order to distinguish individual components of different rates of the leaching reaction (Goslar et al. 2009). The method is based on the supposition of an inversely proportional relationships existing between the reaction rate (based on solubility) and the size of grains in the mortar sample. According to the theory that limestone aggregates react more slowly than those of the binder, in  $^{14}\text{C}$  dating of archaeological mortars it is worth utilizing different time interval to discriminate limestone carbon and binder signals during the collection of  $\text{CO}_2$  (Nawrocka et al. 2009, Nawrocka and Michniewicz, 2011). For Qumran samples a series of back corrections to final dating like the one based on reservoir age correction applied, in order to minimize aging coming from DC contaminations (Nawrocka et al., 2005, Michalska et al. 2013). Dating analysis were performed both by AMS technique (Poznan Radiocarbon Laboratory is equipped with an accelerator mass spectrometer type

1,5 SDH-Pelletron, Model “Compact Carbon AMS”) or a gas proportional counter technique (GPC) in the Gliwice C-14 Laboratory (Pazdur et al. 1999, 2000).

CIRCE modus operandi is linked to the application of the Cryo2SoniC protocol described into methodological (II.2) and applicative (III.1) chapter (Nonni et al. 2013). The analysis through AMS facility (Terrasi et al. 2008) were performed exclusively on suspended fractions produced from each sample (named *susp* and *sand*) obtained pre-treating the bulk mortar.

## Results

AA25 sample from Jericho contains abundant carbonate aggregates, which contains large amount of soft and fragile foraminiferous limestone, that did not allow the collection of a “pure” sample of binder-bound CO<sub>2</sub> even in a very short time of acid leaching (up to 5 seconds). Goslar et al. (2009) reported that crumbled pieces of foraminifera shells can decompose as quickly as the binder, hence the acid-leaching reaction in the very first seconds is very fast. Two portions collected during leaching of the same fraction of AA25 (after 10 and 25 seconds) were <sup>14</sup>C measured confirming that CO<sub>2</sub> collected at the very beginning of the acid leaching is more suitable for dating purposes (Table 13; Goslar et al. 2009); however, also the <sup>14</sup>C date of the first component of the sample from Jericho appeared much older than the wall from which the sample originating (120 – 75 BC). Second fraction collected shows an incredible aging. This can be explained with large amounts of crumbled foraminiferous limestone contained as aggregate, as many pieces of foraminifera shells scattered in the mortar. Fractions collected with Cryo2SoniC protocol produced similar results: a strong aging due to heavy DC contaminations (Table 13). AA25\_*susp* fraction, as Goslar’s fractions, didn’t reach the required binder signal discrimination allowing for accurate dating (Table 13). Evidently foraminifera fragments reach dimensions so fine to be collected together with binder particles.

Analogue problem appeared in Qumran samples from roman settlement. The results of mortar dating presented in the paper of Michalska et al. (2013) are far from the age attested between 2<sup>nd</sup> BC and 1<sup>st</sup> AD century. This incongruence confirms the enormous influence of aggregate on the radiocarbon dating results and it was tried to bypass the aging effect applying a back correction, considering the reservoir effect and the percentage content of carbonate components (Figure 30; SKpopr from Michalska et al. 2013). Even if final results obtained after correction included the archaeological time interval reference, it should be noticed that each measure is affected by an incredibly large uncertainty due to data handling (i.e. 250 years; Table 13; Figure 30). Same samples were performed with Cryo2SoniC protocol with no *a posteriori* correction. Although most of them resulted younger than majority of Michalska samples and sometimes in agreement with

Table 13. Resulting RC Ages from: the Hesmonean Palace of Jericho (AA25), Qumran settlement (Q3, Q4, Q6) and Wielka Waga in Krakow (KR14, KR38). They were measured by Poznan Laboratory (PL; results, from Goslar et al. 2009, Nawrocka and Michniewicz, 2011, Michalska et al. 2013) and by CIRCE Laboratory (CL; bold type). S – binder; SK- binder with aggregate; SKpopr - SK after considering the carbonate components contained in mortar during reservoir age calculation; 45-63,63-80 – fractions of material collected and analyzed after sieving; W- charcoal; \*\* first 40 sec of leaching reaction. Calibration reports only extreme data of final time interval. Our measures are indicated with bold type.

SAMPLE	Lab	RC Age	Err RC Age	Calibrated Age 1 $\sigma$	Calibrated Age 2 $\sigma$	Archaeological Reference
<b>Jericho</b>						
AA25_susp	CL	<b>3283</b>	<b>41</b>	<b>1611 - 1514 BC</b>	<b>1667 - 1455 BC</b>	120 - 75 BC
First 10 sec of leaching	PL	3255	30	1606 – 1464 BC	1611 - 1453 BC	
10 – 25 sec of leaching	PL	6720	40	5668 – 5572 BC	5715 – 5560 BC	
<b>Qumran</b>						
Q3 SK	PL	8750	130	8164 – 7601 BC	8220 – 7588 BC	104 BC - 68 AD
Q3 SKpopr		1915	250	204 BC – 395 AD	520 BC – 645 AD	
Q3 /63-80		4060	40	2833 – 2493 BC	2852 – 2476 BC	
Q6 S	PL	3250	120	1685 – 1415 BC	1880 – 1260 BC	
Q6 SK		9220	80	8543 – 8323 BC	8627 – 8285 BC	
Q6 SKpopr		2270	230	750 – 50 BC	900 BC – 215 AD	
Q6 /45-63		2770	35	975 – 840 BC	1005 – 830 BC	
Q4 SK	PL	6020	80	5007 – 4799 BC	5207 – 4721 BC	
Q4 W		2165	30	351 -171 BC	360 -112 BC	
<b>Q3 sand</b>	CL	<b>3211</b>	<b>34</b>	<b>1503 - 1441 BC</b>	<b>1603 - 1414 BC</b>	
<b>Q3 susp</b>		<b>3152</b>	<b>33</b>	<b>1494 - 1392 BC</b>	<b>1526 - 1301 BC</b>	
<b>Q4 sand</b>	CL	<b>2915</b>	<b>45</b>	<b>1194 - 1028 BC</b>	<b>1264 - 968 BC</b>	
<b>Q4 susp</b>		<b>2847</b>	<b>38</b>	<b>1054 - 931 BC</b>	<b>1125 - 911 BC</b>	
<b>Q6 sand</b>	CL	<b>2657</b>	<b>53</b>	<b>894 - 792 BC</b>	<b>927 - 763 BC</b>	
<b>Q6 susp</b>		<b>2626</b>	<b>39</b>	<b>824 - 787 BC</b>	<b>850 - 792 BC</b>	
<b>Krakow</b>						
KR14 W	PL	355	50	1468 – 1631 AD	1450 – 1640 AD	End of 15 <sup>th</sup> century
KR14 **	PL	330	30	1499 – 1634 AD	1477 – 1642 AD	
<b>KR14 sand</b>	CL	<b>346</b>	<b>32</b>	<b>1486 - 1631 AD</b>	<b>1464 - 1637 AD</b>	
<b>KR14 susp</b>	CL	<b>415</b>	<b>31</b>	<b>1439 - 1485 AD</b>	<b>1428 - 1520 AD (90%)</b>	
KR38**	PL	395	30	1445 - 1615 AD	1439 – 1628 AD	15 <sup>th</sup> century
<b>KR38 sand</b>	CL	<b>651</b>	<b>34</b>	<b>1287 - 1387 AD</b>	<b>1279 - 1395 AD</b>	
<b>KR38 susp</b>	CL	<b>455</b>	<b>75</b>	<b>1402-1516 AD (89%)</b>	<b>1389 -1637 (93%)</b>	

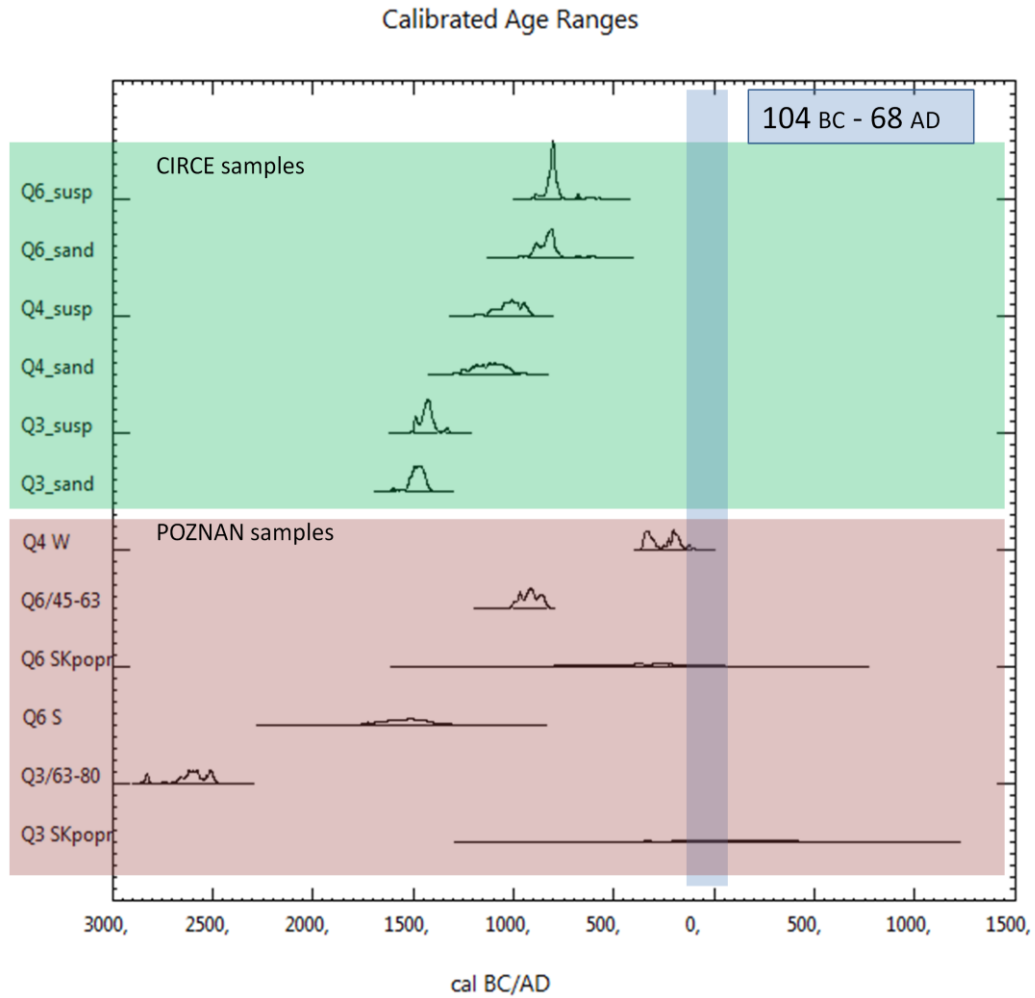


Figure 30. Calibration of dating results of mortars from Qumran Roman settlement. Samples prepared using Cryo2SoniC method (green) by CIRCE team and various methods by Michalska et al, 2013 (violet). Archaeological reference is highlighted with a vertical blue line. It is evident that the back-corrected results are affected by widespread error.

back-corrected Poznan samples, the final age represent the evidence of Cryo2SoniC selection lack of DC suppression.

Krakov samples, discussed by Nawrocka and Michniewicz (2011), showed a double dating on sample KR14 (carbonate fraction collected after leaching digestion and charcoal fragments took from the same sample) while only one for sample KR38, where the dating was performed on a charcoal found encased in mortar. Dating of mortar was made on the bulk mortar after removal of false lime lumps (potential carrier of contamination) and acid leaching. CIRCE team analysed the binder of each sample produced after the pre-treatment with Cryo2SoniC, no vegetal fragments were extracted or dated. The age obtained by radiocarbon dating for analyzed samples seems to be consistent with archaeological and historical expectations both for Poznan and for CIRCE measurements (Table 13, Figure 31).

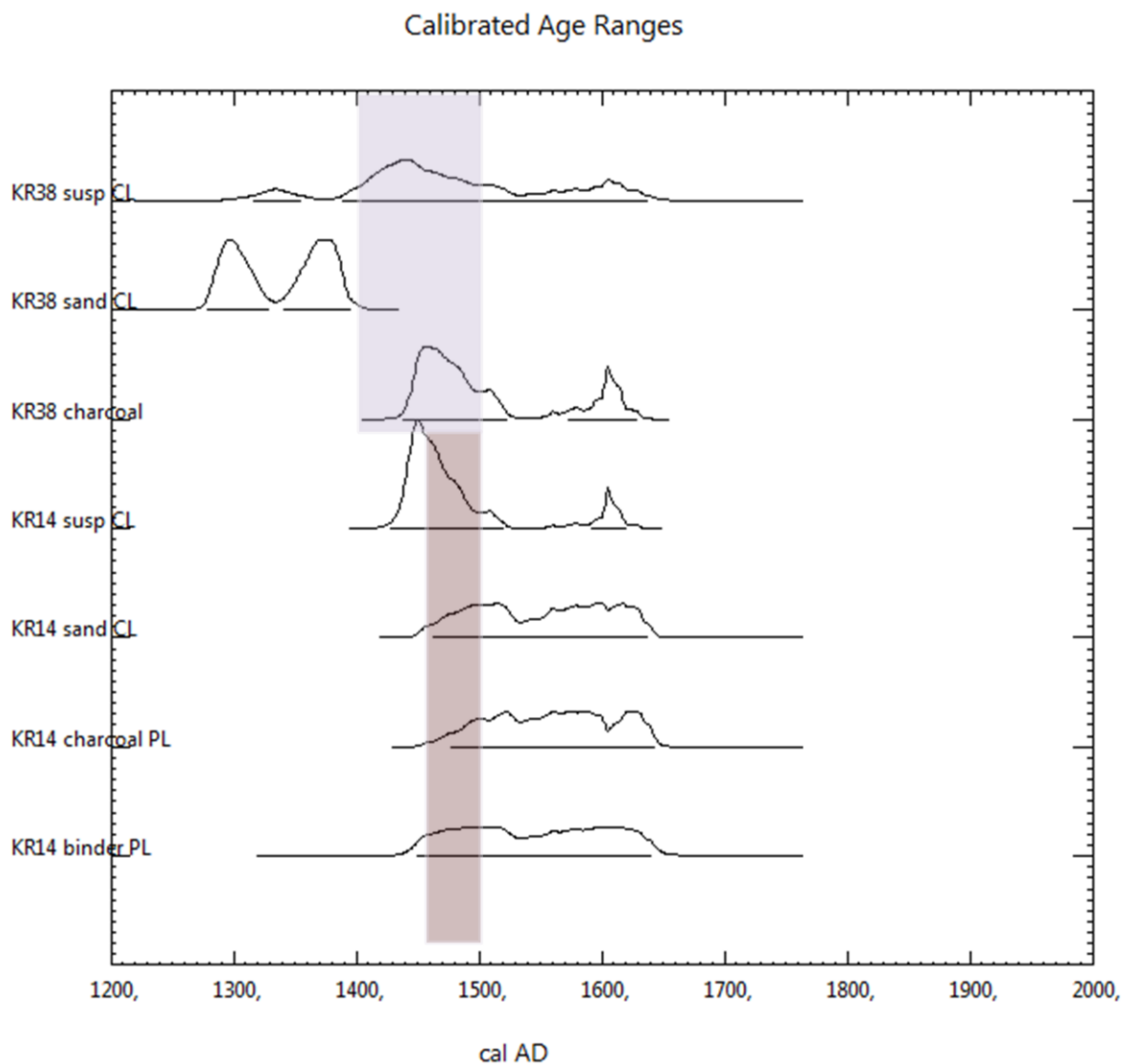


Figure 31. Calibrated age of KR14 and KR38 samples with their respective archaeological references (vertical stripes indicating 15<sup>th</sup> century second half).

### Conclusions

The Cryo2SoniC method has demonstrated to be trustworthy for sample like Great Scales ones, in other words for mortars with a quartz sand aggregate, mostly composed by silica - alluminate minerals. Exclusively on samples from Wielka Waga (Great Scales) building in Krakow, the obtained results were in agreement both with the established archaeological stratigraphic sequence and between each other (Poznan and CIRCE results). On Qumran samples instead Cryo2SoniC efficiency for isolation of a binder fraction representative of carbonation moment failed even if it gave results better than mostly obtained with Michalska methods. The dead carbon contamination coming from aggregate portion is yet too much present to obtain an accurate chronological estimation. As for Qumran samples, mortar from Jericho seem to be not useful for dating with none



of seen methods. The reason is the presence of small, crumbled pieces of foraminiferous limestone and shells scattered which has precluded a successful  $^{14}\text{C}$  dating, whatever is the applied protocol. Once ascertained the necessity to improve Cryo2SoniC protocol, it's important to highlight its potential in DC suppression, which even though insufficient showed a major efficiency than Poznan technique in dating.

## II.8. Resume

It has been seen how the development of a new and more effective selection method allowing to obtain a suitable and representative binder fraction to date was generally obtained at CIRCE. Through the validation of the Cryo2SoniC separation protocol it has been found that it is possible to date successfully, different typologies of real mortars. To facilitate the future choice of the samples potentially analysable by this methodology, it can be useful to report a list of the main positive aspects of the Cryo2SoniC. Generalizing, positive attributes are:

- Capability to suppress contaminated signal coming from unburned limestone residues commonly present inside binder.
- Capability to operate on both main kind of mortars: the aerial and hydraulic ones. Where the hydraulic nature of the binder or the aggregates does not preclude the possibility to obtain an accurate dating. The unique ulterior requirements in these cases is the necessity to select a bigger amount of material to pre-treat, in order to contrast the lower C concentration of such materials.
- Capability to discriminate and avoid contamination deriving from weather activity, producing secondary calcite depositions (able to suppress rejuvenation signal).
- Capability to select a suitable fraction of calcite to date when its original mortar contains calcareous aggregates, but only if this component has a coarse grain dimension and maintain it even if undergone to mechanical stress (low crumbling tendency). That is limestone which composes the aggregate fraction should have such a high hardness to not be notched by physical stress. This capability is a precious evidence on protocol reliability, because till now other selection methods based on differential acid leaching were not able to obtain successful results from this type of materials.

During our experimentation some drawbacks highlighting main developments required in order to produce accurate dating were discovered. In details observed pitfalls were:

- Produce high accuracy variability when dealing with mortars characterised by calcareous fraction of fine grains dimension (i.e. silt, foraminifera shells) and/or of bigger dimensions with fragile habitus. The presence of these kind of materials increases the probability of an erroneous result in dating. An alternative could be searching inside the binder for lime lumps samples to date.
- Fail dating when analysed mortar is strongly contaminated by the presence of secondary calcite depositions, as voids filler or as a partially substitution of binder matrix, when it

derives from groundwater activity. This is an eventuality to take into account when sampled material coming from an underground environment is interested by watertable.

To solve the first of these problems it has been taken into account the possibility to date lime lumps. It could be a positive solution adopted everywhere and especially when it seems to be impossible to perform the dating on bulk mortars due to aggregates nature. It has been already discussed that when dealing with these materials a safer protocol to proceed, is not represented by the dating of bulk lime lumps, but is represented by the dating of a fraction collected after the pre-treatment of lime lump through CryoSoniC protocol. This avoids any kind of dead carbon influx coming from eventual unburned residues.

As a rule, to avoid dating on materials potentially contaminated and wastes of economic resources, a cathodoluminescence analysis is recommended to be performed on suspensions collected after Cryo2SoniC and CryoSoniC pre-treatment.

There are also other possibilities of un-success, but they are not linked to reliability of Cry2SoniC method. Probable fails are often related to a not-correct sampling or to the genesis of mortars. In these cases during the sampling the following behaviour should be avoided: to collect a sample from:

- a situation of reuse where ancient pieces of mortars could be use as inert.
- an inner/deeper part of a structure. It is known that carbonation velocities decrease proportionally to the deep reaches inside a wall, leading to a rejuvenation of the sample than the real age.
- an active volcanic area. It will be probably affected by a strong aging due to fossil atmosphere which entered in contact with.
- a restored structure.
- an area involved in flooding episodes (nowadays or in the past) by alluvial, groundwater or meteoric activities.

These situations should be known and avoided before to start a dating campaign, trying to choose to be dated only most representative samples.

## **III. Applicative Section**

### **III.1. Castle of Shayzar: a Radiocarbon Publication.**

This paper reports the application of Cry2SoniC protocol aiming to  $^{14}\text{C}$  mortar date on some lime mortars from the Shayzar Castle (Syria). Shayzar, a defensive citadel built on a rock massif, is one of the most important examples of medieval fortifications in the Middle East, attended from the second half of X to the beginning of XV century AD (Tonghini, 2005). The  $^{14}\text{C}$  tool represents a fundamental tool to more precisely anchor the already built (by means of other archaeological analyses) site chronology. In this study some mortar samples were dated in order to preliminary evaluate Cryo2Sonic applicability to this study site.

To reconstruct the building chronology and confirm the archaeological expectation a series of  $^{14}\text{C}$  dating by means of new Cryo2SoniC protocol, were applied performed to on some selected samples of mortars. Cryo2SoniC dated samples were chosen among mortars containing encased charcoals, in order to evaluate the mortar dating procedure accuracy by comparison with the  $^{14}\text{C}$  fingerprint of charcoals, extracted from the analyzed mortars.

Petrographic and mineralogical analyses in thin section by optical microscopy, X-ray diffraction and SEM investigations were carried out for the characterization of mortar samples in order to both to investigate mortar typology and to verify the occurrence of some attributes which can influence the outcome of the dating.

## **<sup>14</sup>C MORTAR DATING: THE CASE OF THE MEDIEVAL SHAYZAR CITADEL, SYRIA**

Sara Nonni<sup>1,2,3</sup> • Fabio Marzaioli<sup>2,4</sup> • Michele Secco<sup>5</sup> • Isabella Passariello<sup>2</sup> • Manuela Capano<sup>2,6</sup> • Carmine Lubritto<sup>2,7</sup> • Silvano Mignardi<sup>1</sup> • Cristina Tonghini<sup>8</sup> • Filippo Terrasi<sup>1,2</sup>

**ABSTRACT.** This paper reports the results from applying the Cryo2SoniC (Cryobreaking, Sonication, Centrifugation) protocol to some lime mortars sampled from the citadel of Shayzar (Syria). The overall aims of this project are 1) to use the properties offered by high-precision accelerator mass spectrometry (AMS) radiocarbon dating for the evaluation of absolute chronology with its typical robust time constraints (i.e. 25 <sup>14</sup>C yr), and 2) to apply the dating directly to the citadel structures in order to prevent possible biasing effects potentially affecting indirect <sup>14</sup>C dating on organic materials found at the study site. The analyses presented in this paper have been mainly performed as a preliminary check of the Cryo2SoniC methodology in order to assess its applicability to this study site by comparing observed mortar results with archaeological expectations about the citadel development phasing and charcoals found encased in mortars. Petrographic and mineralogical thin-section analyses by optical microscopy (TSOM), X-ray powder diffraction (XRD), and scanning electron microscopy plus energy dispersive spectroscopy (SEM/EDS) investigations were carried out for characterization of the mortar samples to verify the occurrence of some features, related to their production technology, which may introduce dating offsets. The resulting <sup>14</sup>C calibrated ages were in agreement with the archaeological expectations based on type and stratigraphic site reconstructions, *in situ* inscriptions, and written sources. Such results showed also a general (with 1 exception) statistical agreement among the charcoals and the analyzed mortars simultaneously, confirming the archaeological expectations for the Shayzar citadel. Results presented in this paper indicate good accuracy for the applied procedure for chronology reconstruction and highlight the capability of Cryo2SoniC to further characterize the Shayzar site.

### **INTRODUCTION**

Currently, radiocarbon chronology of archaeological sites is mostly based on the dating of organic materials uncovered during the excavations. The opportunity offered by mortars to establish the age of artifacts represents a sensitive improvement for the <sup>14</sup>C dating of archaeological buildings: mortar naturally records the act of building and represents also a class of materials virtually ubiquitous at archaeological sites, from the Neolithic period on (Rech 2004).

Mortar matrix can be schematically distinguished in 2 portions: the binder and the aggregates. The basis of the production of aerial mortar can be briefly summarized as follows: limestone (mainly CaCO<sub>3</sub>) is burned to quicklime (CaO) and is mixed with water to form slaked lime (Ca(OH)<sub>2</sub>). Slaked lime is then mixed with aggregates of different size and material type (e.g. reworked bricks, silica minerals, marble powder) and, during its hardening, lime mortar absorbs carbon dioxide (CO<sub>2</sub>) from the atmosphere to produce calcium carbonate (CaCO<sub>3</sub>). During mortar setting, contemporary air <sup>14</sup>CO<sub>2</sub> reacts with the slaked lime to form the calcite binder. Therefore, lime mortar binder represents a potential tool to assess the chronology of the different construction phases of buildings by means of <sup>14</sup>C dating.

<sup>1</sup>University of Rome La Sapienza, Department of Earth Sciences, 000185 Rome, Italy.

<sup>2</sup>Centre for Isotopic Research on Cultural and Environmental Heritage, INNOVA, 81020 San Nicola La Strada, Caserta, Italy.

<sup>3</sup>Corresponding author. email: sara.nonni@uniroma1.it.

<sup>4</sup>Second University of Naples, Department of Mathematics and Physics, 81100 Caserta, Italy.

<sup>5</sup>University of Padua, Department of Geosciences, 35131 Padua, Italy.

<sup>6</sup>Second University of Naples, Department of Letters and Cultural Heritage, 81055 Santa Maria Capua Vetere, Caserta, Italy.

<sup>7</sup>Second University of Naples, Department of Environmental, Biological and Pharmaceutical Sciences and Technologies, 81100 Caserta, Italy.

<sup>8</sup>University of Venice Ca' Foscari, Department of Studies on Asia and Mediterranean Africa, 30125 Venice, Italy.

Since the 1960s, mortars have been exploited as a potential material for  $^{14}\text{C}$  dating (Delibrias and Labeyrie 1964), and despite the fact that this methodology appears very simple in its principles, some measured  $^{14}\text{C}$  ages showed evident contradictions with respect to the expected historic ages (Stuiver and Smith 1965; Baxter and Walton 1970; Van Strydonck et al. 1986, 1992; Ambers 1987; Heinemeier et al. 1997, 2010; Mathews 2001; Hale et al. 2003; Nawrocka et al. 2005, 2009; Lindroos et al. 2007).

Therefore, in order to eliminate observed biasing sources, sample preparation procedures have been implemented since the beginning of the mortar radiometric dating method (Delibrias and Libeyrie 1964). Most preparation procedures applied during recent decades consist of a combination of mechanical and chemical treatments (Folk and Valastro 1976; Cherf 1984; Van Strydonck et al. 1986, 1992; Heinemeier et al. 1997; Sonninen and Jungner 2001; Lindroos et al. 2007; Nawrocka et al. 2007, 2009; Goslar et al. 2009). The most common approaches involve the isolation of the binder atmospheric  $^{14}\text{C}$  signal by means of stepped acid digestion based on the evidence that binder carbonates react faster than limestone residuals. To our knowledge, the unique alternative to this methodology is based on the attempt to physically separate the binder carbonates by a combined mechanical/physical procedure (Folk and Valastro 1976; Heinemeier et al. 1997; Nawrocka et al. 2005; Ortega et al. 2012) based on the laboratory isolation of binder calcite.

The CIRCE (Centre for Isotopic Research on Cultural and Environmental Heritage) group developed a protocol based on a development of previously applied mechanical/physical procedures (Nawrocka et al. 2005) called CryoSoniC allowing  $^{14}\text{C}$  dating of mortars. This procedure, described by Marzaioli et al. (2011), was successfully applied to real lime lumps and, after implementation (Cryo2SoniC), to mortars leading to accurate results (Marzaioli et al. 2013). The main advantage of the Cryo2SoniC methodology is 1) the complete digestion of the laboratory isolated mortar fraction, avoiding difficulties in handling time-evolved fractions, and 2) the limited number of analyses per mortar to be performed: one for each sample after methodology accuracy evaluation. While usually in stepped acid digestions from 3 up to 5 aliquots of  $\text{CO}_2$  are produced by means of  $\text{H}_3\text{PO}_4$  (85 wt%) or  $\text{HCl}$  (standard solution 1.15 N), and analyzed for each sample (Van Strydonck et al. 1986, 1992; Heinemeier et al. 1997; Sonninen and Jungner 2001; Lindroos et al. 2007, 2012; Nawrocka et al. 2007, 2009).

The main aim of the Shayzar  $^{14}\text{C}$  dating project is to further improve the already built site chronology.  $^{14}\text{C}$  dating offers some unique advantages to the scientific community working on the site represented by the possibility to precisely define the site chronology using the properties of high-precision accelerator mass spectrometry (AMS) dating (Terrasi et al. 2008). AMS, in fact, in the range identified by a typical relative error on the isotopic ratios ( $\Delta R/R$ ) of 0.3%, allows  $^{14}\text{C}$  dating with a typical uncertainty of 25 yr, helping to clearly disentangle site development chronologies. Moreover, the possibility to directly date, by means of mortars, the manufacture of the structures represents a potential to avoid eventual biases due to the  $^{14}\text{C}$  analysis of organic materials found at the study site. For such materials, in fact, erroneous stratigraphic interpretation and/or on/offsite material reuse leading to age estimation biases cannot be estimated *a priori*, possibly adding extra costs to the development of the study (Bowman 1990; Van Strydonck 1986; Mathews 2001; Hale et al. 2003; Rech 2004).

In this study, the Cryo2SoniC procedure was applied to samples from the Shayzar citadel in Syria. Selected samples came from structures with well-constrained absolute chronologies, aiming to check our procedure potential to site age estimation. Moreover, the co-presence of intact charred wood fragments within the mortars was also used for this purpose as a further time reference.

Indeed, it is well established that while encased charcoals represent a matrix capable of leading to accurate mortar dating (Tubbs and Kinder 1990; Berger 1992; Van Strydonck 1992; Wyrwa et al. 2009; Heinemeier et al. 2010; Al-Bashaireh and Hodgins 2011), possible bias may be introduced due to their history.

To correlate eventual observed offsets with the technological characteristics of the analyzed samples, a series of analyses (i.e. TSOM, XRD, and SEM-EDS) were performed on mortars. They allow, through identification of mineralogical phases and nature of the aggregates, collecting clues about the presence of possible dating contamination sources. For example, the presence of recrystallized calcite plays a primary role in the accurate determination of <sup>14</sup>C ages of the studied samples, raising the risk of rejuvenation in the case of weathering, or aging in the case of water table interactions. Other potentially dangerous identifiable features are calcination relics and biomicritic sand usage; their presence also leads to an aging effect on the final dating.

## ARCHAEOLOGICAL BACKGROUND

The archaeological site known as the citadel of Shayzar (35°16'N", 36°34'00"E) is located on the top of a hill overlooking the Orontes River in central Syria (Figure 1). The structure, partially buried, spans about 500 m N-S, 55 m E-W, and is located at ~220 m above sea level (asl). The citadel was founded in the 10th century on the ancient acropolis of a Hellenistic town originally called *Larissa on the Orontes* and later, in the Roman era, known as *Caesarea on the Orontes*. This fortification played an important military role in the region during the Medieval period, and only after the 15th century did Shayzar progressively lose its strategic function and gradually revert to a village. The remaining buildings represent a cohort of different construction phases that led to the fortification of the site between the 10th and 14th centuries, although the remains of previous structures were also incorporated into the walls of the citadel. The structures related to the Medieval fortification are better preserved on the edges of the plateau, with at least a ring of curtain walls, while the inner area was mainly occupied by the remains of the village belonging to the last phase of occupation (Tonghini et al. 2003, 2005, 2006, 2012).

Archaeological analyses of the remains revealed a clear stratigraphic sequence of the building phases, mostly anchored to a reliable relative chronology describing the temporal evolution of the fortification of Shayzar. This chronology was built by means of the features of masonry typology, stratigraphic data, and some absolute dating elements. Absolute time anchoring refers to 1) written evidence of historical sources and *in situ* inscriptions, 2) contextual data (e.g. pottery remains) retrieved from archaeological excavations, and 3) analogous structures already chronologically constrained from the same region. These data identify 7 periods in the development of the Shayzar site (Tonghini 2012):

- Period I: the earlier phase of occupation of the site covers probably from the 2nd century to the first half of the 10th century;
- Period II: the first fortification of the site from the second half of the 10th to the 11th centuries;
- Period III: from the end of the 11th century to the first half of the 12th century corresponding to the 1157 earthquake swarm;
- Period IV: the great restoration and strengthening of the defenses, from the start of the earthquakes to the early 13th century;
- Period V: a new defensive program, from 1233 to 1290;
- Period VI: partial modification and restoration of the fortification, from 14th to 18th centuries;
- Period VII: conversion of the site to residential use, from 19th century to 1950s.

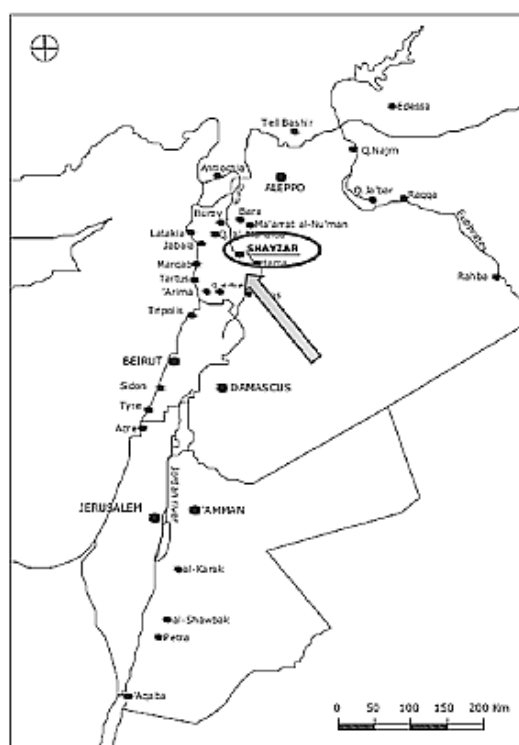


Figure 1 General map of Syria showing the location of Shayzar citadel.

## MATERIALS AND METHODS

### Sample Descriptions

All analyzed samples were collected from structures related to the fortifications (Figure 2) and identified by means of the code corresponding the archaeological code of building ambients (i.e. CF7, CF16, CF18, CF26). Ambient CF26 represents an ancient building, built before the construction of the citadel of the 10th century, later transformed in a defensive curtain in the eastern front between the end of the 10th and the 11th centuries. CF26 mortar was sampled from the remains of wall US 5035 of the same building belonging to its oldest part and, hence, attributable to Period I. Sample CF7 (Figure 2) comes from the top of the vault of wall 6254, inside space 16 of building CF7, in the area of access to the citadel. Building CF7 corresponds to a massive defensive structure on several levels known in the literature as *glacis*; at Shayzar it is attributed to the second half of the 12th century (Period IV). Samples CF16 (from the nucleus of wall US 3008) and CF18 (from the nucleus of wall US 3217) have been collected from 2 towers of the eastern defensive curtain, both attributed to the second half of the 12th century (Figure 2). Their construction postdates the strong earthquake swarm to the end of Period III.

### Mortar Characterization

Samples CF7, CF16, and CF18 underwent characterization. CF26 was not analyzed because of its complete consumption during  $^{14}\text{C}$  dating, but according to its macroscopic aspect, it is presumed to be similar to the others. Information on the composition of both the binder and the aggregates has been obtained by TSOM, XRD, and SEM-EDS analyses of these samples. Mineralogical-petro-



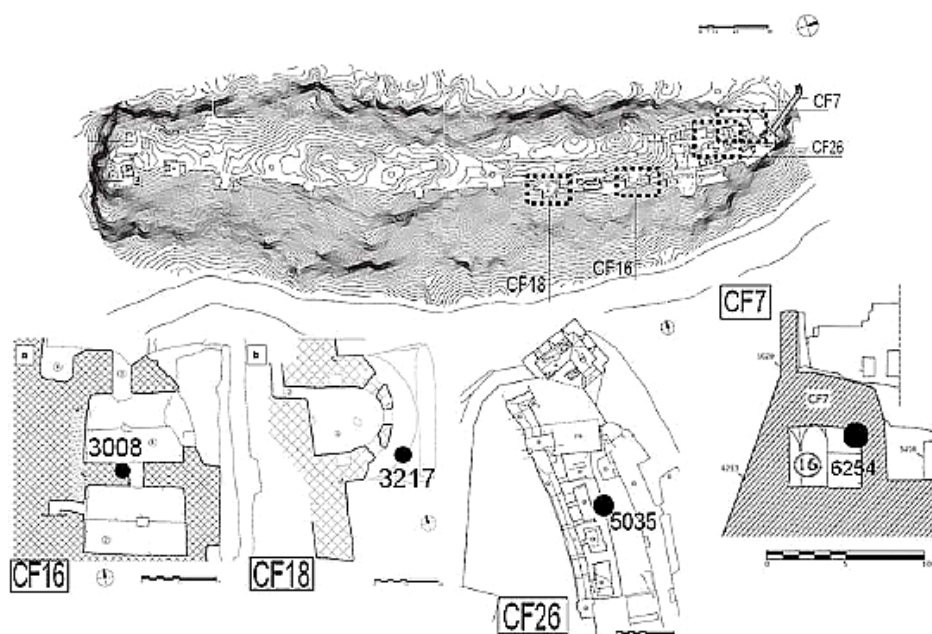


Figure 2 Plan of the Shayzar citadel showing the sampling zones

graphic analyses were aimed to identify 1) the nature of the binder, 2) the occurrence of unburned limestone residues and calcareous aggregates, and 3) the occurrence of recrystallized calcite.

TSOM was performed on thin sections (30  $\mu\text{m}$  thick) with an optical polarizing microscope under parallel and crossed nicols. A Camscan MX 2500 SEM microscope equipped with a LaB6 electron source and an energy dispersive X-ray detector (EDS) was used to collect elemental and structural microanalyses, which gave valuable information on the mineral phase composition and the pore structure of the historic mortars (Figure 3). Previously used thin sections were covered with an ultrathin coating of graphite to prevent the accumulation of static electric fields during imaging. Qualitative spectra interpretations were performed through SEMQuant Phizaf software.

XRD analyses were performed with a Philips X'Pert diffractometer in Bragg-Brentano geometry equipped with a Cu X-ray tube operating at 40 kV and 40 mA ( $\text{CuK}\alpha$  radiation), and an X' Celerator detector, both mounted on a PW1050/37 theta-2theta vertical goniometer. Data acquisition was performed by operating a continuous scan in the range  $3.01\text{--}79.99^\circ [2\theta]$ , at an acquisition rate of  $0.02^\circ$  per second [20]. Diffraction patterns were interpreted with X'Pert HighScore Plus 3.0 software by PANalytical, reconstructing mineral profiles of the compounds by comparison with ICDD and ICSD diffraction databases. XRD analyses were focused on the fractions of the samples with grain size below  $63 \mu\text{m}$ . These fractions were collected, broken up by means of soft hammering, and then dry sieving mortars samples, across a series of dry test sieving (800, 160, and  $63 \mu\text{m}$ ), until the accumulation of 0.25 g of powder, virtually representing the binder fraction. The obtained sample was crushed in an agate mortar before XRD analyses.

#### **<sup>14</sup>C Analyses**

Cryo2SoniC methodology was applied to suppress the C contamination in the analyzed mortar samples by means of a sequence of physical separations: cryobreaking, ultrasonication, and centrifuga-

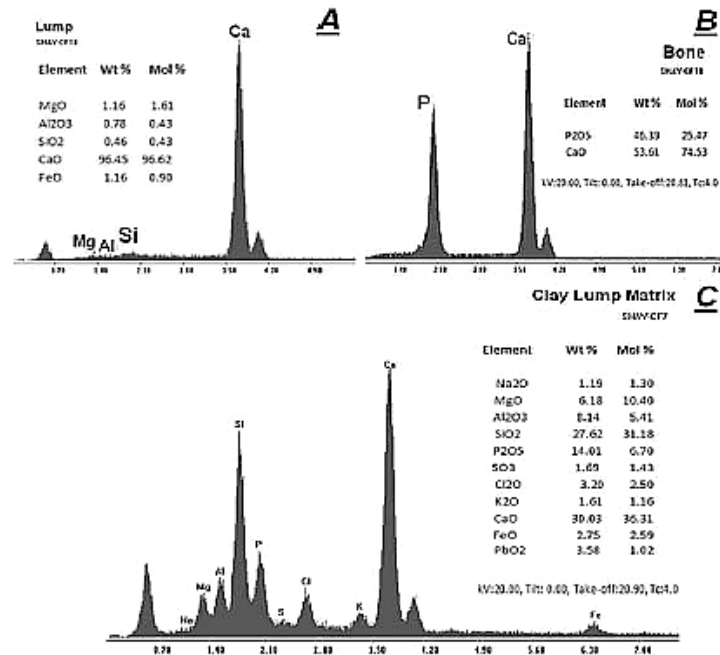


Figure 3 EDS spectra of the core of a lump (A) and of a bone fragment (B) inside sample CF18, and of a clay lump inside sample CF7 (C).

tion (Marzaioli et al. 2013). This procedure is based on the experimental observation that binder carbonates are characterized by an easily breakable structure under a series of ultrasonic attacks. This main selection criterion results from the ultrasonication allowing the isolation of the binder signal from the unburnt limestone residuals by breaking the softer binder structure and originating a suspension of fine particles characterized by a slow sedimentation velocity and, hence, easily recoverable by means of centrifuging. Marzaioli et al. (2011) successfully tested a protocol (CryoSoniC) based on a single step of ultrasonication of 30 min on synthetic mortars, not containing aggregates, and lime lumps. Archaeological mortars are usually produced by adding some aliquots of eventually fine-grained, calcareous aggregates. An improvement to the methodology (Cryo2SoniC) was necessary in order to analyze real samples. This procedure revealed good accuracy also for real mortars (Marzaioli et al. 2013). In this study, Cryo2SoniC involves a double step of ultrasonication, producing different time-evolved suspension fractions from the same mortar matrix. The procedure parameters (i.e. timing) were tuned on experimental age vs. time of suspension evolution profiles. These profiles evidenced, for some mortars, a sudden aging of initially produced suspensions (for 10 min) and an overall rejuvenation of successively produced suspensions, with no statistical difference on suspension ages produced after 30 min and up to 50 min. Data were interpreted as fine carbonaceous aggregates suddenly entering the suspension. These materials, significantly aging the initial suspensions were accurately removed from the samples after 10 min of ultrasonication, producing the so-called *Cryo2SoniC susp\_sand* fraction. In detail, the applied procedure was

1. **Cryogenical breaking.** Following the procedure reported by Nawrocka et al. (2005) and Marzaioli et al. (2011), mortar pieces (~5 g) were submerged in liquid nitrogen until the achievement of thermal equilibrium and immediately transferred into an oven at 80 °C for several minutes. After repeating this freezing/thawing cycle 3 times, the mortars were broken by gentle hammering.

2. **Size selection.** The produced fragments (spanning a wide range of particle size) were sieved and only particles with size below 800  $\mu\text{m}$  were selected and stored in a 75-mL beaker. Then ~40 mL of deionized/decarbonated water (DDW) was added.
3. **1st ultrasonic selection.** After complete sedimentation (~12 hr), the selected powder was re-wetted with 40 mL of DDW and ultrasonicated for 10 min. DDW-containing suspended mortar particles were totally removed and transferred to a Falcon 50-mL centrifuge tube. This fraction of binder represents the fraction potentially affected by dead carbon contamination (*susp\_sand*) due to the probable presence of very fine carbonaceous grains sands entering the suspension easily and before binder particles.
4. **2nd ultrasonic selection.** Residual powder, decanted on the bottom of the beaker after the first sonic attack and the total removal of *susp\_sand*, underwent another ultrasonication for 30 min in an excess (~40 mL) of DDW. About 30 mL of water was collected by siphoning and stored in another Falcon centrifuge tube, taking great care not to induce a new suspension of the sediments. This last fraction, according to our experimental experience, represents the suspension guaranteeing accurate dating (*susp*).
5. **Centrifugation.** The Falcon centrifuge tube containing *susp* carbonates, and the other containing the *susp\_sand* fraction, were centrifuged at 8.0 krpm in a rotor of 10 cm mean radius for 5 min and oven-dried overnight (80 °C).

About 40 mg of *susp* and *susp\_sand* fractions and carbonate standards samples (i.e. IAEA C1 and C2; Rozanski et al. 1992) were digested under vacuum to  $\text{CO}_2$  by means of a complete orthophosphoric acid attack (McCrea 1950) for 2 hr at 85 °C. Charcoal samples found in mortars were mechanically extracted and pretreated according to a modification of Berger's (1992) protocol. Since our samples were easily recognizable and extractable, we applied the conventional AAA (acid-alkali-acid) method (Passariello et al. 2007) with a longer (following Berger's observations) time (12 hr) for the first acid digestion in order to completely remove calcite contaminations, eventually evolving to  $\text{CO}_2$  during the successive combustion phase. Treated charcoals underwent combustion in a run together with normalization/check standards (i.e. IAEA C3 and C5 (Rozanski et al. 1992) and NIST OxII) and background (graphite) samples according to Marzaioli et al. (2008). The developed  $\text{CO}_2$  (both from combustion and acid digestion) was cryogenically purified by other gases, reduced to graphite on iron powder catalyst according to the CIRCE sealed-tube reaction protocol (the zinc process) following Marzaioli et al. (2008), and analyzed to measure  $^{14}\text{C}$  isotopic ratios using the CIRCE AMS system (Terrasi et al. 2008). Measured  $^{14}\text{C}$  ratios were converted to  $^{14}\text{C}$  ages (Stuiver and Polach 1977) and calibrated to absolute (i.e. calendar) ages by means of the CALIB v 6.0 program (Stuiver and Reimer 1993) using the IntCal09 atmospheric calibration data set (Reimer et al. 2009). All  $^{14}\text{C}$  dates in this paper are reported as intervals comprised between the highest/lowest calendar age identified by the projection of measurement intervals (1 or  $2\sigma$ ) on the absolute age axes using the IntCal09 calibration curve.

### Data Analysis

In this study,  $^{14}\text{C}$  ages with dispersion coefficients ( $2\sigma$ ) are compared with charcoal  $^{14}\text{C}$  ages at  $2\sigma$ .  $^{14}\text{C}$  calibrated ages at  $2\sigma$  for both mortar and charcoals were compared with archaeological expectations. A *t* test for the means was used to compare these results. The *t* test indicates no difference between the means if the level of agreement observed lies within 0.05 and 0.95 which, from here on, will be conventionally called the  $2\sigma$  level. When explicitly stated, given a number of  $^{14}\text{C}$  dates referring to coherent samples, the weighted mean of these ages calibrated using IntCal09 is referred to as calibrated weighted age. The calibrated weighted age dispersion is used to estimate the error of the weighted average if a  $\chi^2$  test on the significance of the weighted mean at 0.05 was successful.

## RESULTS AND DISCUSSION

### Mortar Characterization

All analytical techniques performed were necessary to infer the nature of mortars and their characteristics and if they possibly interfere with  $^{14}\text{C}$  dating, such as the co-presence of other calcite sources (i.e. carbonatic aggregates, calcination relicts, or secondary depositions) together with the binder. Macroscopically, all mortar samples show an arenaceous appearance, strong cohesion, and a great abundance of charcoals. Microscopic examinations of the samples show a micritic aspect of the binder carbonate, a homogeneous texture, and a limited amount of sandy aggregates. Therefore, all samples can be classified as fat mortar because of their high binder/aggregate ratios. The results of XRD analyses show that the calcitic binder contains small amounts of magnesium carbonate due to the presence of dolomitic rock fragments (Table 1). Uniformly distributed aggregate is scarce and mainly composed of these dolomitic rock fragments, quartz, biotite grains, a local sand essentially composed of organogenous scraps (*Globigerina* and mollusks), and some biomicritic-globigerina-limestone microfragments. Small fragments of pottery and some minerals of volcanic origin, such as diopsides and zeolites, are dispersed in the binder matrix, together with some clay lumps. These clay lumps contain dispersed chloride salts (halite and sylvine), charcoals, and microfragments of bones (60–300  $\mu\text{m}$ ). In particular, their presence has been confirmed by SEM-EDS results highlighting the presence of apatite. The simultaneous occurrence of clay, charcoal, and phosphate minerals in clay-lumps systems suggests their origin from a different site than the sands, which come from the Orontes River basin according to a previous study (Tonghini 2012). Sporadic crystals of gypsum have been found only in sample CF7. The presence of secondary calcite microcrystals and chlorine salt crystals, in all mortar samples, has been observed in the voids. These features were attributed to restoration and conservation works by Tonghini (2012), but they are more probably ascribable to weathering. Abundant lime lumps of different sizes, showing shrinkage cracks, have been recognized in all samples; however, only some of them contained calcination relicts.

Table 1 Mineralogical composition by XRD (+++ major phase, ++ secondary phase, + minor phase, (+) traces).

	CF7	CF16	CF18
Calcite	+++	+++	+++
Dolomite	++	+	++
Sylvine	(+)	(+)	(+)
Halite	(+)	(+)	(+)
Quartz	(+)	(+)	(+)
Apatite	(+)	(+)	(+)
Diopside	+	+	+
Gypsum	(+)	–	–

### $^{14}\text{C}$ Dating

Mortars have been dated with the aim of confirming and improving the precision of ages of the construction phases of the Shayzar military citadel. Results are summarized in Table 2 and Figure 4, where  $^{14}\text{C}$  ages of both fractions (i.e. *susp* in bold and *susp\_sand*) obtained from Cryo2SoniC procedure are shown for each mortar sample, together with charcoal dates and archaeological expectations. According to the *susp* results shown (Table 2), an overall different age phasing is recognizable: CF7, CF16, and CF18, which identify a later development of the castle (Period III), and CF26, which marks the beginning of the Shayzar fortification (Period I). The calibrated ages of samples CF7, CF16, and CF18 do not differ among each other at a  $2\sigma$  level. They identify a building phase

*<sup>14</sup>C Mortar Dating: Medieval Shayzar Citadel*

with a calibrated weighted age of AD 1022–1278 ( $2\sigma$ ) in agreement with archaeological expectations for the sampled structures and the earthquake swarms discontinuity of AD 1157 representing the end of Period III. The same level of agreement ( $2\sigma$ ) was observed for each individual sample with respect to expectations.

Table 2 <sup>14</sup>C dates of mortars and charcoals. For each analyzed mortar, both *susp\_sand* and *susp* results are shown. Calendar ages ( $1\sigma$  and  $2\sigma$ ) are represented as a continuous distribution spanning the maximum and minimum calibrated values.

Sample	Analyzed fraction	<sup>14</sup> C age (BP)	Calibrated age AD		Archaeological age AD
			1 $\sigma$	2 $\sigma$	
CF7	Susp_sand	1407 ± 41	610–658	568–674	12th century
	Susp	1017 ± 65	902–1151	887–1169	
	Charcoal	869 ± 22	1163–1209	1051–1221	
CF 16	Susp_sand	737 ± 45	1228–1290	1211–1386	12th century
	Susp	868 ± 26	1160–1213	1047–1251	
	Charcoal	923 ± 45	1041–1158	1025–1208	
CF18	Susp_sand	405 ± 35	1441–1614	1432–1630	12th century
	Susp	729 ± 54	1225–1296	1187–1392	
	Charcoal	882 ± 26	1058–1211	1045–1219	
CF26	Susp_sand	1400 ± 27	623–658	603–665	10th century
	Susp	1150 ± 35	784–968	779–976	
	Charcoal	1376 ± 53	608–683	569–771	

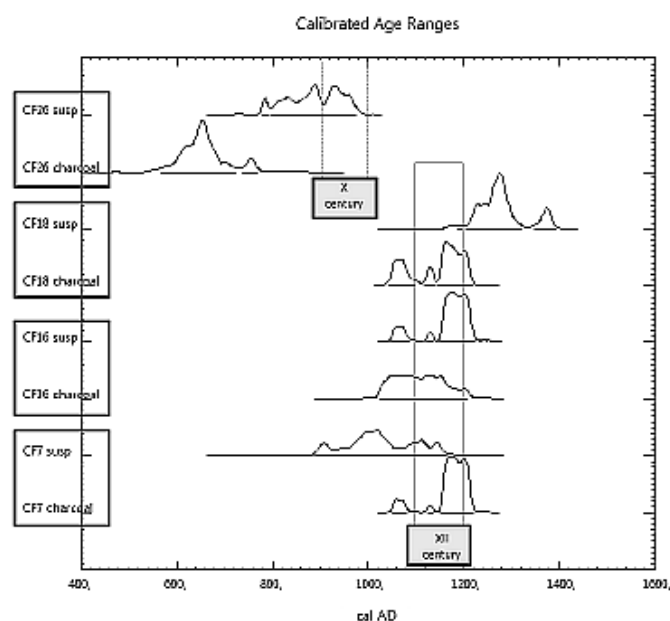


Figure 4 Calibrated dates of each sample (susp and charcoal) with the corresponding archaeological reference.

The same analysis procedure for the *susp-sand* fractions led to a calibrated weighted age of AD 600–1798 ( $2\sigma$ ), again in agreement with the archaeological estimation, but characterized by a drastic failure of the  $\chi^2$  test for the significance of the weighted mean due to a sensitive scatter of the *sand-susp* <sup>14</sup>C ages. For the *susp\_sand* class samples, it should be noted how 2 of these fractions

were  $^{14}\text{C}$  enriched (younger) with respect to the relative *susps* (CF16 *susp\_sand* and CF18 *susp\_sand*) and one was depleted (CF7). A similar behavior is shown by the CF26 calibrated dates. The CF26 *susp* calendar age was in agreement with the castle archaeological chronology, while CF26 *susp\_sand* gave sensitive age overestimation.

Since IAEA C1 and C2 reference materials are routinely used as quality control for Cryo2SoniC quality assurance purposes (they undergo the same pretreatment of mortars), giving no statistical difference from the same materials conventionally treated, any possibility of dissolved inorganic carbon contamination (i.e. rejuvenation) due to the wet attack of ultrasonication can be ruled out *a priori*. Hence, observed  $^{14}\text{C}$  fluctuation for all the *susp\_sand* fractions can be interpreted as a different relative influence of biomicritic microfragments (aging effect) and calcite recrystallization crystals (rejuvenation effect). However, more detailed analyses on the *susp\_sand* fraction should be performed in order to determine such behavior. These results highlight how the *susp\_sand* fraction is generally much more sensitive, with respect to *susp*, to any interfering contaminant introducing also a particular sensitivity to secondary calcite. These observations strengthen our assumption that the *susp* fraction is the most reliable Cryo2SoniC fraction guaranteeing accurate dating.

Looking at the charcoal results, a similar picture is observed: 2 different phases can be identified, charcoals from CF7, CF16, and CF18 belong to a phase coherent with the castle Period III (i.e. calibrated weighted age of AD 1051–1216), while charcoal CF26 alone is dated to AD 569–771. For this kind of material, while matching with expectations is clear for the samples referring to Period III, a statistically significant (i.e. more than  $3\sigma$ ) aging of the sample CF26 is observable. This result is probably attributable, excluding calcite contamination because of the prolonged HCl attack applied during its pretreatment phase, to the CF26 charcoal history. Bowman (1990) also points out this phenomenon as a non-neglectable occurrence when analyzing charcoals encased in mortars.

Regarding the comparison between observed results ( $^{14}\text{C}$  ages) from charcoals and *susp* fractions, a lighter agreement (always comprised between  $2\sigma$  and  $3\sigma$ , becoming  $<2\sigma$  after calibration) is observed with the exception of CF26 being significantly older than the relative analyzed *susp*. Again, this observed mismatch is likely due to wood pre-aging before its usage for mortar production. The observed results are evidence of how  $^{14}\text{C}$  dating of mortar via Cryo2SoniC represents an accurate and precise tool for further deepening the characterization of the Shayzar study site.

## CONCLUSIONS

Despite the simplicity of the carbonatation process leading to the absorption of contemporary  $\text{CO}_2$ , mortar matrices represent a complex system frequently containing other carbonaceous sources mixed in different aliquots, making the  $^{14}\text{C}$  dating of archaeological mortars a difficult task. Efficient extraction methods to isolate the binder (the mortar carbonate fraction merely attributable to carbonatation) are necessary in order to prevent the determination of biased ages. In this framework, the Cryo2SoniC procedure and its further developments were tested to obtain reliable binder fraction isolation. The Cryo2SoniC protocol was applied to mortars sampled from the ancient ruins of the Shayzar site and a series of petrographic characterizations were also performed in order to elucidate mortar production technology. These analyses confirmed the co-presence of both micritic sands and reprecipitated calcite.

The observed results on *susp\_sand* fractions indicate their strong sensitivity to possible biasing agents, confirming the overall more stable and accurate character of the *susp* fractions. In fact, all the calendar ages for this fraction were in statistical agreement with the archaeologically developed absolute chronology for this site.

The co-presence of mortar-encased charcoals also allowed independent estimation of the analyzed sample chronology. The observed results pointed out a general agreement of charcoals vs. *susp* fractions, with the exception of the CF26 sample where only Cryo2SoniC mortar analysis allowed accurate <sup>14</sup>C dating. The application of the Cryo2SoniC protocol showed promising results for accurate determination of the Shayzar chronology, indicating that this method is a promising tool for further mortar <sup>14</sup>C dating.

## ACKNOWLEDGMENTS

The authors would like to thank all people involved in Shayzar Project who allowed the analysis of their samples to test this new protocol of treatment. Thanks also to Prof Gilberto Artioli for his hospitality in the Department of Geoscience at the University of Padua (Italy). The manuscript benefited considerably from the insightful and constructive comments of 2 anonymous reviewers.

## REFERENCES

- Al-Bashaireh K, Hodgins GWL. 2011. AMS <sup>14</sup>C dating of organic inclusions of plaster and mortar from different structures at Petra-Jordan. *Journal of Archaeological Science* 38(3):485–91.
- Ambers J. 1987. Stable carbon isotope ratios and their relevance to the determination of accurate radiocarbon dates for lime mortars. *Journal of Archaeological Sciences* 14(6):569–76.
- Baxter MS, Walton A. 1970. Radiocarbon dating of mortars. *Nature* 225(5236):937–8.
- Berger R. 1992. <sup>14</sup>C dating mortar in Ireland. *Radiocarbon* 34(3):880–9.
- Bowman S. 1990. *Radiocarbon Dating*. Berkeley: University of California Press: 51.
- Cherf J. 1984. Lime mortar C14 dating and the Late Roman fortification of Thermopylai. *Journal of Archaeology* 88(4):594–8.
- Delibrias G, Labeyrie J. 1964. Dating of old mortars by the carbon-14 method. *Nature* 201(4920):742.
- Folk RL, Valastro Jr S. 1976. Successful technique for dating of lime mortar by carbon-14. *Journal of Field Archaeology* 3(2):203–8.
- Goslar T, Nawrocka D, Czernik J. 2009. Foraminiferous limestone in <sup>14</sup>C dating of mortar. *Radiocarbon* 51(3): 987–93.
- Hale J, Heinemeier J, Lancaster L, Lindroos A, Ringbom Å. 2003. Dating ancient mortar. *American Scientist* 91(2):130–7.
- Heinemeier J, Jungner H, Lindroos A, Ringbom Å, Von Konow T, Rud N. 1997. AMS <sup>14</sup>C dating of lime mortar. *Nuclear Instruments and Methods in Physics Research B* 123(1–4):487–95.
- Heinemeier J, Ringbom Å, Lindroos A, Sveinbjörnsdóttir ÁE. 2010. Successful AMS <sup>14</sup>C dating of non-hydraulic lime mortars from the Medieval churches of the Åland Islands, Finland. *Radiocarbon* 52(1):171–204.
- Lindroos A, Heinemeier J, Ringbom Å, Braskén M, Sveinbjörnsdóttir Á. 2007. Mortar dating using AMS <sup>14</sup>C and sequential dissolution: examples from Medieval, non-hydraulic lime mortars from the Åland Islands, SW Finland. *Radiocarbon* 49(1):47–67.
- Lindroos A, Regev L, Oinonen M, Ringbom A, Heinemeier J. 2012. <sup>14</sup>C dating of fire-damaged mortars from Medieval Finland. *Radiocarbon* 54(3–4):1–17.
- Marzaioli F, Borriello G, Passariello I, Lubritto C, De Cesare N, D’Onofrio A, Terrasi F. 2008. Zinc reduction as an alternative method for AMS radiocarbon dating: process optimization at CIRCE. *Radiocarbon* 50(1): 139–49.
- Marzaioli F, Lubritto C, Nonni S, Passariello I, Capano M, Terrasi F. 2011. Mortar radiocarbon dating: preliminary accuracy evaluation of a novel methodology. *Analytical Chemistry* 83(6):2038–45.
- Marzaioli F, Nonni S, Passariello I, Capano M, Ricci P, Lubritto C, De Cesare N, Eramo G, Castillo JAQ, Terrasi F. 2013. Accelerator mass spectrometry <sup>14</sup>C dating of lime mortars: methodological aspects and field study applications at CIRCE (Italy). *Nuclear Instruments and Methods in Physics Research B* 294:246–51.
- Mathews JP. 2001. Radiocarbon dating of architectural mortar: a case study in the Maya region, Quintana Roo, Mexico. *Journal of field Archaeology* 28(3–4): 395–400.
- McCrea JMJ. 1950. Isotopic chemistry of carbonates and a paleo-temperature scale. *Journal of Chemical Physics* 18:849–57.
- Nawrocka D, Czernik J, Goslar T. 2009. <sup>14</sup>C dating of carbonate mortars from Polish and Israeli sites. *Radiocarbon* 51(2):857–66.
- Nawrocka DM, Michczyńska DJ, Pazdur A, Czernik J. 2007. Radiocarbon chronology of the ancient settlement in the Golan Heights area, Israel. *Radiocarbon* 49(2):625–37.
- Nawrocka DM, Michniewicz J, Pawlyta J, Pazdur A. 2005. Application of radiocarbon method for dating of lime mortars. *Geochronometria* 24:109–15.
- Ortega LA, Zuluaga MC, Alonso-Olazaba A, Murelaga X, Insausti M, Ibañez-Etxeberria A. 2012. Historic

- lime-mortar  $^{14}\text{C}$  dating of Santa Maria la Real (Zarautz, northern Spain): extraction of suitable grain size for reliable  $^{14}\text{C}$  dating. *Radiocarbon* 54(1):23–36.
- Passariello I, Marzaioli F, Lubritto C, Rubino M, D'Onofrio A, De Cesare N, Borriello G, Casa G, Palmieri A, Rogalla D, Sabbarese C, Terrasi F. 2007. Radiocarbon sample preparation at the CIRCE AMS Laboratory in Caserta, Italy. *Radiocarbon* 49(2):225–32.
- Rech JA. 2004. New uses for old laboratory techniques. *Near Eastern Archaeology* 67(4):212–9.
- Reimer PJ, Baillie MGL, Bard E, Bayliss A, Beck JW, Blackwell PG, Bronk Ramsey C, Buck CE, Burr GS, Edwards RL, Friedrich M, Grootes PM, Guilderson TP, Hajdas I, Heaton T, Hogg AG, Hughen KA, Kaiser KF, Kromer B, McCormac FG, Manning SW, Reimer RW, Richards DA, Southon JR, Talamo S, Turney CSM, van der Plicht J, Weyhenmeyer CE. 2009. IntCal09 and Marine09 radiocarbon age calibration curves, 0–50,000 years cal BP. *Radiocarbon* 51(4):1111–50.
- Rozanski K, Stichler W, Gonfiantini R, Scott EM, Beukens RP, Kromer B, Van der Plicht J. 1992. The IAEA  $^{14}\text{C}$  intercomparison exercise 1990. *Radiocarbon* 34(3):506–19.
- Sonninen E, Jungner H. 2001. An improvement in preparation of mortar for radiocarbon dating. *Radiocarbon* 43(2A):271–3.
- Stuiver M, Polach HA. 1977. Discussion: reporting of  $^{14}\text{C}$  data. *Radiocarbon* 19(3):355–63.
- Stuiver M, Reimer PJ. 1993. Extended  $^{14}\text{C}$  data base and revised CALIB 3.0  $^{14}\text{C}$  age calibration program. *Radiocarbon* 35(1):215–30.
- Stuiver M, Smith CS. 1965. Radiocarbon dating of ancient mortar and plaster. In: *6th International Conference on Radiocarbon and Tritium Dating*. Pullman, Washington, USA. p 338–43.
- Terrasi F, De Cesare N, D'Onofrio A, Lubritto C, Marzaioli F, Passariello I, Rogalla D, Sabbarese C, Borriello G, Casa G, Palmieri A. 2008. High precision  $^{14}\text{C}$  AMS at CIRCE. *Nuclear Instruments and Methods in Physics Research B* 266(10):2221–4.
- Tonghini C. 2012. Shayzar I: the fortification of the citadel. In: DeVries K, France J, Neiberg MS, Schneid F, editors. *History of Warfare* 71. Leiden: Brill.
- Tonghini C, Montevecchi N. 2006. Muslim military architecture in greater Syria from the coming of Islam to the Ottoman Empire. In: Kennedy H, editor. *History of Warfare* 35. Leiden: Brill. p 201–24.
- Tonghini C, Donato E, Montevecchi N, Nucciotti M. 2003. The evolution of masonry technique in Islamic military architecture: the evidence from Shayzar. *Levant* 35:179–212.
- Tonghini C, Montevecchi N, Finocchietti L, Tavernari C, Vezzoli V. 2005. Il castello musulmano di Shayzar, Siria: nuovi dati dalla campagna 2004 di indagini archeologiche e analisi degli alzati. *Archeologia Medievale* 32:209–234.
- Tubbs LE, Kinder TN. 1990. The use of AMS for the dating of lime mortars. *Nuclear Instruments and Methods in Physics Research B* 52(3–4):438–41.
- Van Strydonck M, Dupas M, Dauchotdehon M, Pachiaudi C, Marechal J. 1986. The influence of contaminating (fossil) carbonate and the variations of  $\delta^{13}\text{C}$  in mortar dating. *Radiocarbon* 28(2A):702–10.
- Van Strydonck M, Van der Borg K, De Jong A, Keppens E. 1992. Radiocarbon dating of lime fractions and material from buildings. *Radiocarbon* 34(3):873–9.
- Wyrwa A, Goslar T, Czernik J. 2009. AMS  $^{14}\text{C}$  dating of Romanesque rotunda and stone buildings of a Medieval monastery in Lekno, Poland. *Radiocarbon* 51(2):471–80.



## III.2. Palazzo Vecchio between antiquity and middle age.

### Abstract

Palazzo della Signoria, better known as Palazzo Vecchio, has been the symbol of the Florence civic power over more than seven centuries. Built between the end of the 13<sup>th</sup> century and the beginning of the 14<sup>th</sup> AD to host the city's supreme governing body, the Priori delle Arti and the Gonfalonier of Justice, over time it underwent to a series of extensions and transformations.

Palazzo Vecchio was build over the ruins of the Roman Theater attributable to the ancient city of Florentia and capable to hold more than 15000 spectators during its golden age. This theater was buried by building projects and the Palace expansion. Through six years of archeological excavations directed by the Soprintendenza ai Beni Archeologici della Toscana, Florentia's ancient theater has been recently uncovered. In this study AMS absolute dating methodology coupled to Cryo2SoniC will be used over this site mortar to ensure archaeological constraints based on different methods of relative chronology, moreover in order to complete mortar samples characterization petrographic analyses where also performed. Cryo2SoniC protocol was applied to two samples of mortar to select suitable fractions to date through AMS. Petrographic analysis was carried out by means of diffraction method (XRD), observation on thin section with optical microscope (OM). In order to complete mortar samples characterization a cathodoluminescence (CTL) investigation was also performed.

### Sampling and Archaeological Setting

Two samples of mortars were collected from the underground excavations comprised inside the area called Terza Corte (Figure 32). The samples were attributed by archaeologists to two different historical periods:

- M201: a fragment of mortar picked up from a central *burella* of the Roman theatre, ascribable to 1<sup>st</sup>-2<sup>nd</sup> centuries.
- M208 : a piece of the plinth at south wall (USD166 - space V) attributed to 14<sup>th</sup> century.

*Burella* is an ancient Tuscan word (by Dante Alighieri) that means 'underground vault of a Roman amphitheatre'. Although the theatre was built during the second half of 1<sup>st</sup> century BC, it was mainly made of wood and the only masonry sections were the scene, the orchestra and seats of honor (Giusberti 1987; Cantini et al. 2009). During the 1<sup>st</sup> century AD the Gens Claudia started restoring works to enlarge the theatre, which prosecute until the strongly renovation of the beginning of 2<sup>nd</sup> century. Probably during this period the main entrance to *platea* (burelle) and the *cavea* (Francovich et al. 2007; Cantini et al. 2009) were built. RC measurements should help to

recognize if sampled structure (i.e. the burella of the theater) belong to first period of constructions or to the theater later modifications. The 13<sup>th</sup> and 14<sup>th</sup> centuries were equally interested by a strongly renovation in the urban aspect, like modifications of Palazzo Vecchio foundations. In details, inside the space V (Figure 32) the walls of a new multilevel building definitively occluded the entrance of the Roman theatre (Cantini et al. 2009). ). 1333 AD can be established as a terminus ante quem (TAQ), an archaeological reference for M208, it has been determined by cross-checking different sources: archive documents, alluvional dating and materials finding like coins and ceramics. Francovich et al. (2007) suggested that the wall of sampling belong to a medieval building built during XIII century (Figure 33) therefore, an archaeological time interval which goes from 13<sup>th</sup> century to the beginning of 14<sup>th</sup> can be inferred as chronological reference.

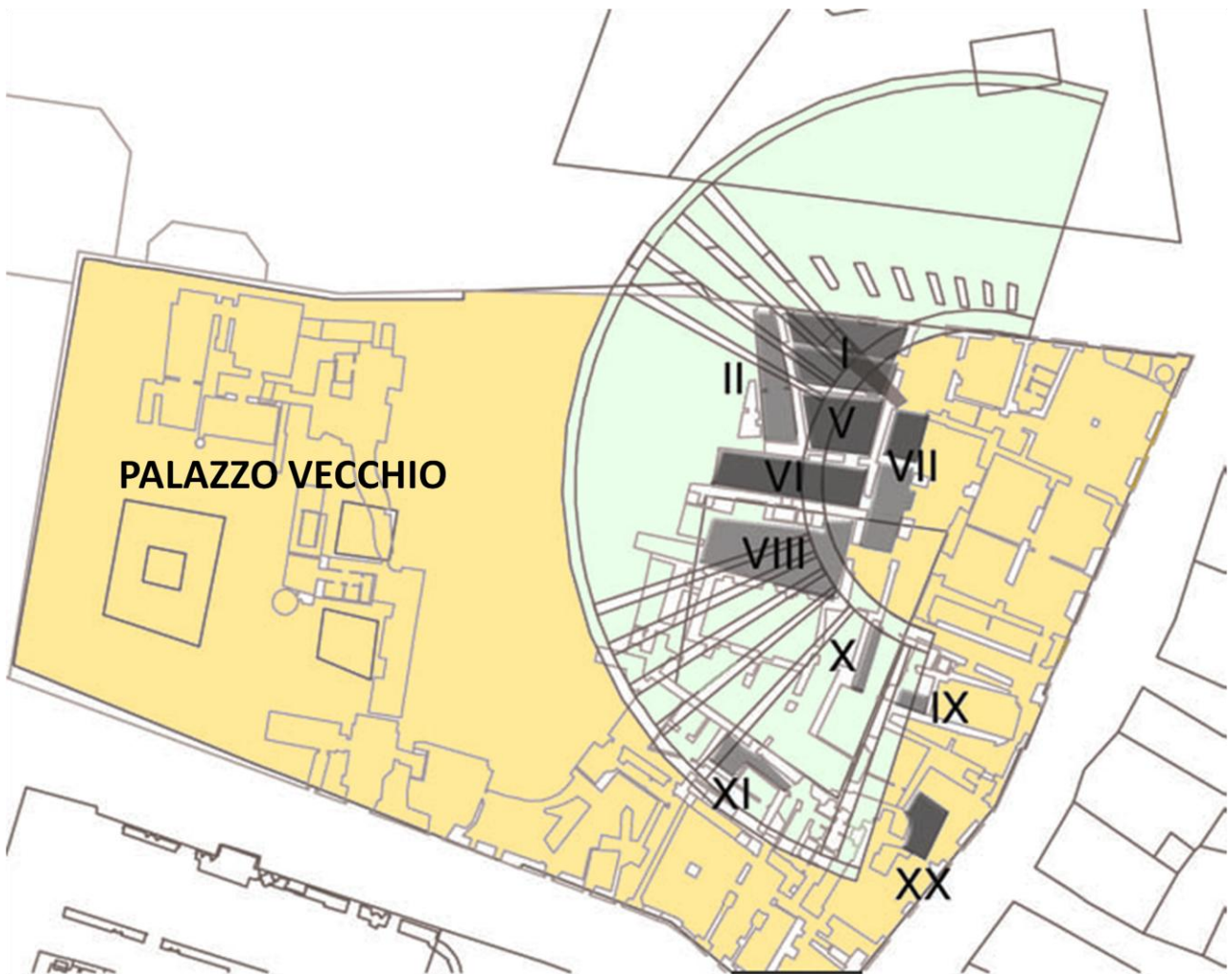


Figure 32 . Plan of Palazzo Vecchio (yellow) with the overlapping of the plan of Roman Amphitheatre. The excavation spaces and space V are highlighted with dark color (modified from Cantisani et al. 2007).

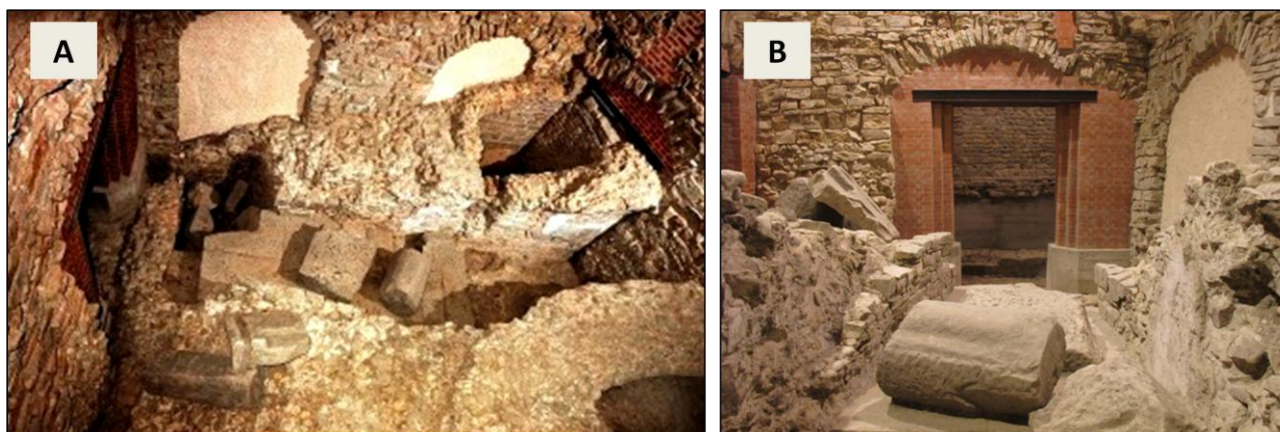


Figure 33. Space V views: i) the entrance of platea (A and B on the left) ii) collapsed vault in the centre of images where M201 was sampled; iii) plinto with two arches supporting a XIII century building where M208 was sampled (A upper side; web source [en.firenze.waf.it](http://en.firenze.waf.it)).

### Analytical Methods

Samples were studied through an optical microscope in transmitted light with a “Zeiss Axioskop 40” microscope. XRD analysis carried out by means of a Bruker D8 Advance diffractometer (Cu-K $\alpha$  radiation, operating at 40 kV and 40 mA). Diffractograms were acquired using a range 3-60° 2 $\theta$ , with a 0.02° 2 $\theta$  step (0.4 seconds step time). To identify the mineralogical phases the DIFFRACplus EVA software was used, comparing spectra with PDF2 database. A binder/aggregate and macroporosity semiquantitative estimation was performed comparing thin section (optical microscope in transmitted polarized light) using tables to estimate minerals proportions (Ricci Lucchi 1980; Myron Best 2003). Cathodoluminescence (CL) analyses was performed on one Cryo2SoniC produced fraction to explain investigate its strange behavior. Prior to CL, powders have been homogenized in an agate mortar and then put on a thin section glass. Cathodoluminescence images were obtained using a petrographic microscope (NIKON Labophot2-POL) equipped with a cold cathode stage (Cambridge Image Technology Ltd, CL8200 MK3 model), a potential difference at 15 KV and current of 200 A. Image collection was performed using a CANON Reflex EOS 600D.

Radiocarbon dating analyses were performed according to the Cryo2SoniC procedure as described in Nonni et al.2013.

In detail, sample M201 was pretreated both as bulk (pre-treating all sample) and as inner portion (only M201\_II fraction) isolating the surface refined layer. M208 sample was pretreated only as bulk due to its homogeneity.

## Petrographic Characterization

First observations on M201 and M208 samples, performed by means of transmitted light scanner, have made it possible to notice some differences. Petrographic observations showed that sample M201 is composed by two distinct layers: an inner one as a rough coat mortar (M201\_II) and an outer one as a very refined plaster of 6mm - called *intonachino* (M201\_I) (Figure 34). On the contrary, M208 sample is an homogeneous mortar without layers distinctions. The mineralogical composition of the aggregate is different for M201 to with respect to M208 and between the two layers of M201. The results of the petrographic study are resumed in Table 14.

M201 external layer (M201\_I) is made almost totally by fragments of spatic calcite, with a mean dimension about 1.50 mm and probably attributable to marble sand (Figure 35). Aggregate distribution is homogeneous, with very angular and low roundness pieces. Binder/aggregate ratio is 1:3. There are some lime lumps, a low macroporosity (about 2%) and a moderate sorted aggregate. XRPD performed on powder collected from M201\_I layer with a lance, has highlighted the almost unique presence of calcite. The inner layer (M201\_II) showed an aggregate typology completely

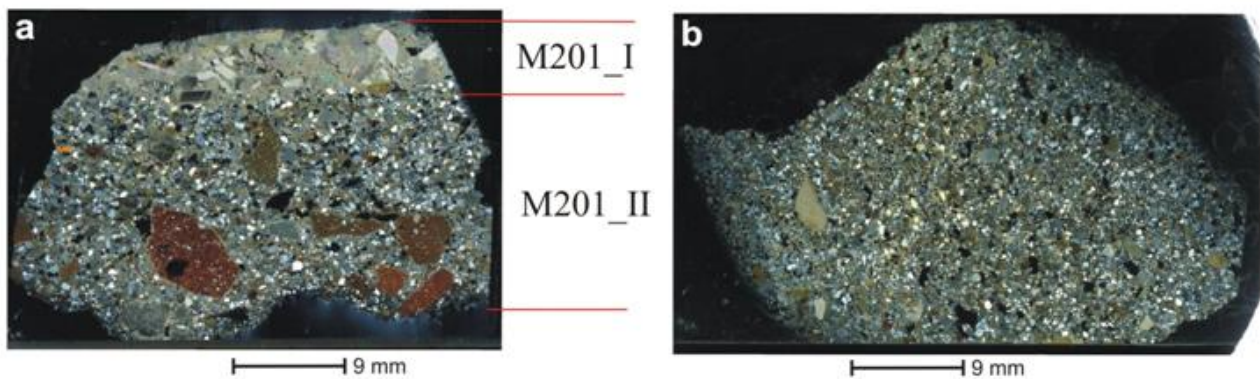


Figure 34. Microphotographs of thin sections under polarized light scanner caption images a)M201 sample b)M208 sample.

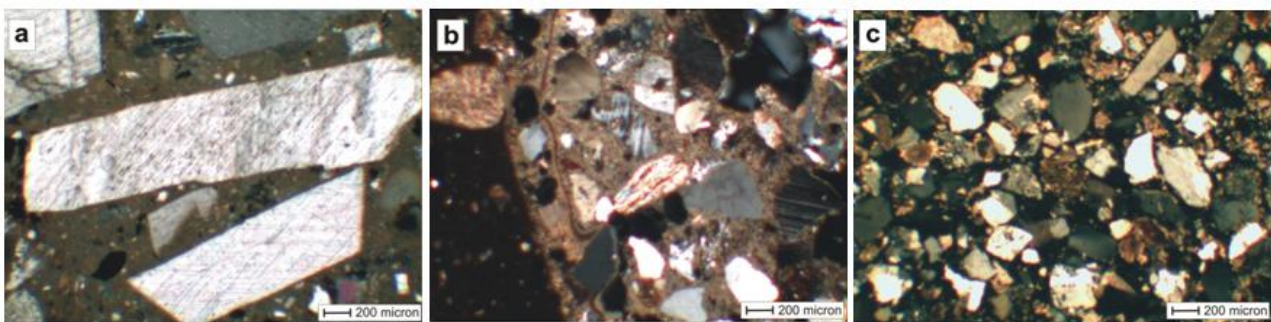
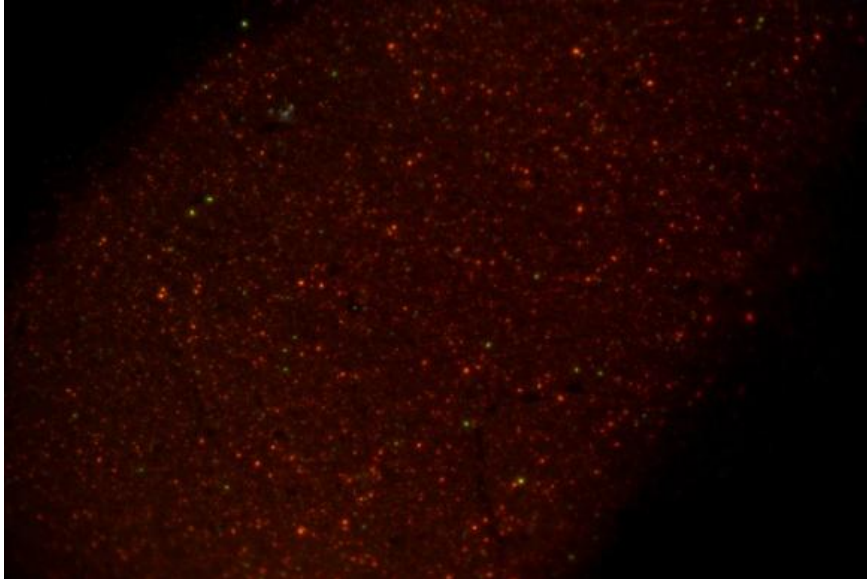


Figure 35. Microphotographs of M210 and M208 samples. External layer of M201 with big angular fragments of spatic calcite, maybe white marble (a); inner layer of M201 sample (b), showing a mineralogical composition very similar to that of M208 sample (c).

different from the first: very pointy and up to 1 mm dimension pieces of ceramics. Mean dimension of broken ceramic is  $> 0.76$  mm. Aggregate sorting is low with a medium roundness and sharpness. Mineral phases are quartz, calcite, plagioclase, microcline, biotite, muscovite and chlorite (Figure 35). There are some fragments of phyllites, sandstones, quartzites and micritic limestones. Even in this case binder/aggregate ratio is about 1:3. Sample M208 has a lower cohesion than M201. The average size of aggregate is 0.48 mm (lower than M201 sample), with a moderate sorting and angular features and a mean roundness. Mineralogical composition of M208 is very similar to that of M201\_II, except for broken bricks fragments and a higher porosity (Figure 35). This last feature is due to strong dissolution phenomena of the calcitic binder, reason of its scarce cohesion. Even in this case binder/aggregate ratio is about 1:3. Aggregate minimum dimension for both sample analyzed is 40  $\mu\text{m}$ . Both samples are characterized by secondary calcite depositions diffuse inside voids.

		M201_I	M201_II	M208
Mean Aggregate Size (mm)		1,50	0,76	0,48
Max Aggregate Size (mm)		3,18	9,00	4,00
Mean Macroporosity Size ( $\mu\text{m}$ )		192,00	600,00	760,00
Max Macroporosity Size ( $\mu\text{m}$ )		760,00	2360,00	2096,00
Sorting	by Jerram et al. (1996)	M.S.	P.S.	M.S.
Roundness	by Powers (1956)	V.A.	An.	An.
Sphericity		L.S.	Me.S.	Me.S.
Size	by Wentworth (1922)	V.C.S.	C.S.	M.Sa.
Mineralogical Phases		Calcite	Quartz, Calcite, Plagioclase, Microcline, Biotite, Muscovite, Chlorite	Quartz, Plagioclase, Calcite, Microcline, Biotite, Muscovite, Chlorite
Fragments of rock		Argillite (rare)	Argillite, Quartzite, Phillite, Micritic Limestone	Argillite, Quartzite, Micritic Limestone, Phillite
Ragments of ceramic		A	P	A
% Aggregate (size $>1/16$ mm)	Semiquantitative visual estimation by polarized microscopy (Ricci Lucchi 1980; Myron Best 2003)	25	20	35
% Binder (size $<1/16$ mm)		73	77	50
% Macroporosity (size $>1/16$ mm)		2	3	15
Lumps		P	A	A



*Figure 36. CTL image of M201\_susp fraction. Clearly visible are light spots which are attributable to grains of geological calcite (orange), quartz (blue) and feldspar (green), diffuse into matrix of binder-calcite. The presence of geological calcite suggests a not accurate selection of fraction to date, which affected the dating with an aging effect.*

## **Results and Discussion**

Experimental data (i.e. RC data) about M201, both on bulk and inner layer, show an incoherence with Cryo2SoniC experimental expectations (i.e. it was experienced to produce two fractions where only *susp* should be unbiased). Final results furnishes ages compatible with archaeological attribution only for M201\_sand but not for M201\_susp and the same behavior was observed for M201\_II fractions. Experimental observations of M201 and M201\_II sand fractions led to results closer to chronological expectations more than M201 and M201\_II susp fractions, exhibiting, respectively, a fair aging and a strong rejuvenation effect. Measurements should be repeated to verify that this inversion is reproducible and to try to understand causes, maybe connected to an inefficient separation. However this was not possible for the absence of further available material. A useless separation should be connected to a mechanical stress owed to pretreatment which probably broke secondary calcite concretions into the voids, uniting youth calcite particles to the binder ones. A CL measurement was performed in order to solve this dating incongruence: the analysis of already dated powder produced an image showing a strong geological calcite contamination into M201\_susp (Figure 36). The absence of further available material did not allow to produce CL measurements on sand fractions too, in order to verify presence of eventual geological calcite grains. On the other hand sand fractions (Table 15) report a visible good matching between their RC results (as M201\_sand and M201\_II\_sand) and the expected 1<sup>st</sup> century AD (Figure 37).

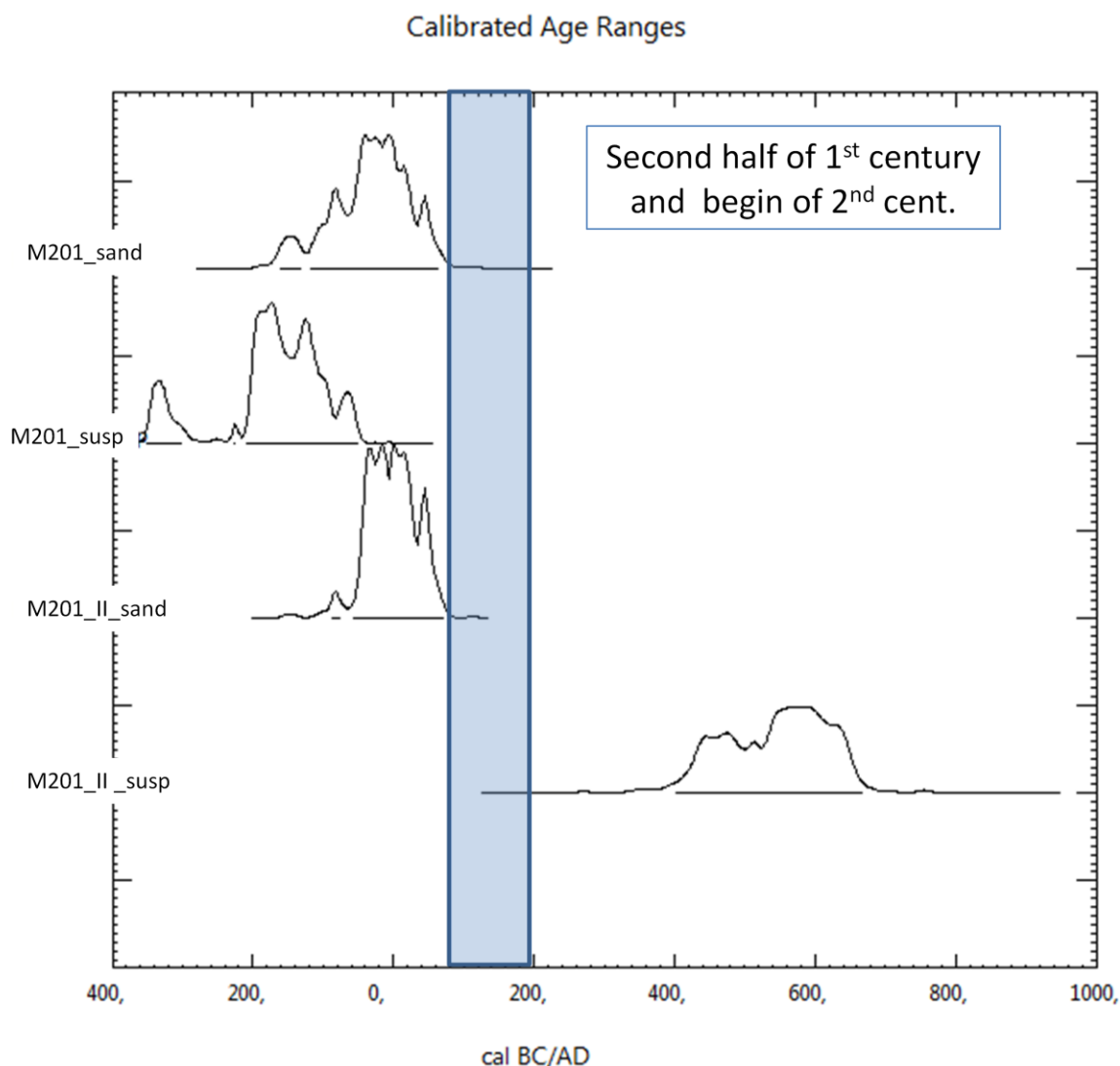


Figure 37. Calibration curves of Roman sample isolated fractions. Are shown susp and sand fractions dating M201 (bulk) and M201\_II (inner layer) together with archaeological attribution to confirm. Archaeological dating goes from second half of 1<sup>st</sup> century to the beginning of 2<sup>nd</sup> century (blue stripe).

Table 15. Radiocarbon measurements, their calibrated ages and the archaeological references. Ages which match with references are highlighted in bold type.

Sample	RC age	Err RC	Calibrated Age 1 $\sigma$	Calibrated Age 2 $\sigma$	Archaeological Reference
M201_sand	2024	40	<b>57 BC -26 AD (87%)</b> <b>42 – 47 AD (4%)</b>	<b>117 BC – 63 AD (94%)</b>	1 <sup>st</sup> -2 <sup>nd</sup> century AD
M201_susp	2130	31	203 - 101 BC	209 – 51 BC (87%)	
M201_II_sand	2003	30	<b>41 BC – 25 AD (99%)</b> <b>44 – 46 AD (1%)</b>	87 – 77 BC (2%) <b>55 BC – 69 AD (98%)</b>	
M201_II_susp	1495	80	441 – 643 AD	402 – 668 AD	
M208_sand	1135	53	864 – 984 AD (92%)	776 – 1013 AD	13 <sup>th</sup> - beginning of 14 <sup>th</sup> century
M208_susp	882	131	<b>1033 – 1252 AD</b>	<b>889 – 1315 AD (98%)</b> <b>1355 – 1389 (2%)</b>	

Absolute chronology determination performed on M208 sample showed a positive feedback with its archaeological attribution chronologically placed the structure between 13<sup>th</sup> and the first half of 14<sup>th</sup> century, respecting also the 1333 AD as TAQ. In this case experimental data are in agreement with Cryo2SoniC principles: M208\_sand is older than M208\_susp (Table 15 and Figure 38). The large error associated to M208\_susp RC age suggests a measurement repetition in the future in order to achieve a lower error (< 50 years). The lack of useful material for a sample reprocessing got made impossible to repeat the dating. In this case RC absolute chronology dating was successfully applied. A light contamination of dead carbon has been isolated using Cryo2SoniC separation method into the sand fraction for M208 sample.

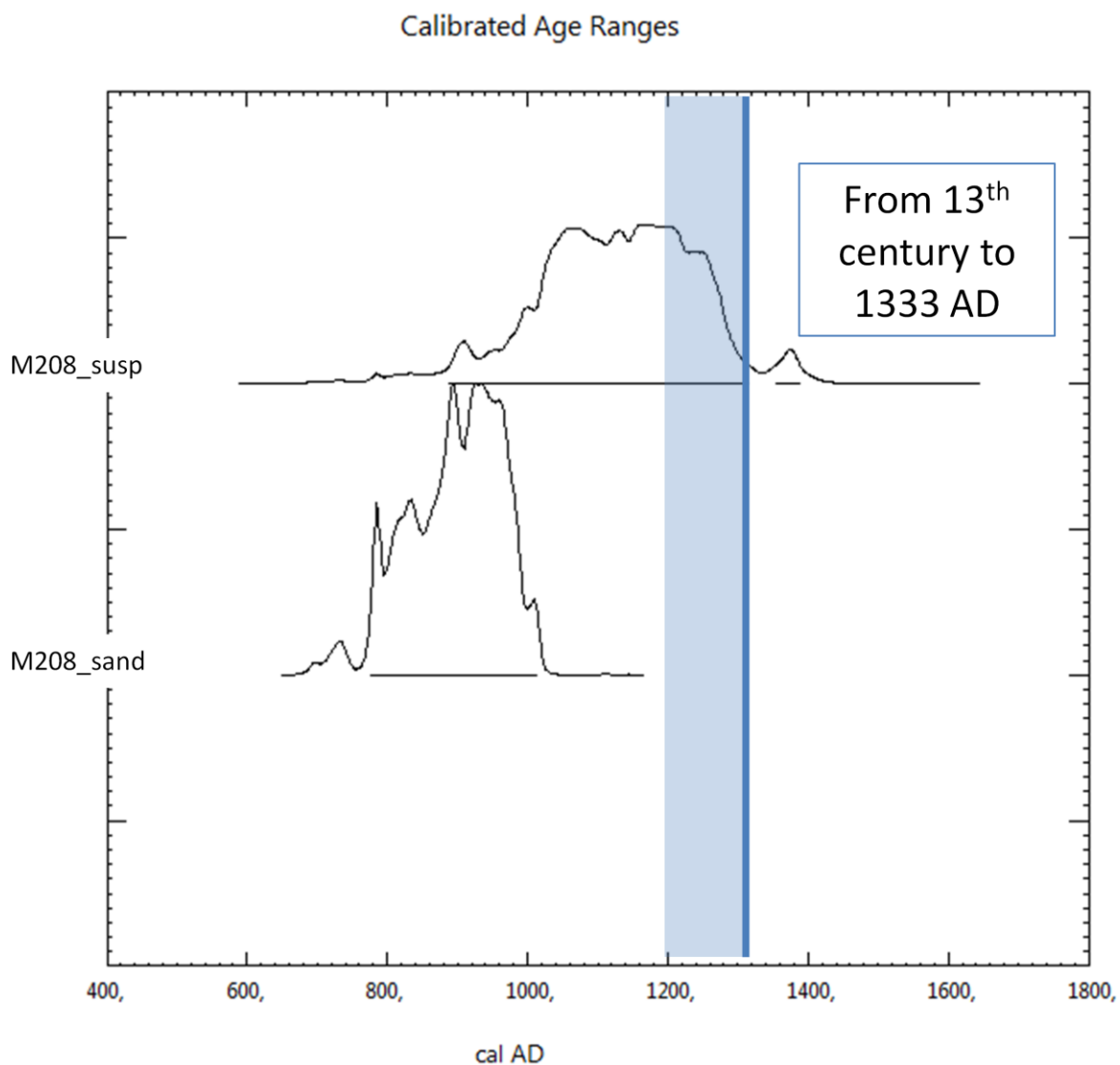


Figure 38. Calibration curves of M208 radiocarbon ages. Only M208\_susp matched with archaeological reference.



## Conclusions

A confirmation on archaeological attributions using an absolute chronology method like RC dating, answered some open questions regarding the study site. Reasons are connected to limits holding to the pretreatment phase and to the same RC dating method. First reason is linked to Cryo2SoniC process of selection of the representative fraction to date that could be conditioned by the presence of fine fraction of carbonate materials into the original mortar. The second reason is connected with a restitution of an interval of dating, that could also widen the final calendar dating time interval. First eventuality has been represented by failure on M201 dating where *susp* fractions showed contaminations from geological calcite grains coming probably from crushing of micritic limestone component, and also from neogenic calcite which fills mortar porosity. On M201 the final dating has been committed to *sand* fractions that confirm the archaeological supposition of belonging to first construction phase: putting the building of the origin *burella* inside first construction phase which allowed to pass from a wooden structure to a more solid one. Inside the same buried space (V) M208 sample has been correctly dated to the 14<sup>th</sup> century confirming the age of medieval structures surrounding the ancient Roman theatre.

## Acknowledgements

Special thank goes to archaeologists Alessandra Pecci, Jacopo Bruttini, Federico Cantini and direction of Soprintendenza ai Beni Archeologici della Toscana for providing these samples. A big thanks goes also to Domenico Miriello and Gino Mirocle Crisci from DiBEST of University of Calabria, that have performed part of all the petrographic and mineralogical characterizations.

### III.3. <sup>14</sup>C Investigation on Circo Massimo remains.

The Circo Massimo in Rome represents one of the most famous buildings of the Italian cultural heritage. From its south-east semicycle (in front of Palatinum hill) nine fragments of mortar collected from three different structures were sampled. From an archaeological point of view they seem to hold to three different epochs. The aim of the research is to understand and verify, through the use of radiocarbon dating of mortars, if the preliminary archaeological guessing attributing them to three different periods could be confirmed.

#### Archaeological Setting

Circo Massimo is an ancient chariot racing stadium and mass entertainment venue situated in a valley between the Aventine and the Palatine hills. It was the first and largest stadium in ancient Rome and could hold about 150,000 spectators (Plinio the Elders, Humphrey 1986). Its aspect nowadays is heavily changed due to historical rearrangements so its few remains still have many uncertainties about chronological attributions. The circus was inaugurated by Cesar on 46 BC with a partial wooden structure, destroyed by a fire in 31 AD and rebuilt during Giulio Claudia dynasty. In particular the main reconstruction was made by emperor Trajan and Domitian, attributions as confirmed by different technical aspects such as the building execution, the utilized materials and the numerous finding of brick-stamps (Lugli 1962). Under Trajan, the *Circus Maximus* found its definitive aspect, last unchanged during centuries, exception made for some monumental additions put on by later emperors such as repairs and renewals to existing fabric. The last extensive change was planned under Caracalla (Humphrey 1986). The last known races was attested in 549 AD; then Circus was progressively abandoned falling into disuse and decay, becoming soon a quarry for building materials (Bowersock 1999). Comparative exams of the structures allows to have an idea of the modifications made during the centuries but the *caput circi* zone, where our samples come, has been inhabited and utilized over the time. These conditions put Circo Massimo to be subject to many transformations and distractions until making remaining roman walls unrecognizable (Ciancio Rossetto 1983, 1988).

#### Materials and Methods

Samples analyzed come from USM 317 (CMAX 1,2,3), USM 314 (CMAX4 and CMAX5), USM 165 (CMAX6 and CMAX7) and USM 300 (CMAX8 and CMAX9) as schematized in Figure 39. Their archaeological attributions, based on structure analyses, attributed:

USM 317 and USM 314 (CMAX 1, 2, 3, 4 and 5) to the first phase of construction, ranging between the 1<sup>st</sup> and 2<sup>nd</sup> centuries;

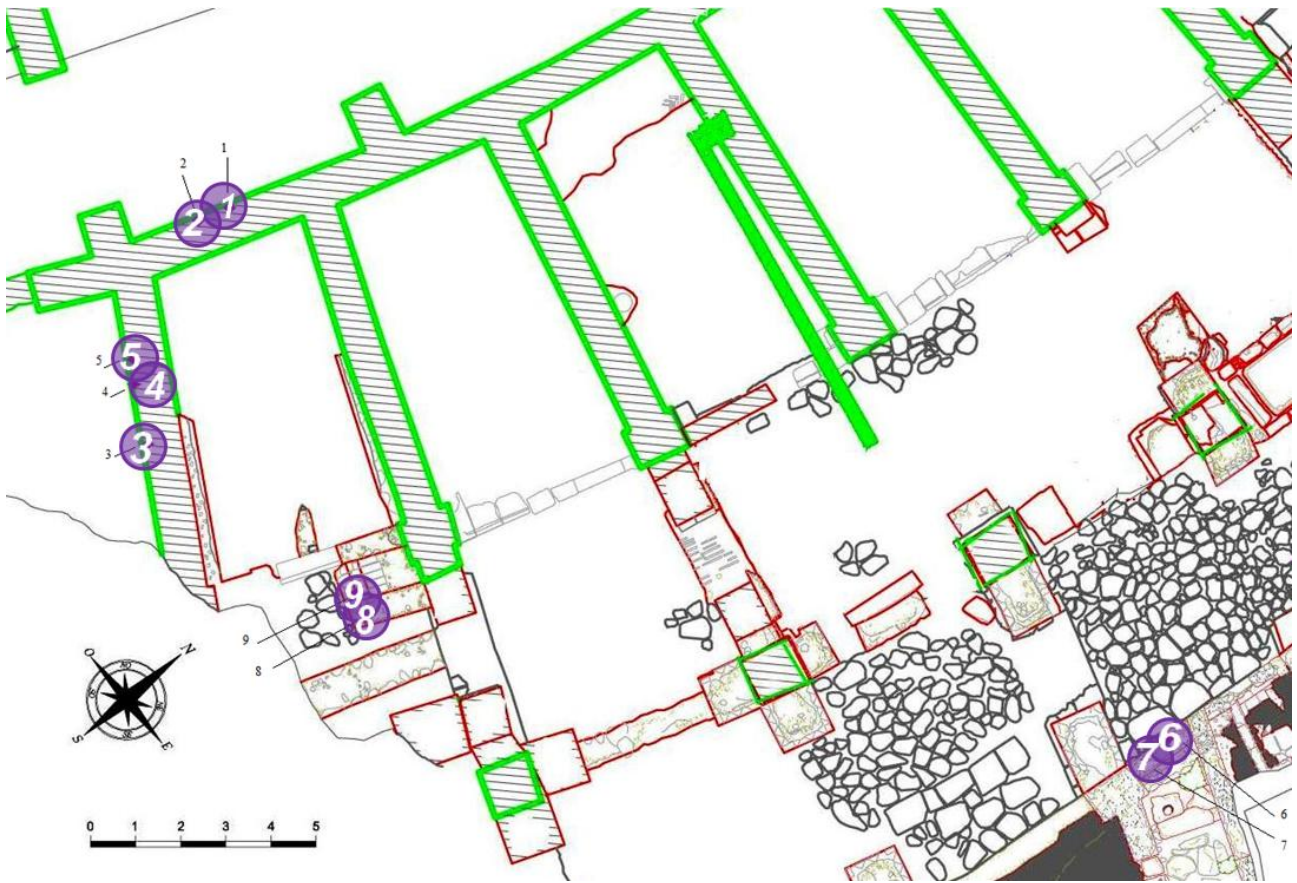


Figure 39. Plan of south-east semicycle of Circus Maximus and relative sampling points.

USM 165 (CMAX 6 and 7) to a Roman late antiquity period, around 4<sup>th</sup> century,

USM 300 (CMAX 8 and 9) to the last period of circus life around the 6<sup>th</sup> century.

Each sample to be dated using the AMS technique (Terrasi et al. 2008) underwent Cryo2SoniC pretreatment as described in Nonni et al. 2013. Samples were characterized by a petrographic point of view by microscopy observations on thin section (TSOM) and by X-ray powder diffraction (XRD).

TSOM was performed on thin sections (30  $\mu\text{m}$  thick) with an optical polarizing microscope (ZEISS D-7082 Oberkochen) under parallel and crossed nicols. XRD was performed with a Seifert MZIV automatic powder diffractometer, equipped with a graphite monochromator using a  $\text{Cu K}\alpha$  radiation and operating at 40 kV and 20 mA. XRD data were collected from  $5^\circ$  to  $60^\circ$   $2\theta$  with a step-size of  $0.02^\circ$  and counting time of 8 s. Diffraction patterns obtained were interpreted with X'Pert HighScore Plus 3.0 software by PANalytical, reconstructing mineral profiles of the compounds by comparison with ICDD and ICSD diffraction databases. Selected fractions of powder to analyze by XRD were obtained crushing bulk sample into an agate mortar.

After Cryo2SoniC pretreatment (see Section II.2), two of produced calcite fractions were analyzed by FTIR according to Chu et al. (2008) experiment, in order to test this methodology as a candidate tool to predict a successful RC dating (see Section II.6.3). FTIR measurements were carried out in transmission mode on KBr pellets containing a suitable amount of sample (0,1%). Measurements were performed in pure dry atmosphere to remove humidity and CO<sub>2</sub> signals with a Fourier Transform Infrared Spectrometer Varian 4100 (Excalibur series), with a resolution of 4 cm<sup>-1</sup> over a spectral range of 4000–400 cm<sup>-1</sup>. The  $\nu_2/\nu_4$  ratio was calculated by dividing the height of the  $\nu_2$  peak by the height of the  $\nu_4$  peak. The baselines were drawn between the closest minima on either side of the measured peak, considering that heights of peaks measured is influenced by the choice of baseline (Chu et al. 1998). The analytical uncertainty in measurement of the  $\nu_2/\nu_4$  ratios was estimated in  $\pm 0.2$ . According to Chu et al. (2008), each sample was measured from two to five times and each measurement was obtained from a different part of the sample.

## Results

Obtained RC ages partially match with archaeological hypothesis, opening the opportunity to discuss also to other archaeological interpretations. First five samples (from CMAX1 to CMAX5) belonging to closer stratigraphic units, were attributed to the coherent period. The archaeological time constraints fix their development between the 1<sup>st</sup> and 2<sup>nd</sup> century, during Trajan emperor age. This building event followed a destructive fire which destroyed the pre-existent wooden structures. Although radiocarbon dating match with the archaeological expectations, they show a shift toward slightly older dates, intercepting the 0 AD (Table 16).

Sample	USM	RC Age	Err RC	Calibrated Age 1 $\sigma$	Calibrated Age 2 $\sigma$	Archaeological Hypothesis
CMAX 1 susp	317	2009	38	47 BC - 49 AD	111 BC - 75 AD	End of 1 <sup>st</sup> and begin of 2 <sup>nd</sup> century
CMAX 1 susp		1995	60	85 BC - 75 AD	165 BC - 127 AD	
CMAX 2 susp		2033	39	92 BC - 21 AD	164 BC - 54 AD	
CMAX 2 susp		2056	59	163 BC - 1 AD	341 BC - 69 AD	
CMAX 3 susp		2048	76	166 BC - 22 AD	352 BC - 124 AD	
CMAX 4 susp	314	1773	79	137 - 341 AD	73 - 423 AD	4 <sup>th</sup> century
CMAX 5 susp		1974	58	43 BC - 80 AD	164 BC - 204 AD	
CMAX 6 susp	165	1926	73	2 BC - 139 AD (88%)	103 BC - 251 AD	4 <sup>th</sup> century
CMAX 7 susp		2066	108	338 BC - 55 AD	379 BC - 129 AD	
CMAX 8 susp	300	1760	85	210 - 384 AD (86%)	67 - 435 AD (97%)	From 6 <sup>th</sup> century on
CMAX 9 susp		1710	65	254 - 402 AD	135 - 437 AD (96%)	

The possibility to attribute the investigated walls to first two centuries, is strongly in contrast with the absence of an architectural characteristic feature: the *opus reticulatum a cubilia* (long side of 6-7 cm) of small dimension representing a stylistic chronological guide. Both sampled walls were built instead by *a laterizi* building technique (Ciancio Rossetto and Buonfiglio, 2007). The small aging effect could be attributed to a light presence of secondary calcite deposition observed in thin sections (Figure 40) although considering their relative uncertainties the measurements could be evaluated as compatible. With an high probability the secondary calcite deposition into porosity should be formed after flooding of the archaeological area with lift groundwater (whose presence is attested in literature; Ciancio Rossetto and Buonfiglio, 2007) or river inundations (Bencivenga et al. 1995). It is known that the Circo area has been affected since the antiquity by the presence of a consistent aquifer water at underground level (Ciancio Rossetto and Buonfiglio, 2007). The sample CMAX4 even if RC age statistically intercept the archaeological attendance within  $2\sigma$  interval, differs from the others just mentioned: it is the unique measurements characterized by a little rejuvenation of age (Figure 42). Rejuvenation could be due to the sampling point: CMAX4 was sampled from a part of the wall inner than CMAX 3 and 5. It is known that inner/deeper parts of a structure carbonates more slowly than the external ones. Finally it could be defined the first group as a compact one in term of dating, where the differences – if there are – should be evaluate as comprise into their relative uncertainties and consequently, statistically absent. Second group of samples, CMAX 6 and CMAX 7, is attributed to a masonry structure of a late antiquity *fornice* (3<sup>th</sup>-4<sup>th</sup> century) but their RC ages did not match with its age, resulting comparable to the first group attributed to the earlier phase of construction, maybe connected with Caracalla remakes (Humphrey 1986). Under a constructive aspect they own to a wall showing different constructive materials,

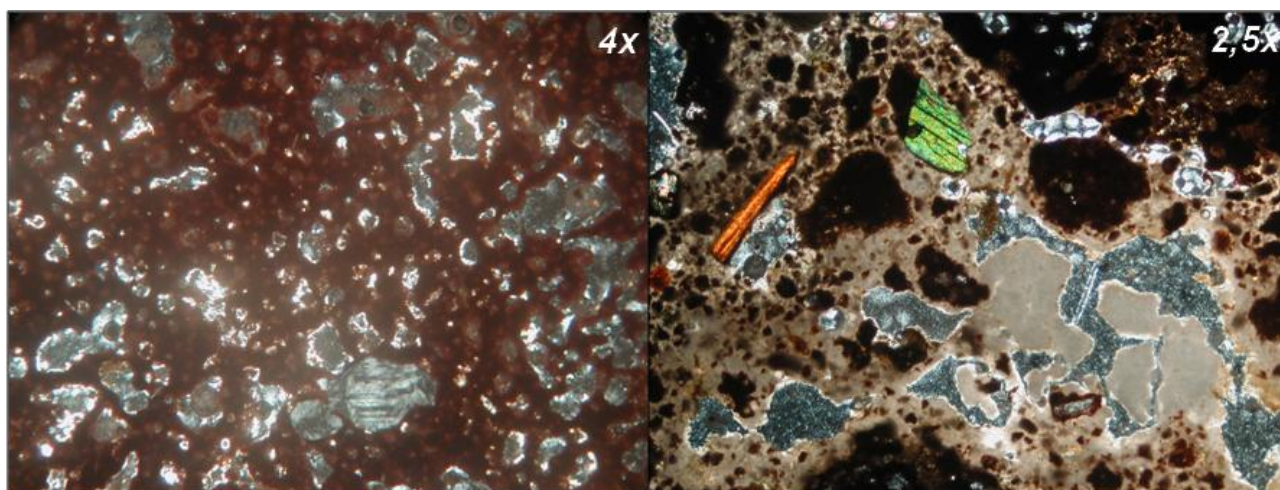


Figure 40. TSOM images captured at crossed nicols, of CMAX3 (left) and CMAX8 (right), showing secondary calcite depositions into voids of aggregate and binder.



Figure 41. A visual check shows difference between structures where mortars were sampled. The picture B shows the wall owns to CMAX 6 and 7 and different from others in A and C pictures. Structures in A and C show the similar constructive technique called a lateritium.

while under a petrographic aspect two group of samples were not evidently different. A further proof was given by FTIR analyses performed on CMAX6<sub>susp</sub> and CMAX7<sub>susp</sub> according to Chu et al. (2008). FTIR analyses allowed the measurement of a  $v_2/v_4$  ratio around 6 implying that the sample ratio falls inside completely calcinated binder defined for calcinated mortars (i.e.  $v_2/v_4$  ratio between 5.8 and 7.2). Considering that FTIR technique should not be yet considered perfectly reliable for this field of application (see Section II.6.3), these results implies that samples were DC contaminants free. Our findings (i.e. petrography, FTIR and Radiocarbon dating) are in apparent contrast with the archaeological hypothesis and on behalf of RC results. The last couple of samples (CMAX8 and CMAX9) comes from a staircase *lacertus* archaeologically attributed to the 6<sup>th</sup> century and following, during the period when Circus felt into disuse (last races were attested in 549 AD under Totila). Radiocarbon analyses produced calendar ages older than the hypothesized ones (attributable to the last centuries of Circus life). Their construction could be probably connected with restoring works made during reign of Diocletian and Constantine, after numerous collapses (first half of 4<sup>th</sup> century; Aurelius Victor 1994). Petrographic analysis suggest that CMAX8 and CMAX9 samples are not different from the others, reporting the same secondary deposition affection (Figure 40) and a similar mineralogical average composition. By an architectonic point of view the building technique of the sampled staircase from which they were sampled is similar to the early imperial one, called a *laterizi* and observable in all sampled structures (Figure 41).

## Conclusions

Radiocarbon dating of mortars coming from Circo Massimo shows a partially agreement with archaeological expectation, limited on five samples (CMAX 1,2,3,4,5) attributed to the first phase of Circus life (1<sup>st</sup> - 2<sup>nd</sup> century; Figure 42). Samples holding to the other two structures (*fornice* and

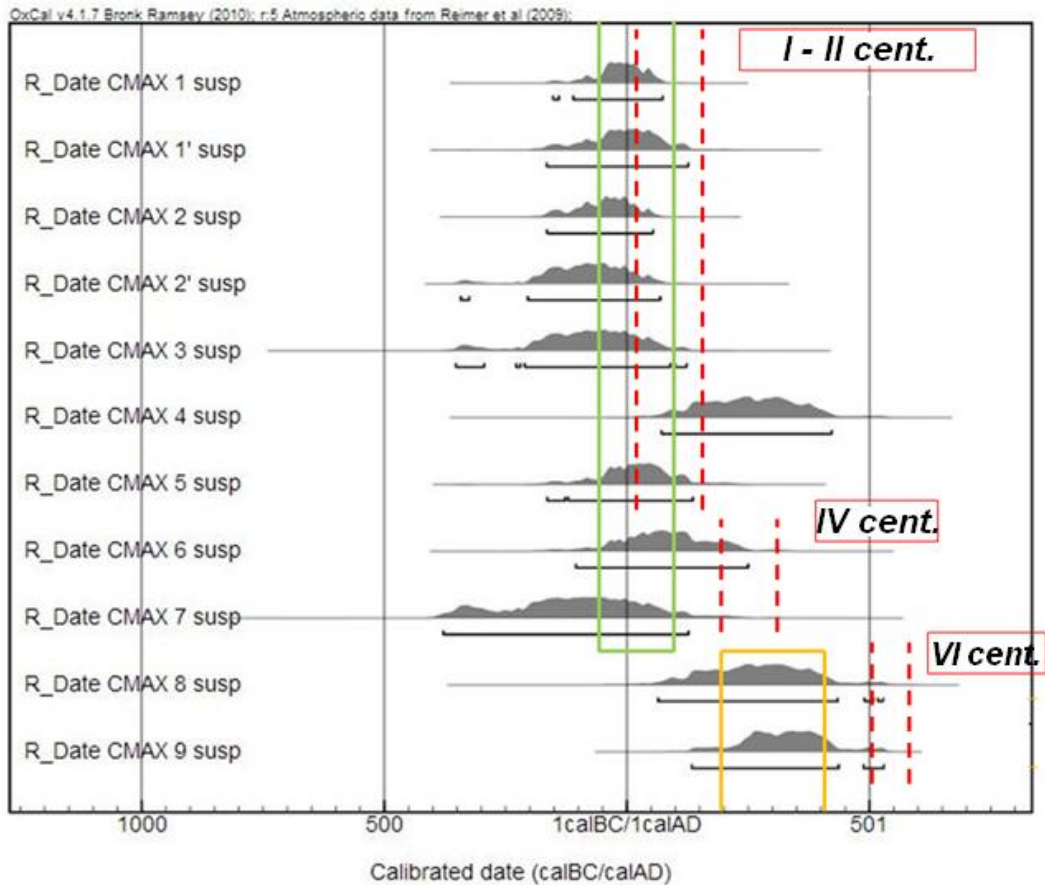


Figure 42. Calibrated ages intervals (vertical continuous lines) compare to hypothesized archaeological age intervals (vertical segmented lines).

staircase), characterized by strong archaeological uncertainties, showed a mismatch between archaeological suppositions and radiocarbon dating (Figure 42).

These observations open new questions about reliability of RC dating on cited structures and suggests a deepest analysis to understand if the observation of older ages is a consequence of a lack of proposed pretreatment procedure (i.e. secondary calcite deposition contaminated by dead carbon) or an holding to different epochs which support a new archaeological interpretation thesis based on RC. In details:

- for CMAX6 and CMAX7 it can be stated that: RC dating chronologically allocated these samples to the extensive rebuilding during Caracalla reign. This dating is supported by: i) FTIR analysis that showing suspended/dated fractions free of DC contaminants guarantee RC dating reliability; ii) petrographic observations which show same main features of samples from Trajan and Domitian era.
- for CMAX8 and CMAX9 it can be stated that they belong to a structure made by a *lateritium* technique, similar to the one used for imperial walls. Hypothesizing: if their

dating was attributed to the last period of life and use of the circus (as experimental data confirm), the building of the staircase could be considered as an act of regular maintenance, while if their dating was attributed to the period of disuse (as hypothesized by archaeologists), the building of a masonry staircase could appear as an act more difficult to explain. Why built a staircase if there was no more its usufruct? In this case the matching of RC dating with the restoration made by Constantine after collapses which involved many parts of the Circus, should be appear as the most plausible hypothesis.

Radiocarbon measurements in this case have not helped to fix all archaeological suppositions and do not want to substitute them, but surely have laid the basis for new interpretations and new archaeological questions to solve.



### III.4. Discovering the Domus Romanae inside Palazzo Valentini

“Buildings can tell you a lots of things, if you allow them to do that” (Piero Angela, 2008). An important excavation project involving Palazzo Valentini in Rome brought to light a series of different construction phases with a complex history. Involved historical periods spans from the early imperial Rome to the closest 19<sup>th</sup> century. This research aims to date various building structures of uncertain chronology through the radiocarbon method, in order to define an absolute chronology which could support archaeologists to confirm their theories of attribution. To achieve this result a series of RC measurements on collected mortar samples using the Cryo2SoniC pre-treatment has been carried out as well as a petrographic study which could help to identify and recognize possible differences in the studied samples.

#### Archaeological setting and sampling

Palazzo Valentini is an ancient noble palace placed in a central area of Rome, which links Foro Romano with the slopes of Quirinale and Campo Marzio. Archaeological excavations made inside underground area of Palazzo Valentini unearthed a series of rooms belonging to the remains of two Roman aristocratic *domus* of the imperial age, including a thermal complex. Their history starts with Traiano or Adriano and goes on to the phase of Constantin when they assumed the complex morphology visible nowadays. The *Domus* were part of a residential complex extended till the Traian Forum area and inhabited by Roman aristocracy. Structures underwent over time to numerous modifications and rearrangements, not only until the late antiquity but also later on from 16<sup>th</sup> to 19<sup>th</sup> century, when they were used as solid bases for the development of a new palace. Initially belonged to Cardinal Bonelli, the palace was dynamically modified until the last century (around II world war) when an air-raid shelter was build (Baldassarri 2008).

For this study a set of mortars constituting different construction phases were sampled, covering all the excavated areas (Figure 43). Belonging to the Roman period, their archaeological ages range from the end of the 1<sup>st</sup> to the beginning of the 4<sup>th</sup> century and they can be divided in three chronological groups.

- The first group is connected to the most ancient layer, a *platea caementitia*, built to waterproofing the overlying street from groundwater (PVAL1 and PVAL16; Baldassarri 2008). The *platea* is attributed to the end of the 1<sup>st</sup> and the beginning of the 2<sup>nd</sup> century and its remains have been found into room 2 (PVAL1) and room 5 (PVAL16).
- The second set of samples was sampled inside masonry structures close to a brick-stamp related to Adrian period (above 123 AD). PVAL 21 and 24, belonging to this second set, have been sampled from two different and distant walls.

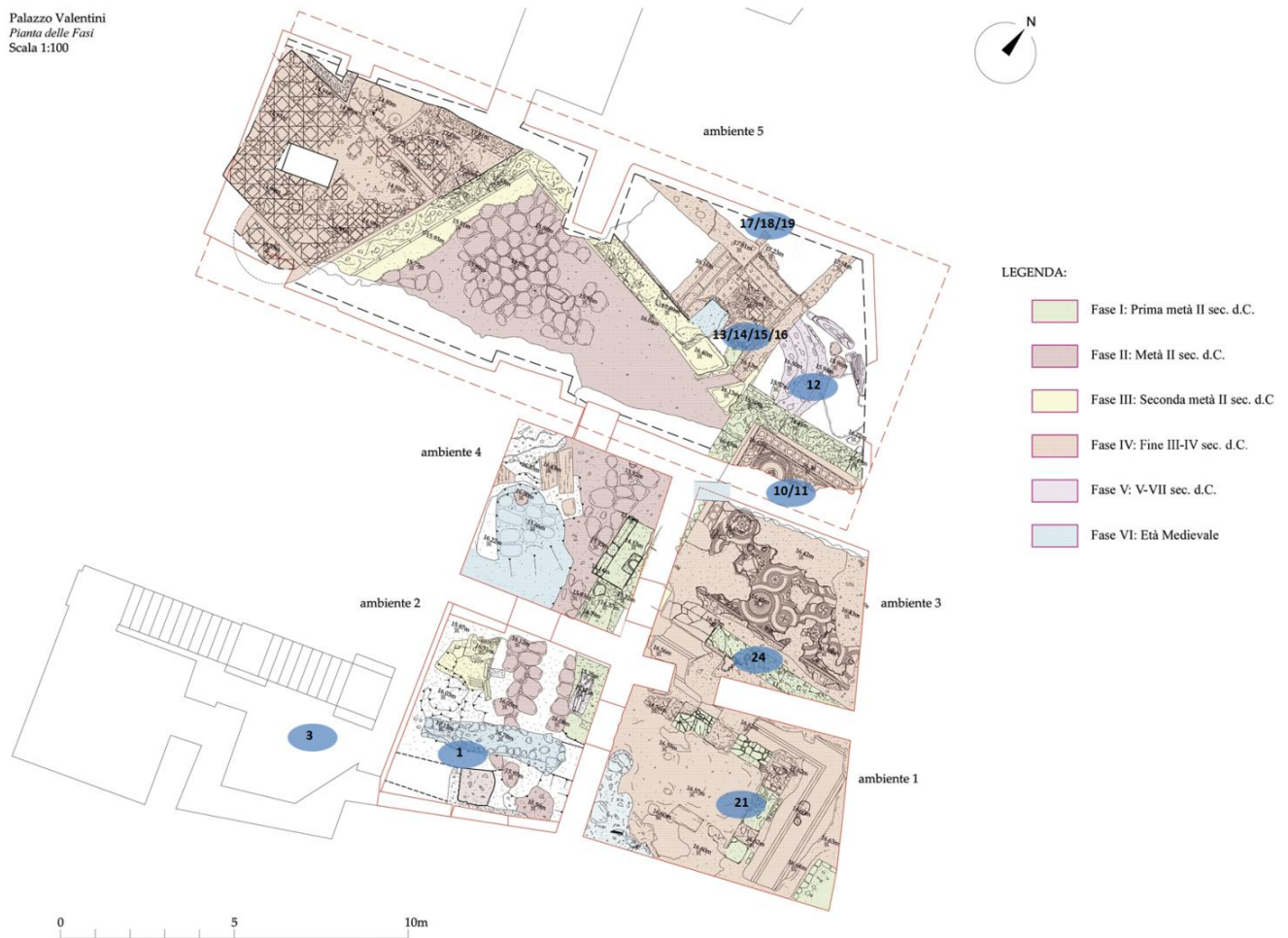


Figure 43. Plan of underground level of Palazzo Valentini where are present both Roman and medieval structures. The sampling points are highlighted in blue.

- The third group includes masonry structures archeologically attributed to the late antiquity and is represented by a barrel vault of the room 5: samples PVAL13 and PVAL14 (the two lateral walls, W and E, respectively) and PVAL15 (their connection vault).

Successive rearrangements of the structure involved the ancient Roman structures appear like additions on pre-existent masonry, as walls from where samples PVAL 3,10,11,12,17,18,19. More precisely:

- PVAL12 was collected from a circular wall structure comprised between two perimetral walls of Roman *domus* (room 5). Archaeologists chronologically place PVAL12 to the late antiquity.
- PVAL3 was collected from a semicircular structure (lower portion of a furnace), that could be dated back to an approximate medieval period.
- A further area to be studied includes a pouring of mortar that cover a Roman mosaic and should represent the basement of a Renaissance floor. From this first zone, samples of PVAL10 and

PVAL11 were collected: they are attributed to the basement casting and to the superior base of the sixteenth floor, respectively (Figure 43).

- A sampling involved a perimetral wall attributed to Renaissance construction phase (room 5). From this zone, three samples (PVAL 17,18,19) from a wood working imprint of the same époque were collected.

## Materials and Methods

Each sample of mortar was dated according to the method described in Nonni et al. (2013) - see section II.2 and II.4 of this Thesis - using Cryo2Sonic as pre-treatment method to select a fraction representative of the binder portion. For some samples (PVAL 13,14,21), dating was performed not only on pretreated bulk material but also on an isolated lime lump, which followed the method described in section II.3, exception made for PVAL3 on which was performed only a dating of its lime lump. Lime lump underwent to a simple acid digestion of the whole lump as is, by a  $H_3PO_4$  attack. At the end of pretreatment, CIRCE AMS facility has been used to retrieve  $^{14}C$  results (Terrasi et al. 2008).

The petrographic study of the samples was carried out by means of X-ray diffraction (XRD), observations on thin sections through ordinary petrographic optical microscope (OM) and a scanning electron microscope (SEM) in order to investigate about technology production differences between samples attributed to different periods.

XRD analyses were performed by means of a Philips X'Pert diffractometer in Bragg-Brentano geometry equipped with a Cu X-ray tube operating at 40 kV and 40 mA (Cu  $K\alpha$  radiation) and an X'Celerator detector, both mounted on a PW1050/37 theta-2theta vertical goniometer. Data acquisition was performed by operating a continuous scan in the range  $3.01-79.99^\circ [2\theta]$ , at an acquisition rate of  $0.02^\circ$  per second  $[2\theta]$ . Diffraction patterns obtained by both XRDs were interpreted with X'Pert HighScore Plus 3.0 software by PANalytical, reconstructing mineral profiles of the compounds by comparison with ICDD and ICSD diffraction databases. XRD analyses were focused on the fractions of the samples with grain size below  $63 \mu m$ . These fractions were collected, broking up by means of soft hammering, and then dry sieving mortars samples, by a series of dry test sieving (800, 160, and  $63 \mu m$ ). It is important to collect almost 0,25 g of material, virtually representing the binder fraction. Powdered samples have to be crushed in an agate mortar before XRD analyses.

OM observations were performed on thin sections with an optical polarizing microscope (ZEISS D-7082 Oberkochen) under parallel and crossed nicols.

SEM analyses were carried out using a Camscan MX 2500 SEM microscope equipped with a LaB6 electron source, with an energy dispersive X-ray detector (EDS) to collect elemental and structural data. To allow measurements, thin sections were previously covered with an ultra thin coating of graphite to prevent the accumulation of static electric fields during imaging.

Not all samples underwent to all kind of analysis for petrographic characterization.

## Results and discussion

On samples PVAL1 and PVAL16, coming from the same archaeological layer of the *platea caementita* but sampled into two different rooms, the absolute chronology investigation used as a tool to confirm archaeological construction hypothesis, did not work. The observed RC ages were older more than a thousand years with respect to the hypothesized ones fixed at the end of 1<sup>st</sup> century AD (Table 17). Petrographic analysis allowed to understand that the mismatching is attributable to a strong presence of secondary calcite into these samples. Secondary calcite is the unique detectable possible source of dead carbon, responsible for this strong aging. In literature the presence of an active underground aquifer is reported (Ventriglia 1971) as well as a significant number of inundations and flooding in that area (Bencivenga et al. 1995); these probably could be the causes of carbonate dissolution/re-precipitation processes. Secondary calcite fills up all voids and profusely substitutes original binder particles, in the spatic or phenocrystalline forms (Figures 44 and 45). The petrographic analysis showed that these mortars were composed by a pozzolanic aggregate, with glass, leucite and zeolites as main components, abundant orthopyroxenes and less abundant biotite. Binder was composed by micritic calcite, partially substituted by newly formed crystals, and hydraulic phases like CSH gel (Calcium Silicate Hydrate), due to reaction between

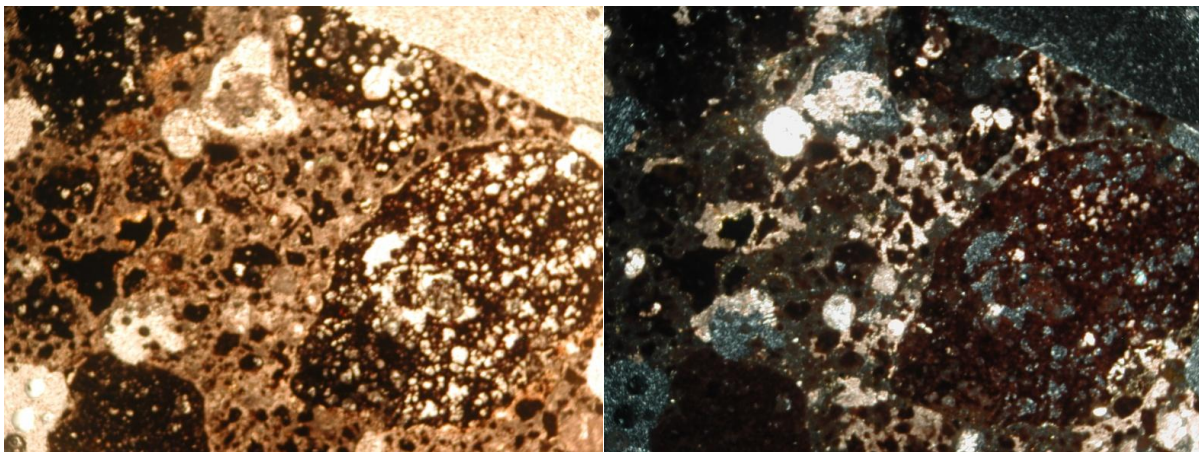


Figure 44 – Microphotographs of sample PVAL1 (crossed nicols- left, and parallel nicols – right; 2.5x). The images show the occurrence of secondary calcite re-crystallization phenomena into the binder matrix; its high birefringence allows to distinguish newly formed crystals from the original ones, concentrated inside pyroclastites voids and binder porosity.

Table 17. RC ages of investigated mortar fragments, with relative errors and calibrations. Calibrated ages show the whole interval without specify different probability distributions, except where specified. Column ‘sample’ indicates *susp* fractions collected with Cryo2SoniC protocol and undergone to dating, with exceptions defined by (L) representing pure lime lumps found inside relative samples and analyzed.

Sample	USM	RC Age	Err RC	Calibrated Age 1σ	Calibrated Age 2σ	Archaeological Reference
PVAL1	292 room2	3005	65	1375 - 1131 BC	1411 - 1053 BC	End of 1 <sup>st</sup> – beginning of 2 <sup>nd</sup> cent.
PVAL16	647 room5	3171	41	1494 - 1415 BC	1523 - 1323 BC	
PVAL21	4008	2306	41	406 - 241 BC	485 - 207 BC	Adrian Period (above 123 AD)
PVAL21 (L)	room1	2015	34	49 BC - 46 AD	109 BC - 68 AD	
PVAL24	NP room3	3453	100	1891 – 1637 BC	2023 – 1522 BC	
PVAL13	654	<b>1670</b>	<b>37</b>	<b>337 - 421 AD</b>	<b>255 - 435 AD</b>	Beginning of 4 <sup>th</sup> cent.
PVAL13 (L)	room5	<b>1787</b>	<b>37</b>	<b>140 – 322 AD</b>	<b>130 – 339 AD</b>	
PVAL14	529	<b>1710</b>	<b>34</b>	<b>259 - 387 AD</b>	<b>250 - 408 AD</b>	
PVAL14 (L)	room5	<b>1758</b>	<b>35</b>	<b>236 – 335 AD</b>	<b>140 – 386 AD</b>	
PVAL15	655 room5	<b>1777</b>	<b>50</b>	<b>140 - 334 AD</b>	<b>129 - 384 AD</b>	
PVAL12	598 room5	<b>1845</b>	<b>49</b>	<b>92 - 234 AD</b>	<b>59 – 322 AD</b>	5 <sup>th</sup> -7 <sup>th</sup> cent.
PVAL3 (L)	37	<b>877</b>	<b>35</b>	<b>1053 -1216 AD</b>	<b>1039 - 1225 AD</b>	12 <sup>th</sup> cent.
PVAL17	632 room5	1644	42	342 -528 AD	261 -537 AD	End of 16 <sup>th</sup> – beginning of 17 <sup>th</sup> cent.
PVAL18		740	52	1225 - 1289 AD	1182 - 1388 AD	
PVAL19		927	54	1039 - 1157 AD	1018 - 1217 AD	
PVAL10		519 room5	<b>445</b>	<b>43</b>	<b>1420 - 1472 AD</b>	
PVAL11	NP room5	1591	39	425 - 533 AD	396 - 556 AD	

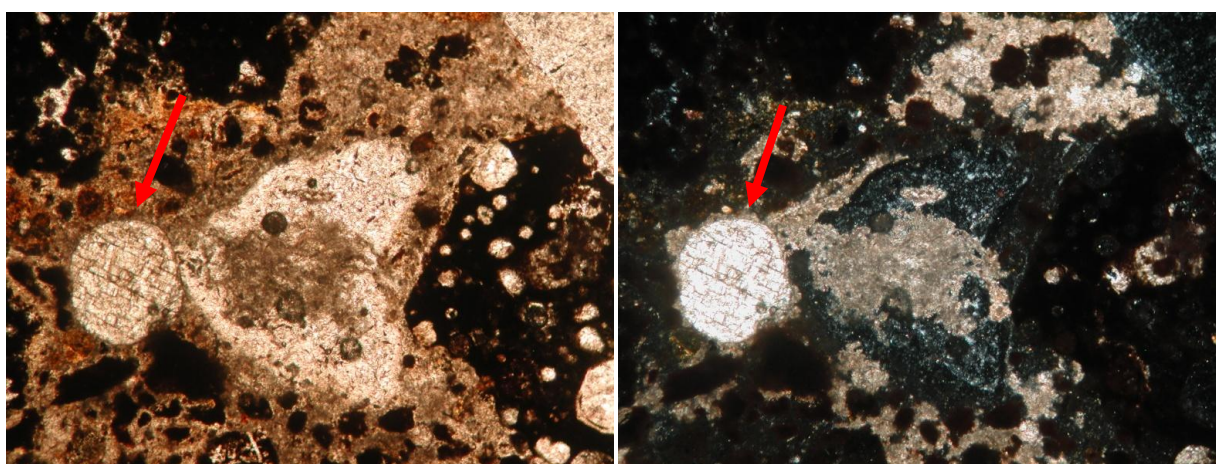


Figure 45 – Microphotographs of sample PVAL1 (parallel nicols -left, crossed nicols- right; 10x). The arrow points to a crystal of secondary calcite grown in a void.

binder and aluminosilicate components of the volcanic ashes, concentrated around pyroclastic fragments. Binder/aggregates ratio is 1:2 for PVAL1 and PVAL16.

Similar results were obtained for PVAL21 and PVAL24 where absolute dating was not compatible with Adrian period hypothesized by the archaeologists. In this case also the samples resulted strongly contaminated by secondary calcite which is the possible carrier of dead carbon (Figure 46; Table 17). Archaeologists also unrevealed the founding of an earthy and muddy substance layer similar to the river silt, emphasized the hypothesis of submerged conditions involving ancient structures analyzed. In this case a flooding caused by an inundation, is an event which happened during the past centuries with a certain frequency, testified by written sources (Bencivenga et al. 1995). Composition and mineralogy of PVAL21 and PVAL24 did not show differences from previous ones, preventing us to attribute these new samples to the constraint Adrian period than to a 1<sup>st</sup> or 2<sup>nd</sup> centuries (Table 18).

Samples from the little barrel vault (PVAL 13, 14 and 15) seem to confirm archaeological expectations which attribute this structure to the first half of 4<sup>th</sup> century (Figure 47, Table 17). Petrographic analyses discovered a mortar similar to the one previously described: a pozzolanic

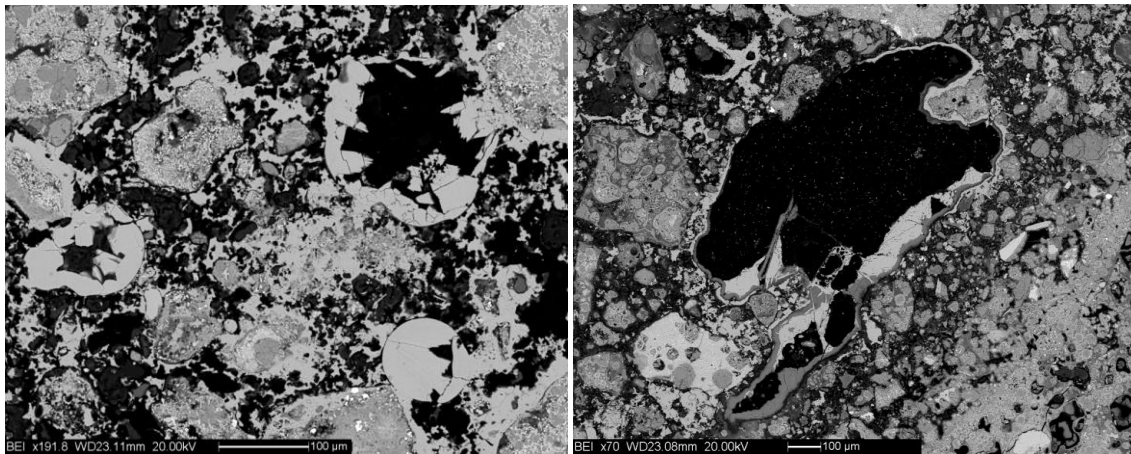


Figure 46. BSE images. Secondary carbonate crystals fill all the porosity and voids in PVAL21 (left) and PVAL 12 (right).

Table 18. XRD results ( +++ prevalent, ++ present, + in trace, ? probably present, - absent).										
Campione	Calcite	Glass	Zeolite	Clinopyroxene	Quartz	Mica	Leucite	Feldspar	Olivina	Anfibole
PVAL12	+++	++	++	++	+	+	++	+	+	-
PVAL17	+++	++	++	++	?	+	++	+	-	-
PVAL18	+++	++	++	++	+	+	++	?	+	+
PVAL19	+++	++	++	++	+	+	+	?	-	++
PVAL21	+++	++	++	++	?	?	+	+	++	+

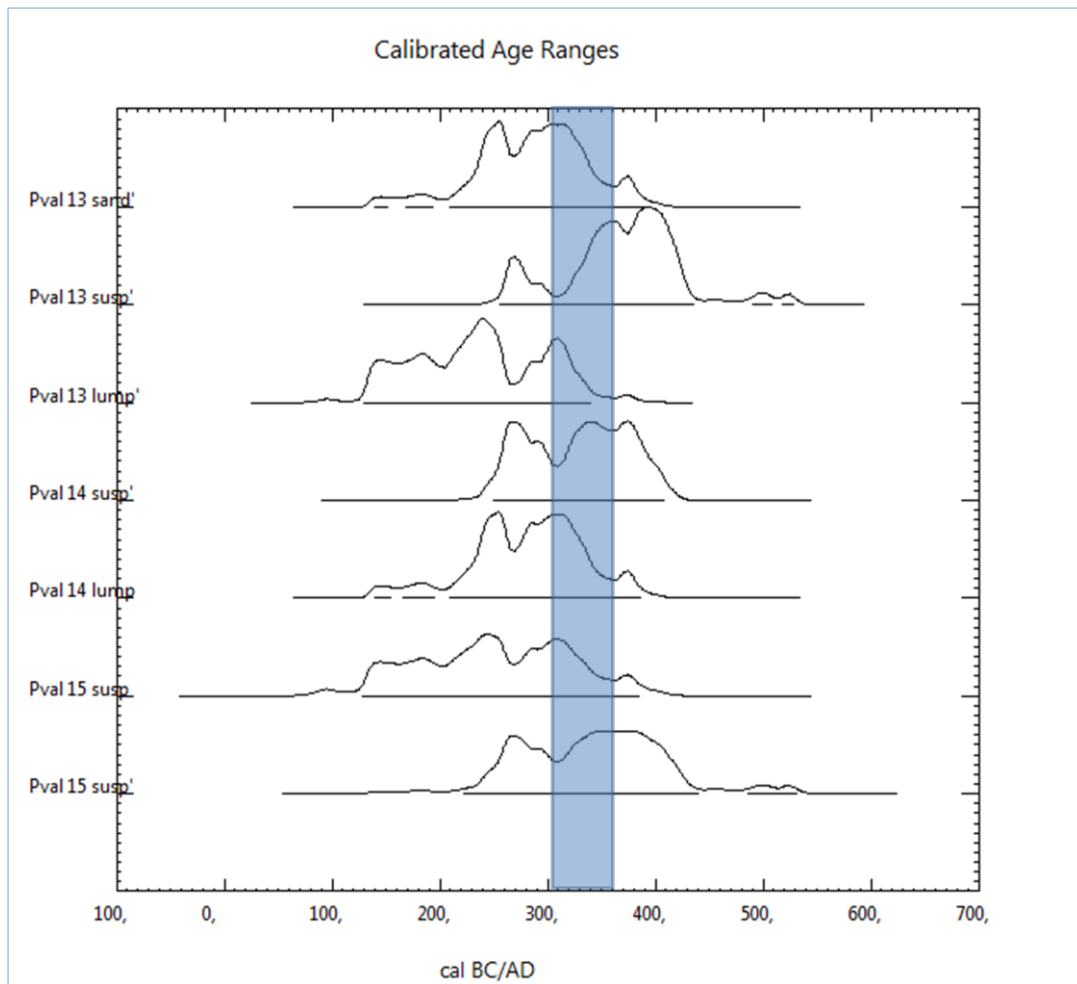


Figure 47. Calibrated ages of PVAL13,14,15 comparing with their archaeological attribution (beginning of 4<sup>th</sup> century).

mortar with black tuffs (PVAL15) or black and yellow tuffs (PVAL14 and 13), with a big vitreous component, abundant leucite (*cart wheel* type), zeolites and orthopyroxenes, discrete quantity of green hornblende and rare biotite (Figure 48). Finding congruent results on analyzed samples coming from two different walls of the same vault represents an important result on the radiocarbon point of view. Limited amounts of secondary calcite crystals have been detected inside voids but their presence did not interfere with RC dating, reporting an agreement between their absolute and relative dating. Upon these consideration with high probability the secondary calcite formation could not be attributed to groundwater or inundation phenomena but maybe to most recent weather activities. PVAL12, belonging to a structure close to this barrel vault, is attributable to 5<sup>th</sup> - 7<sup>th</sup> centuries, but it did not match with archaeological reference resulting older of several centuries. Its aging made it comparable to mortars from the vault, covering the first half of the 4<sup>th</sup> century. Even in this case the massive presence of secondary calcite cannot allow us to understand if the absolute dating age can be affected in terms of accuracy, putting into discussion the archaeological hypothesis (these two structures are close and their relative mortar have similar petrographic

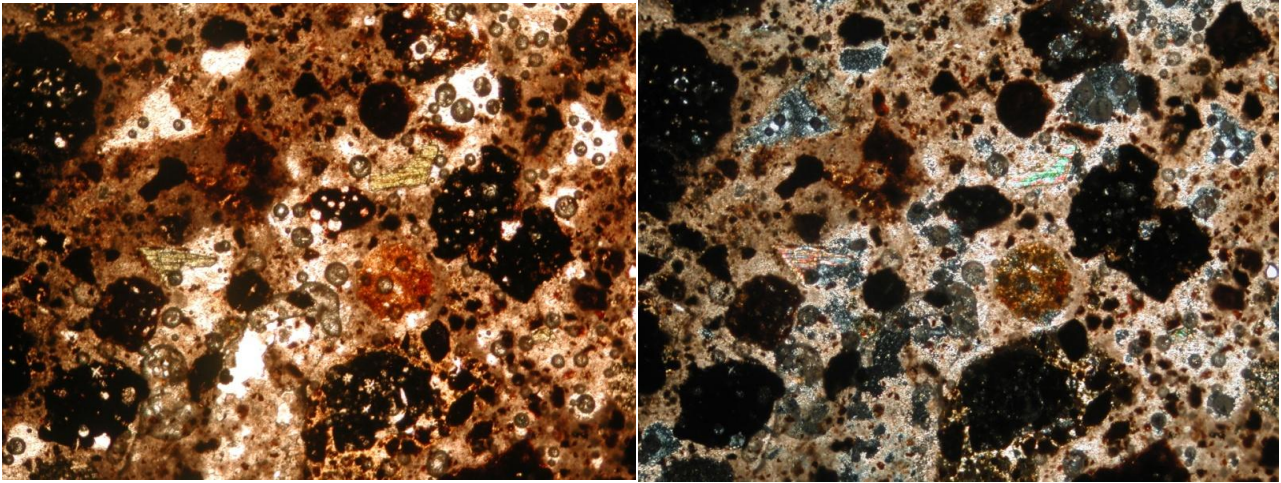


Figure 48. Microphotographs of sample PVAL 14 (parallel nicols - left, crossed nicols – right; 10x). Two kinds of tuffs (yellow and black) and well preserved binder matrix, abundantly filled of hydraulic phases like CSH gels (darkest) are shown. Large crystals of pyroxenes and numerous leucite crystals (cart wheel) are also present.

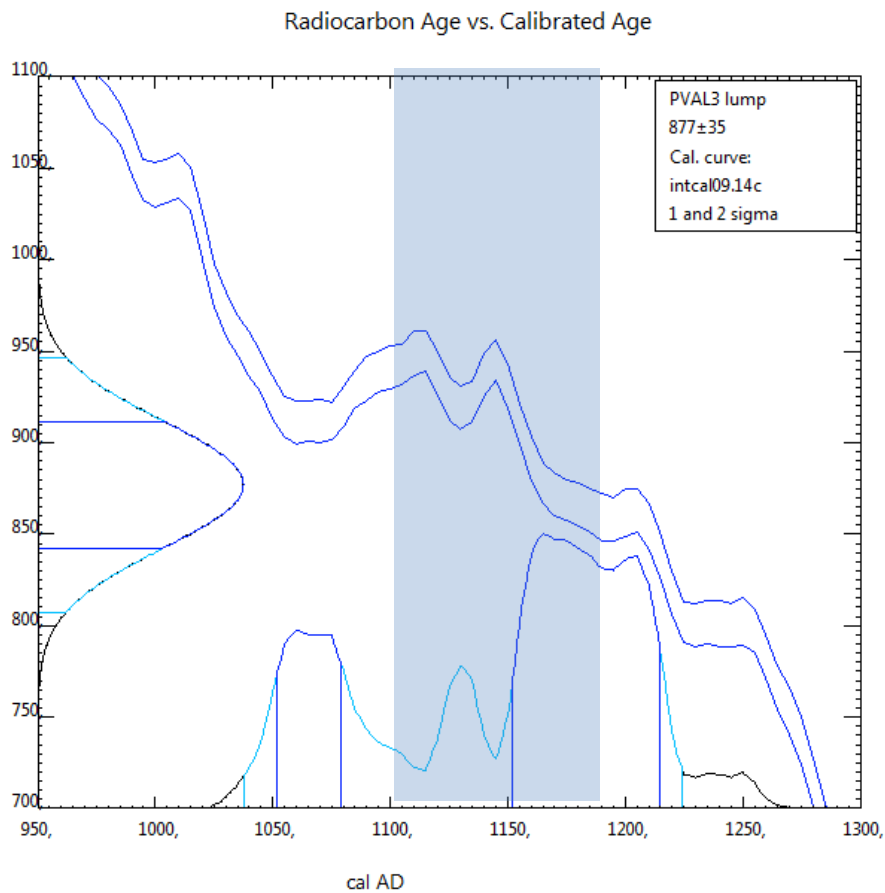
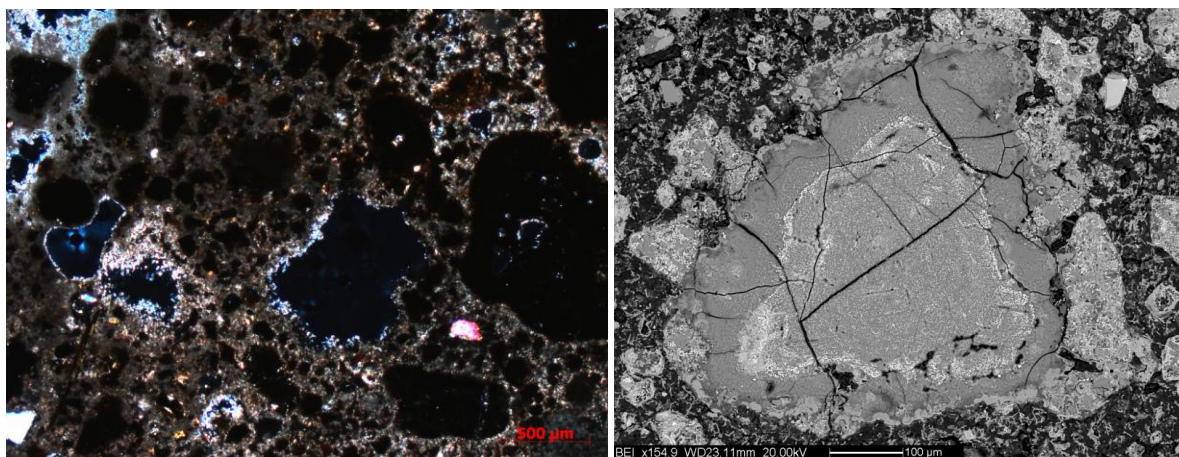


Figure 49. Calibrated age of PVAL3 with its matching archaeological attribution (above the 12<sup>th</sup> century).



features, Table 18), or if gave back a wrong final age due to the fossil influence of DC content from secondary calcite depositions (Figure 46, Table 17).

On PVAL3, a measurement was performed on a lime lump enclashed into the mortar sample. RC age result confirmed the archaeological expectations to the 12<sup>th</sup> century (Figure 49; Table 17) and the absence of inner calcinations relicts (which could contaminate the final result; see section II.3). OM observations showed an overall absence of secondary calcite depositions, clue of the absence of submersion periods during the centuries as it has been seen for many samples of the same site. In this case the observation of an accurate radiocarbon age without any strongly contaminants interference can be quite surely supposed (Figure 49; Table 17). On PVAL 17, 18 and 19 samples, collected from foundations walls of renaissance building, the RC ages did not match the archaeological reference fixed between 16th and 17th centuries. Known Crry2SoniC limits and potentialities (as explained in section II.5), MO observations could explain this bias attributing the aging to the presence of secondary calcite depositions of groundwater origin: its presence was directly proportional to the aging. PVAL18, containing limited amounts of secondary calcite, had a relative low aging comparing to the archaeological reference while PVAL17 and PVAL19, where secondary calcite crystals occluded all voids and partially substituted binder matrix, had a final aging stronger than PVAL18 (Figure 50; Table 17). It could be hypothesized, likely was for many other samples of the same area, that sampling zone was involved in submersion events. Other petrographic features resulted close to the previous, except for a lower B/A ration (Table 18).



*Figure 50. Microphotograph of sample PVAL17 (crossed nicols on left) showing secondary spatic calcite depositions into the voids. BSE image (right) showing hydraulic reaction rims around a tuff fragment.*

Last two samples - PVAL10 and PVAL11 – were expected to give back an absolute chronology what hypothesized with the two samples having the similar ages or a progressive aging never exceeding the beginning of 17<sup>th</sup> century for PVAL10 (upper limit). RC results seem do not seem to confirm this hypothesis implying the two samples of mortar, belonging to the same stratigraphic unit. Final results confirm the attribution of the PVAL10, and consequently of the structure from which it was sampled, to the end of 16<sup>th</sup> and the beginning of 17<sup>th</sup> century, but did not confirm the same age for the underlying PVAL11 (Figure 51, Table 17). Being the latter coming from a big masonry structure directly covering the late roman mosaic and its measured age, older of several centuries than the expected. The almost totally absence of secondary calcite crystals inside voids of PVAL11 made impossible to attribute the aging to this phenomenon, unless it is attested the presence of a different DC source. It is true that the unique possible heavy sources of DC contamination detected inside the studied mortars is the secondary calcite. A possible explanation could be the reuse practice, so diffuse in the past. This eventuality considers this piece of mortar (PVAL11) owing to a bigger fragment of Roman mortar used as an aggregate for the core of new masonry structure, during the Cardinal Bonelli phase. Sampling was partially performed by people differs from operators, as in this case, but an inconvenience like this could be easily avoided taking more care during the sampling phase. Observation in thin sections seems to validate the hypothesis of reuse comparing two mortars and addressing their manufacturing to two different labors. Main evident feature is the distribution of particle dimensions which suggests a granulometric selection on PVAL11, which is apparently absent on PVAL10 (Figure 52).

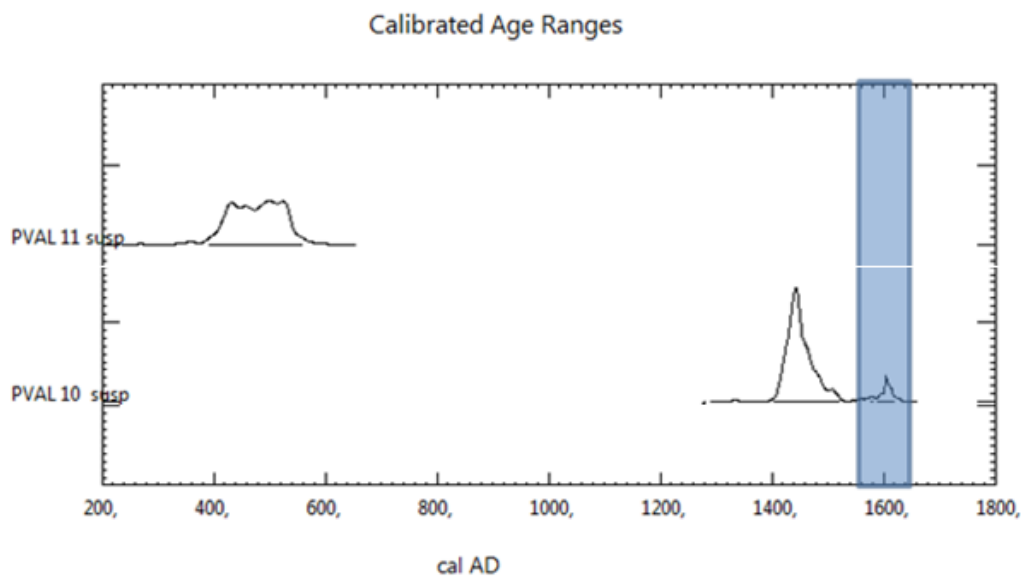
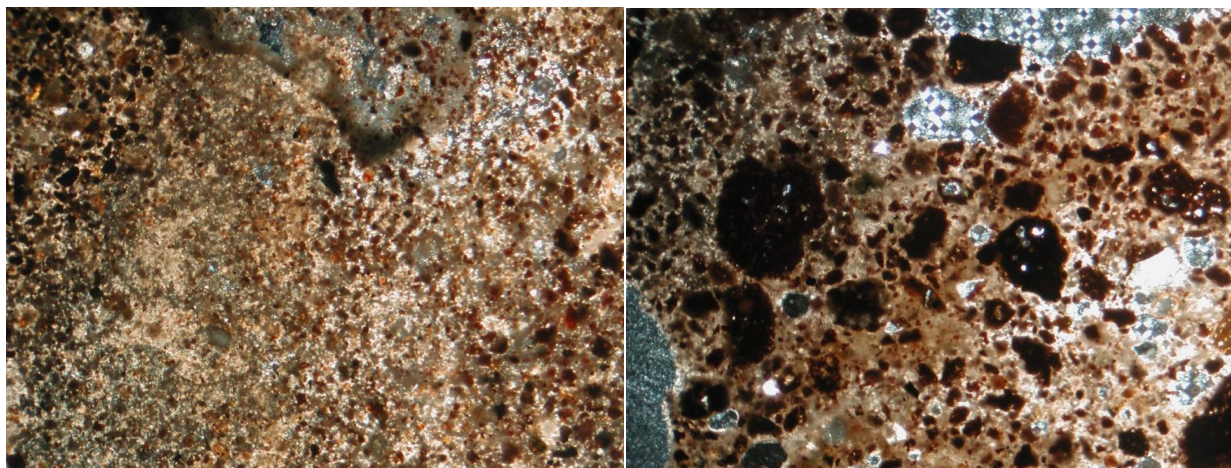


Figure 51. Calibrated ages of PVAL11 and PVAL10 and their archaeological attribution fixed at the construction phase of the Bonelli's palace.



*Figure 52. Microphotographs of samples PVAL11 (left) e PVAL10 (right) (parallel nicols; 10X) showing differences in the sorting of the aggregate. Sample PVAL11 is characterized by a more selected granulometry than sample PVAL10.*

### **Conclusions**

The attempt made to use an absolute dating technique to complete and solve hypothesis done using relative dating and archaeological tools, in this case seem to be useless. Radiocarbon dating on mortars did not allow to easily determine a comparative structure reconstructions on samples coming from the Palazzo Valentini excavations. This incompatibility on results is linked to the presence of a source of dead carbon related to abundant secondary calcite which fills voids and often partially substitutes the binder matrix. The origin of these depositions seems to be linked to the presence of upwelling groundwater phenomena or/and to consequences of attested numerous flooding episodes.

This observation has been useful to better know the history of the archaeological site through the centuries and to consider its submersion tendency to reserve these uncovered and underground structures in the future. Knowing possibility to have a submersion state is an important clue helping the management of an archaeological site. Aging effect did not affect samples picked up from upper structures, where maybe the upwelling groundwater level didn't arrive. This is valid for samples which confirm their archaeological attributions, like mortars sampled from the late Roman barrel vault, the medieval lower portion of a furnace and fragments of 17<sup>th</sup> century floor. Discordant results found on PVAL11 and PVAL12 do not contribute to the final chronological reconstruction but allow the opening of new archaeological questions: i) checking attribution to a 3<sup>th</sup> - 4<sup>th</sup> century instead 5<sup>th</sup> -7<sup>th</sup> century of the circular structures into room 5, placed between two perimetral walls of one *domus* (PVAL12 sampling point); ii) checking the Renaissance structure risen on mosaic into room 5, basements of the 17<sup>th</sup> century floor, by repetition of sampling and RC measure, because the

analyzed one probably owned to a fragment of an older mortar, used as reuse material for the new construction. Archeologists and art historians will have new possibilities of interpretation.

### **III.5. Chronological reconstruction of a Roman Basilica in Canosa di Puglia using the dating on lime lumps.**

Technology applied on mortar investigations will carry us to know about the lime lumps dating resource. Below it will be illustrated some measurements which exploit lime lumps nature to solve situations of unclear chronological attribution as seen into section II.3. The mortars came from the Italian site of Ponte della Lama in the south of Italy and they were analyzed to better know the evolution of the Basilica. Suspended fractions produced from lime lumps encased in mortars will be discussed and compared with dating of charcoals, archaeological references and RC ages of the bulk mortars from which lime lumps were extracted in order to obtain a wide spectrum of answers and to contribute to archaeological questions about constructive phases. The dating procedure performed using lime lumps has been discussed in terms of its accuracy evaluation by the use of CryoSoniC method, focusing on a dating epigraph (481 A.D.).

#### **Archaeological setting and Sampling**

The cemetery complex of Ponte della Lama, displaced nearby of the city of Canosa di Puglia (Apulia, Southern Italy), was discovered at the beginning of the 1950s. The complex developed in a period ranging from 2<sup>nd</sup> to 6<sup>th</sup> century A.D. along the via Traiana and it is composed of different structures. Among them: the catacombs, representing one of the most important examples of funerary sites in the Apulia region for extension and preservation (Nuzzo et al.2008) and the Basilica, founded around the 4<sup>th</sup> century A.D. This artifact plays an important role in the cemetery complex and some questions regarding it are still unsolved. First of all the chronology of the Basilica (such as its development/usage) is not well defined yet. Radiocarbon dating of mortars, combined with petrographic analyses, was applied for the definition of the Basilica chronological development. Ten Wall Stratigraphic Contexts (WSCs) of the Basilica were sampled: CPLM12L, CPLM18L, CPLM34, CPLM42, CPLM48, CPLM55, CPLM56, CPLM62, CPLM63 and CPLM66. Samples belonging to several construction phases spreading over the 2<sup>nd</sup>-5<sup>th</sup> century were analyzed and lime lump selected. An important founding there was during excavations: is a Roman epigraph, discovered in the catacombs side and belonging to the same archaeological context. It has an inscription engraved upon fresh mortar applied during the grave sealing and thanks to this inscription “*Sine collega Flavius Rufius Placidus*” it was possible to attribute the epigraph to 481 A.D.

## Method

Every lime lump was selected and manually cleaned, until obtaining a pure material free of any extraneous matter. Each lime lumps was divided into two sub units. One unit (minimum 30 mg) underwent to the CryoSonic protocol of selection as described into section II.3 and Marzaioli et al. 2013, obtaining a *susp\_lump* fraction from each sample. The second unit of each powdered lime lump was used to be dated as the same (minimum 10 mg) and renamed with *lump* suffix. All fractions underwent to acid dissolution, graphitization and AMS measure to obtain radiocarbon data as described in Marzaioli et al. 2013.

From CPLM 66 and CPLM 63 samples were obtained very few mg of lime lumps, which were preserved to apply exclusively the CryoSonic protocol. Inside CPLM18L mortar an encased charcoal was found, it underwent to sample processing and measurement according to Berger (1992). Charcoal result will be compared with radiocarbon ages of inorganic material. With the aim of the evaluation of the procedure accuracy, one lime lump (*CPLM1\_lump*), its CryoSonic produced fraction was analyzed.

## Results and Discussion

Petrographic observations of the mortars highlighted that Basilica lime mortars contain two possible dangerous sources of dead carbon which could interfered in finding the right date: (i) calcination relics of an unburned biomicritic limestone; (ii) sandy carbonate aggregates (a sensitive fraction of total aggregates) whose size vary from medium to fine (Marzaioli et al. 2013). This is why the direct measurement of the bulk mortar was avoided and was chosen to use preferentially lime lumps, as a simplify system. Contamination deriving from calcinations relics in a lime lump is easier to suppress than ones from very fine biomicritic aggregates in a bulk mortar. Given these considerations, a different way to operate was chosen using lime lumps as raw material. Several studies applied RC dating on the bulk lime lumps with changeable results (as seen in section II.3) depending on pureness of the selected lump. Here it was chosen to apply the most common typology of analysis (the dating of the bulk) backed up with an innovative one (the dating of material collected after CryoSonic). It was performed a double check on same lime lumps, in order to evaluate the accuracy of two methods: the measure of a lime lump as a whole (Pesce et al. 2009, 2012; Pesca and Ball 2012) or as a selected fraction of it (Marzaioli et al. 2013).

Accuracy evaluation on lime lumps dating was performed comparing RC ages of a lime lump (CPLM1) extracted from the epigraph with its archaeological attribution referred to 481 A.D. Observed results on CPLCM1, measured as the bulk of lime lump, indicate a consistent DC effect

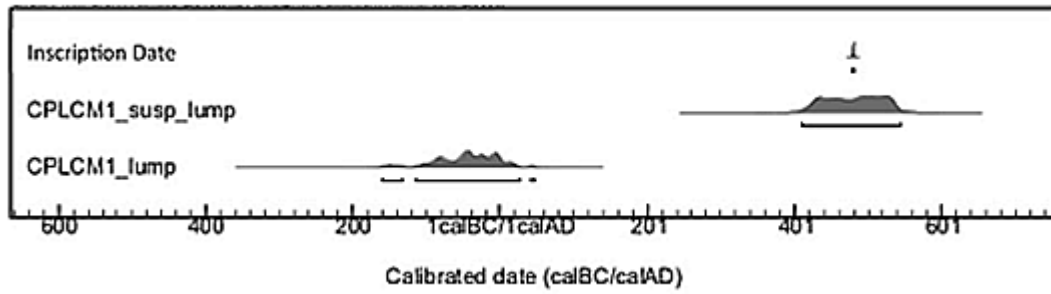


Figure 53. Measured calendar ages for each sample, showing both lump (CPLCM1\_lump), susp\_lump (CPLCM1\_susp\_lump) and the age of the funerary epigraph (Marzaioli et al.2013).

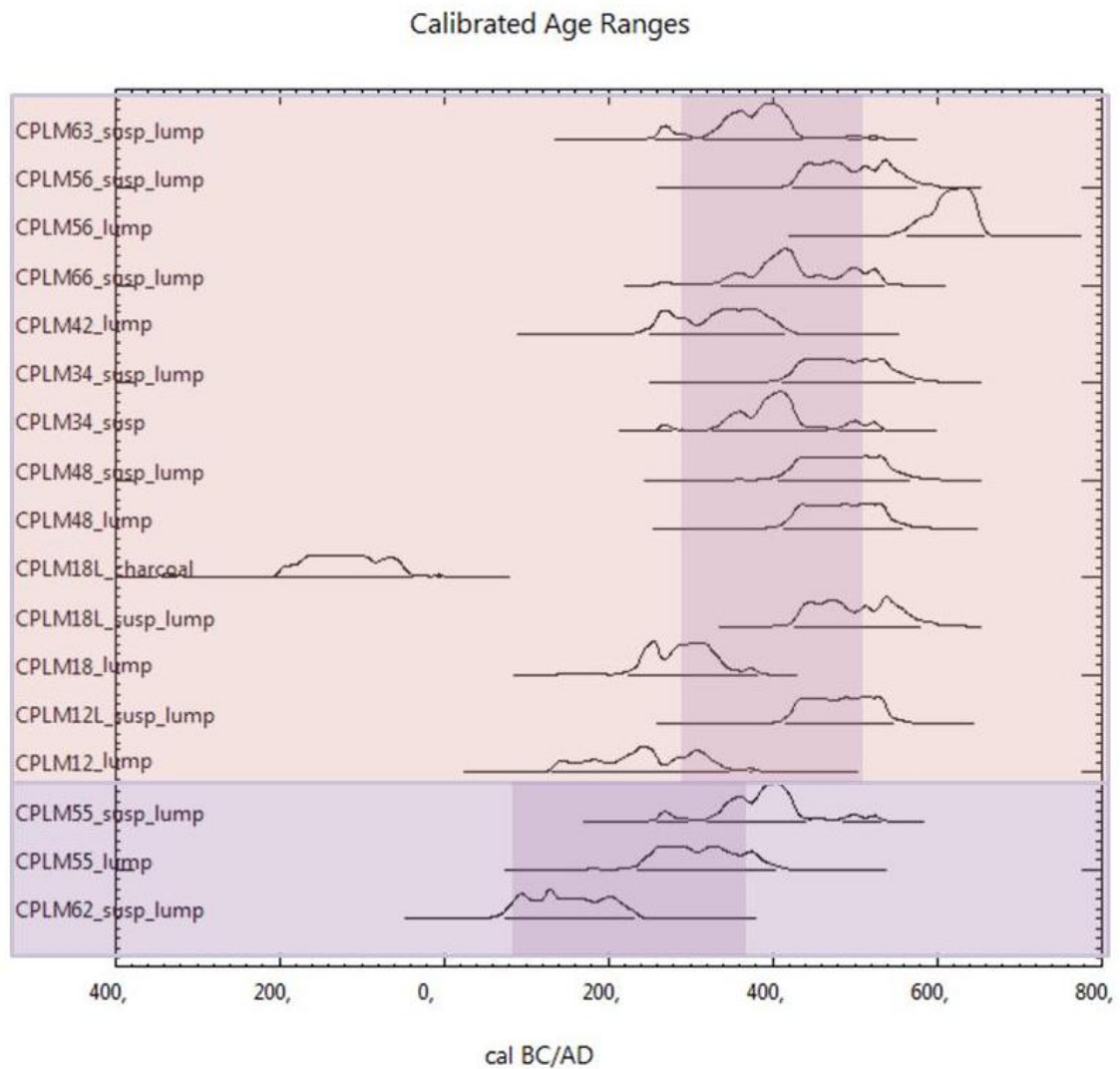


Figure 54. Schematic representation of calibrated ages for analyzed samples. Two different colors divide set of samples owing to Roman Basilica (pink) vs samples attributed to a pre-existent building (blue). Violet underling represents the time interval used as archaeological reference.

Table 19: Samples analyzed are shown with relative Stratigraphic Units (USM), Radiocarbon ages (RC age; years BP), relative Errors (Err RC) and Calibrated Dates according to 1 $\sigma$  and 2 $\sigma$ . Each sample is marked with a suffix which indicates its typology: L lump; SL susp lump; C charcoal.

Sample	USM	RC Age	Err RC	Calibrated Age 1 $\sigma$	Calibrated Age 2 $\sigma$	Archaeological Hypotesis
CPLCM1 L	Epigraph	2038	28	90 BC - 3 AD	161 BC - 47 AD	481 d.C.
CPLCM1 SL		1586	30	<b>428 - 533 AD</b>	<b>413 - 544 AD</b>	
CPLCM1 C		9760	60	9292 - 9206 BC	9324 - 8923 BC	
CPLM62 L	3037	2776	34	803 - 673 BC	812 - 555 BC	Pre-existant structure I ?
CPLM62 SL		1865	32	<b>86 - 212 AD</b>	<b>75 - 231 AD</b>	
CPLM55 L	3046	1729	36	254 - 377 AD	236 - 403 AD	Pre-existant structure II ?
CPLM55 SL		1657	33	<b>346 - 425 AD</b>	<b>259 - 531 AD</b>	
CPLM12L L	3039	1780	38	220-322 AD	131-348 AD	Roman Basilica 4 <sup>th</sup> - 6 <sup>th</sup> century
CPLM12L SL		1579	29	<b>426-539 AD</b>	<b>412-556 AD</b>	
CPLM18L L		1753	26	242-332 AD	227-380 AD	
CPLM18L SL		1548	31	<b>435-557 AD</b>	<b>424-595 AD</b>	
CPLM18L C		2100	36	178-51 BC	341-39 BC	
CPLM48 L	3040	1577	34	433 - 535 AD	409 - 566 AD	
CPLM48 SL		1576	38	<b>433 - 535 AD</b>	<b>409 - 566 AD</b>	
CPLM34 L		1648	33	345 - 431 AD	263 - 533 AD	
CPLM34 SL		1568	38	<b>434 - 538 AD</b>	<b>413 - 572 AD</b>	
CPLM42 L	3044	1702	36	260 - 395 AD	252 - 414 AD	
CPLM42 SL		1635	35	<b>358 - 530 AD</b>	<b>339 - 536 AD</b>	
CPLM66 SL	3038	1556	32	<b>434 - 545 AD</b>	<b>423 - 572 AD</b>	
CPLM56 L		1435	35	601 - 648 AD	564 - 658 AD	
CPLM56 SL		1553	32	<b>434 - 548 AD</b>	<b>424 - 576 AD</b>	
CPLM63 SL	3037	1666	33	<b>345 -418 AD</b>	<b>258 -525 AD</b>	

affecting the radiocarbon age estimation (*CPLCM 1\_lump*; Table 19 and Figure 53). *CPLCM 1\_lump*, results compatible with the 1<sup>st</sup> century B.C. so far from the attended age fixed at end of 5<sup>th</sup> century. The reason of this observed discrepancy can be exclusively attributed to the presence of calcination relics inside lime lumps which was evidently not composed only by binder. This



experimental observation lead us to apply the CryoSonic procedure (section II.1 and II.3) to lime lumps too. It can be noted in Table 19 how the application of CryoSonic efficiently removed the effect of calcination relics on measured radiocarbon ages, leading to unbiased age for the epigraph sample (*CPLCM1\_susp\_lump*; Figure 53). A similar effect (i.e. smaller but significant DC contamination) was observed for the other analyzed lime lumps (*CPLM12L\_lump*, *CPLM18L\_lump*, *CPLM34\_lump*, *CPLM42\_lump*, *CPLM55\_lump*, *CPLM62\_lump*, *CPLM63\_lump* and *CPLM66\_lump*) compared to their relative *susp\_lump* fractions (*CPLM12L\_susp\_lump*, *CPLM18L\_susp\_lump*, *CPLM34\_susp\_lump*, *CPLM42\_susp\_lump*, *CPLM55\_susp\_lump*, *CPLM62\_susp\_lump*, *CPLM63\_susp\_lump* and *CPLM66\_susp\_lump*) (Figure 54). In this case, as before, the application of the CryoSonic procedure has produced *susp\_lump* fractions free of aging effects and whose <sup>4</sup>C ages are coherent each other and in agreement with the archeological hypothesis made about the Basilica (4<sup>th</sup>-5<sup>th</sup> century A.D). On Basilica samples, the lime lumps dating observes a DC effect shifted virtually to zero, placing the dating in the range of 5<sup>th</sup> to 6<sup>th</sup> century, in accord to the archaeological hypothesis of a usage until 7<sup>th</sup> century AD. It is interesting to note that samples coming from same USM showed coherent dates such as: CPLM 12 and 18 samples of USM 3039 (boundary of the apsis) and CPLM 34 and 48 samples from USM 3040 (south side; Figure 55). In particular is important to know that these latter samples, belonging to the internal (CPLM 48) and external (CPLM 34) façade of the same wall, gave identical results and consequently identical ages. Another interesting case is about two samples having consistently different RC ages results. They were a couple of samples from two stratigraphic units linked each other: a structure made of big *isodomi* stones (CPLM62 from USM 3037) and its closer wall (CPLM55 from USM 3046). This whole structure was already presumed to precede the building of the Roman Basilica. Samples relative to the up-mentioned Wall Stratigraphic contexts are *CPLM62\_susp\_lump* and *CPLM55\_susp\_lump*, whose RC dates resulted older than the others found for the Basilica. This aging is compatible with archaeological suppositions, attributing the original structures to earlier period. This discovery allowed to confirm hypothesis about a preceding building and to assign to it a well constraint chronology. The proposed one is arranged between the end of the 1<sup>st</sup> and the 4<sup>th</sup> century. The presence of an earlier building makes possible to advance another question taking into account that 4<sup>th</sup> century represents an upper limit to not exceeded (the birth of the Basilica) and verifying that these two last USM have two different masonry structures, could it be possible to assign sample CPLM55 to the most ancient phase of building? The RC ages suggest that CPLM62 sample owns to the pre-existent structure made with big squared stone blocks (*isodomi*), older than CPLM55 sample owns to a wall made of smaller stone blocks, which could represent or i) a second phase of this pre-existent structure or ii) the oldest testimony of the first basilica walls attested to the

4<sup>th</sup> century. During the following centuries enlargements works were applied to the Basilica as suggested by dating campaign performed on several and widespread sampling points, which highlighted an executive succession from 4<sup>th</sup> to 5<sup>th</sup>-6<sup>th</sup> centuries. An explicative example could be the construction sequence found on a northern wall and involving some closer USM (Figure 56). It shows the coexistence of three construction phases: the first, represented by CPLM62 sample (from USM 3037) holds to a pre-existent construction made of big squared blocks of stones ( $1865 \pm 32$  RC age); the second, represented by CPLM63 sample (from the same USM 3037) but a different

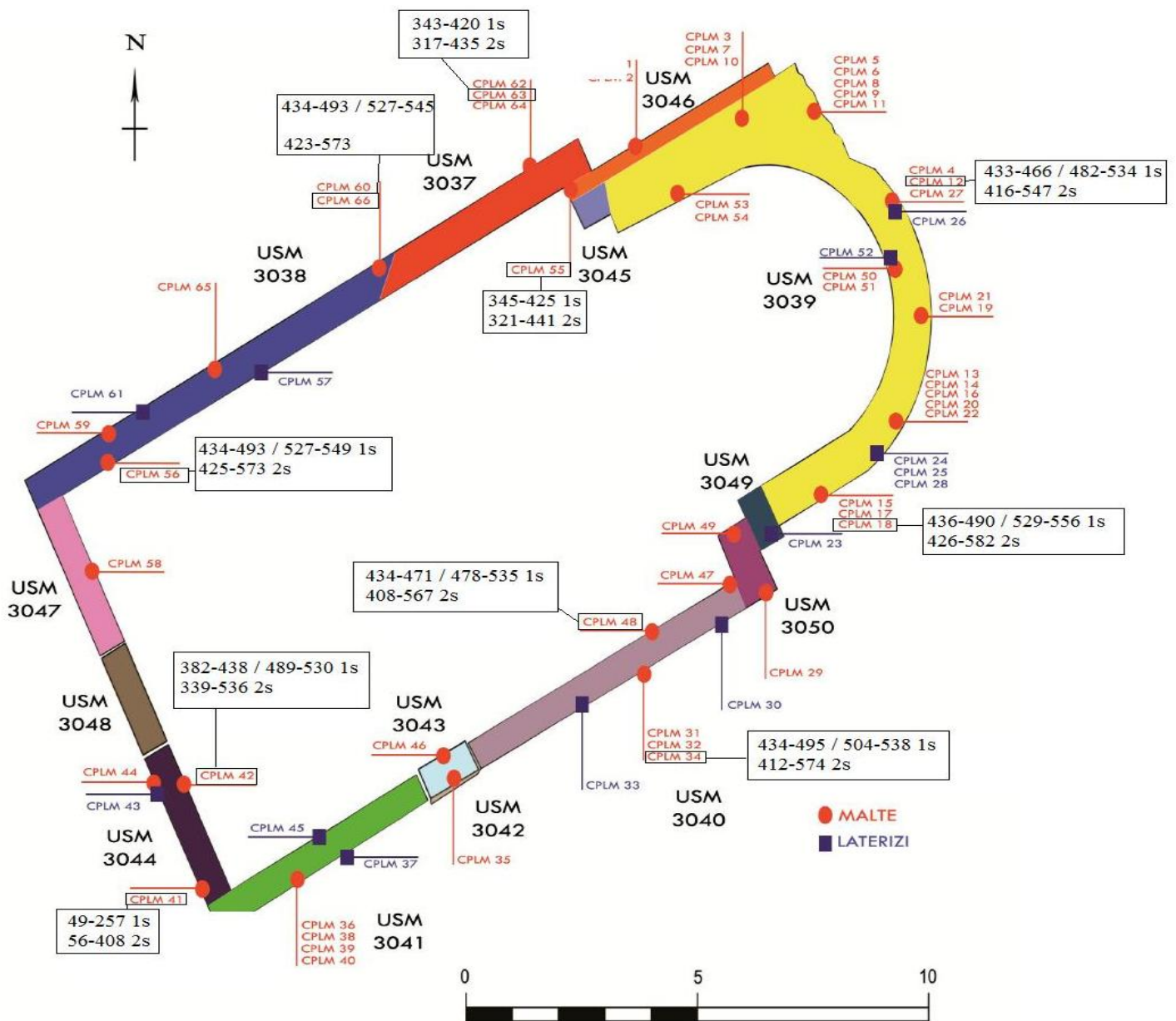


Figure 55: Schematic representation of Roman Basilica of Ponte della Lama, showing stratigraphic units, sampling points and RC ages of susp\_lump fractions.

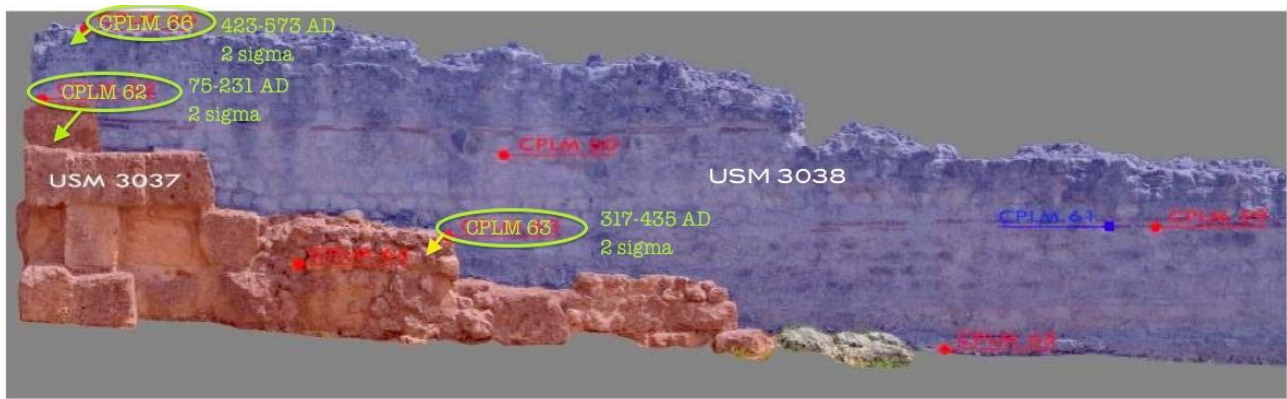


Figure 56. Image of the northern wall of Basilica, where three different construction phases coexist, recognizable from differentiating construction styles and dated back to three different chronological intervals (image modified from Ruggiero 2010).

sampling point building using a different technique ( $1666 \pm 33$  RC age); the third, CPLM66 sample from USM 3038, composed by alternated *tufelli* and bricks ( $1556 \pm 32$  RC age). Observing their progressive ages (Table 19), it is clear these three wall structures are interconnected themselves and their chronological progression explains the different aspects and building techniques used for that wall. It represents a valid example of the evolution of Basilica building from earlier to latest phases.

Difference in the DC contamination affecting the lime lumps analyzed ‘as the same’, helped us to know something more about technology used during mortar production. The epigraph, in fact, represented by *CPLCM1\_lump* appeared sensitively older than others samples picked up from basilica walls. According to the evidence that epigraph mortar manufacture appeared coarser than the ones collected from Basilica walls, it can be deduced that a grosser manufacturing process probably led to higher amounts of calcinations relics in the examined mortar, responsible for the aging. About dating of charcoal intrusions in the mortar matrix, it has revealed a strong DC contamination, evidenced by corresponding calendar ages of 10<sup>th</sup> century BC and 1<sup>st</sup> century BC respectively for charcoals extracted from CPLCM1 and CPLM 18L samples. This observation can be assigned to a lack of carbonate suppression during the coal pretreatment also if ad hoc methodologies (Berger 1992) were applied. Lacks of further material avoided the measure repetition on charcoal.

## Conclusions

Obtained data revealed how the dating of an archaeological site can be easily led to a successful chronological reconstruction if pretreated lime lumps are used to satisfy dating aims. It has been seen how the final dating of this class of materials, if measured as the same and not pretreated, can be affected by significant offsets due to the presence of calcinations relics. Even more so that the

presence of calcinations relicts could be attested only by an accurate observation most of the time by the use of microscope on a thin section. This means that presence or not presence of calcinations relicts has decided after a statistical estimation made on a representative sample and that dating has performed on samples different from the one analyzed, so there are no guarantee of absence of calcinations relicts on them. This uncertainty on the pureness of a lime lump is the main reason to choose a selective pretreatment method like as CryoSoniC rather than measure the bulk of a lime lump as it is. The presence of calcinations relicts inside lime lumps, otherwise, is strictly connected to the technology applied during mortar production so, a mortar whose lime lumps are composed by not completely calcinated lime often is an evidence of a lack of attention during the calcination process. This feature has been observed on 8 upon 11 of the analyzed lumps of the archaeological site of Ponte della Lama, showing evident differences between RC ages of lime lumps measured as the same and the others measured after pretreatment with CryoSoniC. Differences between experimental RC ages in this case have been useful to confirm differences linked to ancient production technologies used to build different parts of the same building. An example is the quality of the binder holding to epigraph, worst than the one of the basilica walls; although they are linked to the same historical period, the epigraph is much more full of calcinations relicts.

CryoSoniC protocol applied on lime lumps helped also to solve doubts about a contemporary presence of different masonry layers into the same wall section, attributing a different age to each layer, reconstructing a chronological sequence and coupling to each building style its chronological framework.

The CryoSoniC pre-treating protocol allows to efficiently remove DC contamination from lime lumps into produced fractions (*susp\_lump*) to date, obtaining a successful dating of different Basilica structures and to reconstruct its building construction sequence (Figure 55). The born of the Roman Basilica was confirmed being between 4<sup>th</sup> - 5<sup>th</sup> centuries on the remains of a pre-existent building. Two possible phases could be distinguished upon this earlier structure by the use of RC technique applied on pretreated lime lumps: the first, from the end of the 1<sup>st</sup> to the beginning of the 3<sup>th</sup> century and the second, from 4<sup>th</sup> to 5<sup>th</sup> century. Application of CryoSoniC protocol to lime lumps has been verified to be a good tool and an alternative resource, to date mortars strongly affected by a potential DC contamination, such as a very fine fraction of carbonatic aggregates (i.e. biomicritic sand).

### **Acknowledgements**

A special thanks to Giacomo Eramo and his equipe, from University of Bari “Aldo Moro”, who performed petrographic investigations and gave us the possibility to analyze these samples.

## VI. General Resume

Buildings can tell you a lots of things, if you allow them to do that. Learning to listen and interpret the several cases of study, has been an useful activity during this experience to find the right way to collect chronological information about them. The way to obtain a successful dating is questioning directly the raw materials, studying their surrounding environment and the history of that archaeological site. To get an absolute dating from an object with an age often difficult to interpret like a wall or a masonry structure, the support of a previous archaeological, historical and petrographic research is needed. The more information are gathered, the more available elements to have a good overview and to reconstruct a chronological path will be. The identification and attribution made by relative dating methods, for example, are important resources to start and aspiring to obtain a more accurate dating, such as an absolute one.

As a final balance about this research it can be affirmed that the use of Cryo2SoniC as separation method, has shown a wide and satisfactory level of applicability, reaching a good degree of dating reliability. Radiocarbon dating of mortar performed on fractions collected with Cryo2SoniC technique, allows to claim that this new separation protocol could be suggested as a novel tool to support archaeological researchers when it's necessary to solve doubts about the chronology of a specific structure if examined age gaps varies over ranges comparable to methodology sensitivity. Of course some issues should taken into account before starting a series of expensive radiocarbon measurements. First of all it is of primary importance to make an accurate selection of samples to be analysed considering not only its archaeological representativeness but also the occurrence of some fundamental attributes to avoid, which could invalidate the final RC result. There are some general behaviour to consider, whatever protocol is used, that should be avoided:

- (a) Sampling of sections of wall so much deeper than the original surface (i.e. the inner part of a probing). Deeper mortar harden more slowly than superficial ones. This could lead to a likely rejuvenation phenomena on RC dating, from few to hundred years.
- (b) Sampling on restored surfaces, where rejuvenation effect on final RC dating will show the restoring moment and not the original one. The same will be for remakes done during building life.
- (c) Sampling surfaces directly exposed to weather action. It should be preferred the sampling of an immediately closer inner layer to the superficial one. The outdoor surfaces of mortar could show a rejuvenation effect on final RC age due to secondary calcite and generally

have a more ruined binder inner structure than the inner layers (with less availability of pure binder).

- (d) Sampling on layers directly exposed to flowing waters, groundwaters or involved in flooding episodes. It is recommended to get information about the presence of floods or groundwater risings at interested areas, in order to avoid bias in RC dating. Meteoric water will rejuvenate while groundwater will age final mortar dating.

Before starting a dating campaign, performing a petrographic characterization of mortars to date it is essential. This should represent the first step of our dating process. Based on observed results future strategies to adopt will be decided. As far as the possibility to obtain a successful RC dating result, the use of Cryo2SoniC protocol should follow some measurements which take into account its qualities and limits. Summarizing:

- (a) A mortar with a sandy aggregate (i.e. quartz, feldspar made of etc.) will be generally successfully dated using Cryo2SoniC pre-treatment.
- (b) A mortar with a pozzolanic aggregate will be generally successfully dated using Cryo2SoniC pre-treatment, with exception of those which could own some calcareous lumps very similar to lime lumps that will bias final RC ages with aging. These lumps, derived from the passage of lava flows through calcareous layers attend under the earth crust, could be easily detected by a CL analysis and discriminated from real lime lumps (anthropogenic origin). It's recommended to perform a selection of all what resembles a lime lump inside a sample of pozzolanic mortar and to start a CL characterization of all them. If some geologic lumps are found in it the sample to date will be inspected and all visible particles of false/true lime lumps should be removed before starting Cryo2SoniC pre-treatment. In this way bias will be avoided. To balance low availability of  $\text{CaCO}_3$ , in pozzolanic mortars (whose binder is full of hydraulic components), it is recommended to collect a larger amount of material during sampling in order to have a bigger quantity of final suspension and consequently a bigger availability of C to date. If CL analysis proof that selected lumps are lime lumps, they could be measured together with the mortar bulk, pre-treating them separately.
- (c) A mortar with a calcareous aggregate will be dated using Cryo2SoniC pre-treatment only if:

- I. Size of aggregate grain will be coarse and hard. Hardness is a fundamental feature to avoid the grains breakage during protocol steps.
  - II. If pure lime lumps are found inside binder, dating will be performed on them (see point (d)).
- (d) A mortar with a calcareous aggregate will be not dated using Cryo2SoniC pre-treatment when it is made of fine size grains (i.e. foraminifera, biomicritic sand or silt) which size is similar to the one of binder particles. In this the case selection protocol will not be able to discriminate good fraction representative of setting moment from one contaminated by the presence of calcareous grains of geologic origin. The only way to obtain an accurate and precise dating of this type of mortar is to check the presence of lime lumps enchased into the binder and perform dating on them:
- III. As it is, entirely without any treatment. Only if CL analyses has given a positive feedback which ensure its powder by the presence of calcinations relics. Only a restrict portion of sampled lie lumps could be used.
  - IV. After CryoSoniC pre-treatment. Always, on the whole of sampled lime lumps without any restrictions. It is recommended when there is no possibility to check a CL analyses on lime lumps powder. This is the recommended protocol which allow to avoid any aging by calcinations relics.

A perfect cleanliness of lime lump surface before applying any protocol, CL analyses or dating measure, should be ensured.

- (e) Any mortar could be dated by application of CryoSoniC protocol on lime lumps, in order to obtain a successful dating representative of the moment of its setting. Pay attention to check lime lumps according to what said in b and d points.

As a final suggestion it is recommended to always check a susp collected after Cry2SoniC protocol by a CL analysis; although CL is a difficult technique to be interpreted, it could be used to preserve any research by an unsuccessful dating without a waste of time and money.

A great and long work finding the best way to obtain a chance to date a mortar has given back a selective protocol, the Cryo2SoniC, able to answer to the most common archaeological questions about a chronological interpretation. From pointing out the protocol phases to the application on real cases of study, this route needed to compare, one by one, all strengths and weaknesses linked to

the Cryo2SoniC method, placing it inside one of the most useful tool in archaeological environments where the only evidence could be constitute by a wall remain or where it could be necessary to have confirmations about a specific chronology. Demonstrating to be a reliable method to pre-treat samples to date with radiocarbon procedure and knowing its limits/potentialities, it can be affirmed that the Cryo2SoniC protocol is a reliable and easy way to date a mortar.



## V. References

- Angela P. 2008. Indagini Archeologiche al Palazzo Valentini. In *Palazzo Valentini. Tra l'antichità ed età moderna: scoperte archeologiche e progetti di valorizzazione*. Provincia di Roma.
- Al-Bashaireh K. 2013. Plaster and mortar radiocarbon dating of Nabatean and Islamic structure, South Jordan. *Archaeometry* 55 (2): 329-354.
- Ambers J. 1987. Stable carbon isotope ratios and their relevance to the determination of accurate radiocarbon dates for lime mortars. *Journal of Archaeological Sciences* 14(6):569-76.
- Angela P. 2008. Indagini Archeologiche al Palazzo Valentini. In *Palazzo Valentini. Tra l'antichità ed età moderna: scoperte archeologiche e progetti di valorizzazione*. Provincia di Roma
- Arbeiter A, Pfüffgen B, Karas U. 1994. Die vor-und fruhromanische Kirche Santos Julian y Basilisa de Aistra bei Zalduondo (Álava). *Madridrer Mitteilungen* 35: 418-439.
- Aurelius Victor. 1994. *De Caesaribus*. Liverpool University Press.
- Artioli G. 2010. Structural Materials II. Cements, mortars and other binders. *Scientific methods and cultural heritage*, Oxford University Press: 242 – 250.
- Azkarate Garai-Olaun A.1988. Arqueología cristiana de la antigüedad tardía en Alava, Guipúzcoa y Vizcaya, Vitoria-Gasteiz.
- Azkarate Garai-Olaun A., Sánchez Zufiaurre L. 2003. Las iglesias prefeudales en Alava: Cronotipología y articulación espacial. *Arqueología de la Arquitectura* 2:25-36.
- Bakolas A, Biscontin G, Moropoulou A, Zendri E. 1995. Characterization of the lumps in the mortars of historic masonry. *Thermochimica Acta* 269/270:809-816.
- Baldassarri P. 2008. Indagini Archeologiche al Palazzo Valentini. In *Palazzo Valentini. Tra l'antichità ed età moderna: scoperte archeologiche e progetti di valorizzazione*. Provincia di Roma.
- Barbera M, Di Pasquale S, Palazzo P. 2007. Roma, studi e indagini sul cd. Tempio di Minerva Medica. *FOLD&R FastiOnLine documents & research* (91): 1-21.
- Baxter MS, Walton A. 1970. Radiocarbon dating of mortars. *Nature* 225(5236):937-8.
- Begin ZB, 1974. *The geological map of Israel* 1:50,000. Sheet 9-III: Jericho. Geological Survey of Israel Mapping Division. Jerusalem.
- Bencivenga M, Di Loreto E, Liperi L. 1995. Idrologia. In Funucielli R. La Geologia di Roma. Il centro storico. *Memorie descrittive della carta geologica d'Italia*. Volume L. Istituto Poligrafico dello Stato: 123-171.
- Beniash E, Aizenberg J, Addadi L, Weiner S. 1997. Amorphous calcium carbonate transforms into calcite during sea-urchin larval spicule growth. *Proceedings Royal Society London Series B* 264: 461 - 465.
- Bensted J. 1997. *Inaugural Lectures Series, University of Greenwich. Cement: past, present and future*. Dartford Greenwich University press, 1997.
- Bensted J, Coleman NJ. 2004. La sorprendente storia del cemento e del calcestruzzo dalle origini dell'età della pietra al 1900 d.C.. *L'industria italiana del cemento* 801, Ed. Gangemi Roma, 2004.

- Berger R. 1992.  $^{14}\text{C}$  dating mortar in Ireland. *Radiocarbon* 34(3):880–9.
- Biasci A. 2000. Il padiglione del "Tempio di Minerva Medica" a Roma: struttura, tecniche di costruzione e particolari inediti. *Science and Technology for Cultural Heritage* 9 (1-2):67-68.
- Bowersock G, Green P, Grabar O. 1999. *Late Antiquity: A Guide to the Postclassical World*, Harvard University Press: 674.
- Bronk Ramsey C. 2005. *OxCal v.3.10*. <http://www.rlaha.ox.ac.uk/orau/calibration.html>
- Bronk Ramsey C. 2009. Bayesian analysis of radiocarbon dates. *Radiocarbon* 51(1): 337–360.
- Bronk Ramsey C. 2010. WEB site: <<http://c14.arch.ox.ac.uk/embed.php?File=oxcal.html>>. Accessed date 20th of August 2012.
- Bruni S, Cariati F, Fermo P, Cairati P, Alessandrini G, Toniolo L. 1997. White limps in fifth to seventeenth century AD mortars from northern Italy. *Archeometry* 39(1): 1–7.
- Bugini R, Toniolo L. 1990. La presenza di grumi bianchi nelle malte antiche. *Arkos* 12:4-8.
- Bus'ko C. 2006. Wstępne wyniki badań archeologiczno-architektonicznych prowadzonych na Rynku Głównym w Krakowie w 2005–2006 roku. *Wiadomości konserwatorskie* 19:67–70
- Callebaut K, Van Balen. 2000. Maintenance and restrengthening of materials and structures: Plaster. *Proceedings of the International workshop on Urban Heritage and Building Maintenance VII*, Zürich: 65–72.
- Cantini F, Bruttini J, Cianferoni C. 2007. Firenze. Indagini archeologiche nell'area della terza corte di Palazzo Vecchio. *Notiziario della Soprintendenza Archeologica della Toscana* 2: 103-106.
- Cantini F, Bruttini J, Scampoli E, Cianferoni C. 2009. Tra il Teatro e il Palazzo: nuovi dati dallo scavo della terza corte di Palazzo Vecchio a Firenze. *V Congresso Nazionale di Archeologia Medievale*, Manfredonia. Ed. All'Insegna del Giglio: 145 – 150.
- Cantisani E, Cecchi A, Chiaverini I, Fratini F, Manganelli Del Fa C, Pecchioni E, Rescic S. 2002. The binder of the "Roman Concrete" of the Ponte di Augusto at Narni (Italy). *Periodico di Mineralogia* 71 (Special Issue: Archaeometry and Cultural Heritage):113-123.
- Cantisani E, Fratini F, Pecchioni E, Rescic S. 2007. The piers of the "Ponte di Augusto" (Narni-Italy): the mortars of the wall core. *Poster presented at GEOITALIA 2007*, Rimini (Italy), September 12-14, 2007.
- Castillo JAQ. 2006. Des poblado de Aistra (Zalduondo), *Arkeoikuska* (Vitoria- Gasteiz) 06: 84-100.
- Castillo JAQ. 2007. Des poblado de Aistra (Zalduondo), *Arkeoikuska* (Vitoria- Gasteiz) 07: 114–122.
- Castillo JAQ. 2008. Des poblado de Aistra (Zalduondo), *Arkeoikuska* (Vitoria- Gasteiz) 08: 209-211.
- Castillo JAQ. 2009. Des poblado de Aistra (Zalduondo), *Arkeoikuska* (Vitoria- Gasteiz) 09: 176-180.
- Castillo JAQ. 2010. *Final report of the Zornotzegi (Salvatierra-Agurain) Archaeological Project*.
- Castillo JAQ, Marzaioli F, Lubritto C. 2011. Dating mortars: three medieval Spanish architectures. *Arqueologia de la arquitectura*, 8:13-24.

- Cazalla O, Rodriguez-Navarro C, Sebastian E, Cultrone G, De la Torre MJ. 2000. Aging of Lime Putty: Effects on Traditional Lime Mortar Carbonation. *Journal of American Ceramic Society* 83(5): 1070-76.
- Cazenave S, Chapoulie R, Villeneuve G. 2003. Cathodoluminescence of synthetic and natural calcite: the effect of manganese and iron orange emission. *Mineralogy and petrology* 78: 243-253.
- Chu V, Regev L, Weiner S, Boaretto E. 2008. Differentiating between anthropogenic calcite in plaster, ash and natural calcite using infrared spectroscopy: implications in archaeology. *Journal of Archaeological Science* 35(4): 905-911.
- Ciancio Rossetto P. 1983. Il Circo Massimo. Indagine Archeologica, in *Roma. Archeologia e progetto*, Catalogo della Mostra: 112-13.
- Ciancio Rossetto P. 1988. *Il Circo Massimo*. Roma: Comune Ass. Alla Cultura.
- Ciancio Rossetto P, Buonfiglio M. 2007. Circo Massimo: riflessioni e progetti. *Orizzonti. Rassegna di archeologia* (VIII): 19-42.
- Courty MA, Goldberg P, Macphail R. 1989. *Soils and micromorphology in archaeology*. Cambridge University press.
- David M. 2011. The Ostia Marina Project. Rewriting the history of a seafront neighborhood. File Pdf in <http://www.storia-culture-civiltà.unibo.it>
- David M, Pellegrino A, Orofino GA, Turci M. 2009. Ostia (Roma). *Ocnus* 17: 198-202.
- David M, Turci M. 2011. Nuove osservazioni da recenti indagini ostiensi. Atti del XVI Colloquio dell'Associazione Italiana per lo Studio e la Conservazione del Mosaico (Palermo-Piazza Armerina, March 2010). *Scripta Manent*: 267-275.
- David M, Gonzales Muro X. 2011. Opus doliare a nuovi bolli laterizi dall'insula IV, IX di Ostia. *Actes du Congrès de la Société française d'étude de la céramique antique en Gaule (SFECAG)*, June 2011, Marseille, Société française d'étude de la céramique antique en Gaule: 389-96.
- Davis JA, Kent DB. 1990. Surface complexation modeling in aqueous geochemistry. *Mineral-Water Interface Geochemistry, Rev. Mineral.* 23: 177-260.
- De Tommasi GB, Manfredonia, Castello. *Restauro in Puglia 1971-1983 II*, Fasano 1983: 312-316.
- Delibrias G, Labeyrie J. 1964. Dating of old mortars by the carbon-14 method. *Nature* 201(4920):742.
- Deloye FX. 1996. La chaux a travers les ages. *Bulletin des laboratoires des Ponts et Chaussées* 201:94-98.
- Drdracky M, Fratini F, Frankeova D, Slizcova Z. In press. The Roman mortars used in the construction of the Ponte di Augusto (Narni, Italy) – a comprehensive assessment. *Journal of Archaeological Sciences*.
- Elsen J. 2006. Microscopy of historic mortar: a review. *Cement Concrete Research* 36: 1416–1424.
- Elsen J, Brutsaert A, Deckers M, Brulet R. 2004. Microscopical study of ancient mortars from Turnai (Belgium). *Materials Characterization* 53: 289-294.
- El Turki A, Ball RJ, Allen GC. 2007. The influence of relative humidity on structural and chemical changes during carbonation of hydraulic lime. *Cement and Concrete Research* 37(8):1233–40.
- Farmer VC. 1974. *The Infrared Spectra of Minerals*. Mineralogical Society, London.

- Folk RL, Valastro Jr S. 1976. Successful technique for dating of lime mortar by carbon-14. *Journal of Field Archaeology* 3(2):203–8.
- Francovich R, Cantini F, Scampoli E, Bruttini J. 2007. *La storia di Firenze tra tarda antichità e medioevo. Nuovi dati dallo scavo di via de' Castellani. Annali di Storia di Firenze*, 2: 1-40.
- Franzini M, Leoni L, Lezzerini M, Sartori F. 1990. On the binder of some ancient mortars. *Mineralogy and Petrology* 67:59-69.
- Gelichi S, Piuze F, Cianciosi A. 2008. *Sacuidic presso Forni Superiore*. All'Insegna del Giglio.
- Genestar C, Pons C. 2003. Ancient covering plaster mortars from several convents and Islamic and Gothic palaces in Palma de Mallorca (Spain). Analytical characterisation. *Journal of Cultural Heritage* 4(4):291–8.
- Giusberti P. 1987. Teatri e anfiteatri romani nella città italiane, *Storia della città* 38-39: 5-38.
- Godwin H. 1962. Half-life of Radiocarbon. *Nature* 195: 984.
- Gottardi V. 1978. *I leganti*. Ed. Pàtron Bologna, 1978.
- Goslar T, Nawrocka D, Czernik J. 2009. Foraminiferous limestone in  $^{14}\text{C}$  dating of mortar. *Radiocarbon* 51(3): 987–93.
- Habermann D, Neuser RD, Richter DK. 2000. Quantitative high resolution spectral analysis of  $\text{Mn}^{2+}$  in sedimentary calcite. *Cathodoluminescence in geosciences*: 331-358.
- Hale J, Heinemeier J, Lancaster L, Lindroos A, Ringbom Å. 2003. Dating ancient mortar. *American Scientist* 91(2):130–7.
- Hale J. 2011. Beyond the eternal city: roman concrete in global perspective. Proceeding of Building Roma Aeterna - Current research on Roman Mortar and Concrete, March 2008. *Commentationes Humanarum Litterarum* 128: 34.
- Heinemeier J, Jungner H, Lindroos A, Ringbom Å, Von Konow T, Rud N. 1997. AMS  $^{14}\text{C}$  dating of lime mortar. *Nuclear Instruments and Methods in Physics Research B* 123(1–4):487–95.
- Heinemeier J, Ringbom Å, Lindroos A, Sveinbjörnsdóttir AE. 2010. Successful AMS  $^{14}\text{C}$  dating of non-hydraulic Lime mortars from the Medieval churches of the Åland Islands, Finland. *Radiocarbon* 52(1): 171–204.
- Hobbs LW, Siddall R. 2011. Cementitious materials of the ancient world. Building Roma Aeterna, *Commentationes Humanarum litterarum* 128: 35-59.
- Hodgins G, Lindroos A, Ringbom A, Heinemeier J, Brock F. 2011.  $^{14}\text{C}$  dating of Roman mortars- preliminary tests using diluted hydrochloric acid injected in batches. Building Roma Aeterna, Proceeding of the Conference March 2008. *Commentationes Humanarum Litterarum* 128: 209- 213.
- Humbert JB, Gunneweg J. 2003. *Khirbet Qumrân et Ain Feshkha*. Academic Press Fribourg, Vandenhoeck & Ruprecht Göttingen.
- Humphrey J. 1986. *Roman circuses: arenas for chariot racing*. University of California Press.

- Ingham JP. 2005. Investigation of traditional lime mortars – the role of optical microscopy. *Proceedings of the 10<sup>th</sup> Euroseminar on Microscopy Applied to Building Materials*, University of Paisley, June 2005: 1-18.
- IUPAC. 1972. Manual of symbols and terminology for physicochemical quantities and units, appendix 2, definitions, terminology, and symbols in colloid and surface chemistry. Part 1. *Pure and Applied Chemistry*, 31: 579-638.
- Jackson M, Marra F. 2006. Roman stone masonry: volcanic foundations of the ancient city. *American Journal of Archaeology* 110: 403-36.
- Jackson M, Logan JM, Scheetz BE, Deocampod DM, Cawoode CG, Marraf F, Vittig M, Ungaroh L. 2009. Assessment of material characteristics of ancient concretes, Grande Aula, Markets of Trajan, Rome. *Journal of Archaeological Sciences* 36 (11): 2481-92.
- Jerram DA, Cheadle MJ, Hunter RH, Elliott MT. 1996. The spatial distribution of grains and crystals in rocks, *Contributions to Mineralogy and Petrology* 125: 60-74.
- Kosednar-Legenstein B, Dietzel M, Leis A, Stingl K. 2008. Stable carbon and oxygen isotope investigation in historical lime mortar and plaster - results from field and experimental study. *Applied Geochemistry* 23(8): 2425–37.
- Kudela K, Bobik P. 2004. Long-Term Variations of Geomagnetic Rigidity Cutoffs. *Solar Physics* 224: 423–431.
- Lancaster LC. 2005. Concrete vaulted construction in Imperial Rome: innovations in context. Cambridge.
- Labeyrie J, Delibrias G. 1964. Dating of old mortars by the carbon-14 method. *Nature* 201: 742.
- Laganara C, Petronella C, Zambetta E. 2011. Elementi dell'edilizia domestica nella Daunia medievale. *Proceeding of 31°Convegno Nazionale sulla Preistoria-Protostoria-Storia della Daunia*, San Severo. In press: 187-210.
- Lanas J, Bernal JLP, Bello MA, Galindo JIA. 2004. Mechanical properties of natural hydraulic lime-based mortars. *Cement and Concrete Research* 34(12): 2191–201.
- Lawrence P, Cyr M, Ringot E. 2003. Mineral admixtures in mortars: Effect of inert materials on short-term hydration. *Cement Concrete Research*, 33(12): 1939-47.
- Leslie AB, Hughes JJ. 2002. Binder microstructure in lime mortars: implications for the interpretation of analysis results. *Quarterly Journal of Engineering Geology and Hydrogeology* 35: 257-263.
- Lindroos A. 2005. *Carbonate phase in historical lime mortars and pozzolana concrete: implication for <sup>14</sup>C dating*. Department of Geology and Mineralogy, Abo Akademi University. Paintalo Gillot.
- Lindroos A, Heinemeier J, Ringbom Å, Braskén M, Sveinbjörnsdóttir Á. 2007. Mortar dating using AMS <sup>14</sup>C and sequential dissolution: examples from Medieval, non-hydraulic lime mortars from the Åland Islands, SW Finland. *Radiocarbon* 49(1):47–67.
- Lindroos A, Heinemeier J, Ringbom A, Brock F, Sonck-Koote P, Pehkonen M, Suksi J. 2011. Problems in radiocarbon dating of roman pozzolana mortars. Building Roma Aeterna, Proceeding of the Conference March 2008. *Commentationes Humanarum Letterarum* 128: 214-230.
- Lugli G. 1962. *Fontes ad topographiam veteris urbis pertinentes* (8). Roma 1962: 383-417,430-432.

- Machel H. 2000. Application of cathodoluminescence to carbonate diagenesis. In Pagel M, Barbin V, Blanc P, Ohnenstetter D. *Cathodoluminescence in geosciences*. Springer Verlag: 271-301.
- Mannoni T. 1984, Metodi di datazione dell'edilizia storica, *Archeologia Medievale* XI: 396-403.
- Maravelaki P, Bakolas A, Maropoulou A. 2003. Physic – chemical study of Cretan ancient mortars. *Cement and Concrete Research* 33(5):651-661.
- Marshall DJ. 1988. Cathodoluminescence of geological materials. Unwin Hyman, Boston.
- Marzaioli F, Borriello G, Passariello I, Lubritto C, De Cesare N, D'Onofrio A, Terrasi F. 2008. Zinc reduction as an alternative method for AMS radiocarbon dating: process optimization at CIRCE. *Radiocarbon* 50(1): 139–49.
- Marzaioli F. 2011. Characterization of a new protocol for mortar dating:  $^{13}\text{C}$  and  $^{14}\text{C}$  evidences. *Nuovo Cimento della Società Italiana di Fisica* 34(5):217-226.
- Marzaioli F, Lubritto C, Nonni S, Passariello I, Capano M, Terrasi F. 2011. Mortar radiocarbon dating: preliminary accuracy evaluation of a novel methodology. *Analytical Chemistry* 83(6):2038–45.
- Marzaioli F, Nonni S, Passariello I, Capano M, Ricci P, Lubritto C, De Cesare N, Eramo G, Castillo JAQ, Terrasi F. 2013. Accelerator mass spectrometry  $^{14}\text{C}$  dating of lime mortars: methodological aspects and field study applications at CIRCE (Italy). *Nuclear Instruments and Methods in Physics Research B* 294: 246-251.
- Massazza F. 1993. Pozzolanic cements. *Cements and Concrete Composites* 15(4): 185-214.
- Mathews JP. 2001. Radiocarbon dating of architectural mortar: a case study in the Maya region, Quintana Roo, Mexico. *Journal of field Archaeology* 28(3–4): 395–400.
- McCrea JMJ. 1950. Isotopic chemistry of carbonates and a paleo-temperature scale. *Journal of Chemical Physics* 18:849–57.
- Medlin WL. 1959. Thermoluminescent properties of calcite. *The Journal of Chemical Physics* 30 (2): 451-458.
- Michalska D, Pazdur A, Czernik J, Szczepaniak M, Zurakowska M. 2013. Cretaceous aggregates and reservoir affect in dating of binding materials. *Geochronometria* 40(1): 33-41.
- Miler K. 1964. *Itineraria Romana: Römische Reisewege an der Hand der Tabula Peutingeriana*. Stuttgart 1916, Roma: Bretschneider 1964: LXVII.
- Miriello D, Barca D, Bloise A, Ciarallo A, Crisci GM, De Rose T, Gattuso C, Gazineo F, La Russa M. 2010. Characterisation of archaeological mortars from Pompeii (Campania, Italy) and identification of construction phases by compositional data analysis. *Journal of Archaeological Sciences* 37: 2207-23.
- Moropoulou A, Bakolas A, Bisbikou K. 2000. Investigation of the technology of historic mortars. *Journal of cultural heritage* 1(1): 45-48.
- Moropoulou A, Bakolas A, Aggelakopoulou E. 2001. The effects of limestone characteristics and calcination temperature to the reactivity of the quicklime. *Cement Concrete Research* 31(4): 633-39.
- Moropoulou A, Cakmak AS, Biscontin G, Bakolas A, Zendri E. 2002. Advanced Byzantine cement based composites resisting earthquake stresses: the crushed brick/lime mortars of Justinian's Hagia Sophia. *Construction and Building Materials* 16(8): 543–552.

- Moropoulou A, Polikreti K, Bakolas A, Michailidis P. 2003. Correlation of physicochemical and mechanical properties of historical mortars and classification by multivariate statistics. *Cement and Concrete Research* 33(6): 891–898.
- Morricone A, Macchia A, Campanella L, David M, De Togni S, Turci M, Maras A, Meucci C, Ronca S. 2013. Archaeometrical analysis for the characterization of mortars from Ostia Antica. Proceeding of Youth in Conservation of Cultural Heritage, YOCOCU 2012. *Procedia Chemistry* (8): 231-238.
- Myron Best G. 2003. *Igneous and Metamorphic Petrology*, Blackwell Publishing, Oxford.
- Nawrocka DM, Michniewicz J, Pawlyta J, Pazdur A. 2005. Application of radiocarbon method for dating of lime mortars. *Geochronometria* 24: 109–115.
- Nawrocka DM, Michczyńska DJ, Pazdur A, Czernik J. 2007. Radiocarbon chronology of the ancient settlement in the Golan Heights area, Israel. *Radiocarbon* 49(2):625–37.
- Nawrocka D, Czernik J, Goslar T. 2009.  $^{14}\text{C}$  dating of carbonate mortars from Polish and Israeli sites. *Radiocarbon* 51(2):857–66.
- Nawrocka D, Michniewicz J. 2011. The radiocarbon dating of mortars from Wielka Waga, The great Scales Building in the Krakow Market Square. *Proceeding of the 37<sup>th</sup> International Symposium on Archaeometry*, Turbanti –Memmi I. Ed. Springer Verlag: 517-524.
- Nonni S, Marzaioli F, Secco M, Passariello I, Capano M, Lubritto C, Mignardi S, Tonghini C and Terrasi F. 2013.  $^{14}\text{C}$  Mortar dating : the case of the medieval Shayzar citadel, Syria. *Radiocarbon* 55 (2-3): 514- 525.
- Norma UNI 10924, 2001. Malte per elementi costruttivi e decorativi: classificazione e terminologia. Ed. UNI (Ente Nazionale Italiano Unificazione) Milano 2001.
- Norma 12/83 UNI 1176. 2006. Descrizione chimico - mineralogico - petrografico - morfologica dei materiali lapidei artificiali. Aggregati Artificiali di Clasti a Matrice Legante non Argillosa: Schema di Descrizione. Ed. UNI (Ente Nazionale Italiano Unificazione) Milano 2006.
- Nuzzo D, Rocco A, Disantarosa G. 2008. Indagini geofisiche nell'area del complesso cimiteriale di Ponte della Lama 2008 (Canosa di Puglia, Bari). *Fasti online* (Associazione Internazionale di Archeologia Classica, Roma).
- Ortega LA, Zuluaga MC, Alonso-Olazabal A, Murelaga X, Insausti M, Ibañez-Etxeberria A. 2012. Historic lime mortar  $^{14}\text{C}$  dating of Santa Maria La Real (Zarautz, Northern Spain): extraction of suitable grain size for reliable  $^{14}\text{C}$  dating. *Radiocarbon* 54(1): 23-36.
- Pachiaudi C, Marechal J, Van Strydonck M, Dupas M, Dauchot-Dehon M. 1986. Isotopic fractionation of carbon during carbon dioxide absorption by mortar. *Radiocarbon* 28(2): 691-97.
- Pagel M, Barbin V, Blanc P, Ohnenstetter D. 2000. *Cathodoluminescence in Geosciences*. Springer Verlag.
- Pazdur A, Bluszcz A, Stankowski W, Starkel L. 1999. *Geo-chronology of Upper Quaternary in Poland in luminescence and radiocarbon dating*. WIND J. Wojewoda-Wrocław.
- Pazdur A, Michczyński A, Pawlyta J and Spahiu P, 2000. Comparison of the radiocarbon dating methods used in the Gliwice Radiocarbon Laboratory. *Geochronometria* 18: 9-14.

- Pesce G, Quarta G, Calcagnile L, D'Elia M, Cavaciocchi P, Lastrico C, Guastella R, 2009. Radiocarbon dating of lumps from aerial lime mortars and plasters: methodological issues and results from S. Nicolò of Capodimonte Church (Camogli, Genoa-Italy). *Radiocarbon* 51: 867-872.
- Pesce G, Ball RJ, Quarta G, Calcagnile L. 2012. Identification, extraction and preparation of reliable lime sample for  $^{14}\text{C}$  dating of plasters and mortars with the “pure lime lumps” technique. Proceeding of the 6<sup>th</sup> International Radiocarbon and Archaeology Symposium. *Radiocarbon* 54(3-4):933-942.
- Pesce G, Ball R. 2012. Dating of old lime based mixtures with the “pure lime lumps” technique. *Radiometric Dating*, InTech: 21-38.
- Piekosin´ski F, Szujski J. 1878. Zestawienie rachunko´w miasta Krakowa z lat 1390–1393, 1395–1405. In *Najstarsze ksiegi miasta Krakowa od 1300 do 1400*. t. II, Krakow (in polish).
- Powers, M.C., 1953, A new roundness scale for sedimentary particles. *Journal of Sedimentology and Petrology* 23: 117-119.
- Rech JA. 2004. New uses for old laboratory techniques. *Near Eastern Archaeology* 67(4):212–9.
- Reimer PJ, Brown TA, Reimer RW. 2004. Discussion: Reporting and Calibration of Post-Bomb  $^{14}\text{C}$  Data. *Radiocarbon* 46 (3): 1299–1304.
- Reimer PJ, Baillie MGL, Bard E, Bayliss A, Beck JW, Blackwell PG, Bronk Ramsey C, Buck CE, Burr GS, Edwards RL, Friedrich M, Grootes PM, Guilderson TP, Hajdas I, Heaton T, Hogg AG, Hughen KA, Kaiser KF, Kromer B, McCormac FG, Manning SW, Reimer RW, Richards DA, Southon JR, Talamo S, Turney CSM, van der Plicht J, Weyhenmeyer CE. 2009. IntCal09 and Marine09 radiocarbon age calibration curves, 0–50,000 years cal BP. *Radiocarbon* 51(4):1111–50.
- Ricci Lucchi F. 1980. *Sedimentologia parte I: Materiali e tessiture dei sedimenti*. Clueb, Bologna.
- Ringbom A, hale J, Heinemeier J, Lindroos A, Brock F. 2006. Mortar dating in medieval and classical archaeology. *Construction History Society Newsletter* 73:11-18.
- Ringbom A, Lindroos A, Heinemeier J, Hale JR, Lancaster L, Brock F. 2008. Radiocarbon dating of mortar, case studies, testing different types of Roman mortar. *Poster presented at the AIA Annual Meeting* January 5, 2008, Chicago.
- Ringbom A, Heinemeier J, Lindroos A, Brock F. 20011. Mortar dating and Roman pozzolana results and interpretations. Building Roma Aeterna, Proceeding of the Conference March 2008. *Commentationes Humanarum Letterarum* 128: 187-208.
- Rittmann EA. 1933. Die geologische bedingte evolution und differentiation des Somma-Vesuvius magmas. *Zeitschrift fur Vulkanologie* 15:1-2.
- Rodriguez-Navarro C, Hansen E, Ginell WS. 1998. Calcium Hydroxide Crystal Evolution upon Aging of Lime Putty. *Journal of American Ceramic Society* 81(11): 3032-34.
- Roth I. 1974. *The geological map of Israel* 1:50,000. Sheet 12-I: Wadi el Qilt. Geological Survey of Israel.
- Rozanski K, Stichler W, Gonfiantini R, Scott EM, Beukens RP, Kromer B, Van der Plicht J. 1992. The IAEA  $^{14}\text{C}$  intercomparison exercise 1990. *Radiocarbon* 34(3):506–19.
- Ruggiero G. 2010. Tesi Ponte della Lama. Relazione preliminare su attività svolta. Unpublished.



Salama AIA, Wilson AD. 2000. Mechanical techniques: particle size separation. Wilson AD, editor. *Encyclopedia of Separation Science*. Oxford Academic Press: 3277–89.

Schiele E, Berens LW. 1976. *La calce. Calcare, calce viva, idrato di calce*. Tecniche ET Milano, 1976.

Seinfeld JH, Pandis SN. 2006. *Atmospheric Chemistry And Physics: From Air Pollution To Climate Change*. John Wiley and Sons.

Sławin'ski S, Niewalda W, Mamica M, Rozbicka D (2008) Badania wschodniej części Rynku Głównego w Krakowie – 2005–2007. Wielka Waga – Architektura (typescript in polish).

Soft Imaging System, 1999. AnalySIS User's guide.

Sonninen E, Jungner H. 2001. An improvement in preparation of mortar for radiocarbon dating. *Radiocarbon* 43(2A):271–3.

Stark J, Wicht B. 1999. Zur Historie des Gipses. *ZKG (Zement, Kalk, Gips)* 52 (10):527-533.

Stefanidou M, Papayianni I. 2005. The role of aggregates on the structure and properties of lime mortars. *Cement and Concrete Composites* 27(9–10): 914–9.

Stuiver M, Smith CS. 1965. Radiocarbon dating of ancient mortar and plaster. *6th International Conference on Radiocarbon and Tritium Dating*. Pullman, Washington, USA. p 338–43.

Stuiver M, Polach HA. 1977. Discussion: reporting of  $^{14}\text{C}$  data. *Radiocarbon* 19(3):355–63.

Stuiver M, Reimer PJ. 1993. Extended  $^{14}\text{C}$  data base and revised CALIB 3.0  $^{14}\text{C}$  age calibration program. *Radiocarbon* 35(1):215–30.

Stuiver M, Braziunas TF. 1993. Modelling atmospheric  $^{14}\text{C}$  influences and  $^{14}\text{C}$  ages of marine samples to 10,000 BC. *Radiocarbon* 35 (1): 137.

Terrasi F, De Cesare N, D'Onofrio A, Lubritto C, Marzaioli F, Passariello I, Rogalla D, Sabbarese C, Borriello G, Casa G, Palmieri A. 2008. High precision  $^{14}\text{C}$  AMS at CIRCE. *Nuclear Instruments and Methods in Physics Research B* 266(10): 2221–4.

Tonghini C, Montevecchi N, Finocchietti L, Tavernari C, Vezzoli V. 2005. Il castello musulmano di Shayzar, Siria: nuovi dati dalla campagna 2004 di indagini archeologiche e analisi degli alzati. *Archeologia Medioevale* 32: 209-234.

Torraiuoli N. 2008. *Storia di Manfredonia - Volume I: Il Medioevo*. Edipuglia: 25-62.

Tubbs LE, Kinder TN. 1990. The use of AMS for the dating of lime mortars. *Nuclear Instruments and Methods in Physics Research B* 52(3–4):438–41.

Utrero Agudo M Á. 2006. Iglesias tardoantiguas y altomedievales en la Península Ibérica. Análisis arqueológico y sistemas de abovedamiento. *Anejos de Archivo Español de Arqueología Madrid*, Instituto de Historia. Madrid. 2006.

Valeri V. 2001. Brevi note sulle Terme a Porta Marina ad Ostia. *Archeologia Classica* 52:306-322.

Van Strydonck M, Dupas M, Dauchotdehon M, Pachiaudi C, Marechal J. 1986. The influence of contaminating (fossil) carbonate and the variations of  $\delta^{13}\text{C}$  in mortar dating. *Radiocarbon* 28(2A):702–10.

- Van Strydonck M, Van der Borg K, De Jong A, Keppens E. 1992. Radiocarbon dating of lime fractions and material from buildings. *Radiocarbon* 34(3):873–9.
- Ventriglia U. 1971. *La geografia della città di Roma*. Edited by Amministrazione Provinciale di Roma, Roma.
- Vitruvius, *De Architectura*, V. Frank Granger's translation (Heinemann) 1931.
- Weiner S, Goldeberg P. 1990. On-site Fourier Transform infrared spectrometry at an archaeological excavation. *Spectroscopy* 5: 46-50.
- Wentworth C.K. 1922. A scale of grade and class terms for clastic sediments. *Journal of Geology*, 30: 377-92.
- White, W.B., 1974. The Carbonate Minerals The Infrared Spectra of Minerals. Mineralogical Society, F.V.C. London: 227-284.
- Wilson R, Spengler JD. 1996. *Particles in our air*. Harvard University Press, Howard.
- [www.biblewalks.com](http://www.biblewalks.com)
- [www.treccani.it/enciclopedia/siponto\\_\(Enciclopedia-dell'-Arte-Medievale\)/](http://www.treccani.it/enciclopedia/siponto_(Enciclopedia-dell'-Arte-Medievale)/)
- Zamba I C, Stamatakis MG, Cooper F A, Themelis PG, Zambas CG. 2007. Characterization of mortars used for the construction of Saithidai Heroon Podium (1st century AD) in ancient Messene, Peloponnesus, Greece. *Materials Characterization* 58:1229–1239.
- Zouridiakis N, Saliege J, Person A, Filippakis S. 1987. Radiocarbon dating of mortars from ancient Greek palaces. *Archaeometry* 29 (1):60-68.

